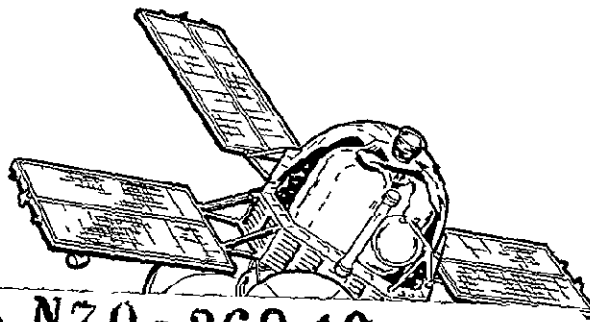


1
2
3
4
5
6
7
8
9
10
11
12
13
14
15
16
17
18
19
20
21
22
23
24
25
26
27
28
29
30
31
32
33
34
35
36
37
38
39
40
41
42
43
44
45
46
47
48
49
50
51
52
53
54
55
56
57
58
59
60
61
62
63
64
65
66
67
68
69
70
71
72
73
74
75
76
77
78
79
80
81
82
83
84
85
86
87
88
89
90
91
92
93
94
95
96
97
98
99
100

LIGHT WEIGHT SOLAR PANEL DEVELOPMENT



FACILITY FORM 602

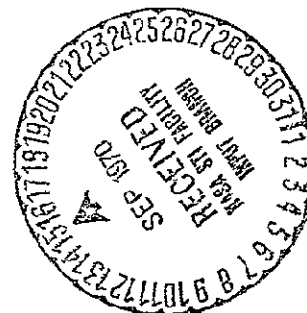
N70-36940
(ACCESSION NUMBER)

198 (THRU)

CR-112869 (PAGES)

03 (CODE)

(NASA CR OR TMX OR AD NUMBER) (CATEGORY)



PREPARED FOR
JET PROPULSION LABORATORY
CALIFORNIA INSTITUTE OF TECHNOLOGY
CONTRACT 952571

THE **BOEING** COMPANY
AEROSPACE GROUP
SPACE DIVISION, SEATTLE, WASHINGTON

Reproduced by
NATIONAL TECHNICAL
INFORMATION SERVICE
Springfield, Va 22151

D2-121773-2

FINAL REPORT

Prepared for
Jet Propulsion Laboratory
Under Contract
JPL 952571

LIGHT WEIGHT SOLAR PANEL DEVELOPMENT

JULY 1970

Prepared by J. A. Lackey
E. L. Leppert
H. M. McDaniel
D. A. Norsen

Approved by


F. W. McAfee
Program Manager

This work was performed for the Jet Propulsion Laboratory, California Institute of Technology, as sponsored by the National Aeronautics and Space Administration, under Contract NAS 7-100.

THE BOEING COMPANY
Aerospace Group
Space Division
Seattle, Washington

CONTENTS

	<u>Page</u>
Abstract	v
List of Illustrations	vi
List of Tables	ix
Glossary	x
1.0 Introduction	1
1.1 Document Organization	1
1.2 Purpose and Objectives	3
1.3 Background	3
1.4 Master Schedule	5
2.0 Summary	7
2.1 Program Objectives	7
2.2 Purpose of Performing Work	7
2.3 Work Description	8
2.4 Conclusions	18
2.5 Recommendations	19
2.6 Significant Program Developments	19
3.0 Program Plan	23
3.1 Program Tasks	23
3.2 Program Changes	26
4.0 Panel Design	29
4.1 Test Panel Requirements	29
4.2 Preliminary Design	33
4.3 Description of Test Panel	37
5.0 Design Analysis	55
5.1 Background	55
5.2 Power Output Analyses	56
5.3 Weight Analyses	60
5.4 Voltage Control	62
5.5 Thermal Analysis	63
5.6 Dynamic and Stress Analysis	65
5.7 Mechanical Analyses	76
5.8 Anomaly Investigations	92

	<u>Page</u>
6.0 Test Program	97
6.1 Modal Survey	97
6.2 Acoustic Test	107
6.3 Random Vibration Test	115
6.4 Sinusoidal Vibration Test	121
6.5 Static Load Test	129
6.6 Thermal-Vacuum-Shock Test	136
6.7 Substrate Frequency Check	144
6.8 Power Output Checks	148
6.9 Damage Evaluation	150
7.0 Manufacturing and Materiel	158
7.1 Manufacturing Plan	158
7.2 Fabrication of Detail Parts	161
7.3 Structure Subassembly Bonding	165
7.4 Substrate Bonding	170
7.5 Structure Final Assembly Bonding	171
7.6 Fabrication of Power Generation System	174
7.7 Final Assembly	181
7.8 Materiel	182
8.0 Quality Assurance	185
9.0 Conclusions	187
10.0 Recommendations	189
11.0 New Technology	193
12.0 References	195

ABSTRACT

This is the final report on the Light Weight Solar Panel Development program conducted under Jet Propulsion Laboratory Contract No. 952571. The report contains technical information concerning the preliminary design, analysis, test article design, fabrication, and test of a light weight solar panel made of built-up beryllium structure, and with 29 square feet of active cell area. This report provides a description of the test article, describes how the tests were performed, and evaluates the results of the modal survey, reverberant acoustic, random vibration, sinusoidal vibration, static load, thermal-vacuum-shock, substrate frequency check, and power output tests.

KEY WORDS

Light Weight Solar Panel	Test Results
Design Analyses	Test Fixtures
Test Analyses	Test Equipment
Procedures	Test Environment
Vibration Test	Acoustic Test
Static Load Test	Modal Survey Test
Thermal-Vacuum Test	Power Output Test
Thermal Shock Test	Test Instrumentation
Thermal Soak	Manufacturing Tooling

LIST OF ILLUSTRATIONS

<u>Figure No.</u>	<u>Title</u>	<u>Page</u>
1-1	LASA Solar Panel	4
1-2	Light Weight Solar Panel Development Program Master Schedule	6
2-1	Light Weight Solar Panels— Installed	9
2-2	Panel Physical Characteristics	11
2-3	Test Panel	13
2-4	Test Plans	14
2-5	Test Results Summary	15
2-6	End Item Delivery Schedule	17
2-7	Weight Comparison	20
3-1	Test Schedule	25
4-1	Light Weight Solar Panel Installation	31
4-2	Solar Panel Design Evolution	35
4-3	Test Panel Assembly	38
4-4	Electrical Design	40
4-5	Test Panel Electrical Installation	41
4-6	Test Panel Structure Assembly	45
4-7	Structural Member Properties	48
4-8	Deployment Equipment	51
4-9	Boost Damper Detail	53
5-1	Power-To-Weight Comparison	57
5-2	Predicted Array Performance in Space	58
5-3	Thermal Characteristics	64
5-4	Idealization Model	68
5-5	Static Stress Margins	72
5-6	Dynamic Margins of Safety vs Deflection	73
5-7	Static Deflection Shapes	74
5-8	Analysis Results - Resonant Frequencies	75

<u>Figure No.</u>	<u>Title</u>	<u>Page</u>
5-9	Deployment Analysis Assumptions	78
5-10	Cruise Damper Force-Deflection Curves	80
5-11	Energy Distribution at End of Deployment	81
5-12	Deployment Time Histories	84
5-13	Deployment Closing Rate vs Damping Coefficient	85
5-14	Temperature Effects on Damping	86
5-15	Boost Damper Test Setup	89
5-16	Boost Damper Test Results	90
5-17	Power Output Check Setup	94
6-1	Test Sequence	99
6-2	Test Program Summary	101
6-3	Test Panel Instrumentation	103
6-4	Modal Vibration Test Setup	104
6-5	First Bending Mode Shapes	108
6-6	First Torsion Mode Shapes	109
6-7	Second Torsion Mode Shapes	110
6-8	Oscillograph Record, First Bending - Decay	111
6-9	Acoustic Test Setup	113
6-10	Average Acoustic Spectrum	114
6-11	Substrate Acceleration Response - Acoustic Test	116
6-12	Random Vibration Test Setup	118
6-13	Random Vibration Test Setup	119
6-14	Random Vibration Test Spectrum	120
6-15	Substrate Acceleration Response - Random Vibration	122
6-16	Sinusoidal Vibration Test Setup	124
6-17	Sinusoidal Vibration Test Levels	125
6-18	Sinusoidal Sweep Test Results - Bending Mode	128
6-19	Static Load Test Setup	130
6-20	Torsional Load Applied	131
6-21	Deflections - 8 g Load	133

<u>Figure No.</u>	<u>Title</u>	<u>Page</u>
6-22	Deflections - 50-Pound Load	134
6-23	Stress Comparisons - Static Load Tests	135
6-24	Thermal-Vacuum-Shock Test History	137
6-25	Thermal-Vacuum-Shock Test Setup	138
6-26	Solar Simulation---Thermal-Vacuum-Shock Test	140
6-27	Thermal-Vacuum-Shock Test Equipment	141
6-28	Low Temperature Soak Setup	142
6-29	Zener Diode Test Data	145
6-30	Setup for Substrate Frequency Check	147
6-31	Setup for Power Output Check	149
6-32	Power Output Test Data	151
6-33	Silver Mesh Pigtail Damage	153
6-34	Silver Mesh Pigtails - Enlarged Photos	154
7-1	Test Panel - Sun Side	159
7-2	Test Panel - Dark Side	160
7-3	Channel Form Die	162
7-4	Hot Platen Press	163
7-5	Stick Assembly Bonding Tool	166
7-6	Frame Bonding - Sun Side Frame	168
7-7	Frame Bonding - Dark Side Frame	169
7-8	Substrate/Frame Bonding	172
7-9	Substrate/Frame Bond Setup	173
7-10	Completed Structural Frame Assembly	175
7-11	Titanium Hinge, Cruise Damper, and Tip Fitting Installation	176
7-12	Seven-Cell Soldering Fixture	178
7-13	Module Soldering Fixture	179
7-14	Solar Cell Soldering Template	180
10-1	Recommended Electrical Installation	191

LIST OF TABLES

<u>Table No.</u>	<u>Title</u>	<u>Page</u>
5-1	Test Panel Weight Summary	61
5-2	Driving Forces - Sinusoidal Tests	91
5-3	Boost Damper Parameters	92
6-1	Modal Test Results	106
6-2	Reported Cracked Solar Cells (c) and Coverglasses (cg)	156

GLOSSARY

BASIC PANEL---A flight configuration panel, consisting only of the cell stack, structure, substrate, and zener diodes, which is used for power output determination. No mechanisms or extraneous equipment are included.

BLOCKING DIODE---A solid state component which allows current to flow in a selected direction and prevents current from flowing in the reverse direction.

CAP STRIP---One of the beryllium sheet parts comprising a structural member, or stick. (See definition of "stick".)

CELL STACK---An assembly of one solar cell and one coverglass, bonded together with an RTV silicone compound.

COVERGLASS---The protective cover bonded to the solar cell.

DARK SIDE---The panel surface away from the sun.

EDM---Electrical Discharge Machining.

FACTOR OF SAFETY---The ratio of the ultimate design load to the limit design load.

FITTING FACTOR---An additional multiplicative factor applied to fittings to account for stress complexities and concentrations.

GENERALIZED MASS---The "effective" mass associated with a vibration shape.

INTERCONNECTORS---Expanded silver mesh strips which connect both parallel groups and series assemblies of solar cells.

LASA---Large Area Solar Array

MARGIN OF SAFETY---A positive margin of safety is defined as:

$$M.S. = \left[\frac{\text{Allowable Load (or Allowable Stress)}}{\text{Design Load (or Design Stress)}} \right] - 1 > 0$$

MEK---Methyl Ethyl Ketone.

MMSA---Mars Mission Solar Array -- an abbreviation used to identify the Light Weight Solar Panel.

MODULE---A group of solar cells connected in series/parallel which produces system voltage and current.

NODE---A point of no motion used in describing vibration mode shapes.

PANEL CONFIGURATIONS---

- INITIAL CONFIGURATION

Proposal Configuration---A panel configuration, as defined in the Boeing Proposal Document D2-114460-3, which supports a relay antenna and other extraneous equipment.

Alternate Configuration---A panel configuration proposed to determine the effect of removing the relay antenna and related mounting provisions.

- TRADE STUDY CONFIGURATIONS (at the time of the Preliminary Design Review)

PDR Baseline Configuration---A refinement of the Proposal Configuration including a relay antenna of reduced weight.

PDR Alternate Configuration A---A panel configuration similar to the PDR Baseline Configuration but with the relay antenna and mounting provisions omitted.

PDR Alternate Configuration B---A set of panel configurations in which extraneous equipment and mounting provisions were included on each of the four panels per array only when the panel would actually support that equipment.

- FINAL CONFIGURATIONS

Test Panel---The light weight solar panel test article with the relay antenna and the deployment equipment omitted and approximately half of the solar cells on the panel not connected electrically to the panel electrical buses.

Flight Configuration---A panel configuration developed for analytical purposes which is identical to the test panel except that the deployment equipment

is included in the mechanical analysis and 100 percent connection of flight-quality solar cells is assumed in the electrical and thermal analyses.

PDR---Preliminary Design Review

PIN-FREE---A panel support condition where the panel hinges are supported by pins which constrain the panel against translation but allow rotation, and where the tip is supported by dampers.

PIN-PIN---A condition where the panel is supported at the hinges and tip in a manner constraining the panel against translation but allowing rotation.

POWER BUSES---Flat copper electrical conductors which pick up the output of each module for transmission to the spacecraft loads.

PULSE SOLDERING---Contact soldering by means of a pulse of electrical energy which heats a small resistance element which contacts the solder.

SHEAR WEB---One of the beryllium sheet parts comprising a structural member, or stick. (See definition of "stick".)

SOLAR CELL ASSEMBLY---Same as Cell Stack.

SOLAR CELL GROUP---Six or seven cells electrically connected in parallel by soldering each cell to a common silver mesh interconnector.

SOLAR CELL MODULE---Two or four submodules joined together in series after submodules have been bonded to the substrate.

STICK---A beryllium structural member of rectangular cross section consisting of two formed channels connected across the facing flanges by a shear web on the substrate side and a cap strip on the opposite side (see Figure 4-6).

STRUCTURAL NODE---A point assumed on the panel structure for analytical purposes, usually at the intersection of structural members.

SUBSTRATE---An assembly of epoxy impregnated fiberglass tapes bonded in a grid pattern and positioned at 45° to the panel structural members. The solar cells

are bonded to the substrate, each cell being located on a tape intersection point (see Figures 4-5 and 4-6).

SUBSTRATE NODE---A point at the center of a substrate bay at which the effective weight of that bay is assumed to be concentrated.

SUBSTRATE PLANE---The planar surface (sun side) of the substrate after it is installed between the sun side and dark side frames of the solar panel.

SUN SIDE---The panel surface facing the sun

ZENER DIODE---A solid state component which limits system voltage to a selected value.

SECTION 1.0: INTRODUCTION

This document provides a record of the work accomplished in compliance with the Jet Propulsion Laboratory (JPL) Contract No. 952571, Light Weight Solar Panel Development. The work was performed by The Boeing Company, Aerospace Group, Space Division, Seattle, Washington, between July 1, 1969, and July 1970.

The entire contract effort is summarized herein with reference to more detail reports for test results and analyses of the design.

1.1 DOCUMENT ORGANIZATION

—

This document provides different levels of detail to suit the readers' requirements.

—

A reporting technique consisting of declarative "headline" statements at the beginning of each topic was used as the format of this report. The headline statements identify the major point of interest in each topic. More detail concerning each topic is provided in the text following the headline statements. The document summary (Section 2.0) and the headline statements provide to the reader a program summary and an identification of significant issues. The major document sections contain the following information:

Section 1.0: Introduction---A discussion of document organization, purpose and objectives, background of preceding work, and the program schedule.

Section 2.0: Summary---A brief summary of program activities, program objectives, purpose, conclusions, recommendations, and significant developments.

Section 3.0: Program Plan---A description of the work accomplished in planning the program, changes made in the plan, and the items delivered.

- Section 4.0:** Test Panel Design---A description of work performed in designing the panel to the specified requirements and a description of the test panel design in detail.
- Section 5.0:** Design Analyses---The analyses performed to evaluate the design, determine test requirements, and predict test results. Analyses included are: power output, weight, electrical/thermal, dynamic and stress, mechanical, closing velocity limitation, deployment mechanisms, boost damper characteristics, and evaluations of test anomalies.
- Section 6.0:** Test Program---The test program, containing a summary of the test setup, conduct, and results of the power output, frequency check, modal survey, reverberant acoustic, random and sinusoidal vibration, static load, and thermal-vacuum-shock tests.
- Section 7.0:** Manufacturing and Materiel---The manufacturing plan and a description of the methods of fabrication and assembly of the structural and electrical elements with a brief description of Materiel activities.
- Section 8.0:** Quality Assurance---A summary report of the activities performed in maintaining configuration control and unplanned event records (UER's) during fabrication and test of the solar panel.
- Section 9.0:** Conclusions
- Section 10.0:** Recommendations
- Section 11.0:** New Technology
- Section 12.0:** References

1.2 PURPOSE AND OBJECTIVES

—
The program objectives were met and the purpose can be fulfilled by using the design on a flight vehicle.

—
The purpose of the Light Weight Solar Panel Development program was to develop a solar panel, using the technology developed in the 50 kilowatt Large Area Solar Array (LASA) program, that would satisfy the requirements for a smaller, one kilowatt solar array with a substantial weight saving (a goal of 20 watts/pound at 1.0 A.U.) over conventional designs (generally about 10 watts/pound).

The primary objective was to develop a light weight solar panel that would meet the type-approval requirements of a solar array for a hypothetical Mars mission within the time period needed to support a 1973 Mars flight. Several secondary objectives are given in Section 2.0.

All program objectives were met. A specific power output of 20.6 watts per pound (without zener diodes) was achieved, the test panel met the static, dynamic, and dimensional requirements, and LASA tools, processes, and techniques were used extensively.

1.3 BACKGROUND

—
The light weight solar panel design is a result of the application of technology successfully developed for the Large Area Solar Array.

—
In October 1968, the second phase of the three phase, LASA development program for a 50 kilowatt, 20-watt-per-pound solar array was successfully completed. The development program verified that a 20-watt-per-pound large area solar array was feasible and that individual LASA solar panels, as shown in Figure 1-1, could be built to satisfy space flight requirements. Phase III of the LASA program was required to determine

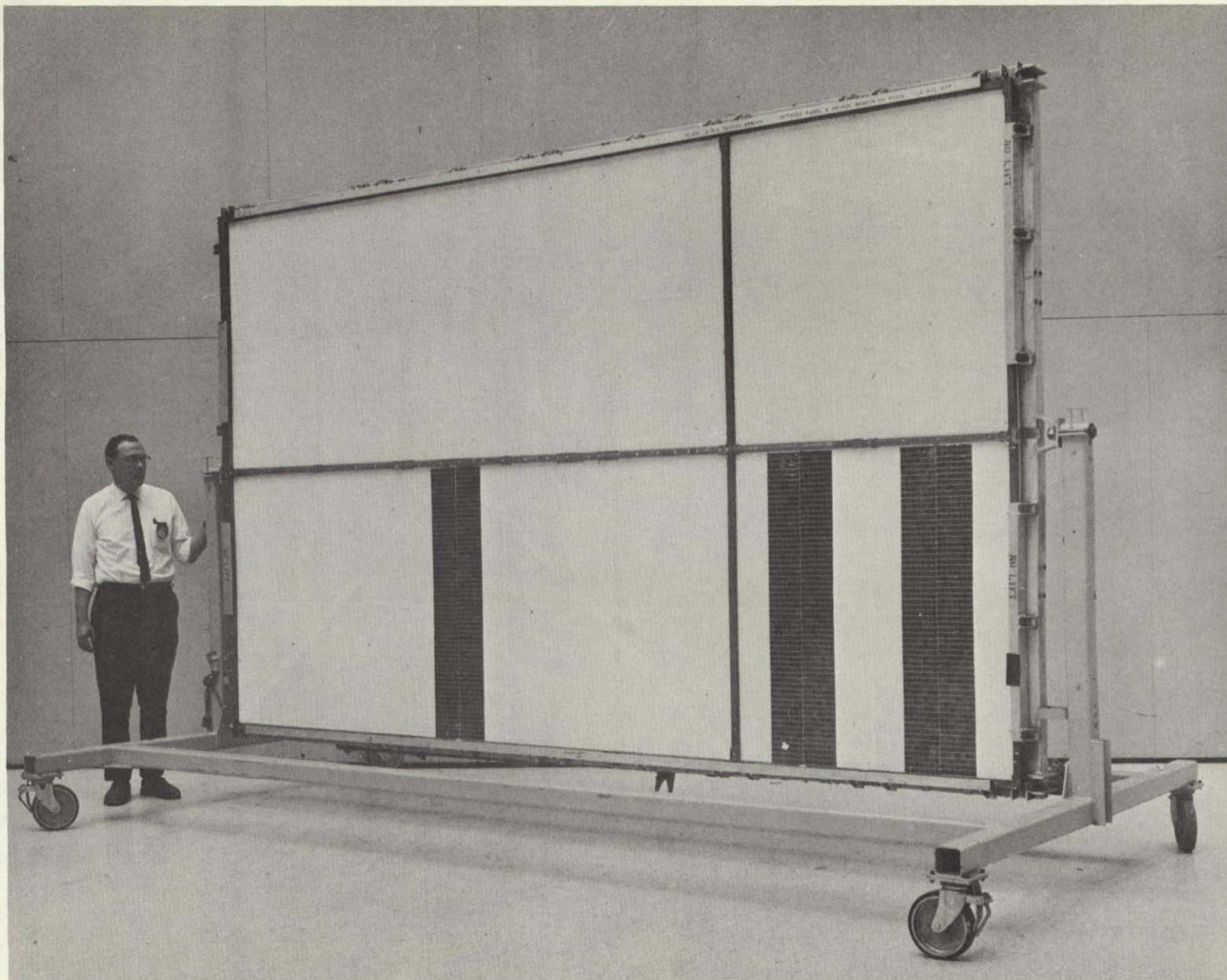


Figure 1-1: LASA SOLAR PANEL

that the LASA could satisfy flight requirements by testing the complete multi-panel array in both the stowed and deployed conditions. Since the purpose of developing the LASA was to power a Mars orbiter mission using electric propulsion, the LASA Phase III was indefinitely postponed because the electrical propulsion mission had been eliminated and the solar array technology was, at that time, ahead of the electric propulsion system development.

The solar panel features developed for the LASA were its high power-to-weight ratio, structural stiffness, desirable thermal characteristics (i.e., balanced thermal coefficients of linear expansion and minimum stable temperature), and its ease of manufacturing compared to other light weight panel designs.

In July 1969, JPL contracted with The Boeing Company to design, fabricate and test a solar panel suitable for a hypothetical Mars Orbiter mission. The panel would be as near to interchangeable with the Viking Orbiter panels as could be determined at the time of the design. The panel would be tested to type-approval levels, as nearly as could be determined at the time, to verify the capability of the light weight design for use on proposed Mars missions.

This document summarizes the results of this contract and provides a record of work accomplished.

1.4 MASTER SCHEDULE

The master schedule shown in Figure 1-2 provided a guide throughout the program for identifying the major milestones and establishing the timing for significant events.

All major milestones were met on schedule and contract revisions did not materially affect the completion of the program tasks as planned. The effects of contract changes and revisions to the test plan on the master schedule are described in detail in Section 3.0.

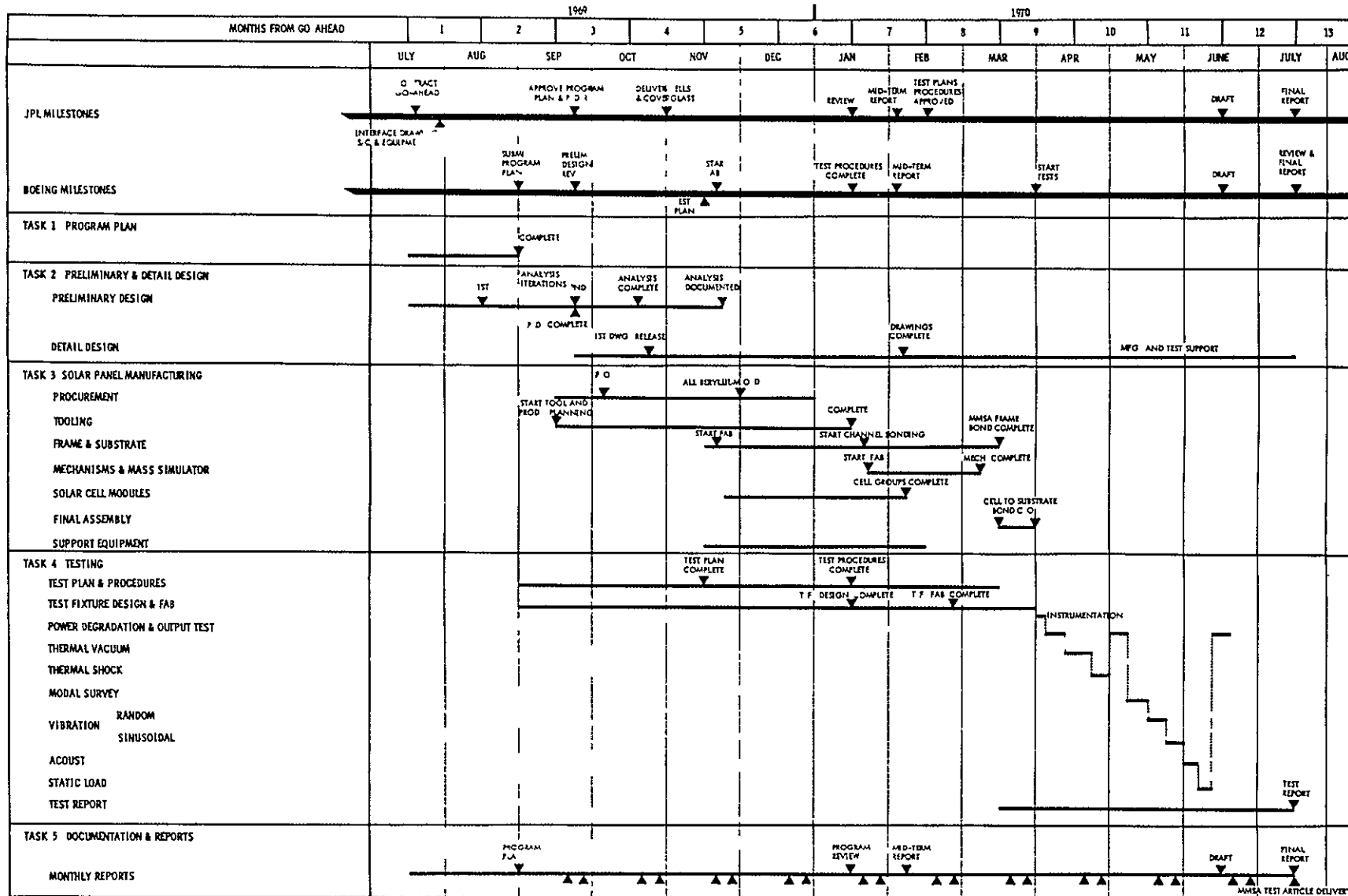


Figure 1-2 LIGHT WEIGHT SOLAR PANEL DEVELOPMENT PROGRAM MASTER SCHEDULE

D2-121773-2

SECTION 2.0: SUMMARY

This section provides a summary description of the work performed and answers the following questions:

- 1) What were the objectives of the work?
- 2) Why was the work done?
- 3) What is the report about?
- 4) What conclusions were reached?
- 5) What recommendations are made?
- 6) What is significant about the work?

2.1 PROGRAM OBJECTIVES

The primary objective of this program was to design, fabricate, and test a light weight solar panel that would meet all the requirements of a Mars orbiter spacecraft, using Large Area Solar Array (LASA) technology to achieve a goal of 20 watts per pound specific power output at 55°C and one A.U. (The LASA design achieved 21.85 watts per pound under comparable conditions.)

Secondary objectives were to:

- 1) Evaluate the effect of using the solar panel to support extraneous equipment.
- 2) Develop additional manufacturing techniques and processes for the light weight solar panel.
- 3) Verify the test panel capability to meet type approval requirements for a Mars orbiter
- 4) Determine zener diode characteristics when installed on the light weight solar panel.
- 5) Be interchangeable, as far as possible, with the Viking Orbiter solar panels.

2.2 PURPOSE OF PERFORMING WORK

The main purpose in performing the work on this contract was to verify the utility of the LASA light weight technology on solar panels of the one kilowatt size and to

show that power-to-weight ratios of 20 watts per pound can be attained while meeting the requirements for a Mars orbiting spacecraft.

Other purposes of this contract were to:

- 1) Provide a light weight solar panel backup design for Mars orbiting spacecraft.
- 2) Develop a small one kilowatt solar panel design using the Large Area Solar Array light weight technology.
- 3) Prepare procedures and processes for fabricating the light weight solar panels.

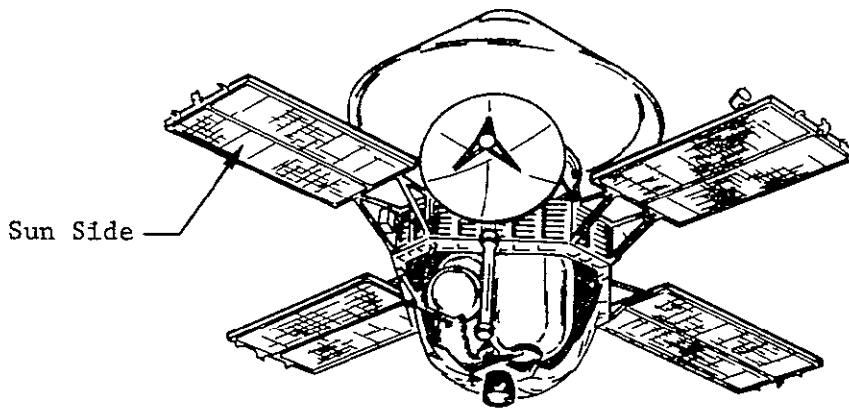
2.3 WORK DESCRIPTION

This report describes the work that was accomplished on the Light Weight Solar Panel Development Contract. The work was divided into five tasks as described below.

Task 1, Program Plan---A program plan was prepared in the first six weeks after the July 9, 1969, go-ahead. The plan presented flow charts of events for Engineering, Manufacturing, and Testing. A master schedule, Figure 1-2, was included in the plan. Following the Preliminary Design Review, the plan was revised by contract modification to change the work statement and use existing surplus materials from the LASA program. After the Test Plan Review, the contract was modified to add the substrate frequency checks, four additional power output tests, a zener diode parametric test, and to change from a heated chamber to a solar simulator heat source for the long term, high temperature soak test.

Task 2, Configuration Review and Detail Design---The first two months of this program were devoted to a configuration review of three four-panel array alternates to determine the effects of supporting extraneous equipment on the solar panels. The assumed launch and deployed configurations for this review are shown in Figure 2-1. The results of the configuration review and the three alternate configurations are shown in Section 5.0, Figure 4-2. The four-panel array configurations compared were:

- The PDR Baseline Configuration — in which each panel included provisions for supporting a 10-pound relay antenna and other extraneous equipment.



DEPLOYED CONFIGURATION

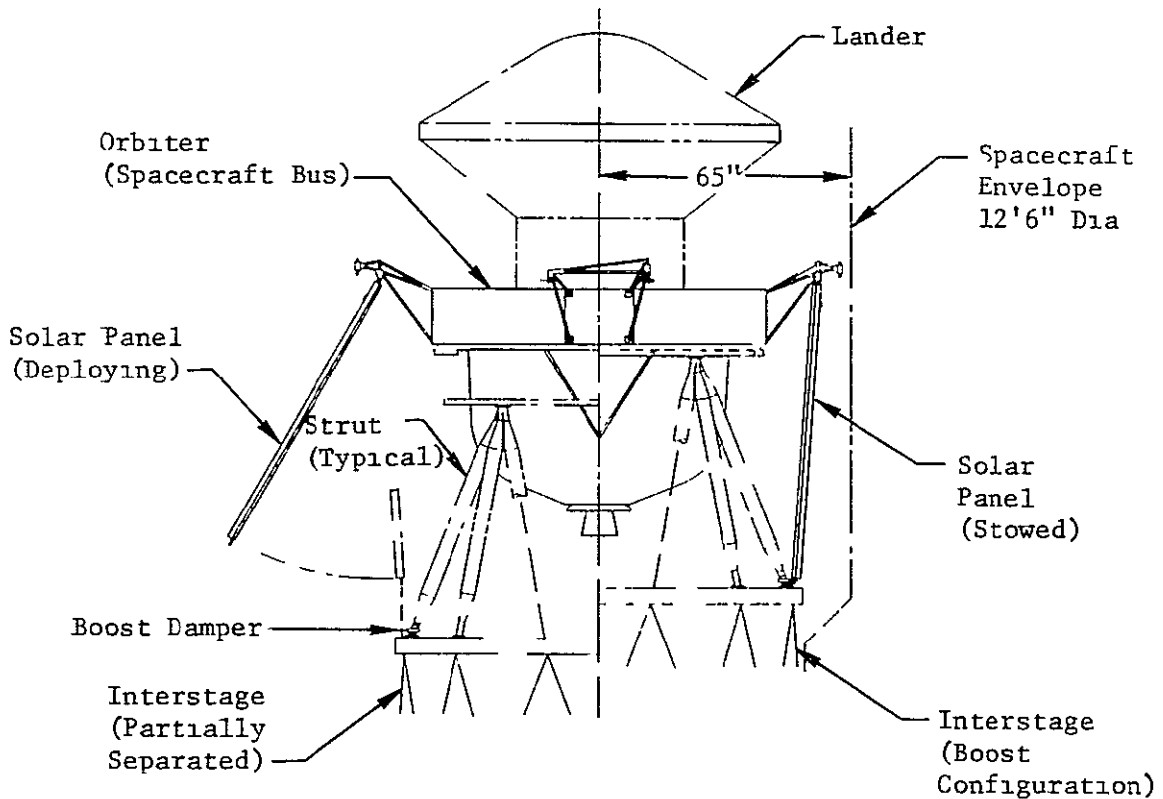


Figure 2-1 LIGHTWEIGHT SOLAR PANELS---INSTALLED

- The PDR Alternate A Configuration — in which the provisions for supporting the relay antenna were omitted from each panel
- The PDR Alternate B Configuration — in which the panels were not interchangeable and only one of the four panels included provisions for supporting the relay antenna

The panels for these configurations were carried to a level of preliminary design to allow a comparison of weight and electrical performance. As shown in the following table, the penalties incurred in supporting the extraneous equipment are minor.

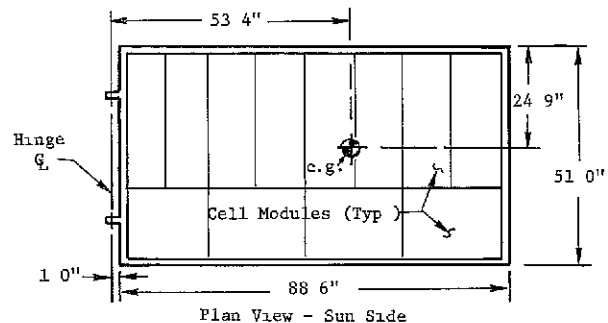
RESULTS OF CONFIGURATION REVIEW
(Based on a Four-Panel Array)

Characteristic	Configuration		
	PDR Baseline	PDR Alternate A	PDR Alternate B
Weight (structure and cell stack only)	56.52 lb.	54.84 lb.	54.36 lb.
Power-to-Weight Ratio (Based on structure and cell stack weight only)	20.5 w/lb.	21.2 w/lb.	21.3 w/lb.

Following the configuration review, detail design was completed for the selected test panel configuration and drawings of the test panel details were released for fabrication. The selected test panel configuration was identical to the PDR Baseline configuration except that the relay antenna was omitted and the deep lateral spar was replaced by an intercostal. A summary of the physical characteristics of the test panel design (flight configuration) is given in Figure 2-2.

Task 3, Test Panel Manufacturing---The test panel structure was fabricated from beryllium, titanium, and fiberglass tape. Material surplused by the LASA program was used. Forty-five percent of the test panel beryllium requirement was obtained by chem-milling heavier surplus stock to the required gages. The remaining beryllium requirement was purchased.

SOLAR PANEL POWER OUTPUT



Plan View - Sun Side

- Overall Panel Area 31.4 Sq Ft
- Cell Module Area 29.0 Sq Ft
- Weight. The Weight Summary for a Four-Panel Array is Given Below

100 Lb (Ref)	Panel Mounted Equipment	
68.44 Lb	S/C & L/V Mechanisms	Panel Mechanisms 0.07 Lb Per Panel
56.28 Lb	Zener Diodes 3.04 Lb/Panel	
33.28 Lb	Cell Stack & Wiring 5.75 Lb/Panel	Basic Panels 17.11 Lb Per Panel
0	Structure 8.32 Lb/Panel	

STRUCTURAL/DYNAMIC CHARACTERISTICS

- Structural Materials
Built-up Rectangular Tubes---Beryllium
Fittings, Clips, and Gaskets ---Titanium
Substrate---Fiberglass Tapes
- Resonant Frequencies (hz)

Condition	Mode	Rigid Rotation	First Torsion	Shear	First Bending	Second Torsion
Pin-Free (35 Lb/In Damper Spring)		7.9	19.2	28.5	34.3	68.6
Deployed (530 Lb/In Spring)		1.61	17.2	27.5	34.5	---

- Maximum Stress (static)
Bending 7400 psi (margin of safety = 0.15)
Torsion 4350 psi (with 50-lb load at one tip fitting)

ELECTRICAL CHARACTERISTICS

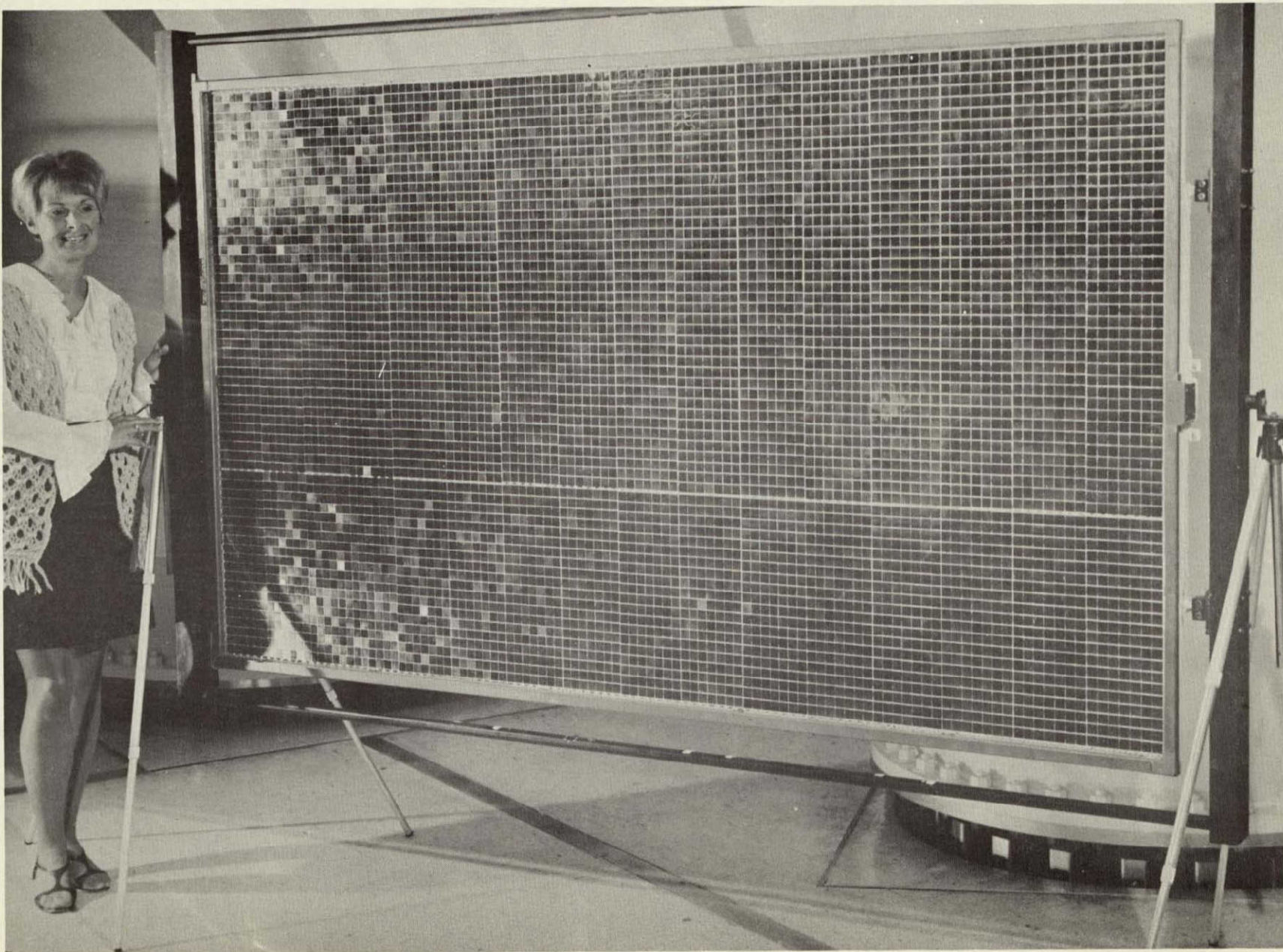
- Test Panel Cell Stack
Cells---2 x 2 cm, 8 mil, N on P
Solderless Silicone, 9% efficient
Coverglass---Plain 3 mil Microsheet
- Cell Modules
Cell Group = 6 or 7 Cells in Parallel
Module = 80 Cell Groups in Series
- Total Cells per Panel = 6480
- Voltage = 33.6 V (Near Earth)
46.4 V (Near Mars)
- Cell Operating Temperature = 45.5°C at 1 A.U.
- Zener Diodes
Design Nominal---Five Diodes, (Dickson Corp Part No. IM3309B, 10-Volt) Per Module

SOLAR PANEL POWER OUTPUT

Conditions (Degradation Not Included)	Output per Panel (Watts)	Specific Power Output (Watts per Pound)		
		No Zener Diodes---Basic Panel (14.07 Lb/Panel)	3 Zener Diodes per Module (15.88 Lb/Panel)	5 Zener Diodes per Module (17.11 Lb/Panel)
Output based on the contract-specified 10 w/sq ft x 29 sq ft	290	20.6	18.2	17.0
Output extrapolated from test measurements • Normalized for 55°C and 130 w/sq ft input intensity (1 AU) • Cell output rating = 0.047 watt at 28°C	282	20.0	17.7	16.5
Possible output of a flight panel at 45.5°C • 45.5°C = predicted cell operating temperature at 1 AU and 130 w/sq ft input intensity* • Cell output rating = 0.055 watt at 28°C (average flight quality)	324	23.0	20.3	18.9

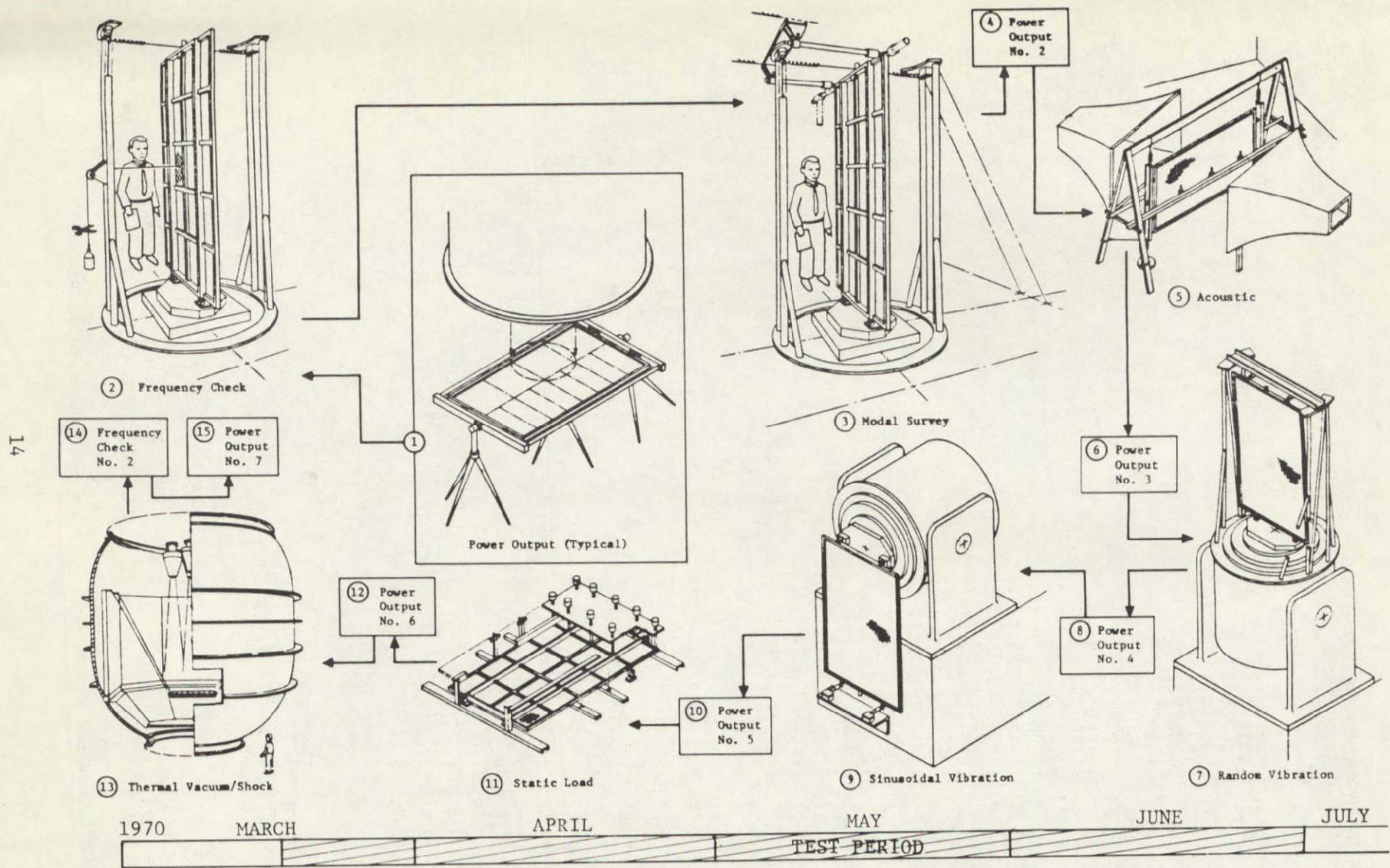
*Neglecting spacecraft thermal interface

Figure 2-2 SOLAR PANEL PHYSICAL CHARACTERISTICS



D2-121773-2

Figure 2-3: TEST PANEL



D2-121773-2

Figure 2-4: TEST PLANS

TEST	OBJECTIVE	MEASURED PARAMETERS				REMARKS																	
MODAL SURVEY	TO DETERMINE MODE SHAPES FREQUENCIES AND MODAL DAMPING OF THE PIN FREE PANEL FOR FREQUENCIES BELOW 100 Hz	MODE	FREQ (Hz)	DAMPING COEFF	MODE	FREQ (Hz)	DAMPING COEFF	<ul style="list-style-type: none"> MODE SHAPES WERE ABOUT AS PREDICTED SEE FIGURES 6 5 6 6 AND 6 7 BENDING STIFFNESS WAS ABOUT 80% AND TORSIONAL STIFFNESS ABOUT 85% OF PREDICTED BECAUSE OF DEFICIENCIES IN ANALYTICAL MODELING RECALCULATED FREQUENCIES INCLUDING TEST EQUIPMENT WEIGHT AND REDUCED STIFFNESS AGREED WITH MEASURED FREQUENCIES 															
		1ST TORSION	12.2	0.037	2ND TORSION	50	0.062																
		1ST SHEAR	22.28	0.037	CHORD BENDING	58	0.062																
		1ST BENDING	28.4	0.110	LARGE SUBSTRATE	68.71	~ 0.075																
		HIGHEST STRUCTURAL STRESS		3 540 PSI																			
REVERBERANT ACOUSTIC	TO EXPOSE THE TEST PANEL TO ACOUSTIC NOISE UP TO 150 db OVERALL FOR 60 SECONDS AND TO DETERMINE RESPONSES			<table border="1"> <thead> <tr> <th>LOC</th> <th>RESPONSE (g rms)</th> <th>LOC</th> <th>RESPONSE (g rms)</th> </tr> </thead> <tbody> <tr> <td>A3</td> <td>15.1</td> <td>A11</td> <td>305</td> </tr> <tr> <td>A5</td> <td>12.3</td> <td>A12</td> <td>200</td> </tr> <tr> <td>A7</td> <td>26.7</td> <td>A13</td> <td>37.5</td> </tr> </tbody> </table>		LOC	RESPONSE (g rms)	LOC	RESPONSE (g rms)	A3	15.1	A11	305	A5	12.3	A12	200	A7	26.7	A13	37.5	<ul style="list-style-type: none"> SUBSTRATE RESPONSES WERE GREATER THAN EXTRA POLATED FROM LASA DATA BECAUSE OF DIFFERENT TEST CONDITIONS NO STRUCTURAL OR CELL BOND DAMAGE OCCURRED 	
		LOC	RESPONSE (g rms)	LOC	RESPONSE (g rms)																		
A3	15.1	A11	305																				
A5	12.3	A12	200																				
A7	26.7	A13	37.5																				
		DIAGRAM I ACCELER LOC S		HIGHEST STRUCTURAL STRESS 4 300 PSI																			
RANDOM VIBRATION	TO DETERMINE THE ADEQUACY OF THE TEST PANEL TO WITHSTAND WIDE BAND RANDOM EXCITATION IN THE LAUNCH DIRECTION (4° OFF THE PLANE OF THE PANEL)	ACCELERATION RESPONSES (SEE DIAGRAM II)				HIGHEST STRUCTURAL STRESS 1 100 PSI	<ul style="list-style-type: none"> STRESS AND ACCELERATION LEVELS WERE LOW AS EXPECTED BECAUSE OF THE NEARLY IN PLANE DIRECTION OF EXCITATION MARINER 67 TYPE DAMPERS WERE USED FOR TIP SUPPORT IN THIS AND THE SINUSOIDAL TEST 																
		<table border="1"> <thead> <tr> <th>LOC</th> <th>RESPONSE (g rms)</th> <th>LOC</th> <th>RESPONSE (g rms)</th> </tr> </thead> <tbody> <tr> <td>A3</td> <td>4.0</td> <td>A11</td> <td>14.5</td> </tr> <tr> <td>A7</td> <td>2.9</td> <td>A12</td> <td>10.5</td> </tr> <tr> <td>A8</td> <td>4.0</td> <td>A14</td> <td>5.3</td> </tr> <tr> <td>A10</td> <td>8.0</td> <td>A16</td> <td>6.1</td> </tr> </tbody> </table>	LOC	RESPONSE (g rms)	LOC			RESPONSE (g rms)	A3	4.0	A11	14.5	A7	2.9	A12	10.5	A8	4.0	A14	5.3	A10	8.0	A16
LOC	RESPONSE (g rms)	LOC	RESPONSE (g rms)																				
A3	4.0	A11	14.5																				
A7	2.9	A12	10.5																				
A8	4.0	A14	5.3																				
A10	8.0	A16	6.1																				
SINUSOIDAL VIBRATION	TO EXPOSE THE PANEL TO SINUSOIDAL EXCITATIONS (NORMAL TO THE PANEL) AT THE TWO HINGE POINTS WHICH WOULD INDUCE STRESSES EQUIVALENT TO THOSE PRODUCED BY A SPECIFIED EXCITATION AT THE FOUR SPACECRAFT ATTACH POINTS	ACCELERATION RESPONSES (SEE DIAGRAM II)				HIGHEST STRUCTURAL STRESS 3 250 PSI (VS 10 900 PSI FOR ZERO MARGIN OF SAFETY)	<ul style="list-style-type: none"> TEST WAS PERFORMED IN SEGMENTS TO AVOID OVERDRIVING ADJACENT MODES (SEE FIGURE 6 17) STRESS AND ACCELERATION LEVELS WERE NOT EXCESSIVE NON LINEARITY OF THE DAMPERS AND HINGE FREE PLAY CONTRIBUTED TO HIGH FREQUENCY HASH SEEN ON THE RECORDED DATA 																
		<table border="1"> <thead> <tr> <th>LOC</th> <th>RESPONSE (g PEAK)</th> <th>LOC</th> <th>RESPONSE (g PEAK)</th> </tr> </thead> <tbody> <tr> <td>A11</td> <td>12.5</td> <td>A10</td> <td>15.0</td> </tr> <tr> <td>A11</td> <td>8.0</td> <td>OTHERS</td> <td>< 5.0</td> </tr> </tbody> </table>	LOC	RESPONSE (g PEAK)	LOC			RESPONSE (g PEAK)	A11	12.5	A10	15.0	A11	8.0	OTHERS	< 5.0							
LOC	RESPONSE (g PEAK)	LOC	RESPONSE (g PEAK)																				
A11	12.5	A10	15.0																				
A11	8.0	OTHERS	< 5.0																				
STATIC LOAD	TO DETERMINE PANEL DEFLECTIONS FOR TWO LOADING CONDITIONS 1) BENDING-UNIFORM 8g LOAD 2) TORSION-50 LB LOAD AT UNSUPPORTED SPAR TIP	BENDING DEFLECTIONS		TORSIONAL DEFLECTIONS		<ul style="list-style-type: none"> THE REDUCTION IN STIFFNESS (FROM PREDICTED) AGREED WITH THAT INDICATED BY THE MODAL TEST LOAD DEFLECTION PLOTS WERE ALL LINEAR AND STRESSES DID NOT EXCEED ALLOWABLES 																	
		<ul style="list-style-type: none"> MAIN SPAR-0.123 MAX OUTBD SPAR-0.118 MAX HIGHEST STRESS-7 400 PSI 		<ul style="list-style-type: none"> EXTREME CORNER-1.65 NEAR LOAD POINT-1.05 HIGHEST STRESS-4 350 PSI 																			
THERMAL-VACUUM/SHOCK	TO MEASURE POWER OUTPUT AND ZENER DIODE PERFORMANCE IN VACUUM AND THERMAL SHOCK CONDITIONS AND TO SUBJECT THE PANEL TO A 12 DAY THERMAL SOAK	POWER OUTPUT		ZENER DIODE PERFORMANCE (DURING THERMAL UP SHOCK)		<ul style="list-style-type: none"> THE TEST PANEL DID NOT DEGRADE WHEN SUBJECTED TO THE THERMAL VACUUM SHOCK ENVIRONMENT POWER OUTPUT AND THERMAL DATA MEASURED IN THIS TEST SUBSTANTIATES PREDICTIONS OF FLIGHT PANEL PERFORMANCE (SEE FIG 2 2) THE TEST PANEL WILL OPERATE SATISFACTORILY WITH ONLY THREE 50 WATT ZENERS FOR EACH 560 CELL MODULE BECAUSE THE STRUCTURE PROVIDES A HEAT SINK FOR ZENER DIODE ENERGY DISSIPATION 																	
		<table border="1"> <thead> <tr> <th>INPUT INTENSITY (MW/CM²)</th> <th>AVERAGE OUTPUT OF A 560 CELL MODULE (WATTS)</th> </tr> </thead> <tbody> <tr> <td>140 (AMBIENT PRESSURE)</td> <td>24.6</td> </tr> <tr> <td>63 (VACUUM COLD WALL)</td> <td>13.7</td> </tr> <tr> <td>140 (VACUUM COLD WALL)</td> <td>27.8</td> </tr> </tbody> </table>	INPUT INTENSITY (MW/CM ²)	AVERAGE OUTPUT OF A 560 CELL MODULE (WATTS)	140 (AMBIENT PRESSURE)		24.6	63 (VACUUM COLD WALL)	13.7	140 (VACUUM COLD WALL)	27.8	<ul style="list-style-type: none"> 3 ZENERS PER MODULE INITIAL PANEL TEMP _____ 202°F INPUT INTENSITY _____ 250MW/CM² ZENERS OPERATED FOR _____ 2.0 MIN ZENER OPERATING TEMP _____ 15°F (230°F = SAFE MAXIMUM) ZENERS CLIPPED VOLTAGE AT 49v 											
INPUT INTENSITY (MW/CM ²)	AVERAGE OUTPUT OF A 560 CELL MODULE (WATTS)																						
140 (AMBIENT PRESSURE)	24.6																						
63 (VACUUM COLD WALL)	13.7																						
140 (VACUUM COLD WALL)	27.8																						
POWER OUTPUT & INSPECTION	TO DETERMINE ELECTRICAL DEGRADATION FOLLOWING EACH ENVIRONMENTAL TEST	POWER OUTPUT (WATTS AT 55°C)		DAMAGE EVALUATION		<ul style="list-style-type: none"> POWER OUTPUT PATTERN OF VARIATION INDICATED NO MEASURABLE DEGRADATION REPLACEMENT OF SILVER MESH PIGTAILS WITH STRANDED WIRE IS RECOMMENDED 																	
		SIX ACTIVE MODULES TESTED RESULTS OF FIVE TESTS OF EACH MODULE HIGH = 29.2 WATTS LOW = 23.3 WATTS AVERAGE = 24.4 WATTS (PREDICTED = 23.0 WATTS)		CELL ASSEMBLIES <ul style="list-style-type: none"> 7 SEVERELY CRACKED IN HANDLING 0.93% (60 OF 6480) SUSTAINED SMALL EDGE CRACKS DURING TESTING SILVER MESH PIGTAILS <ul style="list-style-type: none"> 15 FAILURES DURING MANUFACTURING & TEST 																			
SUBSTRATE FREQUENCY	TO DETERMINE IF ANY CHANGE IN SUBSTRATE FREQUENCY IS CAUSED BY THE ENVIRONMENTAL TESTS	FUNDAMENTAL FREQUENCY-Hz				<ul style="list-style-type: none"> THE 6% DROP IN FREQUENCY REPRESENTS A SMALL RELAXATION OF SUBSTRATE TENSION AND DOES NOT SIGNIFICANTLY AFFECT PANEL PERFORMANCE 																	
			PRE TEST		POST TEST																		
	LARGE SUBSTRATE BAY	74	69																				
	SMALL SUBSTRATE BAY	78	74																				

Figure 2-5 TEST RESULTS SUMMARY

FOLDOUT FRAME

FOLDOUT FRAME 15 & 16

		1969						1970							
		J	A	S	O	N	D	J	F	M	A	M	J	J	A
Contract Article	Item														
2(c)(1)	Program Plan -----			▼											
(2)	P D , Drawings & Specs -----			▼											
(3)	Test Plan -----					▼	▼								
(4)	Monthly Financial Report -----			▼	▼	▼	▼	▼	▼	▼	▼	▼	▼	▼	
(5)	Monthly Progress Report -----			▼	▼	▼	▼	▼	▼	▼	▼	▼	▼	▼	
(6)	Quarterly Financial Report -----							▼			▼				
(7)	Semi-Annual Progress Report -----								▼						
(8)	Mid-Program Briefing -----							▼							
(9)	Final Report Draft -----													▼	
(10)	Final Report -----														▼
(11)	Final Program Briefing -----													▼	
(12)	Final Drawings, Specs, Test Rpt -----													▼	
(13)	Solar Panel -----													▼	

D2-121773-2

Figure 2-6 END ITEM DELIVERY SCHEDULE

The solar cells and coverglasses used were obtained from the LASA surplus materials. These were nominal nine percent efficient, 8 mil thick, 2 cm by 2 cm, N on P silicon cells with 3 mil thick, 2 cm by 2 cm microsheet coverglass with no filter coatings. All coverglass-cell assemblies and cell module assemblies were made using LASA fabrication techniques and processes.

The final assembly of the test panel structure, which joins the fiberglass substrate, sun side frame, and dark side frame, was accomplished without incident. Installations of the bus bars, diodes, connected and unconnected solar cell modules were accomplished without incident except for the silver mesh pigtail power leads which were difficult to handle without damaging. The complete test panel is shown in Figure 2-3.

Task 4, Test Program---The test program was generally conducted in accordance with the test plan and procedures. The tests were performed in the sequence and according to the schedule shown in Figure 2-4. Test results of major significance are tabulated in Figure 2-5.

Task 5, Reporting and Documentation---All reports and documentation were submitted under this task according to plan. The scheduled submittal of all reports and documents is given in Figure 2-6. The dates on which items were submitted are indicated by milestone markers.

2.4 CONCLUSIONS

It is concluded from the review of the detail design, fabrication methods, and test results that

- 1) Substrate tension does not decrease when exposed to high temperature (212°F) for twelve days or when exposed to extreme temperature changes at rates as high as 200°F/minute.
- 2) The panel structure is suitable for the specified static and dynamic loads.
- 3) The solar cell stack is suitable for the specified environments.

D2-121773-2

- 4) The solar module and submodule expanded silver mesh power leads are susceptible to damage in handling and test and are not suitable for the fabrication and test conditions to which they were exposed.
- 5) Three zener diodes per solar cell module are adequate.

2.5 RECOMMENDATIONS

It is recommended that

- 1) The silver mesh power leads be replaced by wires, as shown in Figure 10-1, to provide a more reliable design.
- 2) The basic light weight panel design be considered suitable for flight hardware on Mars orbiters by virtue of having met the requirements of this contract.
- 3) Composite materials having structural properties close to beryllium be investigated for replacement of the beryllium parts to reduce raw material costs.
- 4) The number of zener diodes per solar cell module be reduced from five to three to reduce weight.

2.6 SIGNIFICANT PROGRAM DEVELOPMENTS

The following items, resulting from this contract, are considered to be of major significance

- 1) Work on this contract has demonstrated that the technology developed on the Large Area Solar Array program can be used to produce smaller, light weight solar panels of about one kilowatt capacity and with a power output of 20 watts per pound.
- 2) The weight of various features of flight-configuration solar panels of the design developed on this program is compared with the weights of contemporary panels of conventional designs in Figure 2-7. The panel designs, for comparison, are

MM '71 Solar Panel---This panel is the current design for the Mariner Mars 1971 flight and the weights are based on the best estimated weight available at this time. The panel is constructed from aluminum sheet and formed sections bonded together to produce a flat aluminum surface to which a dielectric and solar cell modules are bonded. The basic structure consists of two main beams supporting an aluminum sheet stiffened by aluminum corrugations. The cells are 2 cm by 2 cm, 18 mil thick, N on P silicon solar cells with 20 mil coverglass. The assumed power output of the cell is 60 milliwatts.

Solar Panel	MM-71	MM-71 Equivalent to Light Weight Panel		Light Weight Solar Panel
Array Power at 1 Au 55°C No Degradation	910 watts	MM-71 Cells	Light Weight Cells	1,232 watts
		1,232 watts	1,232 watts	
No. and Type of Cells	17,472 2 cm x 2 cm 60 mw 18 mil Silicon 20 mil Cover	23,600 w cm x 2 cm 60 mw 18 mil Silicon 20 mil Cover	25,920 2 cm x 2 cm 55 mw 8 mil Silicon 3 mil Cover	25,920 2 cm x 2 cm 55 mw 8 mil Silicon 3 mil Cover
Array Cell Stack and Wiring	54.80 lb	 73.6 lb	23 00 lb	23.00 lb
Array Structure	57.20 lb	 78.51 lb	 84.90 lb	33.28 lb
Total Weight	112 00 lb	152 1 lb	107 90 lb	56.28 lb
Difference in Array Weight	57.72 lb	97.8 lb	51 62 lb	Zero (without zener diodes)
	43.56 lb	83 56 lb	39.46 lb	Zero (with zener diodes)



Cell Stack and Structure Weight Increased Proportional to No of Cells

Figure 2-7 WEIGHT COMPARISON

Light Weight Solar Panel---The configuration of this panel is a synthesized flight article identical to the Light weight test panel structure with the power output increased by using higher efficiency cells. Cell output assumed was 55 milliwatts per cell at 28°C at a light intensity of 140 milliwatts per square centimeter. The power of the array was calculated as 1232 watts at 55°C at a light intensity of 140 milliwatts per square centimeter. The panel structure is the typical LASA beryllium frame, fiberglass tape substrate, and titanium fittings, with all bonded construction.

MM '71 Equivalent to Light Weight---There are two synthesized flight panels compared. Both will provide the same power as the Light Weight Solar Array. Both use the typical aluminum construction used on the Mariner Mars '71 solar panels. They differ in that one uses the same solar cell stack as the Mariner Mars Solar Panel and the other uses the solar cells that are used by the Light Weight Solar Panel. There was no effort expended to redesign the panels to produce minimum weights. The weight was determined to provide comparative figures and was calculated as a direct ratio of the number of cells. The number of cells required for the thicker 18 mil Mariner Mars '71 cells was reduced by increasing the solar cell power output from 55 milliwatts used for the 8 mil cells to 60 milliwatts for the 18 mil cells.

The weight comparisons given in Figure 2-7 show that a four-panel array of the Light Weight Solar Panel Design is 51 pounds lighter than the lightest conventional design array (the MM '71 design with 8 mil solar cells).

SECTION 3.0 PROGRAM PLAN

The program plan divided the effort on this contract into five different tasks which were defined in detail, scheduled, documented, and published. This section reports the manner in which each task was accomplished in accordance with the plan and how changes to the contract were integrated into the plan. The original plan is shown in Figure 1-2. The plan was followed and all major milestones were met except where modifications were necessary to meet revisions in the work statement. Only the areas where revisions were necessary are explained in the remainder of this section.

3.1 PROGRAM TASKS

—

Changes in program tasks were accomplished with a minimum impact on the schedule.

—

The five tasks into which the work was divided are Program Plan (Task 1), Preliminary and Detail Design (Task 2), Solar Panel Manufacturing (Task 3); Testing (Task 4), and Documentation and Reports (Task 5).

Program Plan (Task 1)---Six weeks after contract go-ahead, a Program Plan, Boeing Document D2-121318-1, was submitted to JPL for approval. This plan was unchanged for the entire program except for the following revisions.

- The Preliminary Design Review (PDR) generated changes which reduced the contract work. These changes allowed the use of Large Area Solar Array (LASA) residual solar cells and coverglasses already assembled, eliminated the requirement to support the relay antenna on the panel, deleted the requirement to design and build cruise dampers, eliminated the requirement to provide the boost dampers, allowed the use of LASA residual beryllium in the panel structure, and included a Test Plan Review to be held at JPL. These changes did not require any rescheduling of significant items.
- The Test Plan Review generated four revisions in the Test Plan and contract statement of work by requiring the following additional testing four additional

power output tests, one after each significant environmental test, a zener diode test to obtain parametric data on panel voltage control when using three, four, and five zener diodes per module; a substrate frequency check after the first power output test and before the final power output test, and the substitution of a solar simulator heat source for the heated vacuum chamber in the high temperature soak test.

Preliminary and Detail Design (Task 2)---A Preliminary Design Review (PDR) was held two months after contract go-ahead. Before the PDR, minor changes had been made in the panel requirements (e.g., the attitude control jet weight had been doubled). Subsequent to the review, design requirements for cruise and boost dampers, panel deployment, equipment support, and antenna deployment were deleted or reduced.

Solar Panel Manufacturing (Task 3)---The original manufacturing schedule was revised to accelerate the delivery of the test panel by approximately three weeks. In the early part of the program, the supplier of the beryllium raw material encountered a quality control problem. As a result the beryllium was accepted in two separate lots. The last lot was delivered three weeks behind schedule, but material on hand was used for the long lead parts so that the end delivery date was not affected.

Testing (Task 4)---The program plan for testing provided a schedule for preparation of the test plan and test procedures, conduct of the tests, and reporting of the tests. The original plan was revised following the PDR and Contract Modification No. 2 to include the changes described in Section 3.2. Additional tests were scheduled following the test plan review and Contract Modification No. 3 (see Section 3.2). By using a two-shift operation, the original overall time schedule was maintained. However, revisions to the sequence of performing the tests and insertion of additional tests were accomplished with a minimum change to the plan. The revised test schedule is shown in Figure 3-1.

Documentation and Reports (Task 5)---All reports and documents were submitted as scheduled. The end item delivery schedule is shown in Figure 2-6.

No.	Test	Month	March			April				May			June		
		Day	16-20	23-26	30-3	6-10	13-17	20-24	27-1	4-8	11-15	18-22	25-29	1-5	8-12
P1	Power Output		■												
1	Frequency Check		■												
2	Modal Survey			■											
P2	Power Output			■											
3	Acoustic				■										
P3	Power Output					■									
4	Static Load					■	■								
P4	Power Output						■								
5	Random Vibration						■	■							
P5	Power Output								■						
6	Sinusoidal Vibration									■	■				
P6	Power Output										■				
7	Thermal-Vac-Shock											■	■	■	
8	Frequency Check														■
P7	Power Output														■

D2-121773-2

Figure 3-1 TEST SCHEDULE

3.2 PROGRAM CHANGES

There were four modifications to the contract. Changes are described by modifications as follows

- 1) Modification No. 1 added the Quarterly Financial Reports.
- 2) Modification No. 2 revised the following paragraphs in Article 1
 - a) Paragraph 3.3 Electrical Power This paragraph was revised to specify that nominal power output for calculations shall be 10 w/sq ft.
 - b) Paragraph 3.3.2 Solar Cell Cover The coverglass required was changed from 0.006 inch thick with a filter to 0.003 inch, 0211 microsheet with no filter.
 - c) Paragraph 3.4.1 Panel Configuration This paragraph revised the equipment support requirements by substituting JPL Drawing 23835, Rev. B, dated 2-10-70, for Attachment 1.
 - d) Paragraph 3.4.2 Attitude Control System Support This requirement was changed to increase the attitude control jet weight to 2.8 pounds from 1.4 pounds
 - e) Paragraph 3.5.5 Dynamic Requirements The analytical dynamic analysis of a single solar panel configuration was deleted. Only deployment rate limiters and dampers were required to be defined.
 - f) Paragraph 3.2.2 Torsional Loading The location of the application of the 50-pound load was changed from the corner of the panel to the unsupported tip latch point
 - g) Paragraph 3.2.1.4 Acoustic Test Requirements The overall db level was changed from 148 to 150 ± 3 db and the chart showing the required test spectrum was changed accordingly

Other changes to the program were

- a) Paragraph (b)(a)(3) The specification to use solar cells and coverglasses supplied by JPL was changed to allow the use of surplus cells and coverglasses from the LASA program
- b) Paragraph (a)(7)(c) This item, which required a test plan briefing at JPL, was added.

- c) Paragraph (b) Item (1): The specification that JPL would supply cells and coverglasses was deleted. Reference was made to the transfer of LASA residual materials, stored at Boeing, from which cells and coverglasses would be selected.
- 3) Modification No. 3 revised Article 1(a)(4) to require tests be performed in accordance with Boeing Document D2-121321-1, "Mars Mission Solar Array Test Plan," dated November 1969, and Boeing Letter No. 2-1109-3400-085, dated February 4, 1970. The following is a description of the changes which occurred in the work statement.
- a) Paragraph 5.1 Power Output Tests A change was made to perform power output tests after each environmental test and after the static load test. The power output tests were used to determine electrical degradation. Monitoring of power output during the thermal-vacuum and thermal shock test was also specified.
- b) A substrate frequency check was added after the first power output test and before the last power output test. The frequency checks compared the results of the first test with the last test to determine if there was a shift in the resonant frequencies which would indicate a change in the substrate tension.
- c) Page 24, paragraph 5.3 Thermal Shock and Voltage Limiting Test The test plan was changed to obtain parametric data on the zener diode installation with 3, 4, and 5 zener diodes per module. The zener diodes for modules 5, 9, and 10 were instrumented to provide for monitoring zener current. These modules each had one zener thermocouple. The zener diodes for modules 3, 7, and 11, were connected to external power supplies. These modules had one thermocouple per zener diode. The power supply furnished constant current, and temperatures were monitored by CRT display. Zener diode temperatures, current and voltage were recorded.
- d) Page 23, paragraph 5.2 Thermal Vacuum Test The test requirements changed to require the test to be conducted in Boeing's Vacuum Chamber A with the panel supported horizontally in the chamber in a "sun-oriented" position perpendicular to the incident radiation. The temperature of the test article was controlled by radiation to liquid nitrogen cold shrouds and by incident radiation from the solar simulator at a test pressure of 10^{-5} torr or less. The panel temperature was raised until the panel control thermocouple indicated $+212^{\circ}\text{F} \pm 3.6^{\circ}\text{F}$ by activating the solar simulator at the power level necessary to control the rate of temperature rise of the panel to a maximum of 9°F per minute.
- 4) Modification No. 4 required no changes in the work statement. This modification provided changes in negotiated price for the work changes required by Modification No. 3.

SECTION 4.0 TEST PANEL DESIGN

The design of the test panel is described in this section. The design of a flight configuration panel, similar to the test panel, is also described. The light weight solar panel installation on a Mars mission spacecraft is shown in Figure 4-1. The flight configuration panel differs from the test panel primarily in that the electrical performance predictions are based on 100% connected, flight quality, solar cells and the deployment mechanisms are not excluded from the flight configuration panel.

4.1 TEST PANEL REQUIREMENTS

—

Minor changes to the test panel requirements have been incorporated.

—

The test panel was designed to satisfy the functional and test requirements of the JPL specification entitled, "Detail Requirements for Light Weight Photovoltaic Array Structure Technology, 20 Watts/Lb," as required by the JPL Statement of Work, Article 1, JPL Contract No. 952571. The important requirements are summarized below

- 1) An approximate panel size and hinge point location was specified.
- 2) The mounting on the panel of mass-simulated equipment, as described herein, was required.
- 3) Static and dynamic requirements (detailed in Section 5.6.1) included the following frequency limitations:
 - a) Deployed---No natural frequency below 1.0 Hz.
 - b) Stowed (pin-pin)---No natural frequency below 20 Hz.

In addition, the following changes were negotiated:

- 1) Removal of the relay antenna.
- 2) Removal of the maneuver antenna.

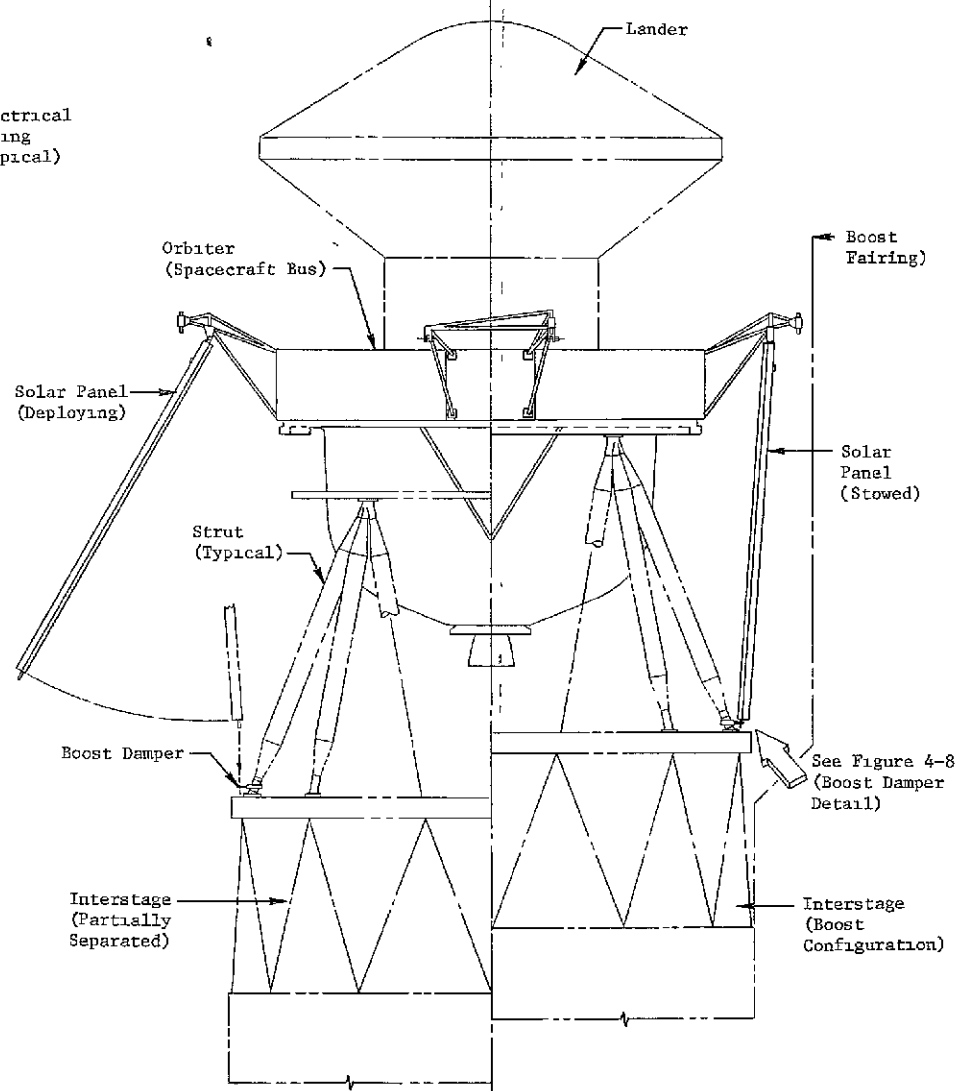
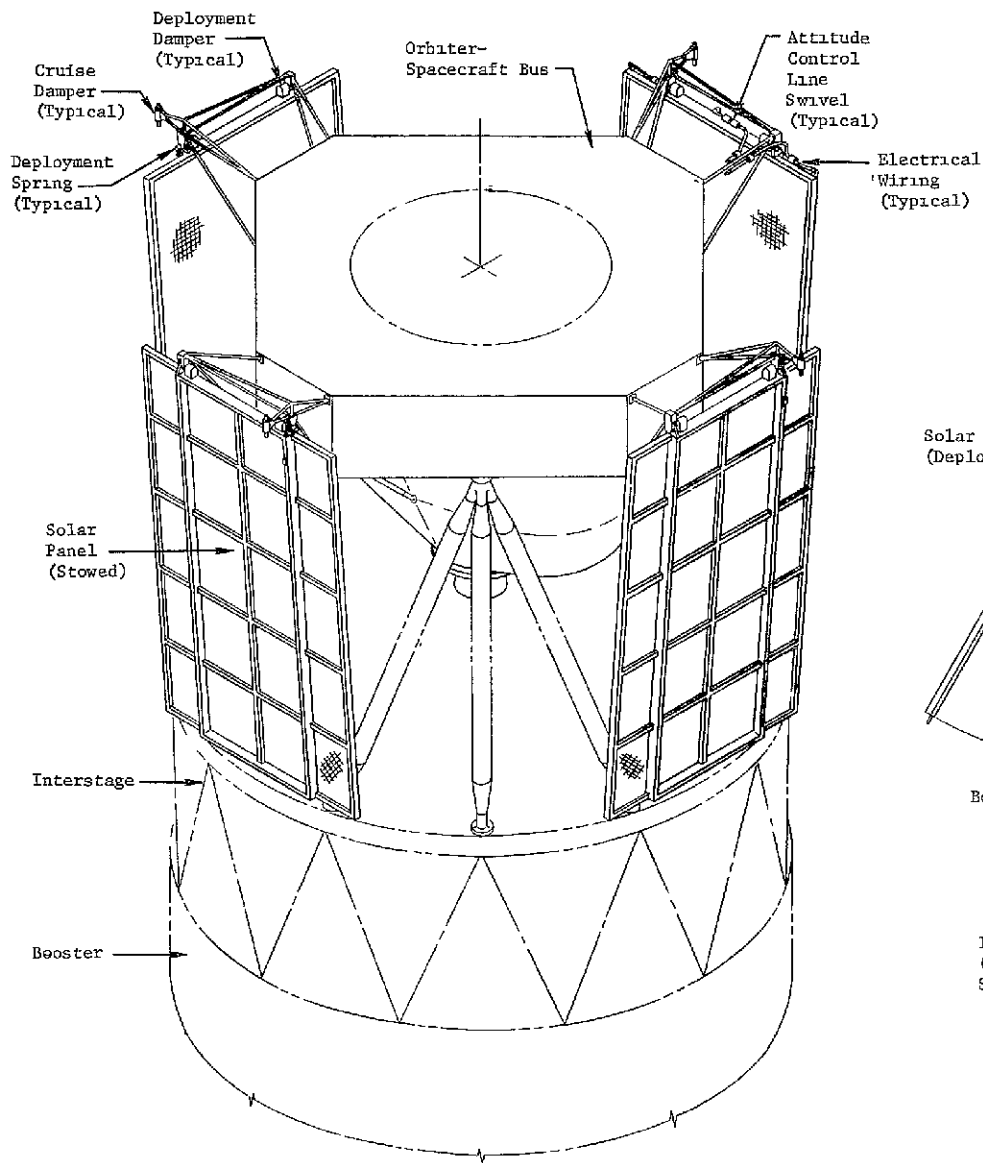


Figure 4-1 LIGHTWEIGHT SOLAR PANEL INSTALLATION

FOLDOUT FRAME (

- 3) Relocation of the mass-simulated sun sensor from the outboard corner of the panel to the outboard center of the panel.
- 4) Doubling the weight of the simulated attitude control jets to 2.8 pounds.
- 5) Increasing the acoustic test requirements from 148 db overall sound pressure level to 150 ± 3 db overall.
- 6) Changing the low frequency limit of the sinusoidal vibration test.
- 7) Substituting LASA cells and 3 mil coverglasses without interference filters for JPL-furnished cells and coverglasses.

The above changes were incorporated in the test panel design.

4.2 PRELIMINARY DESIGN

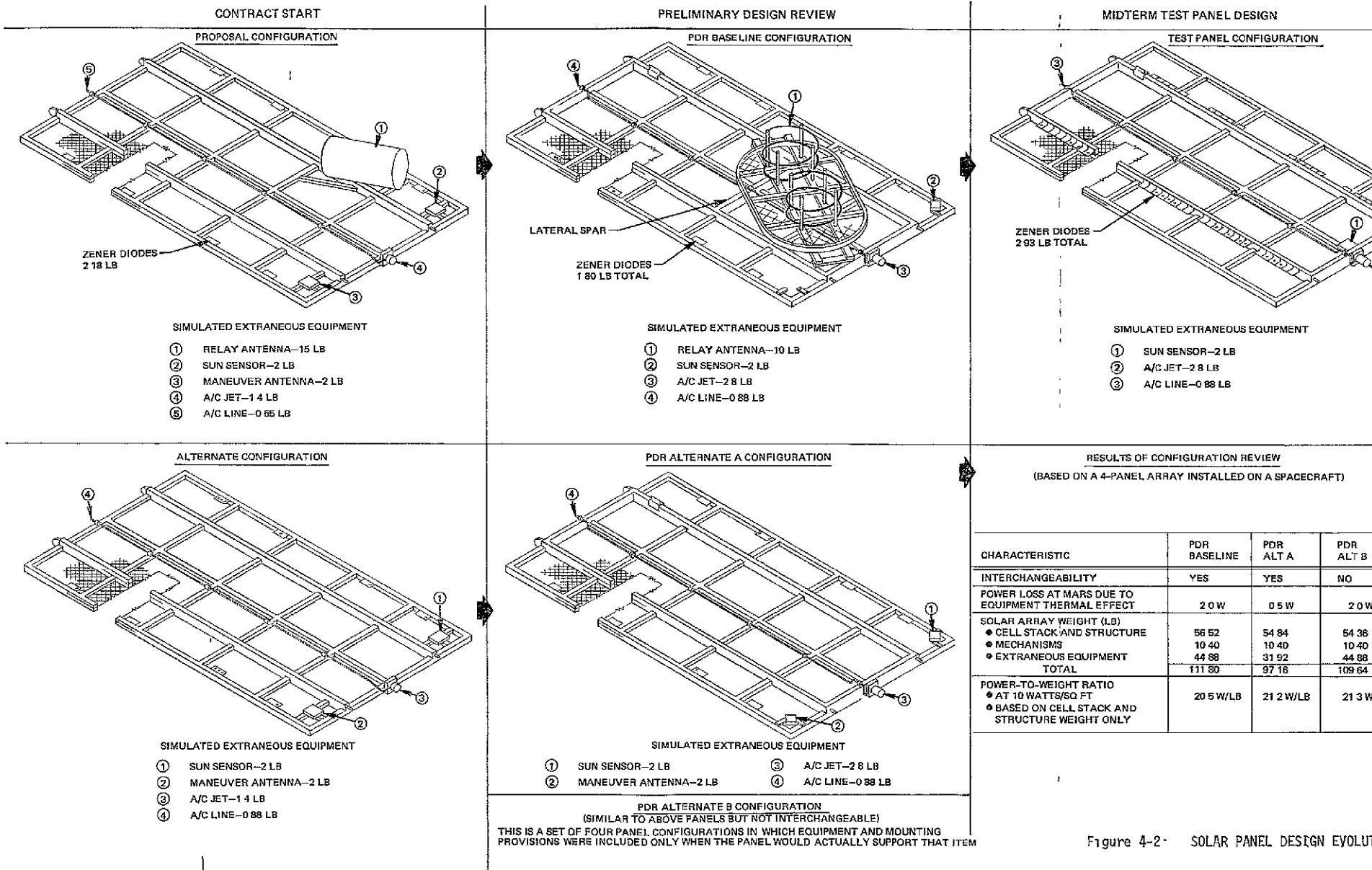
—

Minor performance penalties are incurred when extraneous equipment is mounted on a panel.

—

A preliminary design of a basic panel was made and a configuration review was conducted to evaluate the effect of mounting extraneous equipment thereon. The resulting solar panel design evolution and study results are summarized in Figure 4-2. The preliminary design effort was begun with the proposal configuration and an alternate from which the large relay antenna was omitted (see Alternate Configuration, Figure 4-2). Design coordination between Boeing and JPL resulted in revisions to the proposal configurations which were incorporated in the Preliminary Design Review (PDR) configurations shown in the center block of Figure 4-2. These configurations are the "PDR Baseline," "PDR Alternate A," and "PDR Alternate B." The primary revisions from the proposal configurations to the PDR configurations were

- 1) The structural member spacings were revised to improve the cell module arrangement and to decouple the chord bending mode.
- 2) The simulated relay antenna weight was reduced from 15 pounds to 10 pounds and the antenna mass was centered on the panel long axis to improve stowed dynamic responses.



FOLDOUT FRAME

Figure 4-2. SOLAR PANEL DESIGN EVOLUT

FOLDOUT FRAME

- 3) An idealized relay antenna model was developed to allow a more meaningful thermal and dynamic analysis. This involved producing a preliminary design of the relay antenna as shown in the PDR Baseline Configuration, Figure 4-2. Also an idealized dynamic model was assumed for the dynamic analysis.

The configuration study consisted of comparing the PDR baseline and the two alternate configurations. A comparison of the results of the configuration study shown in Figure 4-2 shows only minor penalties in weight and thermal-electrical performance when extraneous equipment was supported by the panel. However, the decision reached at the PDR was to proceed with the PDR baseline configuration design, omitting the relay antenna, the deep lateral spar, and relocating the simulated sun sensor on the longitudinal centerline. The relocation and increase in weight of the zener diodes, as shown in the test panel configuration, Figure 4-2, was the result of a decision to derate the zener diodes.

4.3 DESCRIPTION OF TEST PANEL

—

The test panel is similar in design to the Large Area Solar Array beryllium-structure subpanels.

—

The basic design of the test panel consists of the solar cell assemblies connected in submodules and bonded to a pretensioned fiberglass tape substrate grid which is supported by a beryllium structural framework. Other equipment, shown in Figure 4-3, includes electrical connections, buses, diodes, the simulated attitude control subsystem, simulated sun sensors, and mechanical elements such as the hinges and boost damper pins. This design is similar, though smaller and more rigid, to the 8' x 13' subpanel constructed by Boeing for the Large Area Solar Array (LASA) program, JPL Contract 951934 (see Figure 1-1). Much of the experience gained in the design, fabrication, and testing of the LASA panel and sample components has been directly applicable to this contract. For example, design control of the test panel manufacturing processes was achieved by using the Boeing LASA Process Document D2-113354-1.

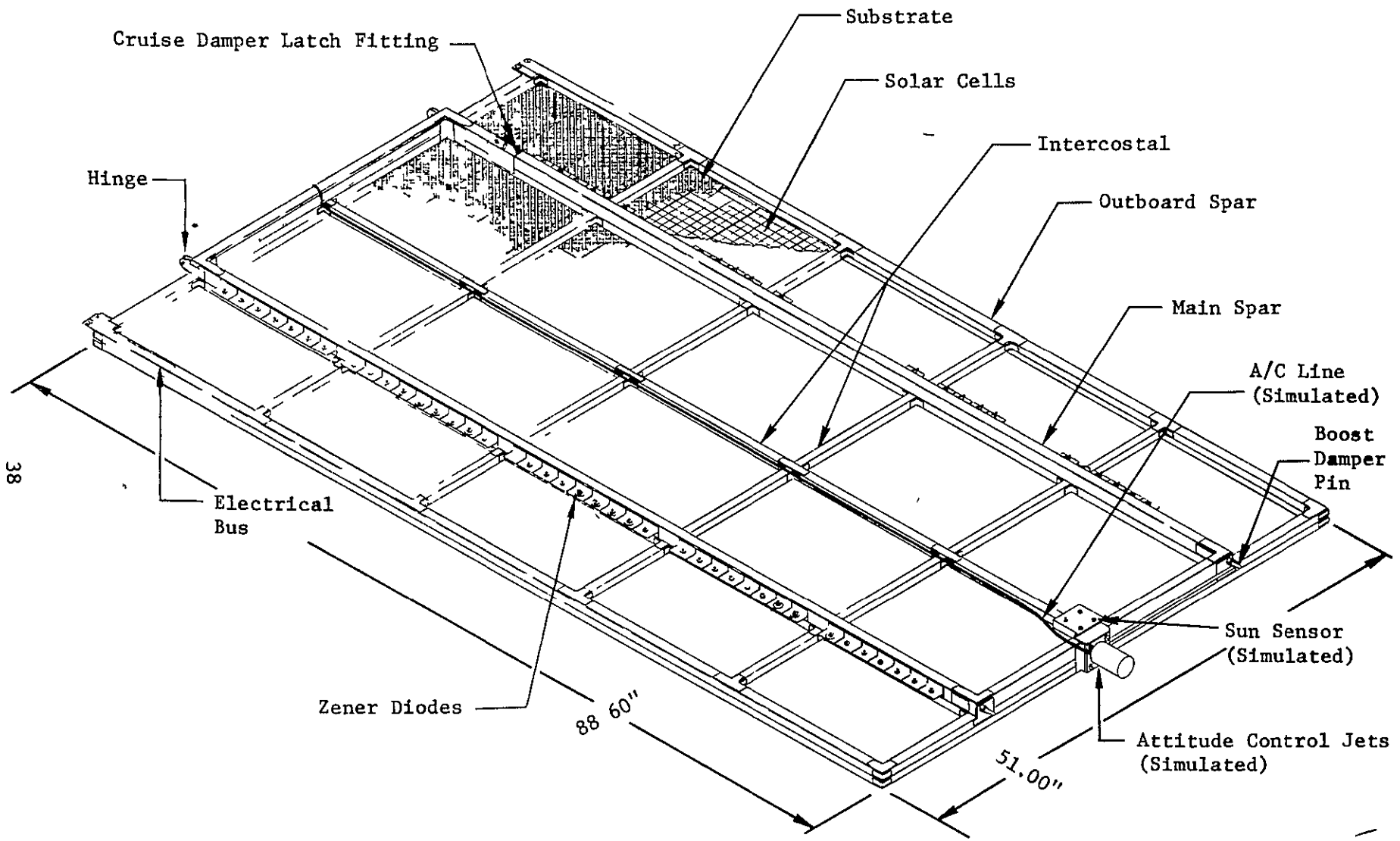


Figure 4-3 TEST PANEL ASSEMBLY

4 3.1 ELECTRICAL DESIGN

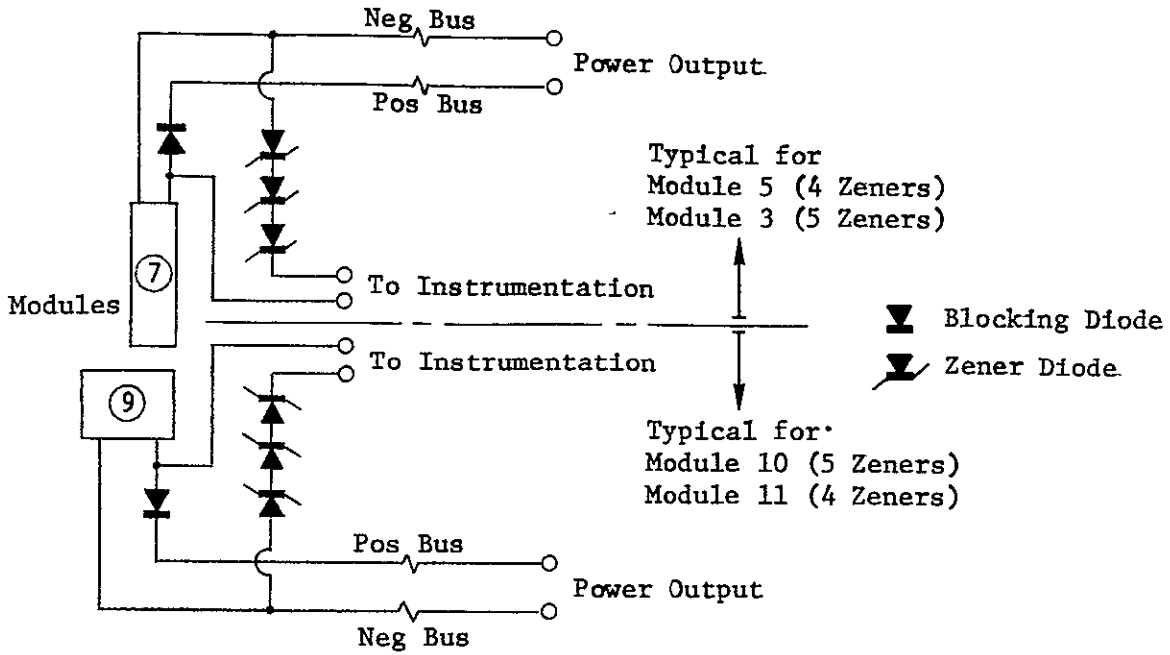
—

The light weight solar panel electrical design was derived from the LASA design with the addition of zener diodes.

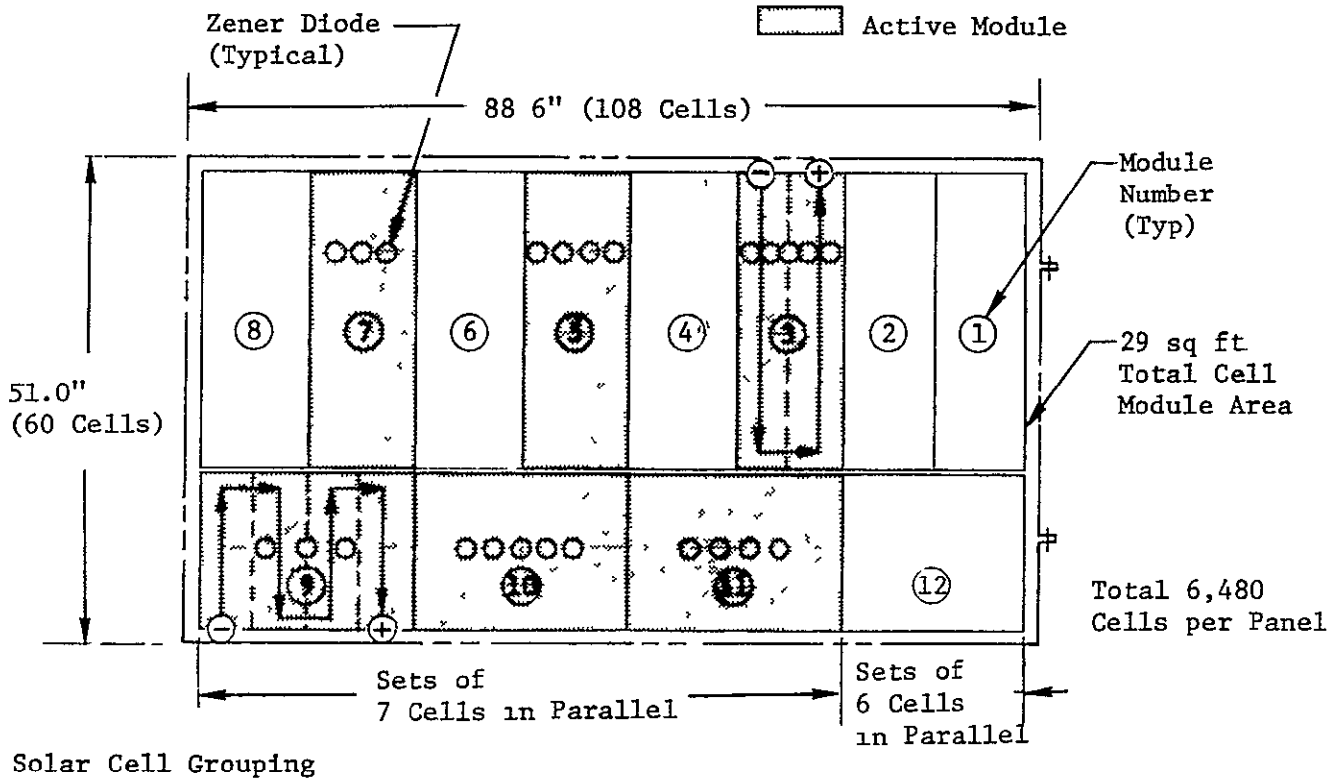
—

The electrical design includes 12 solar cell modules per panel, arranged and connected as shown in Figure 4-4. Zener diodes are used to limit the maximum voltage to 50 volts and blocking diodes are used to prevent reverse current flow. The test panel electrical installation and details of components are shown in Figure 4-5. The solar cell module buildup and installation, and the design of the buses was derived directly from the LASA design. The zener diode installation was developed for this program (the LASA panel did not include zener diodes).

Submodule Installation and Hookup---The cell stacks are bonded to the panel substrate in the form of submodules. Each submodule is 6 or 7 cells wide by 20 or 40 cells long. The cell groups of 6 or 7 cells are connected in parallel by expanded silver mesh strips which are folded and connected to the opposite contacts on the adjacent cell group to provide a series connection of 80-cell groups for each module. Connection is by means of three pairs of pulse-soldered spots per cell. The submodules are bonded to the substrate using RTV-40 (a silicone rubber compound produced by General Electric) which serves as both an adhesive and a thermal control coating on the dark side of the cells. In the bonding process, the RTV-40 is applied onto the dark side of the submodules. The sun side of the substrate is coated and the two are bonded together. The dark side of the fiberglass tape is not coated because the thermal emissivity of the fiberglass substrate tapes is about the same as the RTV-40, therefore, an additional coat of RTV-40 is unnecessary for thermal control. After bonding, the submodules are connected in series by soldering the expanded silver mesh pigtail from a submodule positive interconnect to the negative silver mesh interconnect on the adjacent submodule. Pigtails are also used to connect the modules to the buses as shown in Figure 4-5. This figure shows the positive terminal pigtail soldered to a test terminal clip. On a flight panel this pigtail would be spliced directly to the blocking diode lead. The



TEST PANEL SCHEMATIC



Solar Cell Grouping

Modules 1, 2, & 12 6 Cells per Group x 80 Groups in Series = 480 Cells per Module
 Modules 3 thru 11. 7 Cells per Group x 80 Groups in Series = 560 Cells per Module

CELL MODULE ARRANGEMENT

Figure 4-4. ELECTRICAL DESIGN

- 1 Test Connection
- 2 Flight Connection

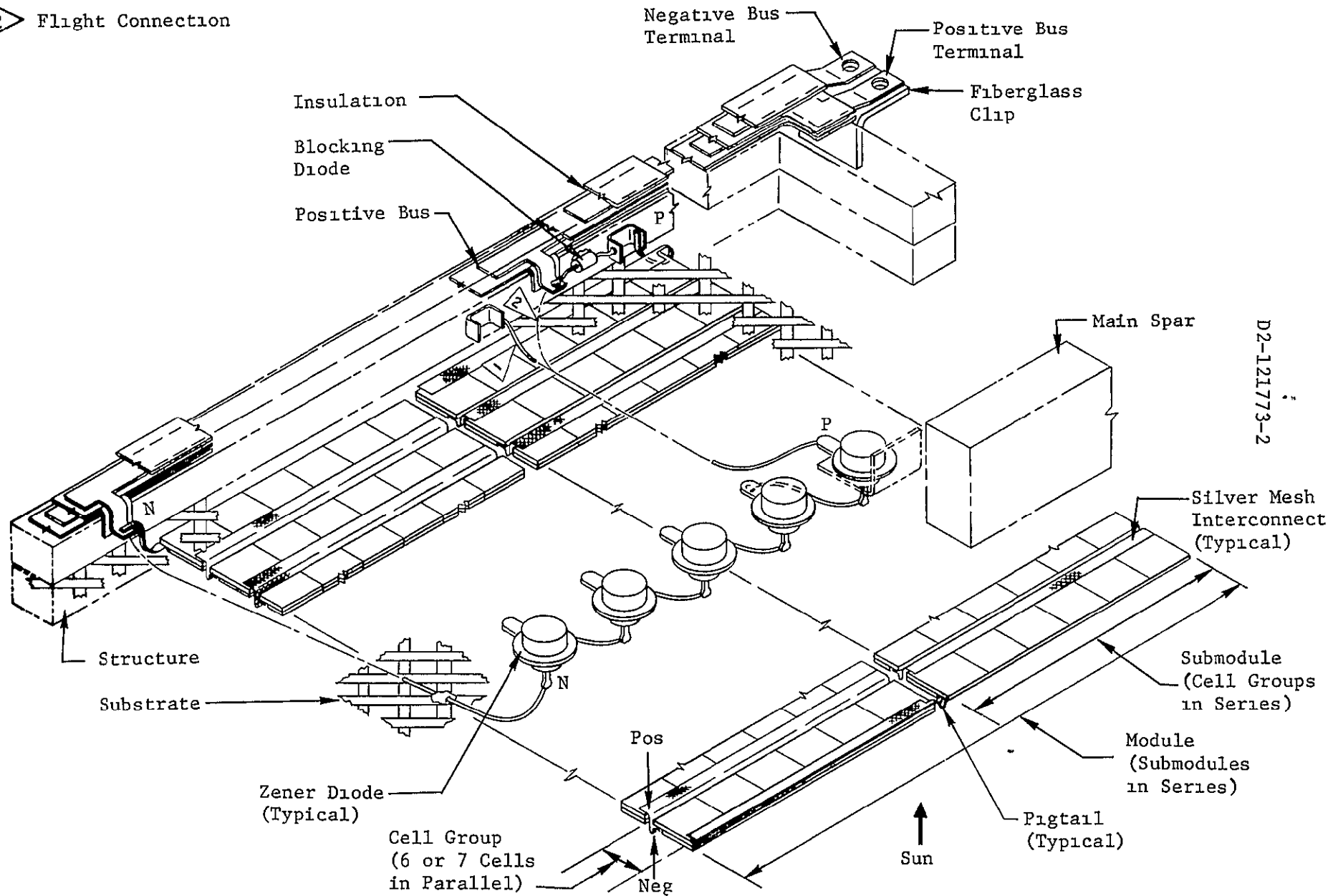


Figure 4-5 TEST PANEL ELECTRICAL INSTALLATION

pigtail feature, although used successfully on the LASA panel, was found to be subject to breakage during handling and the more severe testing on this program. A description of the failures and recommended design changes are given in Sections 6 and 10 of this report.

Zener Diode Installation---In the flight configuration, each module is electrically connected to five 10-volt zener diodes, Dickson Corporation part number IN3309B, connected in series to limit the module output to 50 volts. The test panel configuration has three 16-volt zener diodes for modules 7 and 9, four 12-volt diodes for modules 5 and 11, and five 10-volt diodes for modules 3 and 10. The test panel schematic for modules 7 and 9 is shown in Figure 4-4. The remaining diodes are mass-simulated to provide weight equivalent to five diodes for each of the twelve modules. Beryllium clips attached to the main spars with RTV-630 adhesive are used to mount the zener diodes. Each diode is on a separate clip to minimize interference with the panel structural characteristics. All faying surfaces of the zener diode assemblies are coated with RTV-40 on installation to provide maximum heat transfer to the beryllium clips which function as heat sinks. The diodes and clips are also coated with RTV-40 to improve thermal emittance. The diode leads are bonded to the panel substrate and routed to the bus or test clip connections as shown in Figure 4-5

Electrical Power Buses---The electrical power buses are integrated with the outboard spars. Bus assemblies are made from alternate layers of Kapton film (1 mil thick), thermoplastic polyester resin (1 mil thick), and copper strip (5 mils thick). The film is wider than the copper so that the conductors are completely encapsulated. The assembly is attached to the structure with RTV-630, a silicone elastomer. The inboard power terminal and bus construction is shown in Figure 4-5.

4.3.2 STRUCTURAL DESIGN

—

The beryllium structural design meets the test panel requirements and provides minimum structural weight.

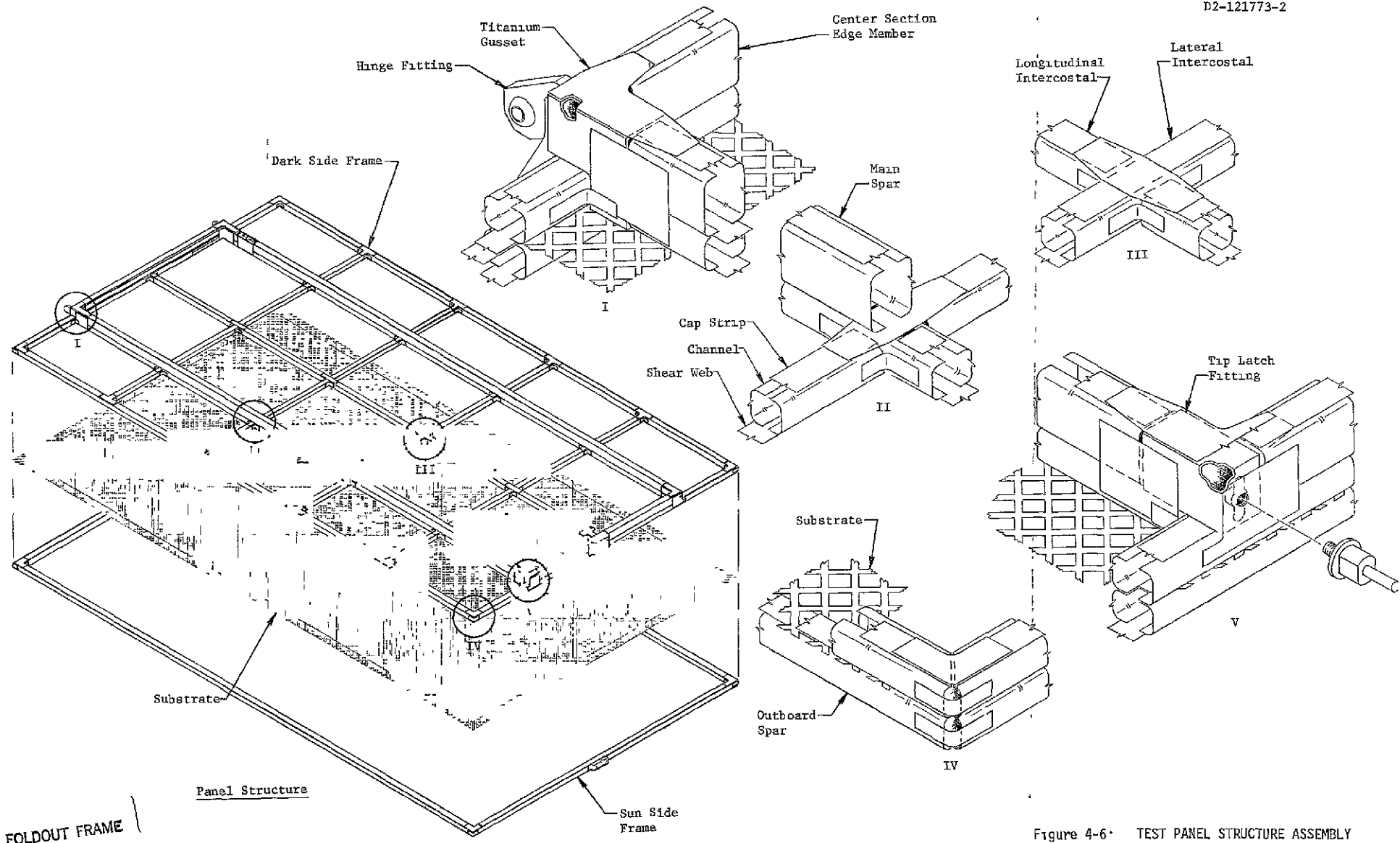
—

The structural design criteria for the test panel are contained in the Contract Work Statement, Detail Requirements for Light Weight Photovoltaic Array Structure Technology, dated November 3, 1969. Briefly summarized, they include the following

- 1) In the pin-pin condition the panel shall withstand an 8 g load normal to its surface without yielding.
- 2) Supported at 3 points, the panel shall be subjected to a 50-pound load at the unsupported fitting.
- 3) The panel in all configurations shall be capable of withstanding a 1 g field.
- 4) In the pin-pin condition, there shall be no natural frequency under 20 Hz.

A more detailed discussion of static and dynamic structural criteria is given in Section 5.0.

The test panel structural design consists of a pretensioned fiberglass tape substrate sandwiched between sun side and dark side bonded beryllium frames as shown in Figure 4-6. The frame assembly is rectangular in plan view. The dark side frame includes outboard spars and edge members which form the perimeter of the frame, two longitudinal main spars, a center longitudinal intercostal, and lateral intercostals. The sun side frame consists only of perimeter members. All primary structural bonding, including the beryllium spars and intercostals and the final frame-to-substrate-to-frame bond, is accomplished with AF-126 (Boeing Specification BMS 5-51) adhesive which is a modified epoxy film supported with dacron fibers. This adhesive is the same as that used on the LASA panel except that a liquid primer (Boeing Specification BMS 5-89) is used in place of EC 2370 (3M Co.) primer. Titanium is used at concentrated load points and joints between structural components where titanium is more



FOLDOUT FRAME

Figure 4-6. TEST PANEL STRUCTURE ASSEMBLY

suitable, because of its toughness, high strength-to-weight ratio, and thermal coefficient of expansion. Machined fittings are held to a minimum to reduce costs. Electrical discharge machined titanium fittings are used for the spacecraft attachment hinges, and the tip latch fittings, which support the tip latch pins. All structural connections are made by adhesive bonding to reduce stress concentrations. Titanium shear clips, gussets, and splices are used at panel joints as illustrated in Figure 4-6.

The solar cell adhesive (RTV-40) between the solar cells and the fiberglass substrate is used as a thermal control coating on the dark side of the cells. However, the dark side of the substrate is not coated with RTV-40. The RTV-40 thermal control coating is also used on the exposed surfaces of the sun side structural frame.

All spars and intercostals are fabricated from powder-derived beryllium sheet which was purchased to Boeing Specification BMS 7-183. The basic cross section of any member consists of two hot-creep formed channel sections attached by a top cap strip and bottom shear web. Figure 4-7 shows structural member properties of the beryllium members in a cross section of the test panel.

The fiberglass tape substrate, to which the solar cells are bonded, is positioned at 45 degrees to the edge members to provide additional in-plane shear stiffness. The tapes are pretensioned to a final average value of 6.82 pounds per tape which is equivalent to an average load on the frame edge members of 12 pounds per lineal inch. Stress calculations for the beryllium members include this static load in the combined stress totals. Due to the differential thermal expansion between the tapes and the beryllium frame, the tapes are initially tensioned to 9.77 pounds per tape in the tension frame during the final bond cycle in order to achieve the final value of 6.82 pounds after cool down. In order to verify the calculated final tape pretension load, a long duration (12 days) tension creep test of a tape specimen was performed at 212°F. Test results showed that permanent tape elongation and adhesive creep could be neglected. This test increases the confidence level of the tape pretension values used in the dynamic analysis.

ADHESIVE

BERYLLIUM MEMBER THICKNESSES
CHANNELS 0.015 INCH (TYPICAL)
CAP STRIPS AND SHEAR WEBS, 0.010 INCH TO 0.020 INCH

87

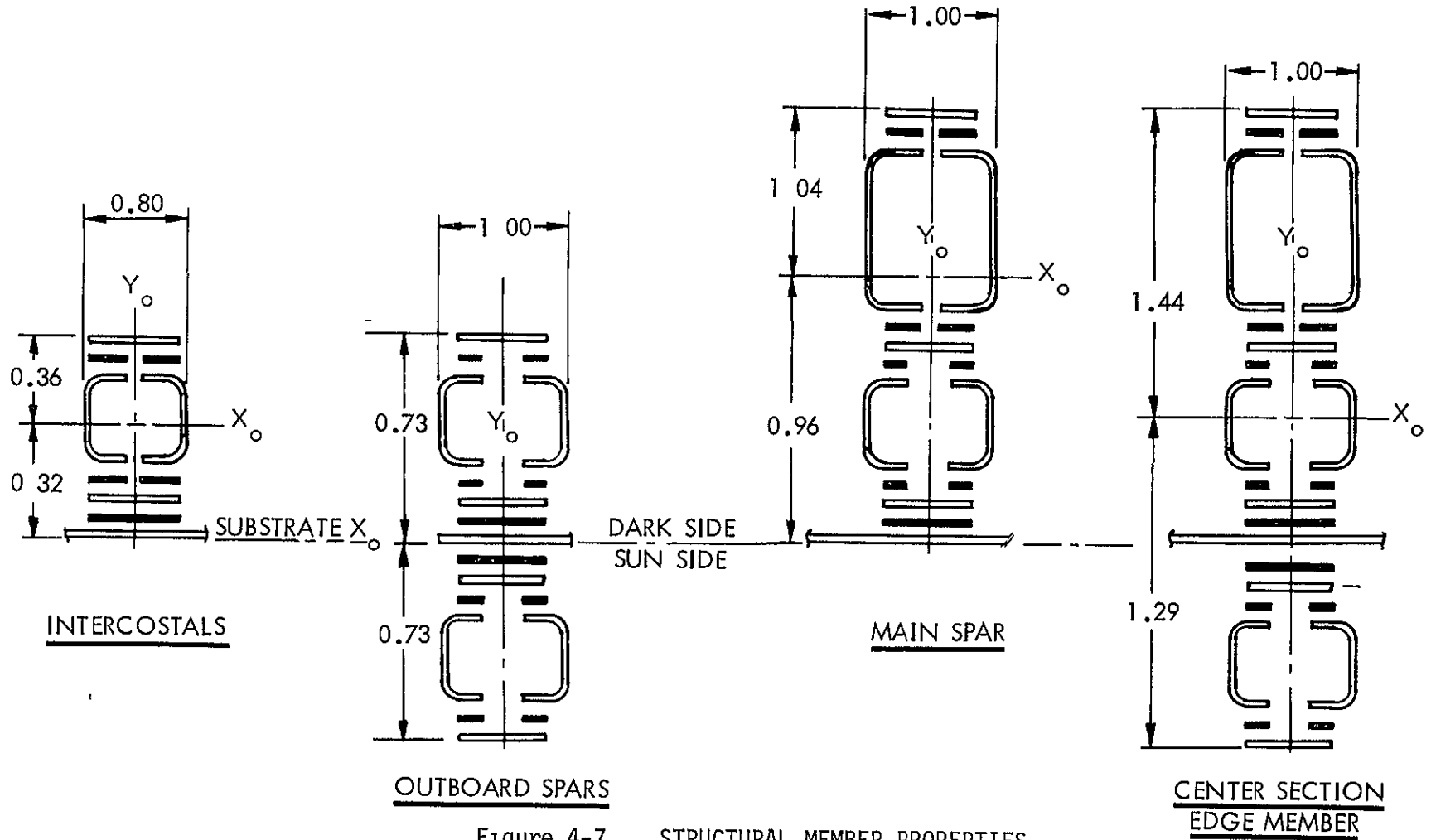


Figure 4-7 STRUCTURAL MEMBER PROPERTIES

D2-121773-2

The following mass-simulated equipment is mounted to the structure

- 1) Cruise Latch---No attempt has been made to simulate the actual latch hardware except for the weight allowance and weight distribution on the panel structure. The simulated cruise latch is machined from mild steel as a cylinder with mounting tabs attaching it to two titanium brackets bonded to the main spar.
- 2) Sun Sensor---This item is simulated by a block of steel. It is attached to the test panel by bolting to titanium clips bonded to the panel structure.
- 3) Attitude Control Equipment---The weight of the dual attitude control jets is simulated by a steel cylinder with mounting flanges. The 2.8-pound cylinder is shaped to provide the assumed correct center of gravity distance from the titanium mounting bracket bonded to the panel structure. The attitude control tubing is simulated by a stainless steel tube clamped at several locations along the center longitudinal intercostal. There was no attempt to install electrical control circuit simulation or tubing swivel joint simulation at the deployment centerline.

The estimated weights of major elements of the test panel are summarized below. A detailed breakdown of calculated and actual weights is given in Section 5.2.1.

TEST PANEL ESTIMATED WEIGHT

Item	Weight	
Structure	8.32 lb.	
Cell Stack and Buses	<u>5.75 lb</u>	
Subtotal (Basic Panel)		14.07 lb.
Diode Installation	3.04 lb.	
Simulated Equipment	5.82 lb.	
Panel Mechanisms	<u>.07 lb</u>	
Total		23.00 lb.

4.3.3 MECHANICAL DESIGN

—

Deployment equipment and boost damper components have been defined.

—

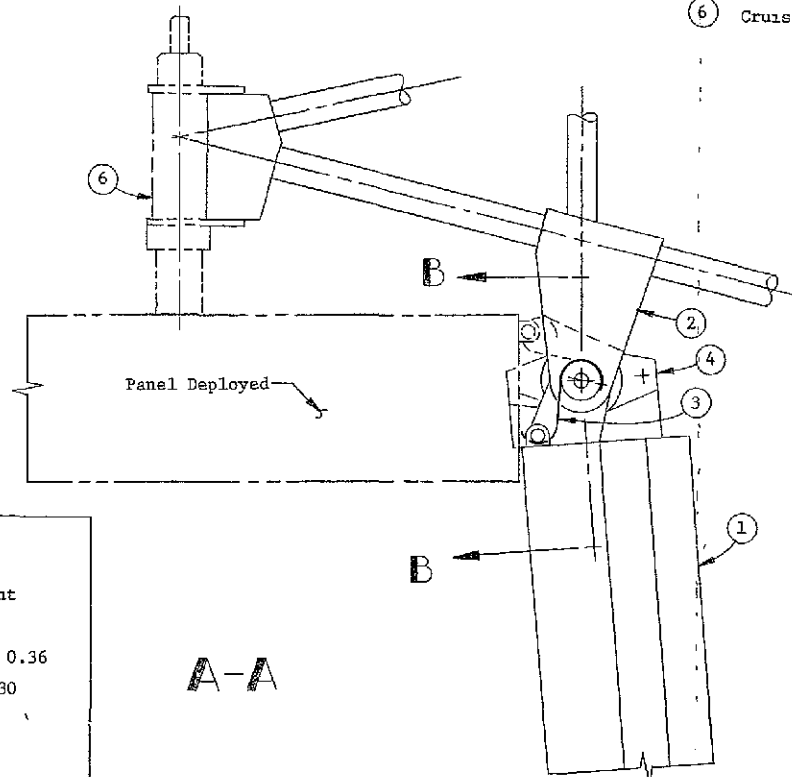
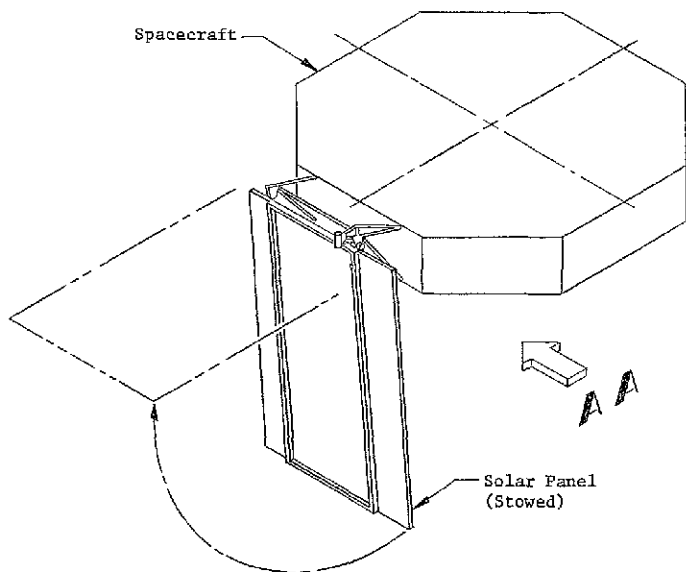
Deployment Equipment---Design has been performed in sufficient depth to support the analysis and selection of deployment equipment described in Section 5.4.2 of this report. The deployment equipment defined is shown in Figure 4-8. This equipment includes.

- 1) Deployment Spring---A constant-force Negator type RW (reverse wound) spring.
- 2) Rotary Dampers---Sesco Manufacturing, Inc., part number 1025-800 or equivalent, one at each hinge, two per panel.
- 3) Roller---This device consists of a pin and a sleeve on which the spring winds to provide a deploying moment. The sleeve is of a self-lubricating material such as Teflon or Fabroid and rotates on the pin to reduce friction as the spring winds.
- 4) Bearings---The panel-to-spacecraft hinge bearings are a self-aligning monoball type. Faying surfaces of the aluminum balls and the bearing races are coated with a baked-on molybdenum disulfide type space lubricant. In any flight installation, as in the test installation, one bearing will be mounted to resist all shear forces while the opposite bearing will provide end play to accommodate manufacturing tolerances and thermal expansion differences.

The first three items above were carried through the design phase only and were not included on the test panel.

Boost Dampers---The flight installation of the boost dampers is shown in Figure 4-9. Dampers of the Mariner Venus (MV) 1967 type were used in this installation for the vibration tests of the test panel. These dampers feature silicone oil as the damping fluid. The oil is worked in shear in the radial clearance between two concentric tubes. The damping fluid is trapped between "O" rings at each end of the cylinder.

Tests of several dampers were performed to verify suitability and to select two dampers for use on the test panel. As a result of these tests and related analysis, discussed in Section 5.4.3, the two selected dampers were modified as follows:



- ① Solar Panel
- ② Hinge Fitting - Spacecraft
- ③ Spring - Negator Type "RW"
- ④ Rotary Damper (One at Each Hinge)
- ⑤ Roller
- ⑥ Cruise Damper (REF)

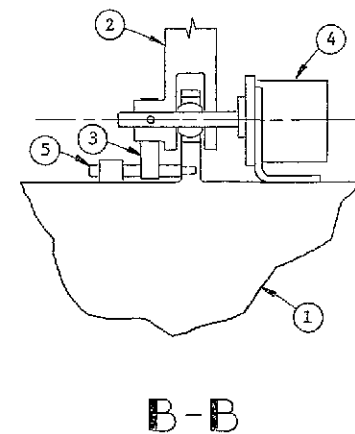
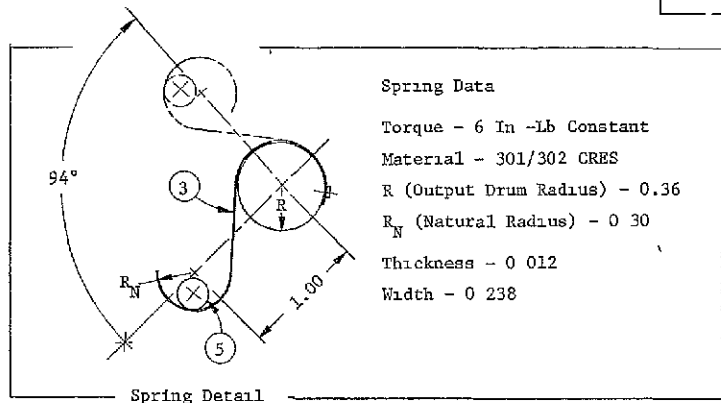


Figure 4-8 DEPLOYMENT EQUIPMENT

FOLDOUT FRAME

51 & 52

FOLDOUT FRAME 2

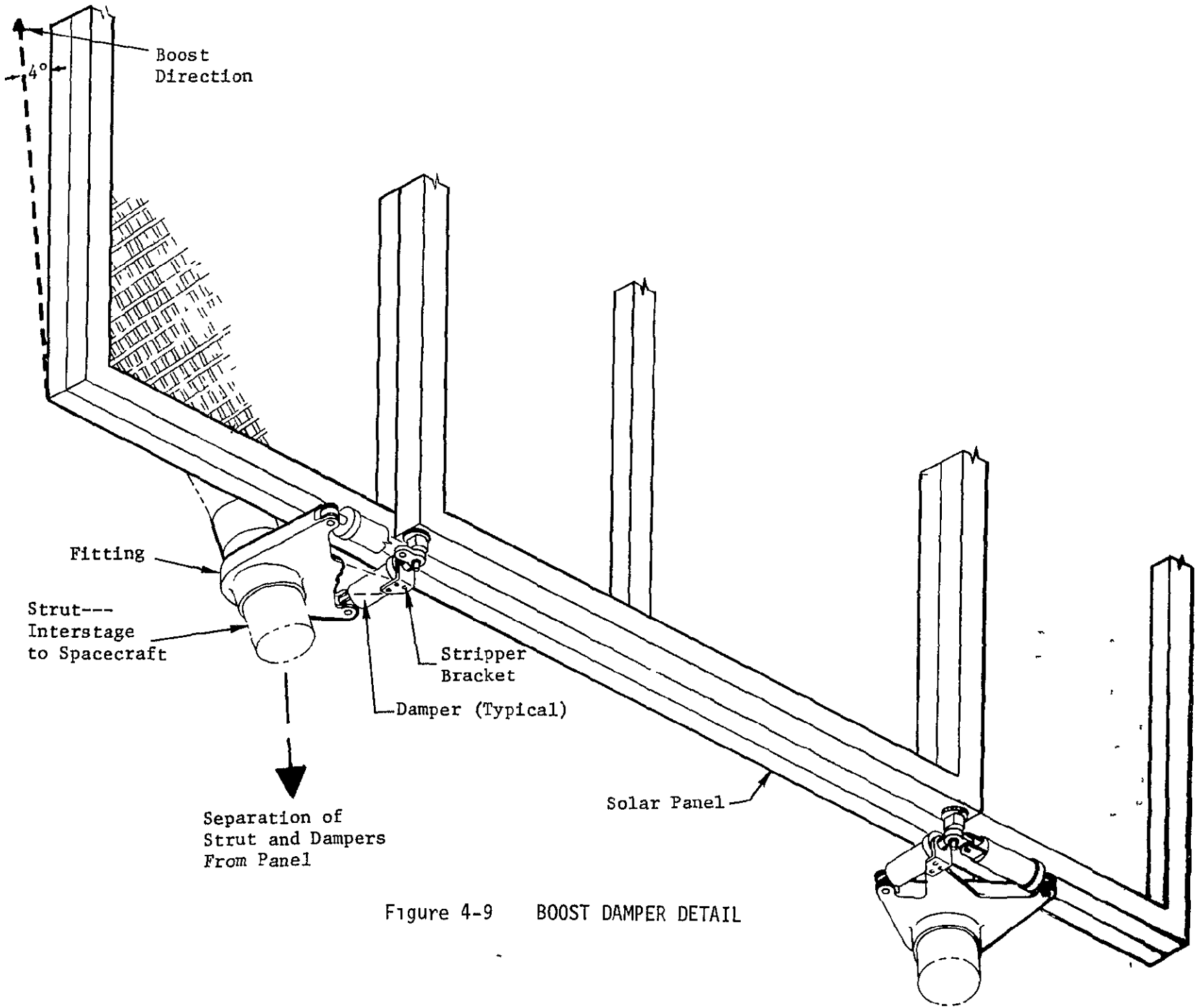


Figure 4-9 BOOST DAMPER DETAIL

53

D2-121773-2

D2-121773-2

- 1) Two of the four "O" rings were removed from each damper piston and 30,000 centistoke silicone oil was selected for use in the dampers. This was done to reduce breakaway forces or "stiction."
- 2) The centering springs were ground to a shorter length and spacers were added to increase the spring rate from 20 lbs/inch to about 33 lbs/inch.

SECTION 5.0: DESIGN ANALYSIS

Analyses have been performed as described herein to verify that the Light Weight Solar Panel meets the specified requirements, to provide detailed test requirements, and to predict the performance of the test panel configuration and of a flight-suitable panel of comparable configuration.

5.1 BACKGROUND

—

Iterations of the analyses performed on configuration variations expedited the test panel design evolution.

—

Major areas of effort described in this section include the power output analysis, the dynamic and stress analysis, and the mechanical analysis. The power output analysis, which included the thermal/electrical predictions of panel performance and the weight calculations to determine specific power output, were performed initially for the proposal configuration and were performed in more detail for the PDR configurations and the test panel configuration. A major constraint on the dynamic and stress analyses was to provide an adequate definition of the beryllium members in the first two months to allow procurement of beryllium material commensurate with fabrication schedules. Additional effort included the evaluation of stress and dynamic characteristics of the PDR configurations, with and without the 10-pound relay antenna and the deep lateral spar, and the refinements of the original analyses to predict test panel performance and determine test requirements. Mechanical analyses were performed to define deployment equipment and to select the boost damper configuration for dynamic testing.

5.2 POWER OUTPUT ANALYSES

The specific power output goal of 20 watts per pound, based on 10 watts/square foot, and the weights of the solar cell stack, structure and electrical buses, was achieved.

A goal of the light weight solar panel design was to provide 20 watts of electrical power output per pound of panel weight at one A.U., 55°C, and with a solar intensity of 140 mW/cm². Based on 10 watts per square foot and a total solar array cell area of 116 square feet, the predicted output for the flight configuration is 1160 watts, and the required cell efficiency is 9.6%. The final predicted weight of a four-panel array is 56.28 pounds without zener diodes, 68.44 pounds with five zener diodes per module, and 63.53 pounds with three zener diodes per module. The resulting power-to-weight ratios, excluding mechanisms and extraneous equipment and assuming a solar cell efficiency of 9.6% are:

20.6 watts per pound without zener diodes

17.0 watts per pound with 5 zener diodes per module

18.2 watts per pound with 3 zener diodes per module

The power output analysis results based on the contract specified 10 watts per square foot, are summarized graphically in Figure 5-1, which includes the proposal and PDR baseline configurations for comparison. The power output of a four-panel array was also analyzed to determine the effects of degradation factors and higher efficiency cells that might apply in space. The results are shown in Figure 5-2. The measured test panel output normalized to 1 A.U. and 55°C, is plotted to show that by using more efficient cells than used on the test, the panel will produce more than 10 watts per sq. ft. The predicted values are calculated by using measured cell outputs of the same production lot as the cells used on the panel. The cell efficiency is 8.86% as determined by measurement of the cell output at 28°C and 140 mW/cm². This value is determined by

$$\text{Efficiency } \eta = \frac{P_M}{A_S} = \frac{\text{Maximum Cell Output}}{\text{Active Cell Area} \times \text{Solar Intensity}}$$

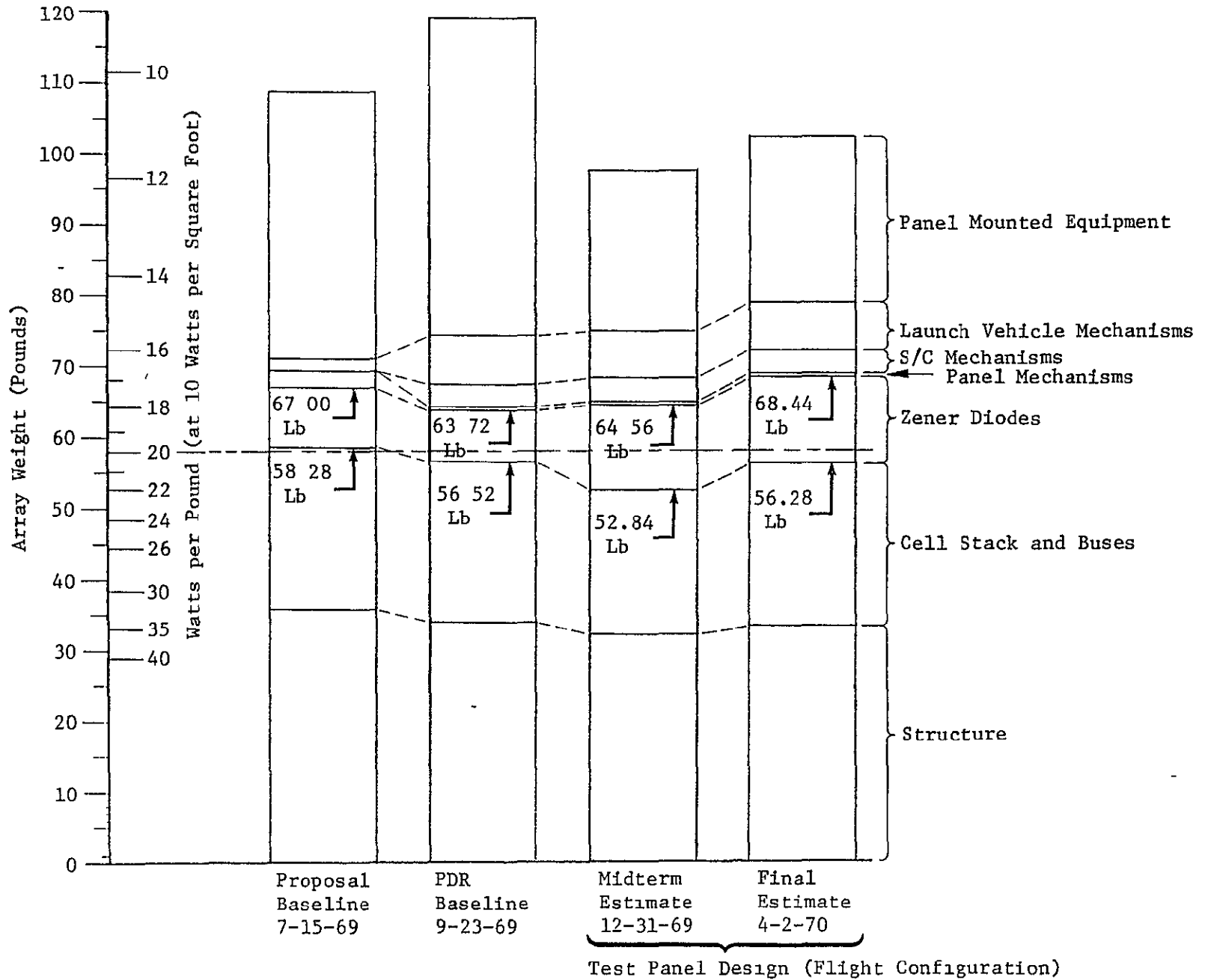


Figure 5-1 POWER-TO-WEIGHT COMPARISON

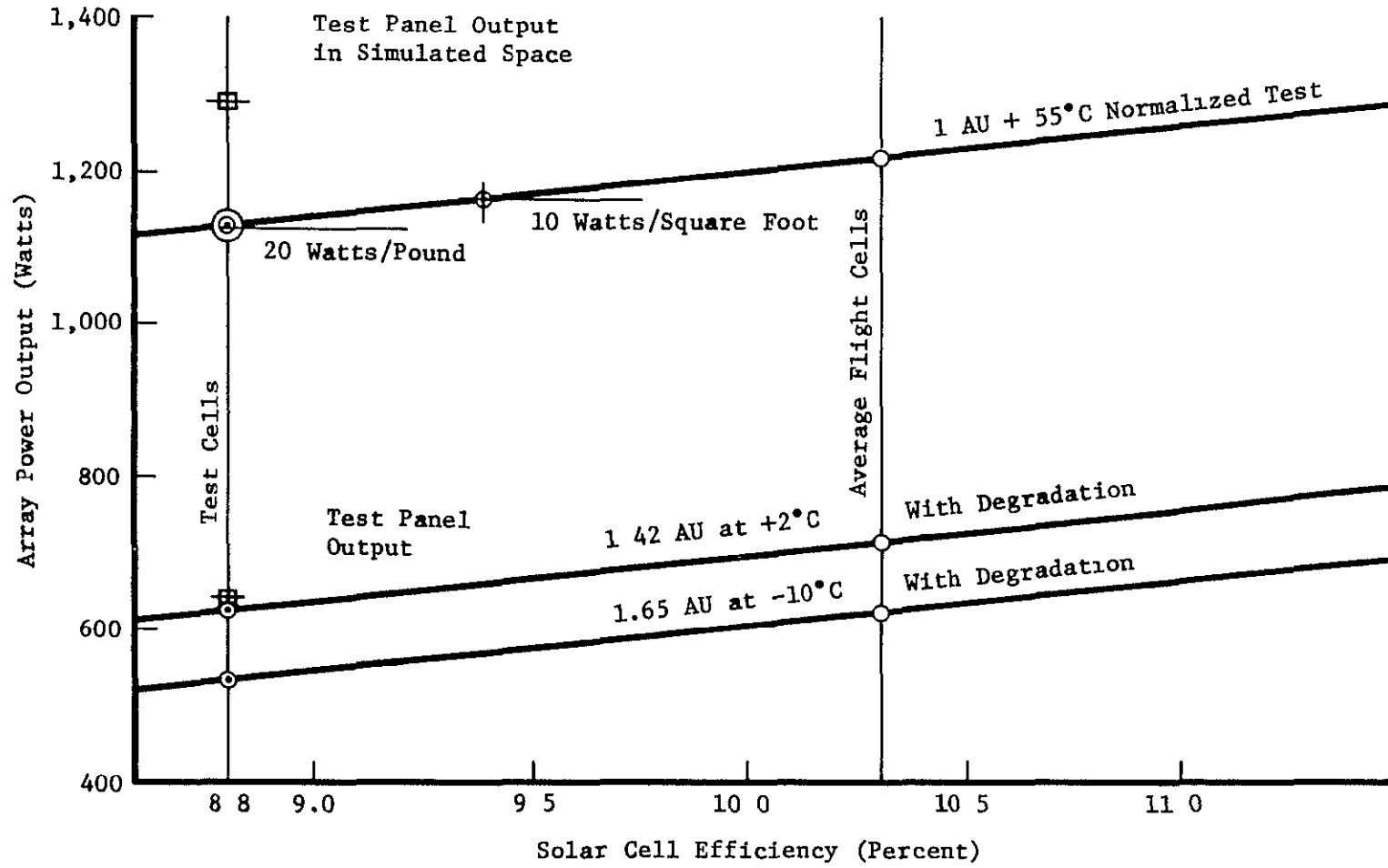


Figure 5-2 PREDICTED ARRAY SPACE PERFORMANCE

The output of the 560-cell test modules were calculated from the average output of the solar cells used for the modules. The following formula was used:

$$P_{MOD} = (N) (P_{cell}) (K)$$

- Where:
- P_{MOD} = Module maximum power
 - N = Number of cells per module
 - P_{cell} = Average power output of the cells at 1 A.U., 55°C and 140 mW/cm²
 - K = $K_1 \times K_2 \times K_3$ degradation factors as follows:
 - K_1 = Coverglass loss 0.97
 - K_2 = Radiation degradation 0.97
 - K_3 = Seasonal solar intensity variation, spectral response deviations, and standard cell calibration error and process degradation = 0.96

The predicted module power output for the 560-cell modules on the test panel at one A.U. with no radiation factor but a degradation factor of 0.931, is 21.4 watts at 55°C and 140 mW/cm² for the 8.86% cell. The power output of the panel can be obtained by multiplying the output of a 560-cell module by the equivalent number of modules per panel, or 11.57. The total panel power output is 248 watts or 992 watts per array.

The power output can be calculated for space conditions of 1.42 A.U. at a panel temperature of + 2°C and for 1.65 A.U. at a panel temperature of -10°C. The results of the calculations are plotted for cell efficiencies from 8.75 to 12.00 percent in Figure 5-2.

The power output of the test modules were averaged and normalized to 55°C, 140 mW/cm², and plotted for comparison with the predicted.

5.3 WEIGHT ANALYSIS

—
The weight of the basic panel (structure, cell stack, and wiring) is 14.07 pounds.
—

The weights given in Figure 5-1 were calculated for a flight configuration panel of the test panel design. The final estimate of the total panel weight is 1.11 pounds greater than the total given in the mid-term report because of adjustments based on the actual weight of the test panel components. A detailed weight summary of the mid-term and final estimates and the test panel actual weights is given in Table 5-1. The increase in the basic panel weight, on which power output figures are based, is 0.97 pounds. The remaining 0.4 pound increase is in the clips, clamps, and fasteners used for the mass-simulated attitude control equipment.

The column in Table 5-1 labeled "Test Panel Actual" consists of actual weight test data for components of the test panel or for identical components from the LASA program. Where weight tests were not made, the detailed weights are noted as being estimated. The total of this column varied from the measured weight of the completed test panel by 0.33 pounds. The most probable source of this variance is the sum of the estimated weights: about 5.41 pounds. These weights include thermal coatings, wires, and miscellaneous parts and are generally of an unestablished accuracy. An average error in these items of 6% would account for the weight to absorb the 0.33 pound discrepancy. The remaining 4.81 pounds of items estimated from LASA data are unchanged from their LASA counterparts and errors in excess of 1% are unlikely.

Error trends for this program were much the same as the LASA program. Formed structural parts were typically lighter and machined parts typically heavier than predicted. No verification was obtained for the weights of certain coatings, wires, and small parts, partly because the fabrication sequence did not allow individual weight tests. Weight of such components has a tendency to increase because small items which appear on the product escape detection on preliminary drawings which are used for

TABLE 5-1
TEST PANEL WEIGHT SUMMARY

	<u>Mid-Term Estimate (Lbs)</u>	<u>Final Estimate (Lbs)</u>	<u>Test Panel Actual (Lbs)</u>
<u>CELL STACK & BUSES (TOTAL)</u>	(5.15)	(5.75)	(5.75)
Solar Cells, 6480, 2cm x 2cm, 8mil thick	2.49	2.49	2.49 L
Coverglasses, 3 mil microsheet, 2cm x 2cm	.91	1.02	1.02 L
Cell Adhesive	.30	.30	.30 L
Coverglass Adhesive	.12	.12	.12 L
Solder and Connectors	.38	.42	.42 L
Buses and Terminals	.45	.60	.60 E
Thermal Coating	.50	.80	.80 E
<u>PANEL STRUCTURE (TOTAL)</u>	(8.06)	(8.32)	(8.30)
Main Spars	1.68	1.68	1.66
Outboard Spars	1.56	1.54	1.40
End Members	1.21	1.21	1.20
Lateral Intercostals	.76	.76	.70
Longitudinal Intercostals	.34	.34	.33
Substrate	.46	.46	.46 L
Clips, Splices, Gussets	.68	.73	.75
Thermal Coating	.35	.38	.38 E
Fittings	.68	.68	.88
Miscellaneous	.34	.54	.54 E
<u>SUBTOTAL (STRUCTURAL & ELECTRICAL)</u>	<u>(13.21)</u>	<u>(14.07)</u>	<u>(14.05)</u>
<u>DIODE INSTALLATION (TOTAL)</u>	(2.93)	(3.04)	(3.05)
Zener Diodes	2.45	2.45	2.45
Mounting Strips	.48	.59	.60
<u>ATTITUDE CONTROL (Simulated)</u>	(3.68)	(3.82)	(3.85)
R/C Jets	2.80	2.80	2.83
Tubing Installation	.88	1.02	1.02 E
<u>PANEL MECHANISMS</u>	.07	.07	.07
<u>SUN SENSOR</u>	(2.00)	(2.00)	(2.00) E
<u>TOTAL</u>	<u>21.89</u>	<u>23.00</u>	23.02
Variance between predicted and measured (1.43%)	-----	-----	<u>+ .33</u>
Measured Total	-----	-----	<u>23.35</u>

L = LASA Weight Test Data Used
E = Estimated

pre-manufacturing weight estimates. This explains a part of the increase from the mid-term to the final weight estimate.

The center of gravity location was determined by measurement of the test panel shown in Figure 4-3 and is as follows:

Longitudinal datum:	53.4 inches from the hinge centerline
Lateral datum:	24.9 inches from the outer edge of the outboard spar adjacent to modules 1 through 8

This includes all dummy masses. The center of gravity is 0.6 inch off the longitudinal centerline (because of the off-center distribution of the zener diodes) and nearer the outboard end of the panel.

5.4 VOLTAGE CONTROL ANALYSIS

Panel power and voltage requirements can be achieved for the flight configuration with twelve solar cell modules, each with 80-cell groups in series and five zener diodes.

Power and voltage data for given cell temperatures were obtained from the curves published by E. L. Ralph, "Performance of Very Thin Silicon Solar Cells," (ref. 7). The cell, defined by Boeing Specification 20A22514, used in this analysis, provides 0.0475 watts at the contract-specified 140 mW/cm^2 intensity and 55°C temperature. A total of 6480 such cells per panel provides about 308 watts with a gross cell module area of about 29 square feet, resulting in 10.6 watts per square foot, more than the required 10 watts per square foot. The ratio of cell module area to gross panel area (29 square feet to 31.4 square feet) is greater than 92-1/2%. The design goal was 93% or greater, which could be attained by reducing the outer member width and increasing the weight.

Twelve modules, each with 80-cell groups in series was used to obtain an optimum cell module and structure packaging arrangement. This arrangement provides 33.6 volts near Earth and 46.4 volts near Mars. The application of zener diodes to overvoltage

protection was analyzed. Two cases were considered: (1) a spacecraft emerging from behind Mars at 1.62 A.U. after orbit occultation, and (2) near-Earth maneuvers where the array may be off-sun for up to 90 minutes. The near-Earth condition was found to be the most severe with the cell temperature as low as -198°C and a worst-condition module output of 42.5 watts, without considering cell warm-up characteristics. The wattage per diode for 3, 4, 5, and 6 zener diodes per module are:

<u>Zener Diodes Per Module</u>	<u>Watts per Diode</u>
3	14.2
4	10.6
5	8.5
6	7.1

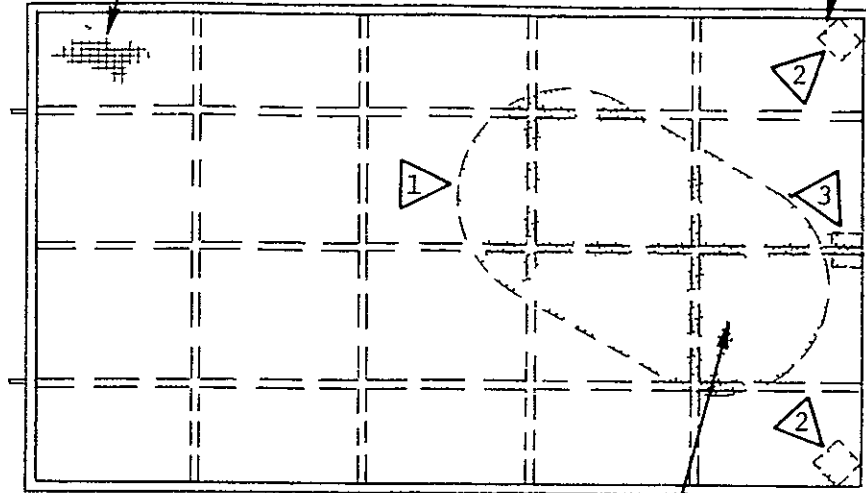
Assuming zener diodes rated at 50 watts and a conservative rated power to dissipated power ratio of 4 to 1, each zener can accommodate up to 12.5 watts. This indicates that either four 12-volt zeners or five 10-volt zeners per module would provide a conservative design. Because of the short cell warm-up time provided by the open fiberglass tape substrate design, the voltage is above the maximum for only a short period and the peak power per module that must be dissipated is more nearly 35 watts, which allows the use of three zeners per module with about 11.7 watts being dissipated by each zener.

5.5 THERMAL ANALYSIS

The solar cell operating temperatures are controlled by the RTV-40 thermal control coating on the cell dark sides. Figure 5-3 shows the thermal analysis results for near-Earth conditions. The normal operating temperature for a flight configuration panel is 45.5°C (as compared to the 55°C design point) and the temperature is 71.0°C in the area of sun sensor blockage of the cell dark sides. This blockage results in a power loss of about 1/4 watt for one sensor. The antenna blockage, analyzed for the PDR baseline configuration, resulted in a 1.5 watt power loss. Beryllium mounting clips combined with RTV-40 coating provide control of the zener diode operating temperatures.

Normal Solar Cell
Operating Temperature
114°F (45.5°C)

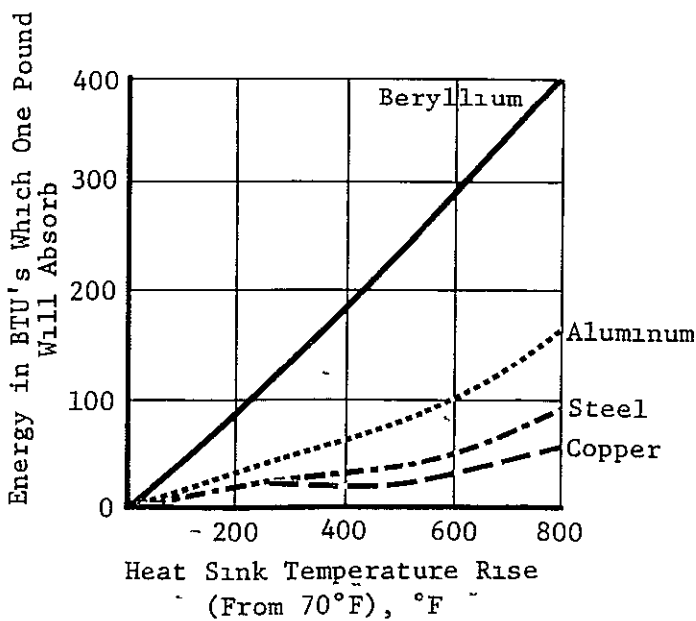
Solar Cell Temperature
160°F (71°C) in Detector
Projected Area
(Typical)



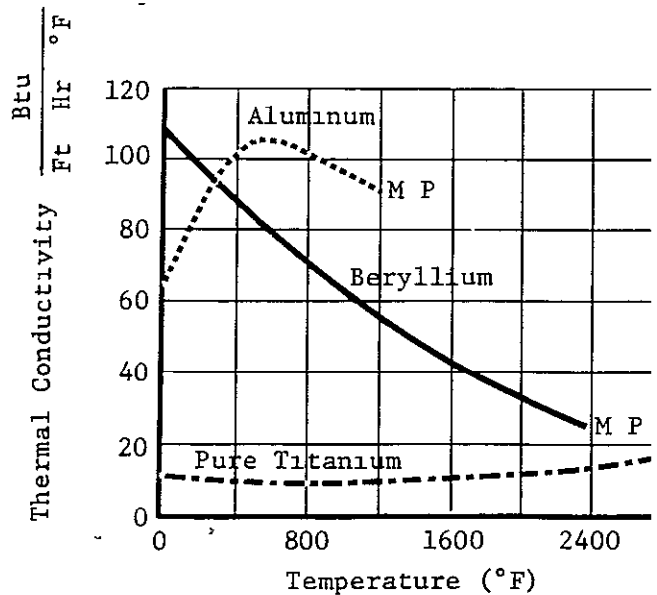
- 1 Relay Antenna (PDR Baseline Configuration)
- 2 Detectors (PDR Baseline Configuration)
- 3 Sun Sensor (Test Panel Configuration)

Solar Cell Temperature
Average 125°F (51.5°C)
for Area Projected Fro
Antenna Substrate

THERMAL ANALYSIS RESULTS



BERYLLIUM AS A HEAT SINK



THERMAL CONDUCTIVITY

Figure 5-3 THERMAL CHARACTERISTICS

Beryllium was chosen as the heat sink for the zener diodes support because of its high thermal conductivity and specific heat as shown in Figure 5-3. In addition the beryllium supports for the diodes match the beryllium structure thermally.

5.6 DYNAMIC AND STRESS ANALYSES

—

A weight-effective boost stowage design was developed by using a pin-free condition.

—

During the preliminary design phase, the initial dynamic and stress analyses showed that panel weight could be minimized by designing the panel to meet the static and frequency requirements and by providing sufficient damping to control the dynamic stresses. The selected boost support condition allows tip motion by connecting the main spar tips to "ground" through the damper springs. The resulting pin-free mode exhibited a node near the c.g. of the 10-pound antenna, reducing its dynamic effect. When, as a result of the PDR, the antenna was removed, the dynamic and stress analyses were refined to include the revised weight and the minor structural changes which resulted in the test panel configuration. These later analyses are described in the remainder of this section.

5.6.1 ANALYSIS REQUIREMENTS

—

Requirements for the dynamic and stress analyses were revised as a result of the Preliminary Design Review.

—

Contract changes after the PDR removed the requirement for a complete dynamic analysis of a panel in the deployed condition and substituted the requirement to define specific equipment as described in Section 5.7. The remaining requirements for dynamic and stress analyses are summarized below:

Static Loading

- 1) The panel shall withstand a one "g" field in all boost and deployed support conditions.
- 2) With the panel supported at the two hinges and one of the tip latch points, loading normal to the panel at the other tip latch point shall be considered (the static test requirement is for a 50-pound load).
- 3) With the hinges and the tip latch points supported in a pin-pin condition, a uniform load normal to the panel shall be considered (the static test requirement is for an 8 "g" distributed load).

Frequency Requirements

- 1) In the pin-pin configuration, no frequency below 20 Hz shall be exhibited.
- 2) In the deployed configuration, with proper cruise dampers and with rigid hinge and damper supports, the lowest damped natural frequency of the rigid body mode must be greater than 1.0 Hz with damping between 0.3 and 0.7 critical.

Analyses to Satisfy Test Requirements

- 1) Analysis shall be made to predict the resonant frequencies and mode shapes in the boost configuration for all significant modes below 100 Hz.
- 2) A dynamic analysis shall be made to predict acceleration response at specified locations on the panel, and to predict the member loads, resulting from a sinusoidal acceleration input of 1 "g" at the resonant frequencies below 100 Hz. The analysis shall simulate the boost configuration, may use appropriate dampers if deemed necessary, and shall include base in-plane and base normal-to-plane excitations. This was later deleted and replaced by a requirement for specifying damper characteristics (see Section 5.4.3). The test requirement specifies excitation at the panel hinges to produce stresses equivalent to those resulting from a sinusoidal input at the four panel attach points.

5.6.2 PROBLEM IDEALIZATION

—

The analytical idealization (modeling) of the test panel included the distribution of the panel mass at structural and substrate nodes.

—

Solutions for the deflections and member loads due to static requirements and for the

resonant mode shapes, frequencies, and dynamic loads for the normalized deflections were obtained with the Boeing ASTRA (Advanced Structural Analyzer) computer program. The program is designed to analyze large complex structures using the direct stiffness matrix method (damping is not included) and is written for the IBM 360 computer. It is essentially an improved version of the program used during the Large Area Solar Array contract and is similar to the JPL "SAMIS" program. The program defines structural members by nodes. A node was assumed at each structural member intersection, at the center of each substrate bay, and at the mass-centers of the simulated sun sensor and attitude control jet as shown in the idealization model in Figure 5-4.

The basic rectangular framework was idealized with beam elements between the nodes. Substrate bays were represented by an "overlay" of plate elements which provide only shear stiffness equivalent to that of the fiberglass diagonal tapes for in-plane vibrations. For out-of-plane vibrations, the substrate stiffness was represented by a pair of diagonal beams having only bending stiffness. Short, stiff beam elements were used for the damper fittings (outboard support points), for the hinge fittings, and for the supports required for the sun sensor and the guidance and control jet assembly.

Concentrated weights at the nodes represented the distributed weight. It was assumed that $1/2$ of the weight of each member ending at a node was effective at the node. For static loads, $1/4$ the weight of each substrate bay was assigned to the corner structural nodes. For in-plane (shear) dynamic analysis, the substrate weight was distributed to the corner nodes, similar to the static loads. For out-of-plane vibration, the early analyses assumed that the generalized mass for the fundamental substrate mode ($1/4$ of the total substrate mass) was at the center of the substrate bay with the remaining $3/4$ distributed to the corners.

Cross sections of the structural framework members were defined and the structural stiffness characteristics of each member were defined in the computer input by the cross section area, torsional stiffness, shear areas and bending (stiffness) moment of inertias in two directions, and by elastic properties of the material.

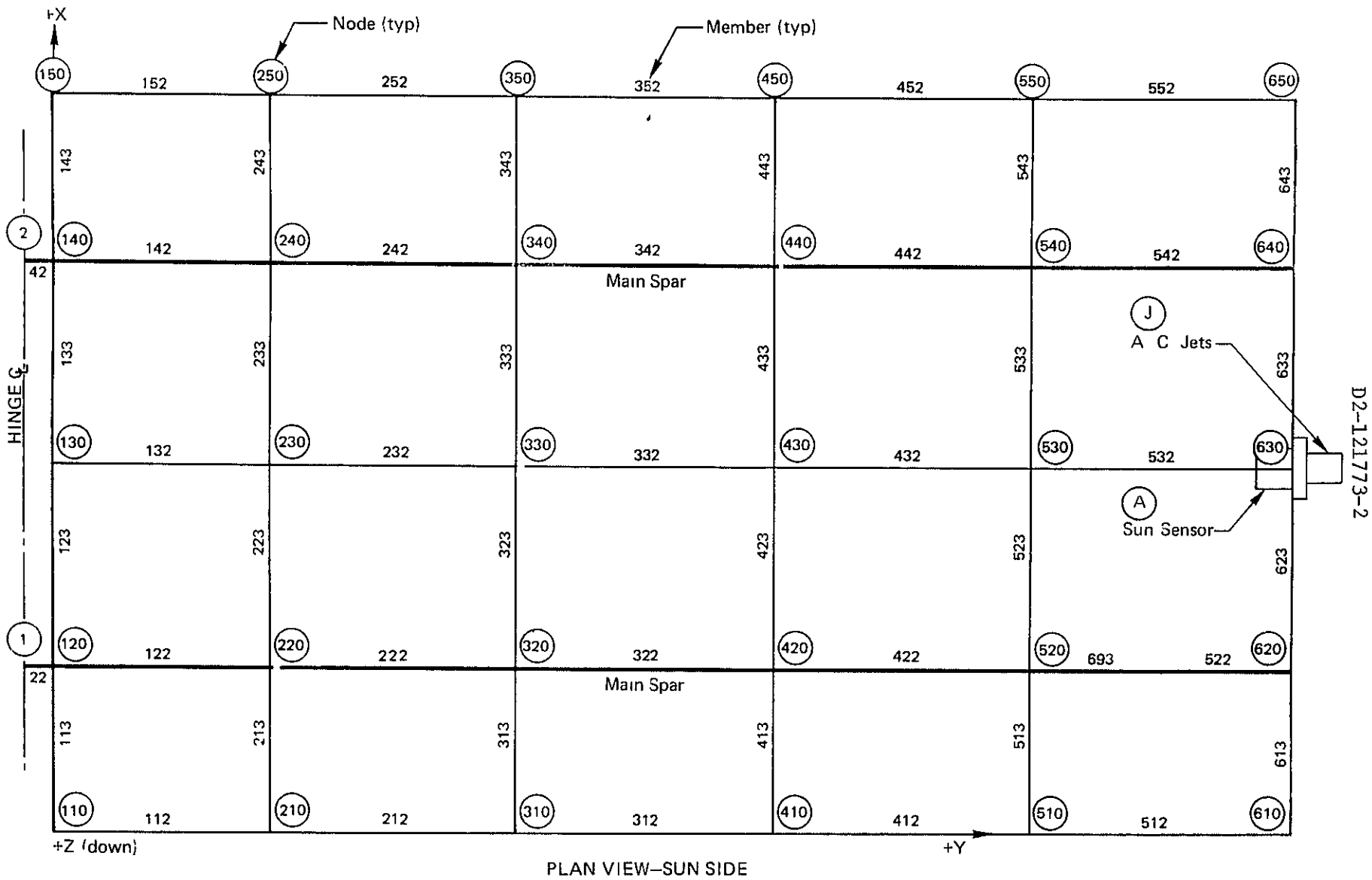


Figure 5-4 IDEALIZATION MODEL

The stiffness of the diagonal beams representing the substrate in out-of-plane bending was selected to result in a specified frequency when loaded with the generalized mass at the intersection of the beams. The frequency was determined by scaling the measured frequency in air from LASA tests. The analyses presented in this report were made with the substrate nodes suppressed by increasing the beam stiffness by a factor of 10, thereby raising the lowest resonance to above 100 Hz. Early analyses, with the substrate modes included, showed a band of 20 closely spaced frequencies starting at 42.5 Hz, effectively masking the structural modes in the region. Because the ASTRA program cannot include damping, the effect of the substrate modes on resonances within the 20-frequency band is exaggerated. To provide visibility for the basic structural modes, the unrealistic undamped response of the substrate was removed. This provided a close approximation of the resonant frequencies and refinement could be made at a later date if necessary.

5.6.3 ANALYSIS METHODS

—

Methods were selected to determine member loads, margins of safety, and dynamic responses.

—

Stress Analysis---The output of the ASTRA program provided the complete loading (end loads, shears, bending, and torsion) for each member for both the static and dynamic solutions with damping excluded. Stresses due to tape tension and to manufacturing straightness tolerances are combined with those from the external loads. An example of an analysis of a main spar member is included in Boeing Document D2-121718-1, "Mars Mission Solar Array - Analyses Documentation," (ref. 3) to illustrate the analysis techniques and the methods for calculating allowable stresses and margins of safety.

Member loads were calculated for a total load of 8 times the weight distributed to the nodes and for a 50-pound load applied to one outboard support. Stresses were then calculated for the two load conditions without the 1 "g" load added, and deflections were obtained for comparison with test measurements.

Margins of safety for the dynamic cases were calculated for selected percentages of the normalized amplitude to define the limiting amplitude for a positive margin of safety. This, in turn, defines the damping force required to limit the motions, as discussed in Section 5.7.3.

The analyses used the same factors of safety and basic allowables that were used in the LASA program. All limit loads are multiplied by 1.25 to obtain the ultimate design load. Where appropriate, they are also multiplied by a 1.15 fitting factor.

Dynamic Analyses---Dynamic solutions for the resonant frequencies and mode shapes are derived from the ASTRA computer program, as are the generalized inertia and stiffness matrices.

Response calculations were originally made by use of a supplementary program which retrieved stored data from ASTRA tapes to obtain the complex response of the normal modes (pin-free) coupled by the damper and driven by the inertia coupling between the excitation motion and the driven modes. Examination of the results showed a simplified approach was possible. This utilized the "pin-free" normal modes with the panel tip connected to ground through the damper springs. The modal coupling due to the damping forces was neglected and the driving inertial forces were hand-calculated. At resonance, the driving force is balanced by the damper force, conservatively assuming that the panel damping is small.

5.6.4 ANALYSIS RESULTS

—

Margins of safety for the test panel are all positive.

—

At the PDR, a panel design for the baseline configuration (with a 10-pound antenna and a 2-pound sun sensor) had been evaluated for satisfaction of the two frequency requirements, and the primary members had been stress analyzed for satisfaction of the 8 "g" and 50-pound load requirements. Fittings and the adjacent structure were given a preliminary design check. Limiting allowable amplitudes for the primary

dynamic modes were established for strength, and Mariner '69 dampers were found to have adequate energy absorption required to control the amplitude. These results are tabulated in the mid-term report, Boeing Document D2-121319-1, "Mars Mission Solar Array Semi-Annual Progress Report," and will not be repeated here. The following analysis results are based on the test panel configuration.

Stress Analysis Results---Analysis results are shown for the static load conditions in Figure 5-5, and for the critical dynamic conditions in Figure 5-6. These results reflect the test panel weights given in Table 5-1 (section 5.3) in the column headed "Mid-Term Estimate." These detailed analyses resulted in the addition of doublers (i.e., structure reinforcement) which improved the margins of safety where required.

The deflection shapes for the 8 "g" and 50-pound static load conditions are shown in Figure 5-7.

Dynamic Analysis Results---The calculated resonant frequencies for four support configurations are tabulated in Figure 5-8. These calculated values are obtained with the substrate frequencies increased by a factor of about 3, to provide visibility for the structural modes.

The first configuration relates to the boost configuration and the sinusoidal sweep tests, the second, to the modal test. From the computer-calculated mode shapes and the excitation motions of translation (specified requirement) and hinge excitation (test requirement), the driving forces for each mode are calculated for a 1 "g" input.

From these values the sinusoidal test levels are derived as explained in Section 5.7.3. The modal test setup introduced a rigid rotation mode at about 1 Hz, but did not affect the tabulated frequencies.

The third configuration tabulated (pin-pin) shows that the minimum calculated frequency exceeds the required (20 Hz) by a considerable margin. The minimum deployed configuration frequency, which was calculated using a Mariner '69 cruise damper spring at a 7.0 inch arm, is 1.6 Hz. With a 6.5 inch arm and 0.7 critical damping, the frequency is 1.07 Hz, which is greater than the required minimum frequency of 1.0 Hz.

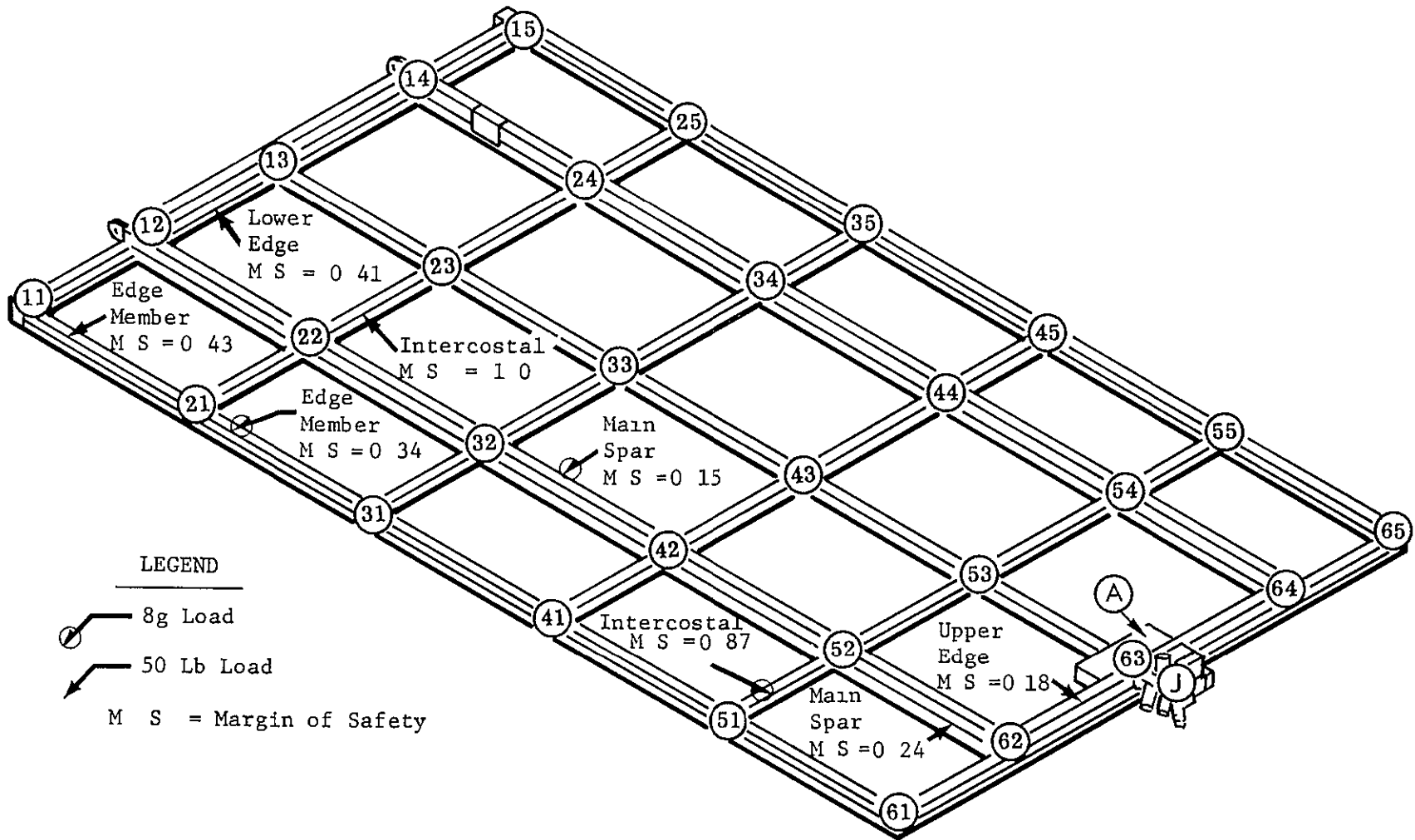


Figure 5-5 STATIC STRESS MARGINS

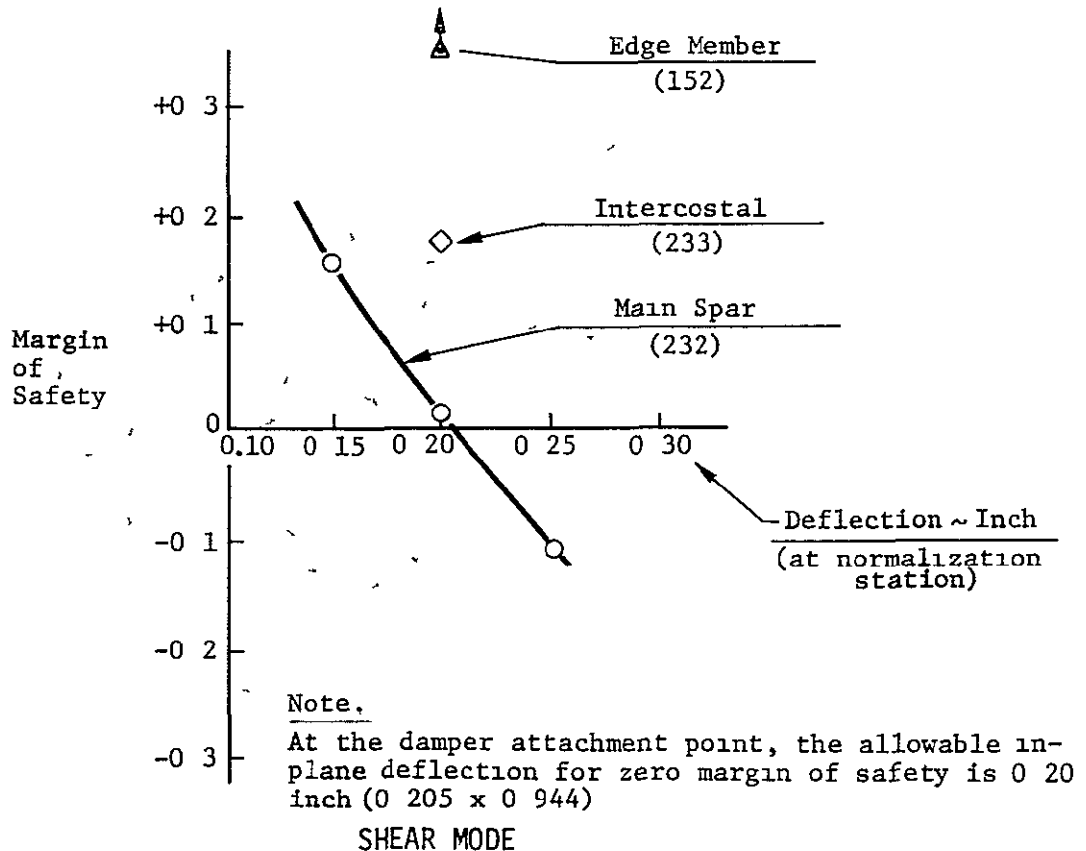
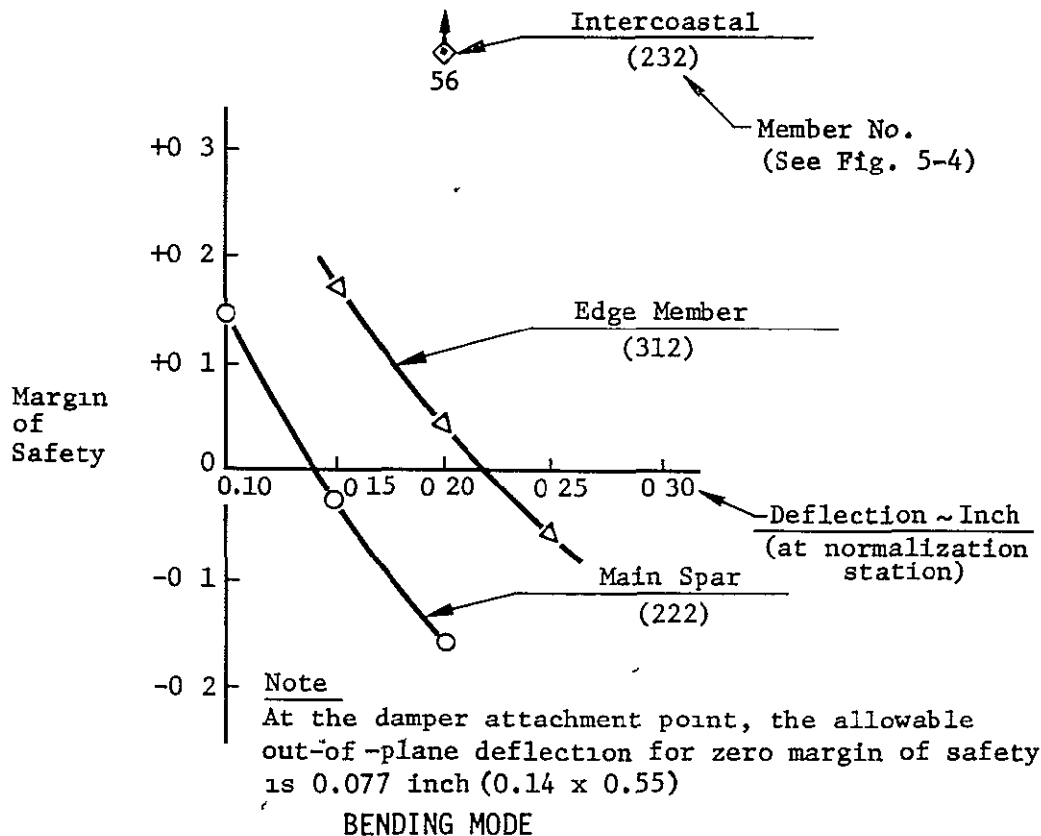
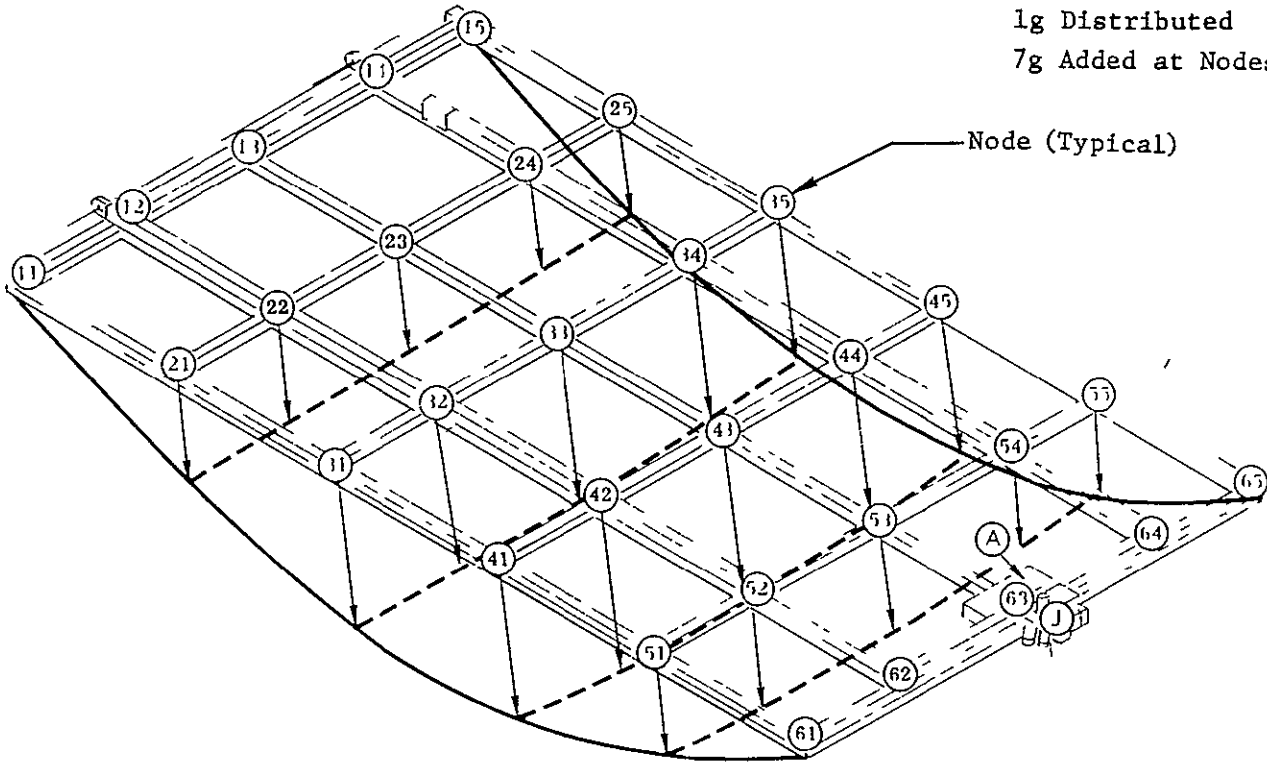


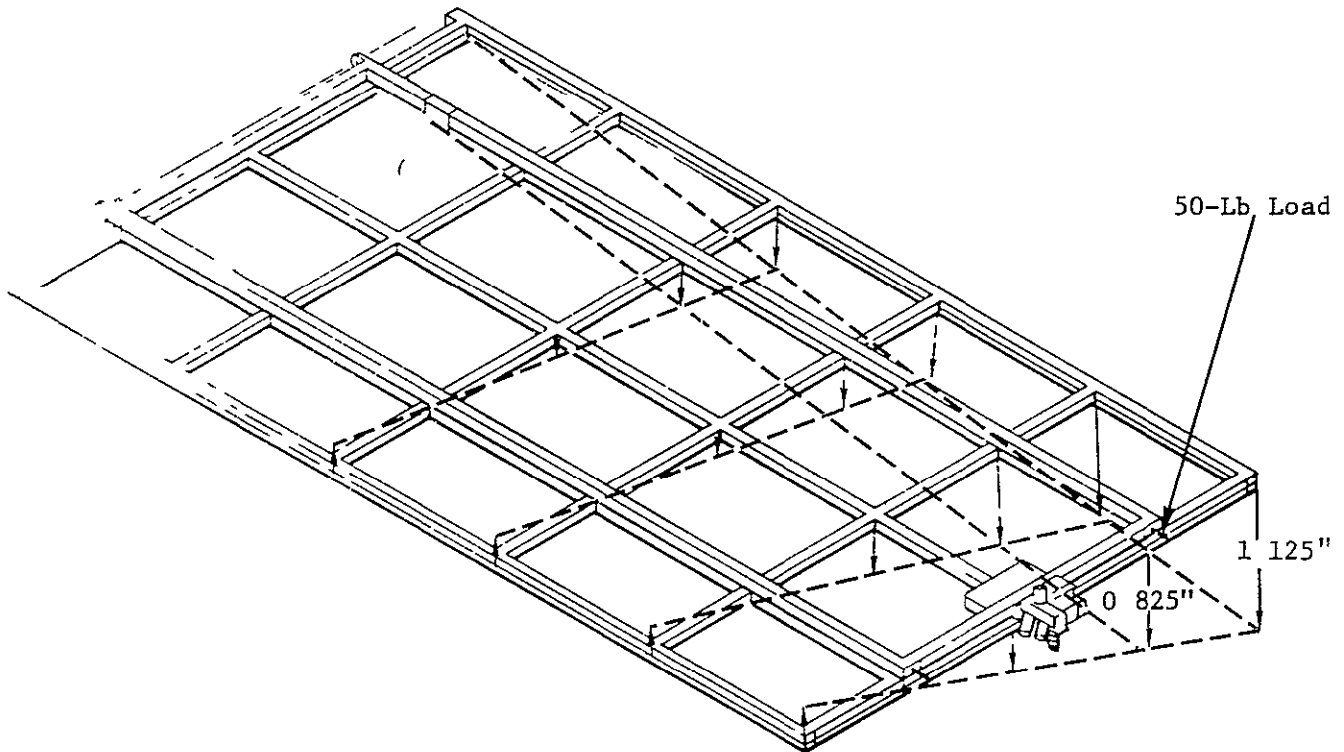
Figure 5-6 DYNAMIC MARGINS OF SAFETY VS. DEFLECTION

1g Distributed
7g Added at Nodes

Node (Typical)



8 G LOAD (BENDING)



50 LB LOAD (TORSION)

Figure 5-7 STATIC DEFLECTION SHAPES

Support Condition \ Mode	1	2	3	4	5	6	7
Pin-Free (35-lb/In. Springs in Boost Dampers)	7.9	19.2	28.5	34.3	68.6	80.9	103.3
Pin-Free (Modal Survey)	---	17.0	27.5	33.9	67.9	80.9	103.0
Pin-Pin	---	45.6	27.4	28.8	---	79.6	99.6
Deployed (530-Lb/In. Springs in Cruise Damper)	1.61	17.2	27.5	34.5	---	---	---

- (1) Rigid Rotation
- (2) First Torsion
- (3) Shear
- (4) First Bending
- (5) Second Torsion
- (6) Chord Bending
- (7) Second Bending

Resonant Frequencies in HZ

Figure 5-8 ANALYSIS RESULTS, RESONANT FREQUENCIES

5.7 MECHANICAL ANALYSES

—

A maximum deployment closing velocity was established and equipment specifications for the deployment mechanisms and the boost dampers were defined.

—

The objectives of these analyses were: (1) to establish a maximum deployment closing velocity based on the energy-absorbing capability of the panel when the deployment motion is arrested by the engaging of the cruise damper, (2) to provide data necessary to define the deployment mechanism equipment, including deployment springs and rotary dampers, (3) to select the boost dampers for the dynamic tests. The analytical approach, an explanation of assumptions and methods, and the analysis results are provided in this section.

5.7.1 ANALYSIS TO ESTABLISH CLOSING VELOCITY LIMITATION

—

A deployment closing velocity limitation of 0.22 radians per second maximum has been established.

—

The approach used in this analysis was as follows:

- 1) Determine the kinetic energy of the deploying panel for several closing velocities.
- 2) Determine the maximum energy-absorbing capability of the panel.
- 3) Determine the maximum energy-absorbing capability of the cruise damper for several closing velocities.
- 4) Select a closing velocity at which:
 - a) The total kinetic energy is absorbed about equally by the bending of the panel and by the deflection of the cruise damper.
 - b) The ratios of energy absorbed to absorption capability of both the panel and the cruise damper do not exceed an arbitrary 60% limit.

This approach provides a conservative approximation of the maximum closing velocity. A more detailed analysis has not been performed because a higher closing velocity limit would not significantly affect deployment mechanism requirements. For example, if the closing velocity could be increased from 0.22 to 0.24 radian per second, two rotary dampers would still be required.

The assumptions used in this analysis are diagrammed in Figure 5-9. The deploying panel is idealized as a single spar with 17.02 pounds of the panel weight evenly distributed along the spar length. Torsional loads on the spar have been included in establishing the 960 inch-pound maximum spar bending moment. The 4.87 pounds of tip-mounted equipment is assumed to be concentrated on the end of the spar 80 inches from the hinge. The effect of the cruise damper latch is assumed to be included in the 530 pounds per inch spring rate of the cruise damper spring. The damping coefficient of the cruise damper is assumed to be 80 pounds per inch per second. The value, d , described in Figure 5-9, has been neglected in the development of cruise damper force-deflection curves but is considered in the 60% limit of energy absorption capability, mentioned previously.

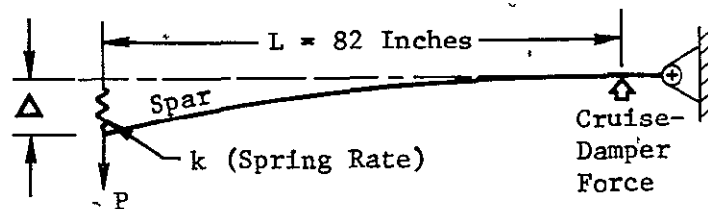
Following the outline of the approach:

- 1) Kinetic energy of a deploying panel is found by the formula,

$$KE = (1/2) I \dot{\theta}^2, \text{ where } I = 18.5 \text{ slug-ft}^2 \text{ and } \dot{\theta} = \text{angular velocity at closing.}$$

- 2) The energy absorbing capability of a panel spar is found as follows:

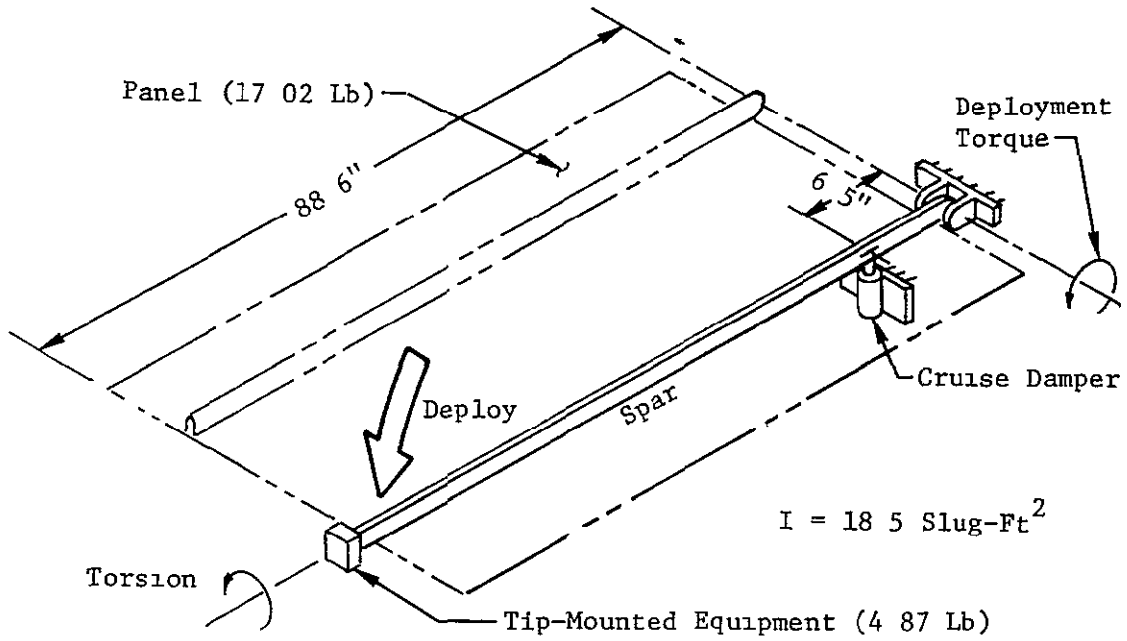
Given. Maximum spar bending moment, $M = 960 \text{ in-lb}$, $P = \frac{M}{L} = 11.7 \text{ lb}$.



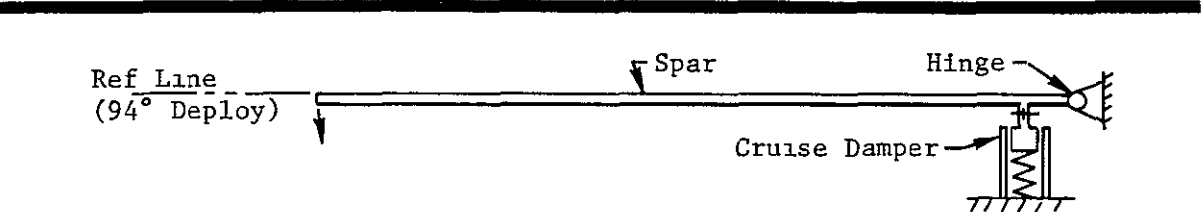
$$\Delta = \text{tip deflection} = 0.75 \text{ inch}$$

$$k = \text{spar rate} = \frac{P}{\Delta} = 15.6 \text{ lb/inch}$$

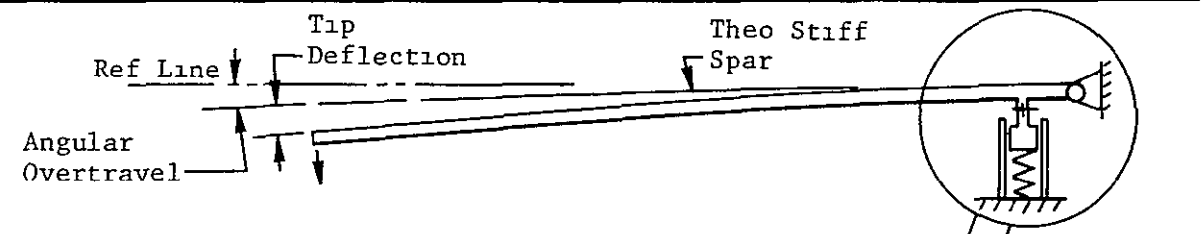
$$\text{Potential Energy} = (1/2) K \Delta^2 = 4.36 \text{ inch-lb (maximum spar capability)}$$



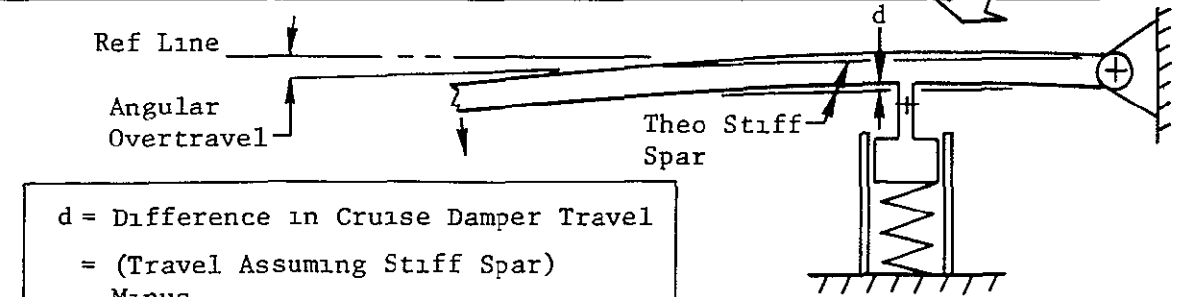
DEPLOYMENT CLOSING IDEALIZATION



① FIRST CONTACT



② EXTREME OVERTRAVEL POSITION



d = Difference in Cruise Damper Travel
 = (Travel Assuming Stiff Spar)
 Minus
 (Actual Travel as Affected by Spar Bending)

Figure 5-9 DEPLOYMENT ANALYSIS ASSUMPTIONS

- 3) The energy absorbing capability of the cruise damper is found by integrating the force-deflection curves for the damper and the damper spring and adding these for each closing velocity considered, as shown in Figure 5-10. In developing these curves, the spar is assumed to be infinitely stiff in bending. Thus, for each small increment of time from first contact to the final position, the acceleration given by:

$$\frac{(\text{initial velocity}) - (\text{final velocity})}{\text{time interval}} \text{ is equal to the acceleration given by}$$

$$\frac{(\text{cruise damper force}) (6.5 \text{ inch moment arm})}{18.5 \text{ slug-ft}^2}$$

A time limit of 0.063 seconds was used for the cruise damper force-deflection curves. This limit is based on a 4-cycle-per-second bending frequency of the spar and the assumption that the highest bending loads will occur in the first 1/4 cycle, or in 0.063 second. In an actual deployment closing, the panel is expected to reach its maximum deflection after 0.063 second, then the tip will start back, driven by the restoring forces in the bent spar and the compressed cruise damper spring. At this point, the total energy absorbed by the bending of the panel and the compression of the cruise damper will equal the original kinetic energy of the panel at first contact.

It was assumed that the cruise damper piston is of a minimum mass and can be accelerated from rest to the panel velocity in no more than 0.004 second.

The total kinetic energy and energy-absorption allocations to the panel and the cruise damper are given for four different closing velocities in Figure 5-11. The selected maximum closing velocity of 0.22 radian per second provides the following characteristics:

- Kinetic energy of panel 5.35 in-lb
- Energy absorption allocated to panel spar bending 2.62 in-lb
- Energy absorption allocated to cruise damper 2.73 in-lb

In an actual deployment the distribution of energy between the panel and the cruise damper will probably be lower than a 2.62 to 2.73 ratio, however, a good margin of safety is provided. For example, if the energy distribution between the panel and the cruise damper is in a three-to-two ratio, the panel spar will absorb 3.21 inch-pounds

Damper Force-Deflection Curve	Area Under Curve (In -Lb)	Spring Force-Deflection Curve	Area Under Curve (In -Lb)	Total Area (Energy) (In -Lb)
① 0 30 Rad/Sec	7 97	S ₁	1 42	9 39
② 0 25 Rad/Sec	5 02	S ₂	0 98	6 00
③ 0 22 Rad/Sec	3 85	S ₃	0 77	4 62
④ 0 20 Rad/Sec	3 39	S ₄	0 63	4 02

F = Damping Force at Initial Closing Velocity

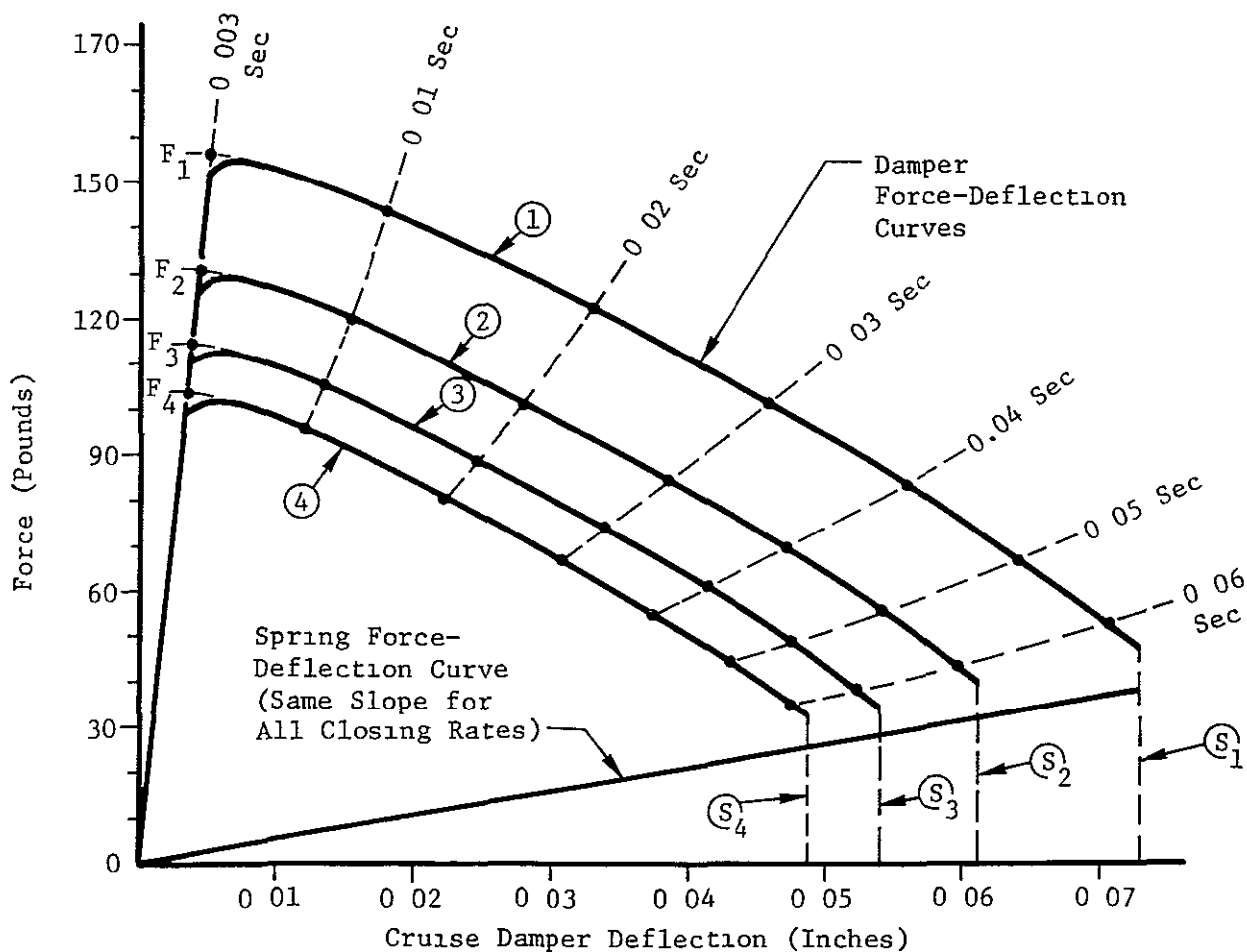
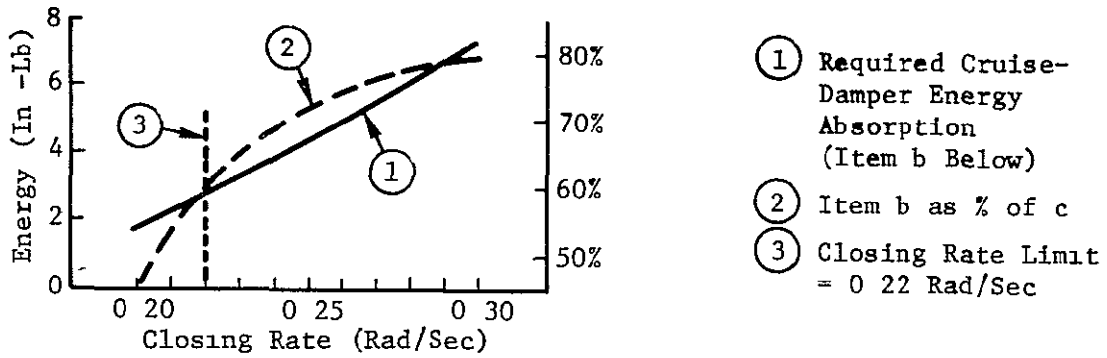


Figure 5-10 CRUISE DAMPER FORCE-DEFLECTION CURVES



- a = Energy Absorption Allocated to Panel Bending = 2.62 In -Lb Constant (60% of Item d)
- b = Energy Absorption Allocated to Cruise-Damper
- c = Capability of Cruise-Damper to Absorb Energy (Assuming No Bending of Panel Spar)
- d = Maximum Allowable Energy in Bending of Panel = 4.36 In -Lb

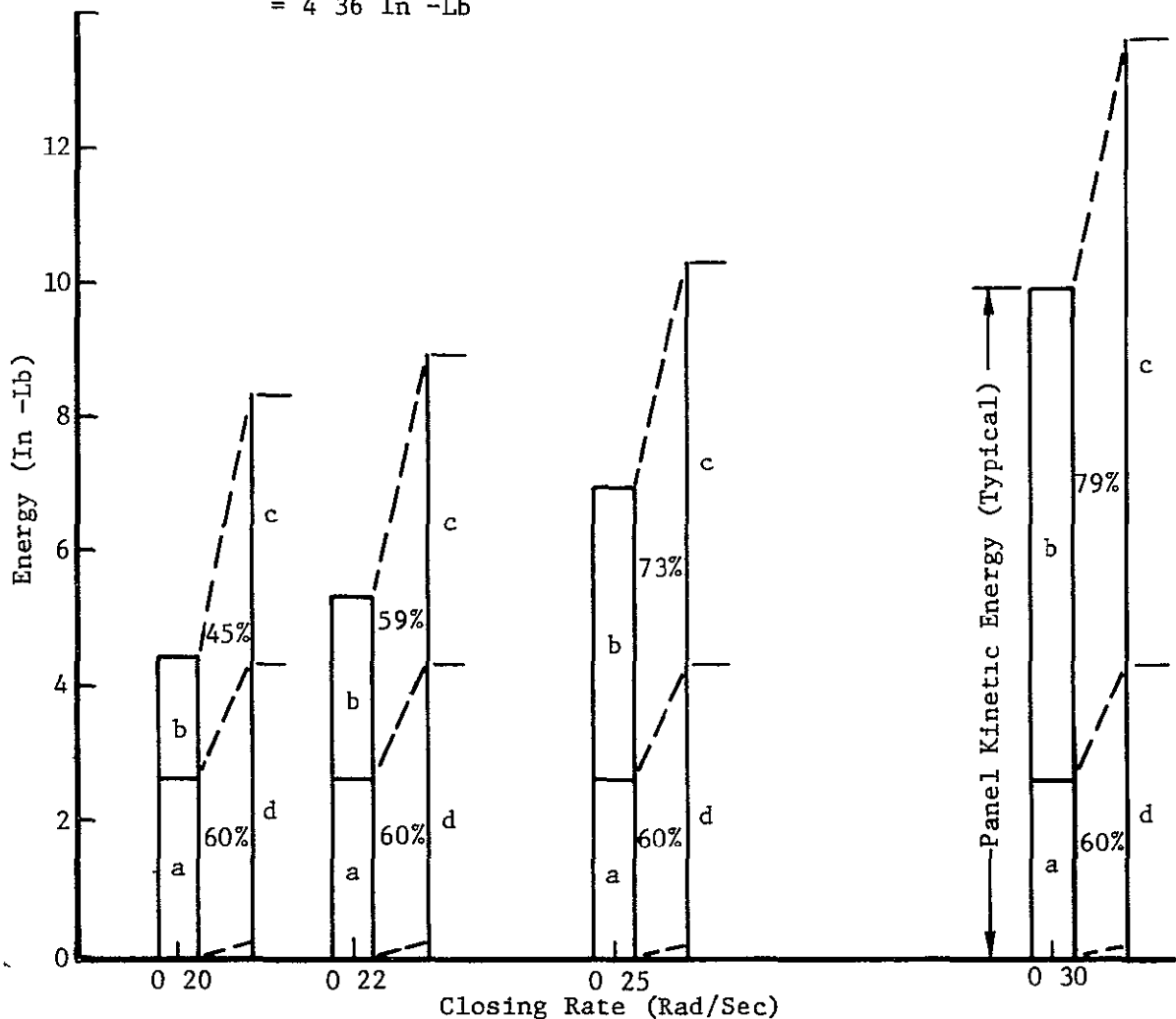


Figure 5-11 ENERGY DISTRIBUTION AT END OF DEPLOYMENT

or 74% of its capacity which is based on a conservative maximum spar bending moment of 960 inch-pounds. In determining the maximum moment, pre-stressing of the beryllium channels was included, assuming the channels to be originally formed to the extreme out-of-straight tolerance condition, then deflected to the straight condition during the bonding of the spar. Actually, the forming consistency was such that the straightness of all channels was well within tolerances.

5.7.2 ANALYSIS TO DEFINE DEPLOYMENT MECHANISMS

-

A constant-force Negator spring and two rotary dampers have been defined for panel deployment.

-

The approach used in this analysis was as follows

- 1) Determine deployment spring torque parameters which will provide adequate deployment torque over a range of deployment positions and friction conditions without producing excessive closing velocities.
- 2) Determine rotary damping effects for several candidate spring torques.
- 3) Select an optimum spring-damper combination which will provide closing velocities no greater than 0.22 radian per second over a range of damper temperatures and friction losses

Deployment Spring Torque---An important assumption in determining deployment spring torque requirements concerns friction losses. These losses result from the friction of the bearings and spring and the resistance to deployment of the electrical wiring and the attitude control gas hoses or swivel connections. For analytical purposes, it is assumed that these losses can vary from zero to three inch-pounds at any point throughout deployment. Based on this assumption, two candidate types of springs have been examined a conventional torsion spring and a Negator RW (reverse wound) constant force spring. The conventional spring, as described in Boeing Document D2-121319-1, "MMSA Semi-Annual Progress Report," (ref. 4) has the disadvantage of minimum torque at the end of deployment. When the friction losses and rotary

damping coefficient are assumed to be maximum (the low temperature condition) the closing velocity is 0.044 radian per second and the net torque at closing is 1.0 inch-pound. This may not be sufficient to engage the cruise damper latch. For comparison, the constant-force spring, under the same extreme conditions, provides a closing velocity of 0.063 radian per second with 3.0 inch-pounds of torque at closing. At the other extreme, assuming no damping and no friction losses, both types of springs provide about the same closing velocity of 0.30 radian per second. For these reasons, a definition of the deployment spring has been established as follows:

Spring Type	Constant force (Negator RW type)
Spring Torque	6.0 inch-pounds nominal

Rotary Damper Effects---To determine rotary damping effects on deployment closing velocities, several deployment time-history curves were developed. These are shown in Figure 5-12. From these time-histories, damping coefficient versus closing rate curves were developed as shown in Figure 5-13. An attempt was made to use existing rotary dampers similar to those used on the Large Area Solar Array (LASA) program. The LASA dampers were modified by removing two of the four vanes to reduce the damping coefficient. For deployment of the MMSA panel, two dampers of this type, but not modified, will provide adequate deployment velocity limitation. However, as shown in Figure 5-14, these dampers are temperature sensitive. Also, LASA test experience has shown that these dampers behave more consistently with the regulating valve in the closed or near-closed position. Therefore, curve No. 1 of Figure 5-14 has been selected as the centerline definition of rotary damping characteristics. These curves were developed for SESCO Manufacturing, Inc., Rotary Damper Part No. 1025-800, however, comparable dampers could be substituted.

Spring-Damper Combinations---Curve No. 1 of Figure 5-13 is the result of combining the centerline spring and dampers and assuming friction losses to be zero. This curve indicates that the damper temperature should be limited to a maximum 102°F to stay within the closing velocity limit. This can be done by shielding or thermal coating of the dampers. Controlling the minimum damper temperature may be more difficult. Point 2 of Figure 5-13 shows the condition with the damper temperature at 0°F and with

	Closing Rate (Rad/Sec)	Damping Coefficient (In -Lb/ Rad/Sec)	Net Torque (In -Lb)	Damper Temperature (°F)
1	0.232	15	6	120
2	0.206	20	6	80
3	0.164	32	6	32
4	0.122	48	6	0
5	0.182	20	5	80
6	0.063	48	3	0
Ref	0.218	32	7	32
7	0.044	48	7+1	0

Zero Friction Loss

1 In -Lb Friction Loss

3 In -Lb Friction Loss

Zero Friction Loss and 7 In -Lb Spring

3 In -Lb Friction Loss and Conventional Spring

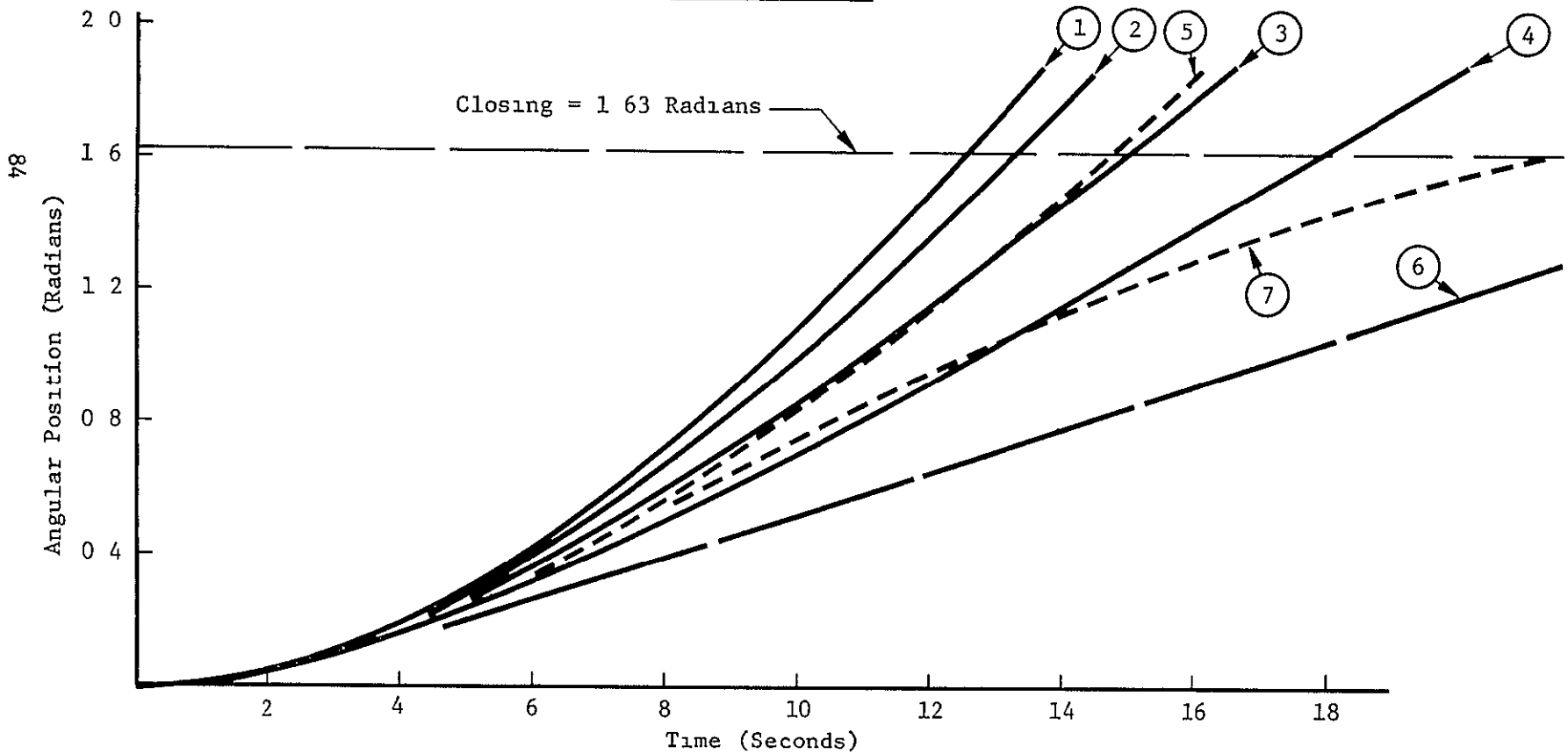


Figure 5-12 DEPLOYMENT TIME HISTORIES

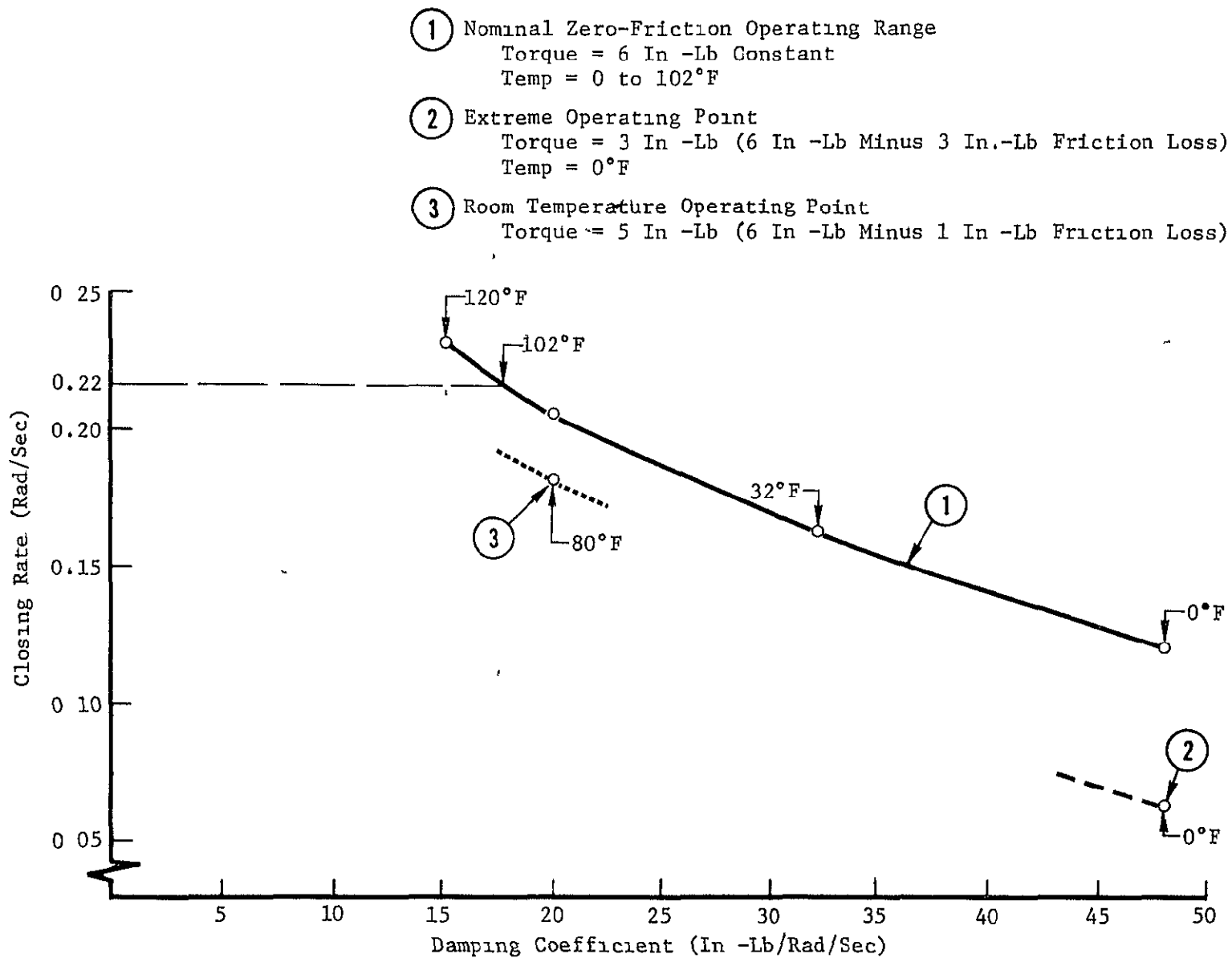
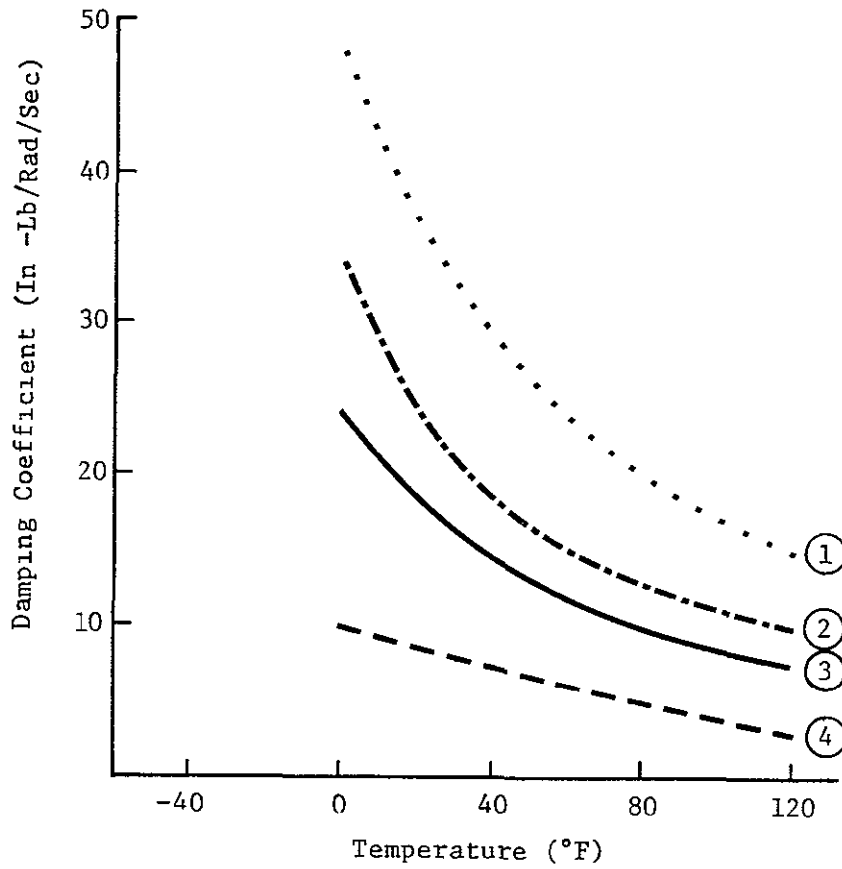


Figure 5-13 DEPLOYMENT CLOSING RATE VS DAMPING COEFFICIENT

These Curves Extrapolated
From SESCO Mfg Co Data
(Damper Manufacturer)



- ① Two Dampers
Valves 20-25% Open
- ② Single Damper
Valve 20-25% Open
- ③ Ref - Single Damper
Valve Fully Closed
- ④ Ref - Single Damper
Valve Fully Open

Figure 5-14 TEMPERATURE EFFECTS ON DAMPING

3.0 inch-pounds friction losses. A closing rate of 0.063 radian per second results. The silicone oil used in the dampers allows operation at temperatures as low as -65°F , however, below 0°F , the closing velocity may be too low to allow latching of the panel to the cruise damper. Two alternatives are possible:

- 1) Insulation of the dampers to retain the latent heat at launch.
- 2) Design of the latch to operate at low closing velocities. The constant force spring provides a minimum latching force of 0.46 pounds regardless of closing velocity. However, the total time to deploy and latch might be several minutes.

It is recommended that both insulation of the dampers and a design of the latch to operate at low closing velocities be used to increase reliability of the deployment latching.

5.7.3 ANALYSIS OF BOOST DAMPER CHARACTERISTICS

—
Modified dampers of the Mariner Venus '67 type were found acceptable for the sinusoidal vibration test.

—
The selected boost configuration for the panel requires dampers attached to the outboard end of the main spars in a manner similar to that used for Mariner spacecraft solar panels. Initially, a modification of the latest Mariner dampers or development of a new damper design was intended. At the time of the preliminary design review, the Mariner damper characteristics were expected to be satisfactory, except that the experimental characteristics for amplitudes between 0.05 and 0.10 inch and between 0.10 and 0.20 inch level were not available. Interpolation between these values was not feasible because of the unpredictable characteristics of the dampers.

A contract change then deleted the damper design effort and a set of six Mariner-Venus '67 damper parts were supplied by JPL for use in the random and sine vibration tests. A set of tests on these dampers was made to verify their capability to supply the required damping and to select two damper assemblies for test usage.

The tests differed from those in the JPL Test Report 605-168 for the Mariner '69 dampers in two respects: (1) excitation was at four selected frequencies with a sweep amplitude, and (2) the damper spring was removed. At specified amplitudes, the oscillograph paper speed was increased briefly to provide visibility of the wave shapes. The selected frequencies were at 7.9, 19, 29, and 34 Hz. A set of initial tests was made with four "O" rings and using 30,000 and 60,000 centistoke oil. Amplitudes were from 0.03 to beyond 0.15 inch. The setup of the damper and the measuring transducers on the shaker is shown by Figure 5-15.

The result of the initial tests showed that the effect of viscosity was much less than expected, that good repeatability was not possible, and that extrapolation toward zero amplitude was not feasible. Each damper showed anomalies in the curve shapes. The possibility of an undesirably high static friction was indicated. On the basis of examinations of plotted data from these tests, two "overall best" dampers were selected for use in the panel dynamic tests. Additional tests of these dampers, with two "O" rings and 30,000 centistoke oil to reduce friction, were then made. The results of the tests on these two damper assemblies are shown by Figure 5-16.

The initial portion of the oscillograph records for these tests was recorded with gradually increasing force in an attempt to obtain the force at which motion began. The background electrical noise of the system was large enough to mask the initiation of motion. Extrapolation of the response curve to zero indicated that the breakaway force was at least between 1 and 2 pounds. Initial friction is important because the beam will oscillate as a pin-pin beam without damper motion unless the forces at the damper exceed the "stiction" force. The importance is magnified because the actual test excites the panel only at its hinges, whereas the simulated test environment is for translation of all four panel attachment points. As a consequence, the forces at the damper are appreciably less than they would be for the translation conditions, even though the hinge excitation is increased to excite the panel modes to equivalent amplitudes. The result is that the concentrated weights at the outboard end (jet assembly and sun sensor) have minimum motion during the test excitation, but translate at the same excitation level as the hinge during the actual (specified) excitation.

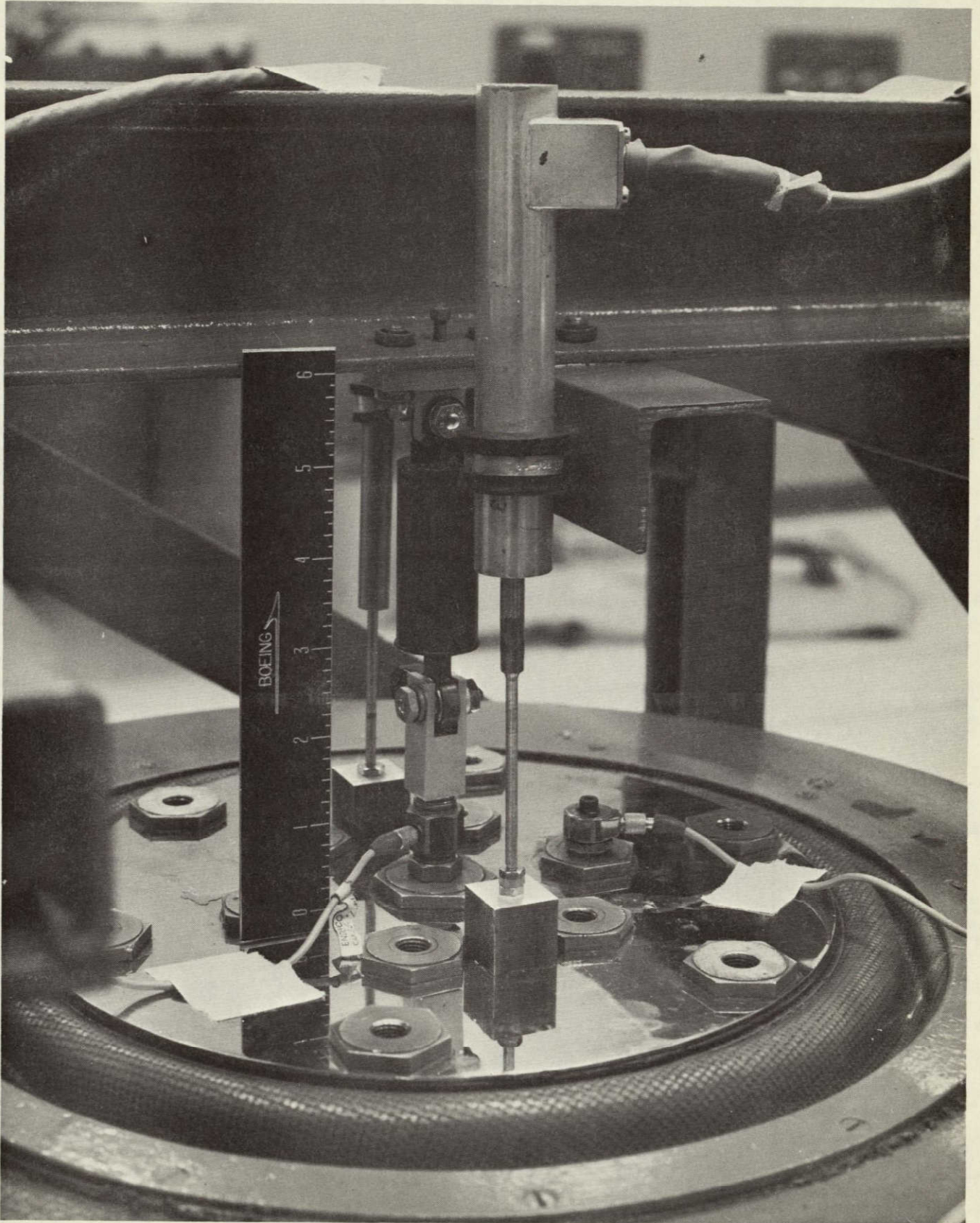


Figure 5-15: BOOST DAMPER TEST SETUP

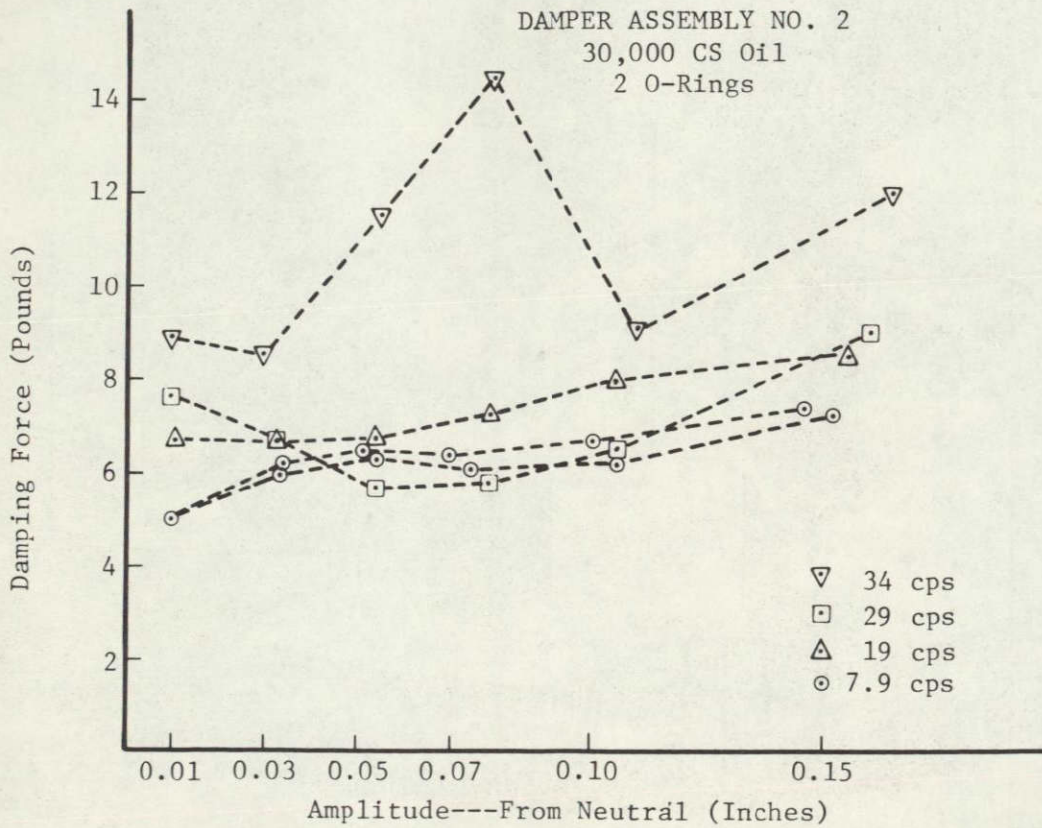
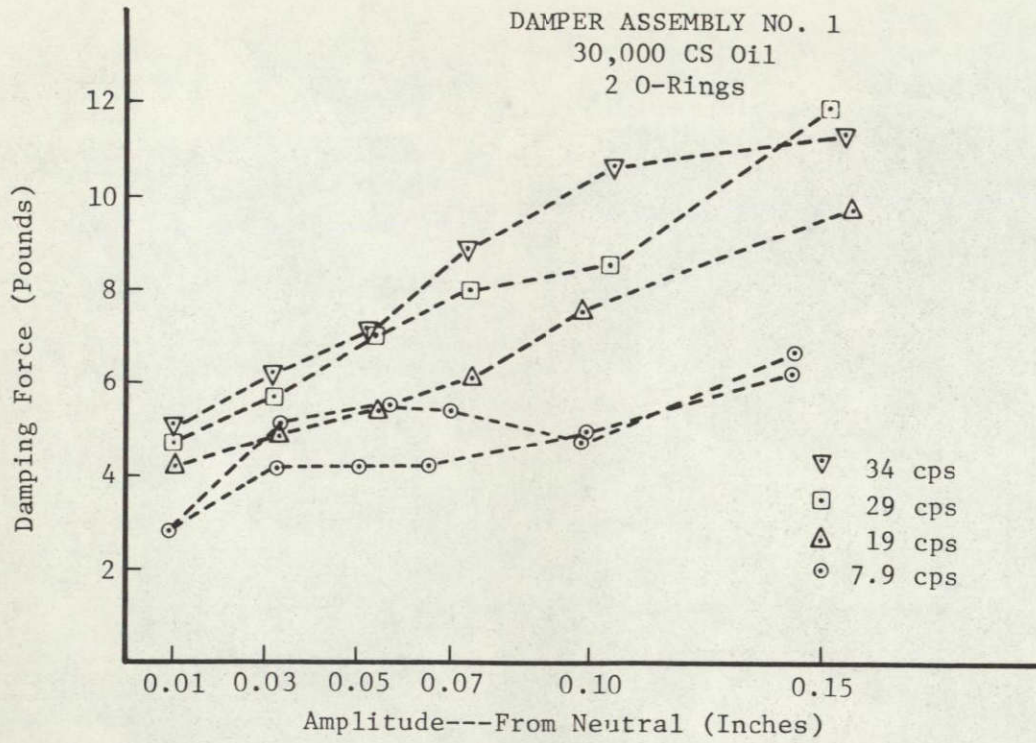


Figure 5-16: BOOST DAMPER TEST RESULTS

Assuming no structural damping, the requirement for the dampers is to provide (at least) the required generalized damping force at the amplitude for zero margins of safety. At resonance the generalized damping force must equal the generalized driving force.

The dynamic analysis of a flight panel considers excitation in translation at four points: the two hinges and the two damper locations at opposite ends of the panel. However, the random and sinusoidal vibration of the test panel is accomplished by exciting the panel only at the hinges, with the dampers attached to ground. The uniform translation driving forces for both of these conditions (based on a one "g" excitation) are given in Table 5-2. The modes underlined in this table are the three which are significantly excited below 100 Hz by the 0.707 "g" test requirement. The spec/test ratio is used to determine equivalent excitations at the hinge points for the specified 0.707 "g" test excitation. The ratio for each mode is multiplied by 0.707 "g", resulting in a range of values from 4.57 "g" for the rigid rotation mode to 0.67 "g" for the first bending mode.

TABLE 5-2
DRIVING FORCES - SINUSOIDAL TEST

Mode	Driving Force at 1 "g" Excitation		Spec/Test
	Spec (4 points)	Test (2 points)	
<u>Rigid Rotation, 7.9 Hz</u>	<u>13.53 Lb</u>	<u>2.09 Lb</u>	<u>6.47</u>
First Torsion, 19.2 Hz	-0.105 Lb	-0.048 Lb	2.09
<u>First Shear, 28.6 Hz</u>	<u>13.82 Lb*</u>	<u>2.81 Lb*</u>	<u>4.93</u>
<u>First Bending, 34.3 Hz</u>	<u>4.24 Lb</u>	<u>4.49 Lb</u>	<u>0.94</u>
Second Torsion, 68.6 Hz	-0.031 Lb		
Chord Bending, 81.0 Hz	-0.017 Lb	-0.065 Lb	0.25

*Based on excitation in the in-plane direction

For the analyzed panel configuration, the generalized driving forces and the limiting amplitudes at the damper locations are given in Table 5-3, Columns A and D, respectively, for the important modes. The total damping force (Column C in Table 5-3) is

equal to the generalized driving force divided by the normalized modal amplitude at the damper locations (Column B in Table 5-3).

TABLE 5-3
BOOST DAMPER PARAMETERS

Mode	A	B	C	D
	Generalized Driving Force for 0.707 "g"	Amplitude at Damper Location (Normalized)	Total Damping Force Required (2 Dampers)	Limiting Amplitude at Dampers (for Zero Margin of Safety)
Rigid Rotation	9.6 Lb	1.0	9.6 Lb	0.15 inch
First Shear	9.8 Lb	1.0	9.8 Lb	0.20 inch
First Bending	3.0 Lb	0.462	6.5 Lb	0.077 inch

Examination of the damping force curves (Figure 5-16) shows adequate excess force over the damping force required to control the responses of the panel within amplitude limits. (The damping forces shown in Figure 5-16 can be doubled because two dampers are used.)

5.8 POWER OUTPUT MEASUREMENT ANOMALY INVESTIGATION

The analyses and investigations performed to resolve the power output measurement anomaly is recorded in this section.

Power output tests of the six live cell modules were performed before and after the modal survey. The values obtained for maximum power for all six modules in both tests were consistently about 25% below predicted values. Because of the consistent power output values of the six modules in the first test, and repeatability of the values in the second test and a requirement to obtain repeatability rather than a specific power output, the figures were assumed to be correct. The third power output test, performed after subjecting the panel to a reverberant acoustic spectrum, produced power values close to those predicted. Five subsequent power output tests produced the higher power levels of the third test. These were performed after the acoustic, random vibration, sinusoidal vibration, static load, and thermal-vacuum-shock tests.

An investigation of the power output check setup shown in Figure 5-17 was made to determine possible causes of the power output discrepancies. The following possible causes were identified and investigated:

- 1) Item---Determination of current at the output end of the electronic load bank requires measurement of the voltage used to drive the recorder. The multimeter internal resistance would be added to the load bank circuit if the multimeter was switched to read current instead of voltage. This would reduce the indicated current of the solar panel module.

Result---Curves were plotted using the multimeter switched to the "current" reading position to set the recorder graph coordinates. Various electrical lead lengths to the multimeter were used to introduce lead resistances. The curves obtained were close but not the same as the anomalous curves recorded during the first two power output tests. The panel module short circuit current could be duplicated but the open circuit voltage was somewhat higher than had previously been recorded.

- 2) Item---The X-Y plotter scales may have been set incorrectly. It appeared that if 200 mA was set at 0 that the suspect curves could be duplicated.

Result---The plotted V-I curve did not duplicate the curves of the first two power output runs.

- 3) Item---An internal resistance in the load would cause an apparent loss of power.

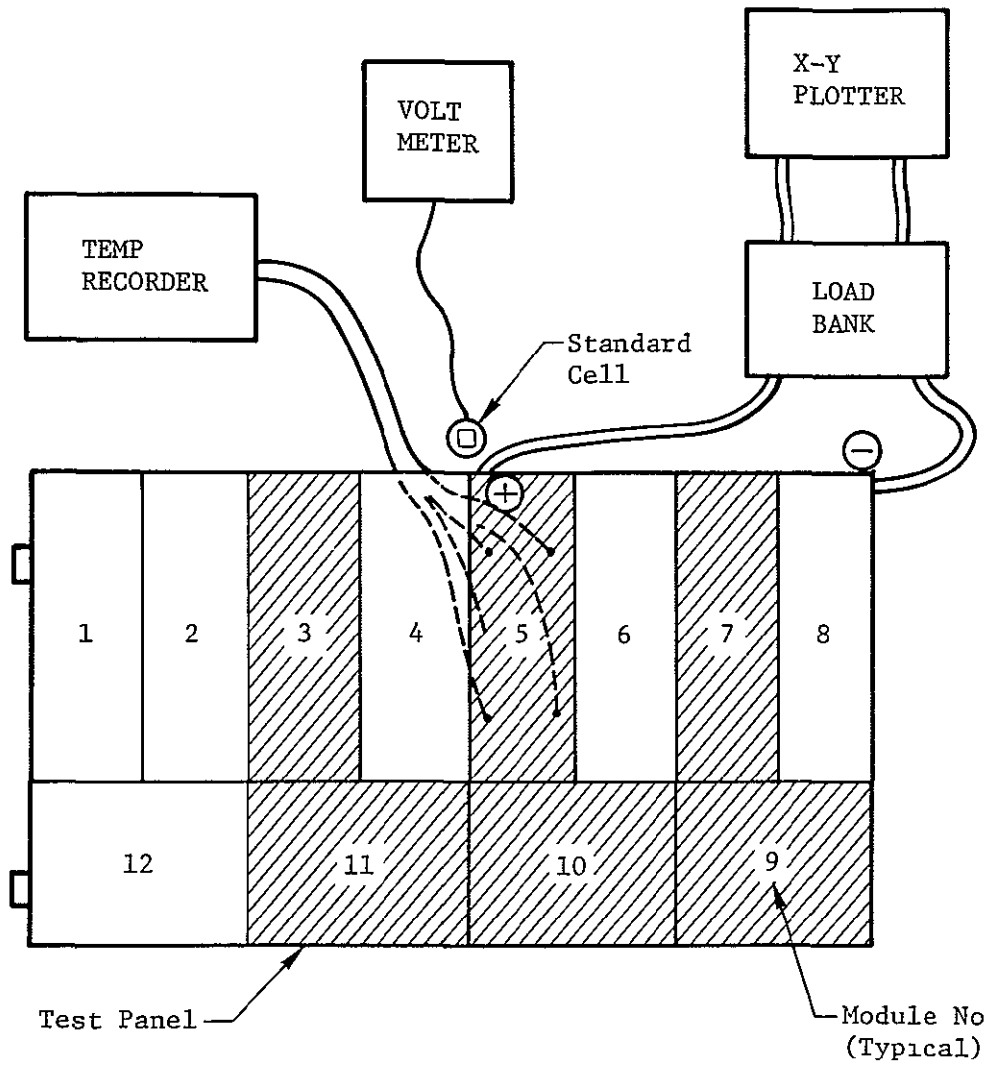
Result---The load bank was carefully checked. No sources of resistance could be found. A resistor was purposely paralleled with the load bank. It proved impossible to plot V-I curves similar to the curves of the first two power output runs.

- 4) Item---The intensity of the solar simulator may have been low.

Result---Intensity is verified with a JPL standard cell, four beam monitor cells, a differential radiometer, power input to the simulator, and panel temperature recordings. These checks indicated the same beam intensity for all runs.

- 5) Item---A short or open circuit may have occurred in a power lead from the test panel.

Result---The leads were inspected for shorts and open circuits. No shorts could be found. An intermittent open circuit was found on one lead, but apparently had occurred after testing. Intentional open circuits to the recorder did not product V-I curves similar to the curves of the first two power output tests.



Note Live Cell Modules Shown Shaded

Figure 5-17 POWER OUTPUT CHECK SETUP

6) Item---A combination of Item 1 and an open circuit may have occurred.

Result---The recorded open circuit voltage was low and the V-I curve shape was significantly different from the curves of the first two power output tests.

None of the suspected causes could be verified as the one which caused the initial low values of power. Six live modules were checked. Three of the modules had a common positive terminal and separate negative terminals. The remaining three modules also had a common but separate positive terminal and individual negative terminals. In this way each module could be checked individually. This rules out an electrical resistance in the panel because tests of individual modules showed similar results. All of the solar cells cannot physically change in the manner indicated thereby ruling out the possibility that the cells actually were producing less power on the first two tests. The solar simulator light intensity and spectral distribution did not change. Therefore, the anomaly is attributable to an unknown error or factor. Although Item 1 produced results close to those recorded in the first two power output tests, the slightly higher (4%) open circuit voltage than the voltage recorded in the first two power output tests, resulted in the decision to disregard the data of the first two power output tests and to determine degradation by comparing results of power output tests conducted after the acoustic test. The values recorded in the power output tests made after the acoustic test were compatible with calculated values.

SECTION 6.0. TEST PROGRAM

This section summarizes the test activities and results of the "type approval" test program to which the prototype test panel was subjected. The overall test sequence is diagrammed in Figure 6-1, and a summary of the test program is given in Figure 6-2. A complete test report is provided in Boeing Documents D2-121321-2 and D2-121321-3, "Test Report, Light Weight Solar Array Panel Development," Volumes II and III.

Accelerometer and strain gage instrumentation, used for the environmental tests, is shown in Figure 6-3. Thermocouple installations for the thermal-vacuum test are shown in Section 6.6.

6.1 MODAL SURVEY

—

The modal survey test was conducted to determine the mode shapes, frequencies, and modal damping of the test panel for the resonant frequencies below 100 Hz.

—

Before testing, analyses were made to predict the resonant frequencies and mode shapes for the test panel configuration in the pin-free condition, which was the modal test condition. Selection of instrumentation locations was based on these analyses. The following paragraphs describe test activities and results, and provide a comparison of predicted and measured values.

6.1.1 TEST ACTIVITIES

—

The modal test objectives were met.

—

The panel was supported at its hinges in a floor-mounted fixture as shown in Figure 6-4. The panel was held in a vertical position by two pre-tensioned, soft springs attached to the simulated attitude control jets at the outboard center of the panel. Excitation was provided by means of small voice coils attached at two positions at

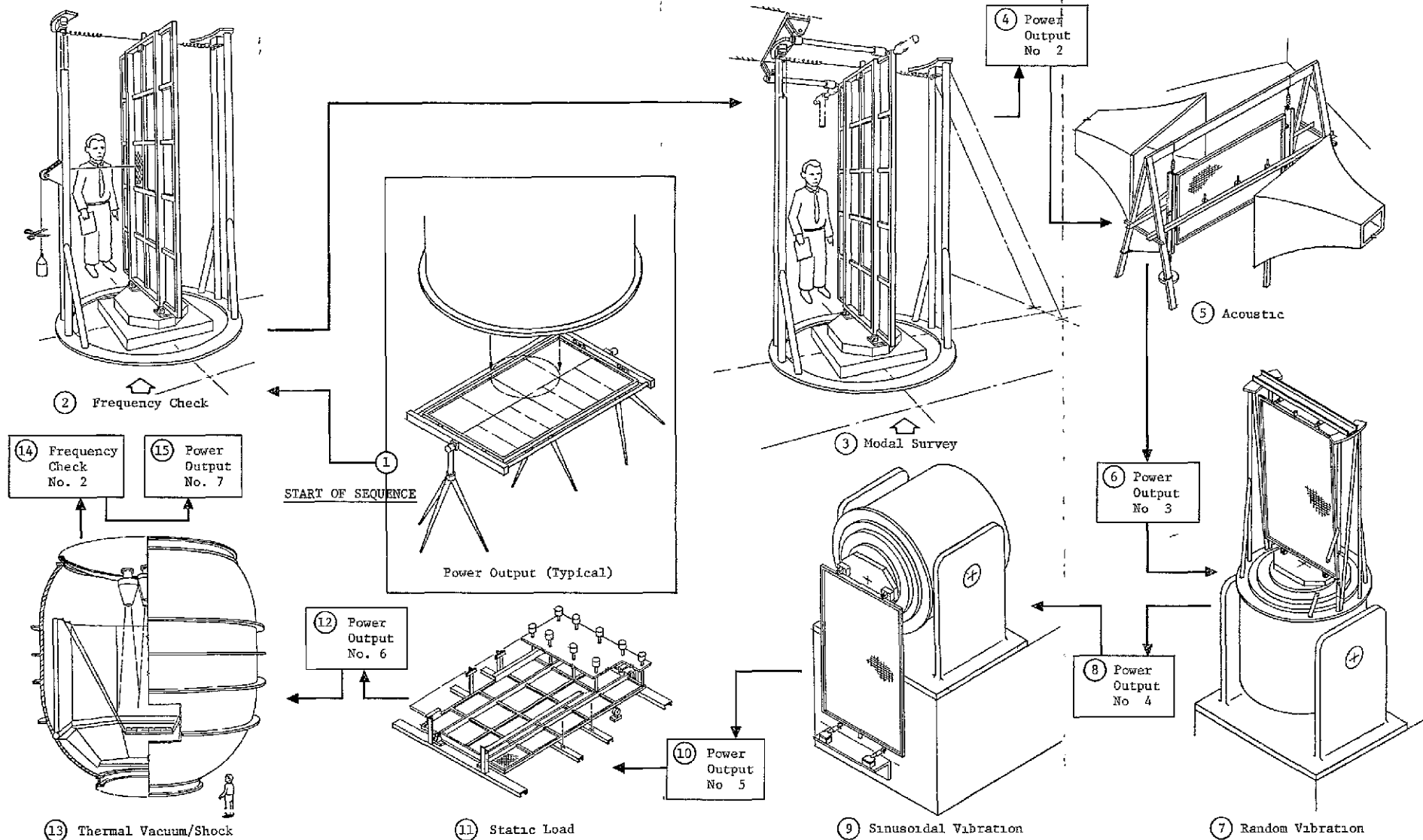
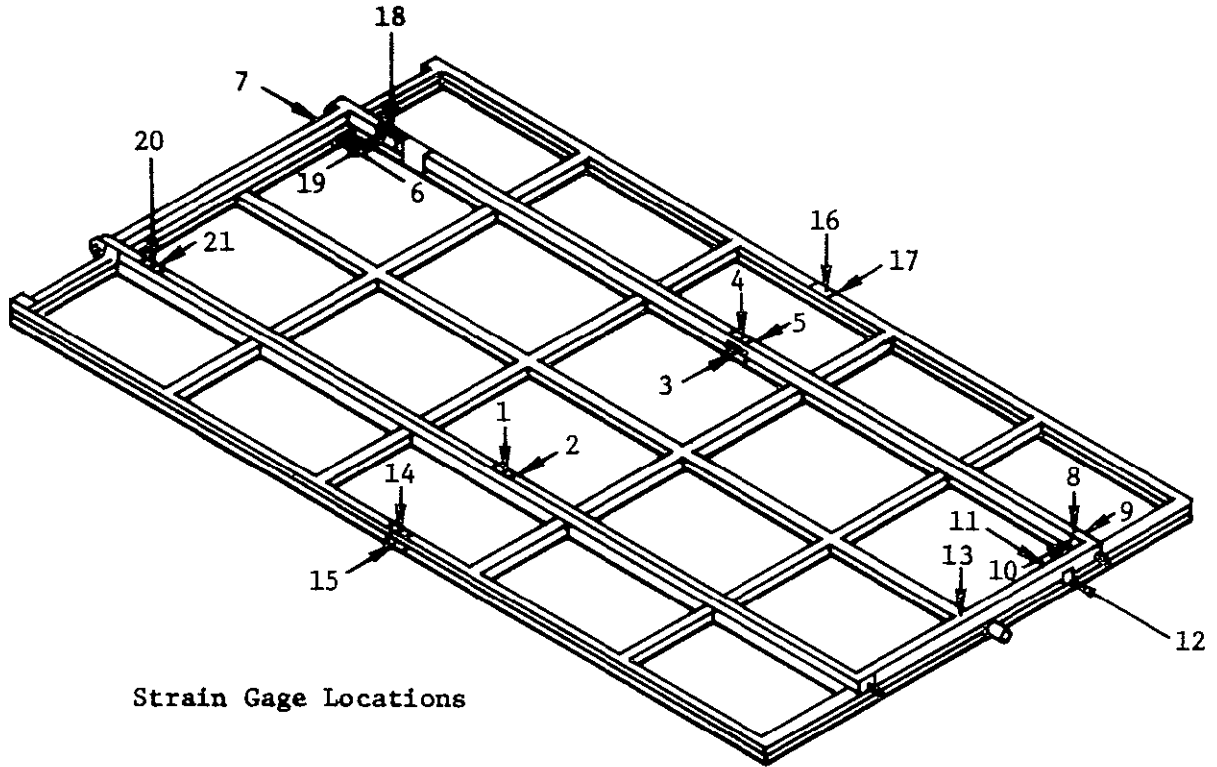


Figure 6-1 TEST SEQUENCE

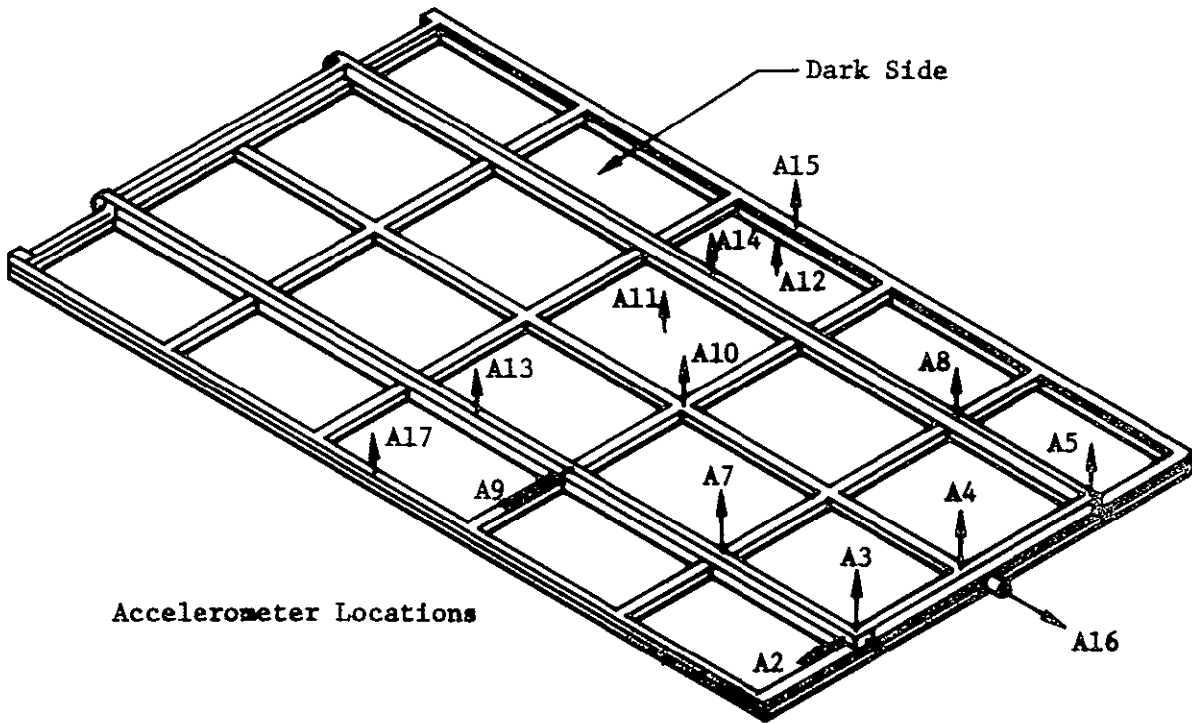
TEST	OBJECTIVE	MEASURED PARAMETERS						REMARKS																				
		MODE	FREQ (Hz)	DAMPING COEFF	MODE	FREQ (Hz)	DAMPING COEFF																					
MODAL SURVEY	TO DETERMINE MODE SHAPES FREQUENCIES AND MODAL DAMPING OF THE FIN FREE PANEL FOR FREQUENCIES BELOW 100 Hz	1ST TORSION	12.2	0.037	2ND TORSION	50	0.062	<ul style="list-style-type: none"> MODE SHAPES WERE ABOUT AS PREDICTED SEE FIGURES 6.5, 6.6 AND 6.7 BENDING STIFFNESS WAS ABOUT 80% AND TORSIONAL STIFFNESS ABOUT 65% OF PREDICTED BECAUSE OF DEFICIENCIES IN ANALYTICAL MODELING RECALCULATED FREQUENCIES INCLUDING TEST EQUIPMENT WEIGHT AND REDUCED STIFFNESS AGREED WITH MEASURED FREQUENCIES 																				
		1ST SHEAR	22.28	0.037	CHORD BENDING	58	0.062																					
		1ST BENDING	28.4	0.110	LARGE SUBSTRATE	68.71	~ 0.075																					
		HIGHEST STRUCTURAL STRESS 3.540 PSI																										
REVERBERANT ACOUSTIC	TO EXPOSE THE TEST PANEL TO ACOUSTIC NOISE UP TO 150 db OVERALL FOR 60 SECONDS AND TO DETERMINE RESPONSES			<table border="1"> <thead> <tr> <th>LOC</th> <th>RESPONSE (g rms)</th> <th>LOC</th> <th>RESPONSE (g rms)</th> </tr> </thead> <tbody> <tr> <td>A3</td> <td>15.1</td> <td>A11</td> <td>305</td> </tr> <tr> <td>A5</td> <td>12.3</td> <td>A12</td> <td>200</td> </tr> <tr> <td>A7</td> <td>26.7</td> <td>A13</td> <td>37.5</td> </tr> </tbody> </table>		LOC	RESPONSE (g rms)	LOC	RESPONSE (g rms)	A3	15.1	A11	305	A5	12.3	A12	200	A7	26.7	A13	37.5	<p>HIGHEST STRUCTURAL STRESS 4.300 PSI</p>		<ul style="list-style-type: none"> SUBSTRATE RESPONSES WERE GREATER THAN EXTRAPOLATED FROM LASA DATA BECAUSE OF DIFFERENT TEST CONDITIONS NO STRUCTURAL OR CELL BOND DAMAGE OCCURRED 				
LOC	RESPONSE (g rms)	LOC	RESPONSE (g rms)																									
A3	15.1	A11	305																									
A5	12.3	A12	200																									
A7	26.7	A13	37.5																									
		DIAGRAM 1 ACCELER LOC S																										
RANDOM VIBRATION	TO DETERMINE THE ADEQUACY OF THE TEST PANEL TO WITHSTAND WIDE BAND RANDOM EXCITATION IN THE LAUNCH DIRECTION (4° OFF THE PLANE OF THE PANEL)	<p>ACCELERATION RESPONSES (SEE DIAGRAM 1)</p> <table border="1"> <thead> <tr> <th>LOC</th> <th>RESPONSE (g rms)</th> <th>LOC</th> <th>RESPONSE (g rms)</th> </tr> </thead> <tbody> <tr> <td>A3</td> <td>4.0</td> <td>A11</td> <td>14.8</td> </tr> <tr> <td>A7</td> <td>2.9</td> <td>A12</td> <td>10.6</td> </tr> <tr> <td>A8</td> <td>4.0</td> <td>A14</td> <td>5.3</td> </tr> <tr> <td>A10</td> <td>8.0</td> <td>A15</td> <td>6.1</td> </tr> </tbody> </table>				LOC	RESPONSE (g rms)	LOC	RESPONSE (g rms)	A3	4.0	A11	14.8	A7	2.9	A12	10.6	A8	4.0	A14	5.3	A10	8.0	A15	6.1	<p>HIGHEST STRUCTURAL STRESS 1.100 PSI</p>		<ul style="list-style-type: none"> STRESS AND ACCELERATION LEVELS WERE LOW AS EXPECTED BECAUSE OF THE NEARLY IN PLANE DIRECTION OF EXCITATION MARINER 67 TYPE DAMPERS WERE USED FOR TIP SUPPORT IN THIS AND THE SINUSOIDAL TEST
LOC	RESPONSE (g rms)	LOC	RESPONSE (g rms)																									
A3	4.0	A11	14.8																									
A7	2.9	A12	10.6																									
A8	4.0	A14	5.3																									
A10	8.0	A15	6.1																									
		ACCELERATION RESPONSES (SEE DIAGRAM 1)																										
SINUSOIDAL VIBRATION	TO EXPOSE THE PANEL TO SINUSOIDAL EXCITATIONS (NORMAL TO THE PANEL) AT THE TWO HINGE POINTS WHICH WOULD INDUCE STRESSES EQUIVALENT TO THOSE PRODUCED BY A SPECIFIED EXCITATION AT THE FOUR SPACECRAFT ATTACH POINTS	<p>ACCELERATION RESPONSES (SEE DIAGRAM 1)</p> <table border="1"> <thead> <tr> <th>LOC</th> <th>RESPONSE (g PEAK)</th> <th>LOC</th> <th>RESPONSE (g PEAK)</th> </tr> </thead> <tbody> <tr> <td>A11</td> <td>12.5</td> <td>A10</td> <td>15.0</td> </tr> <tr> <td>A11</td> <td>8.0</td> <td>OTHERS</td> <td>< 5.0</td> </tr> </tbody> </table>				LOC	RESPONSE (g PEAK)	LOC	RESPONSE (g PEAK)	A11	12.5	A10	15.0	A11	8.0	OTHERS	< 5.0	<p>HIGHEST STRUCTURAL STRESS 3.260 PSI (VS 10.900 PSI FOR ZERO MARGIN OF SAFETY)</p>		<ul style="list-style-type: none"> TEST WAS PERFORMED IN SEGMENTS TO AVOID OVERDRIVING ADJACENT MODES (SEE FIGURE 6.17) STRESS AND ACCELERATION LEVELS WERE NOT EXCESSIVE NON LINEARITY OF THE DAMPERS AND HINGE FREE PLAY CONTRIBUTED TO HIGH FREQUENCY HASH SEEN ON THE RECORDED DATA 								
LOC	RESPONSE (g PEAK)	LOC	RESPONSE (g PEAK)																									
A11	12.5	A10	15.0																									
A11	8.0	OTHERS	< 5.0																									
		ACCELERATION RESPONSES (SEE DIAGRAM 1)																										
STATIC LOAD	TO DETERMINE PANEL DEFLECTIONS FOR TWO LOADING CONDITIONS 1) BENDING-UNIFORM 8g LOAD 2) TORSION-50 LB LOAD AT UNSUPPORTED SPAR TIP	<p>BENDING DEFLECTIONS</p> <ul style="list-style-type: none"> MAIN SPAR-0.123 MAX OUTBD SPAR-0.118 MAX HIGHEST STRESS-7.400 PSI 			<p>TORSIONAL DEFLECTIONS</p> <ul style="list-style-type: none"> EXTREME CORNER-1.65 NEAR LOAD POINT-1.05 HIGHEST STRESS-4.350 PSI 			<ul style="list-style-type: none"> THE REDUCTION IN STIFFNESS (FROM PREDICTED) AGREED WITH THAT INDICATED BY THE MODAL TEST LOAD DEFLECTION PLOTS WERE ALL LINEAR AND STRESSES DID NOT EXCEED ALLOWABLES 																				
		POWER OUTPUT																										
THERMAL-VACUUM/SHOCK	TO MEASURE POWER OUTPUT AND ZENER DIODE PERFORMANCE IN VACUUM AND THERMAL SHOCK CONDITIONS AND TO SUBJECT THE PANEL TO A 12 DAY THERMAL SOAK	<table border="1"> <thead> <tr> <th>INPUT INTENSITY (MW/CM²)</th> <th>AVERAGE OUTPUT OF A 560 CELL MODULE (WATTS)</th> </tr> </thead> <tbody> <tr> <td>140 (AMBIENT PRESSURE)</td> <td>24.6</td> </tr> <tr> <td>53 (VACUUM COLD WALL)</td> <td>13.7</td> </tr> <tr> <td>140 (VACUUM COLD WALL)</td> <td>27.8</td> </tr> </tbody> </table>		INPUT INTENSITY (MW/CM ²)	AVERAGE OUTPUT OF A 560 CELL MODULE (WATTS)	140 (AMBIENT PRESSURE)	24.6	53 (VACUUM COLD WALL)	13.7	140 (VACUUM COLD WALL)	27.8	<p>ZENER DIODE PERFORMANCE (DURING THERMAL UP SHOCK)</p> <p>3 ZENERS PER MODULE</p> <ul style="list-style-type: none"> INITIAL PANEL TEMP _____ 202°F INPUT INTENSITY _____ 250MW/CM² ZENERS OPERATED FOR _____ 2.0 MIN ZENER OPERATING TEMP _____ 15°F (230°F = SAFE MAXIMUM) ZENERS CLIPPED VOLTAGE AT 49v 				<ul style="list-style-type: none"> THE TEST PANEL DID NOT DEGRADE WHEN SUBJECTED TO THE THERMAL VACUUM SHOCK ENVIRONMENT POWER OUTPUT AND THERMAL DATA MEASURED IN THIS TEST SUBSTANTIATES PREDICTIONS OF FLIGHT PANEL PERFORMANCE (SEE FIG 2.2) THE TEST PANEL WILL OPERATE SATISFACTORILY WITH ONLY THREE 50 WATT ZENERS FOR EACH 850 CELL MODULE BECAUSE THE STRUCTURE PROVIDES A HEAT SINK FOR ZENER DIODE ENERGY DISSIPATION 												
INPUT INTENSITY (MW/CM ²)	AVERAGE OUTPUT OF A 560 CELL MODULE (WATTS)																											
140 (AMBIENT PRESSURE)	24.6																											
53 (VACUUM COLD WALL)	13.7																											
140 (VACUUM COLD WALL)	27.8																											
		* INTENSITY VARIATION = ±10%																										
POWER OUTPUT & INSPECTION	TO DETERMINE ELECTRICAL DEGRADATION FOLLOWING EACH ENVIRONMENTAL TEST	<p>POWER OUTPUT (WATTS AT 65°C)</p> <p>SIX ACTIVE MODULES TESTED</p> <p>RESULTS OF FIVE TESTS OF EACH MODULE</p> <p>HIGH = 25.2 WATTS LOW = 23.3 WATTS AVERAGE = 24.4 WATTS (PREDICTED = 23.0 WATTS)</p>			<p>DAMAGE EVALUATION</p> <p>CELL ASSEMBLIES</p> <ul style="list-style-type: none"> 7 SEVERELY CRACKED IN HANDLING 0.93% (60 OF 6480) SUSTAINED SMALL EDGE CRACKS DURING TESTING <p>SILVER MESH PIGTAILS</p> <ul style="list-style-type: none"> 15 FAILURES DURING MANUFACTURING & TEST 			<ul style="list-style-type: none"> POWER OUTPUT PATTERN OF VARIATION INDICATED NO MEASURABLE DEGRADATION REPLACEMENT OF SILVER MESH PIGTAILS WITH STRANDED WIRE IS RECOMMENDED 																				
		FUNDAMENTAL FREQUENCY-Hz																										
SUBSTRATE FREQUENCY	TO DETERMINE IF ANY CHANGE IN SUBSTRATE FREQUENCY IS CAUSED BY THE ENVIRONMENTAL TESTS	<table border="1"> <thead> <tr> <th rowspan="2"></th> <th colspan="2">PRE TEST</th> <th colspan="2">POST TEST</th> </tr> <tr> <th>LARGE SUBSTRATE BAY</th> <th>SMALL SUBSTRATE BAY</th> <th>LARGE SUBSTRATE BAY</th> <th>SMALL SUBSTRATE BAY</th> </tr> </thead> <tbody> <tr> <td></td> <td>74</td> <td>78</td> <td>69</td> <td>74</td> </tr> </tbody> </table>			PRE TEST		POST TEST		LARGE SUBSTRATE BAY	SMALL SUBSTRATE BAY	LARGE SUBSTRATE BAY	SMALL SUBSTRATE BAY		74	78	69	74			<ul style="list-style-type: none"> THE 6% DROP IN FREQUENCY REPRESENTS A SMALL RELAXATION OF SUBSTRATE TENSION AND DOES NOT SIGNIFICANTLY AFFECT PANEL PERFORMANCE 								
	PRE TEST		POST TEST																									
	LARGE SUBSTRATE BAY	SMALL SUBSTRATE BAY	LARGE SUBSTRATE BAY	SMALL SUBSTRATE BAY																								
	74	78	69	74																								
		FUNDAMENTAL FREQUENCY-Hz																										

Figure 6-2 TEST RESULTS SUMMARY

EOL DOUT FRAME



Strain Gage Locations



Accelerometer Locations

Figure 6-3: TEST PANEL INSTRUMENTATION

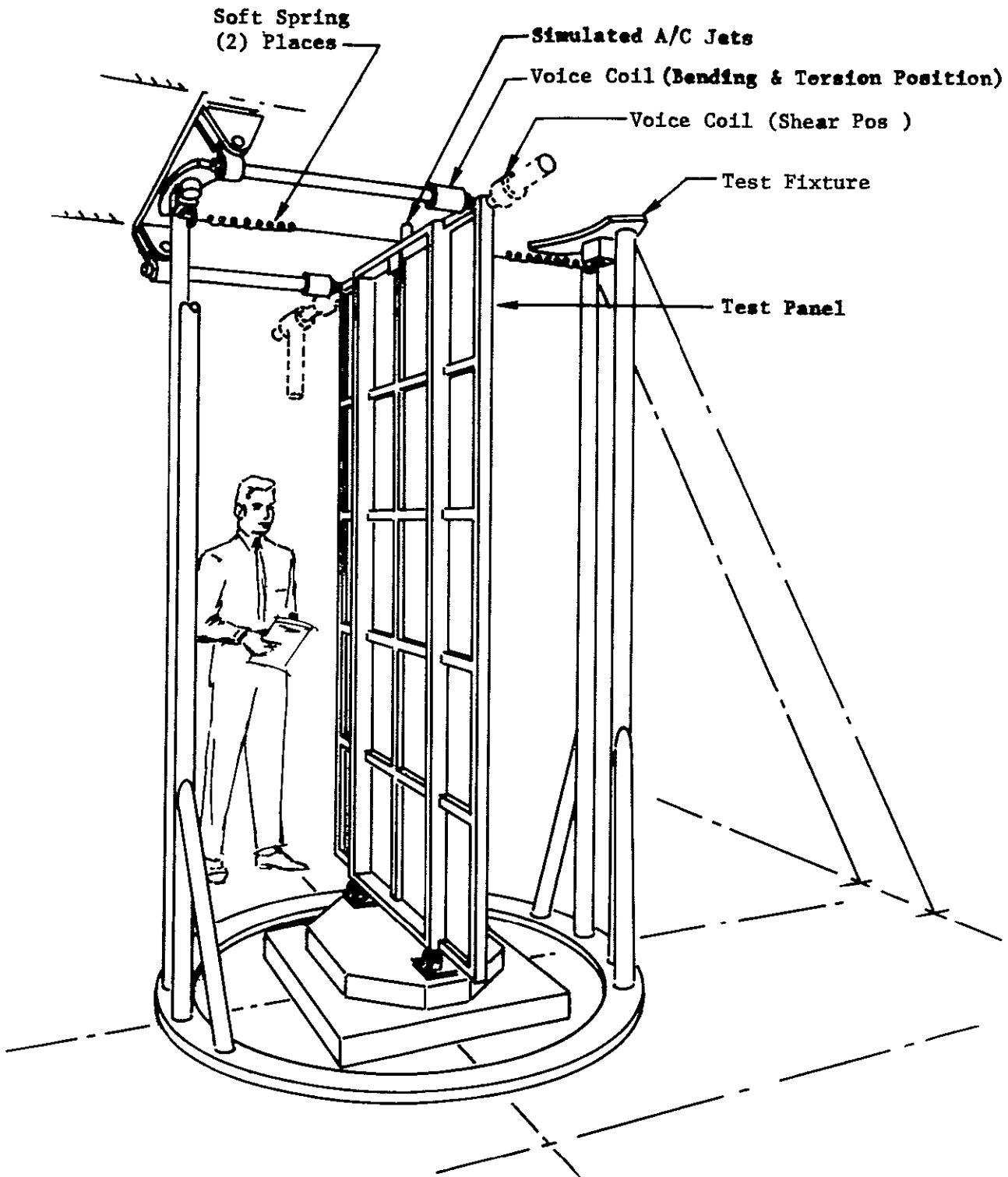


Figure 6-4 MODAL VIBRATION TEST SETUP

the outboard end of the panel. The initial set of voice coils, attached to the main spars on the first three runs, M101, M102, and M103, were not adequate to produce the desired power. Later runs used a more powerful and heavier set of voice coils attached at the outboard edge spars, to excite bending and torsion. A third set was used to excite the panel in shear (in-plane excitation). Measurements of panel motions were made with accelerometers and stresses were measured with strain gages located as shown in Figure 6-3.

Test data for the bending excitation were obtained satisfactorily. However, during the first sweep in the torsion mode, the amplitude increased rapidly at about 13 Hz, causing the monitoring limiter to shut down the excitation. Subsequent sweeps, with the limiter adjustment relaxed, showed that the panel torsional stiffness was less than expected. Some difficulty was encountered in the shear mode at about 24 Hz where a sudden amplitude increase was encountered, accompanied by high frequency content and acoustic noise. This was attributed to a free play tolerance buildup between the panel hinges and the fixture.

An attempt to measure panel motion at points other than the fixed accelerometer locations was made, but the roving pickup measurements were unsatisfactory because the pickup would influence the panel or it would bounce and not follow the panel vibration frequency. However, node positions were successfully determined by sensing no-motion points with the finger tips.

6.1.2 EVALUATION OF TEST RESULTS

—

The panel stiffness was less than expected.

—

The measured frequencies and a comparison with the calculated frequencies for the various modes is given in Table 6-1. When allowances were made in the calculations for the added instrumentation weight, the calculated results still indicated a higher stiffness than found by test for both the bending and torsion modes. The bending stiffness was about 80% of calculated, the torsion stiffness was about 65% of calculated.

Table 6-1
MODAL TEST RESULTS

Mode	Frequency Hz		Damping Coefficient	
	Measured	Calculated	X-Y Plot	Decay
First Torsion	12.2	17.0*	0.038	0.035-0.038
First Shear	22 (X-Y) 28 (Decay)	27.5*	N.G.	0.037
First Bending	28.4	33.9*	0.11	0.104
Second Torsion	50	67.9*	0.062	0.062
Chord Bending	58	80.9*	0.062	0.063
Large Substrate	68-71		0.066-0.085	None
Small Substrate	78		0.063	None
Unidentified	90±	103.0*	0.045	0.033-0.036

*Calculated frequencies not corrected for final measured weight or for instrumentation weight.

This was later substantiated by the static load tests, see Section 6.5.

Damping factors determined by the two methods given in Table 6-1, showed acceptable agreement. The minimum measured damping was equivalent to a magnification of 30 for the first torsion and shear modes. The maximum damping, for first bending, was equivalent to a magnification of 10.

The mode shapes generally agreed with the calculated values for all but the highest frequency measured. Selected mode shapes are diagrammed in Figures 6-5, 6-6, and 6-7. The decay record for the first bending mode is shown in Figure 6-8.

The resonant frequencies of the two different substrate bays were appreciably greater than predicted by a simple extrapolation of LASA measured data. The difference is attributed to the smaller substrate bays and the differences in the structure between LASA and the light weight test panel.

6.2 ACOUSTIC TEST

—

The acoustic test was conducted to expose the test panel to an overall acoustic noise level of 150 ± 3 db and to determine the panel responses.

—

The test panel was exposed to a reverberant acoustic noise field of 148.2 db overall. The specific 1/3 octave band levels and tolerances were the controlling levels. No acoustic response analysis was made to predict test results. However, a measure of the expected response was obtained by extrapolation of results from the testing of the SCS-43 panel in the Large Area Solar Array (LASA) program. Results of the comparison are discussed in Section 6.2.2.

Frequency = 28.4 Hz

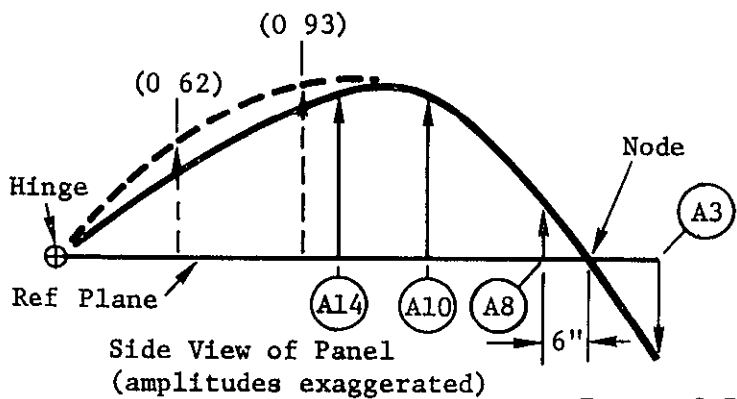
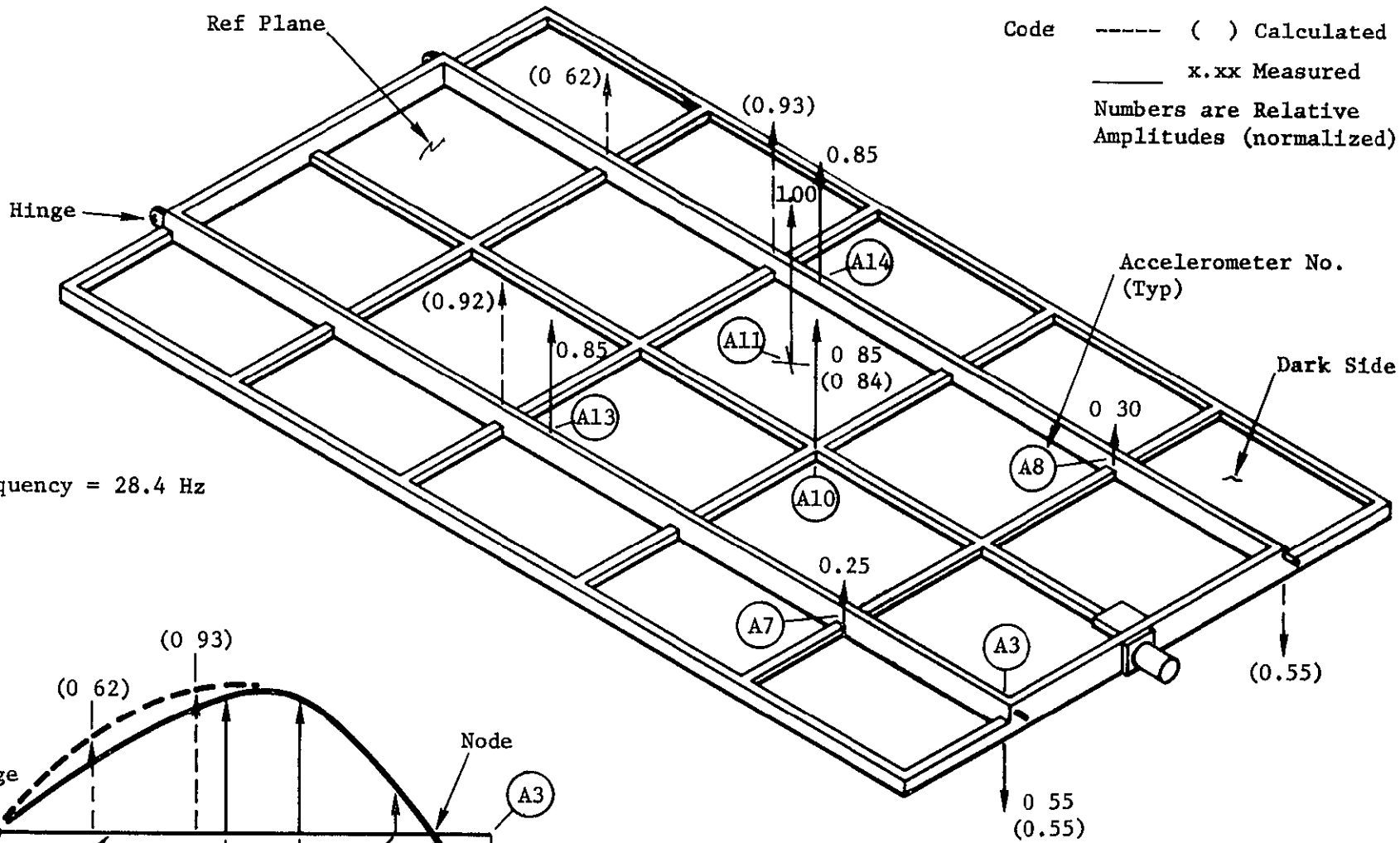


Figure 6-5 FIRST BENDING MODE SHAPE

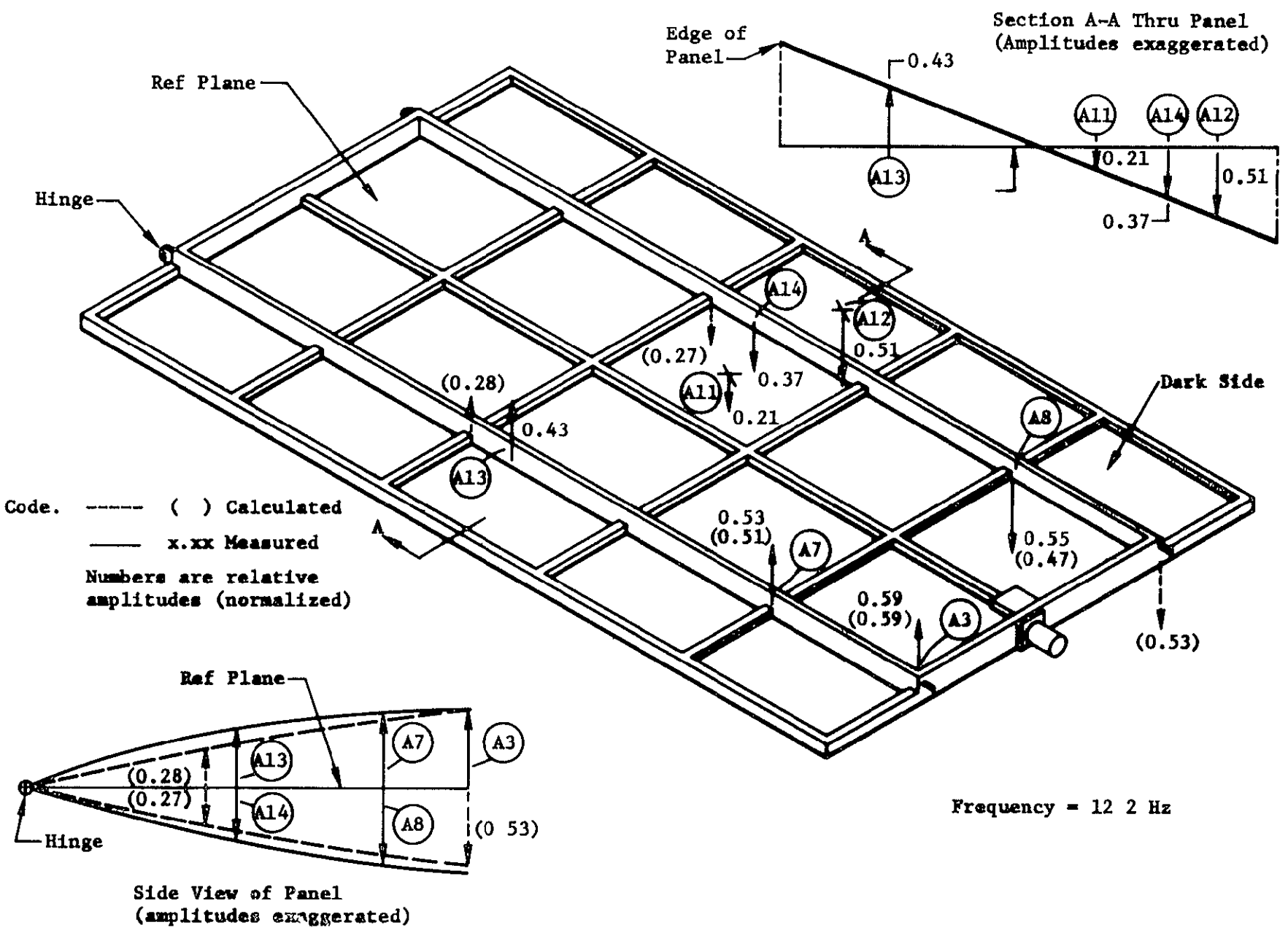
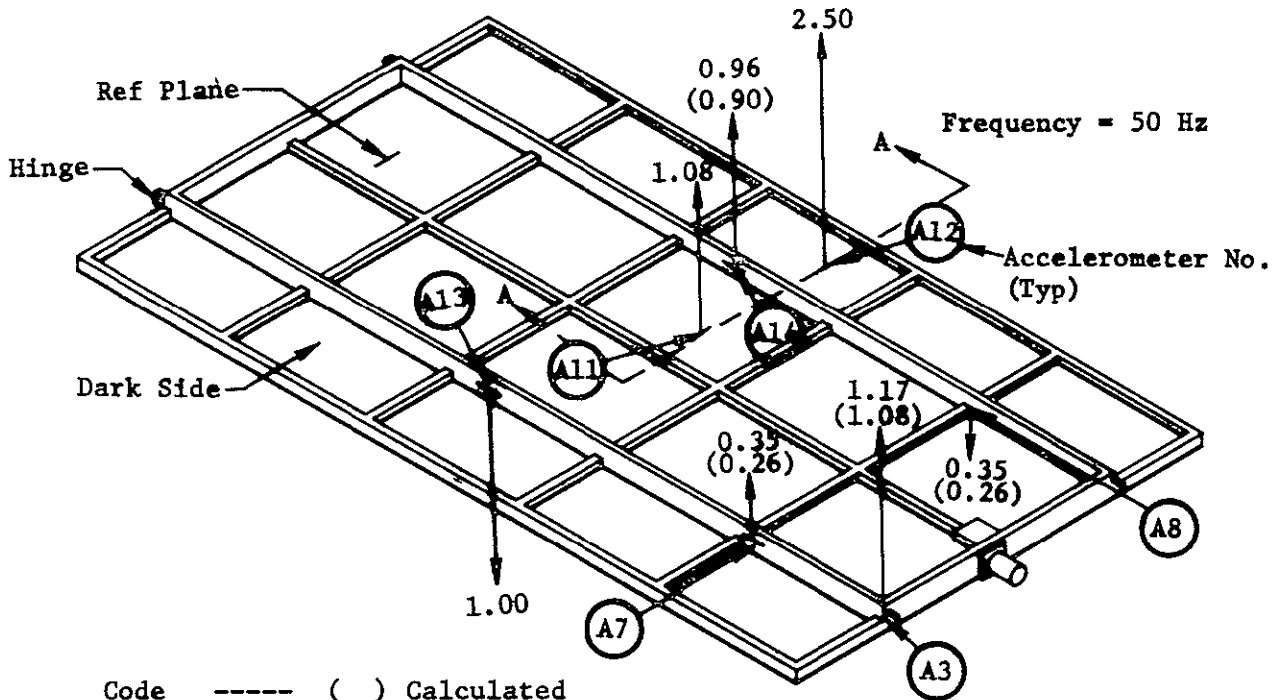


Figure 6-6 FIRST TORSION MODE SHAPES

D2-121773-2



Code ----- () Calculated
 _____ x xx Measured
 Numbers are relative
 amplitudes (normalized)

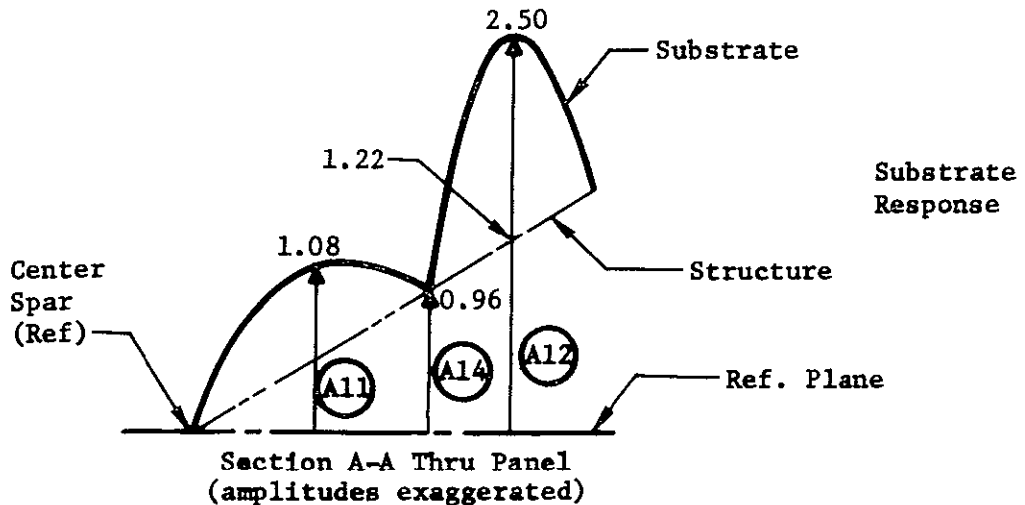
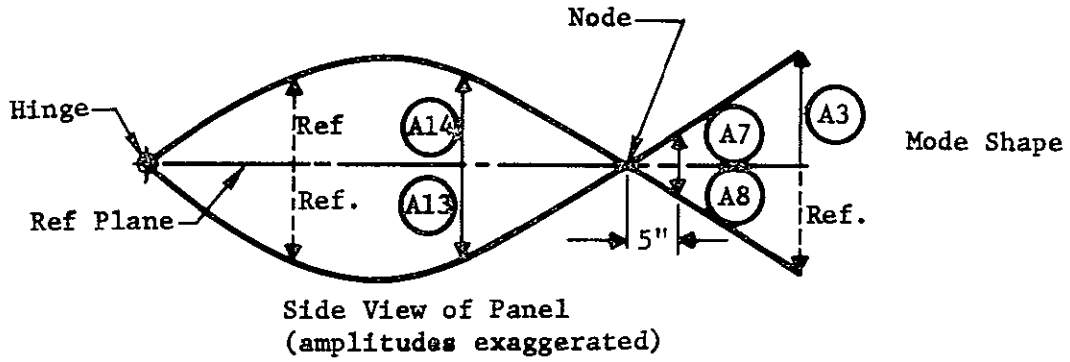


Figure 6-7. SECOND TORSION MODE SHAPES

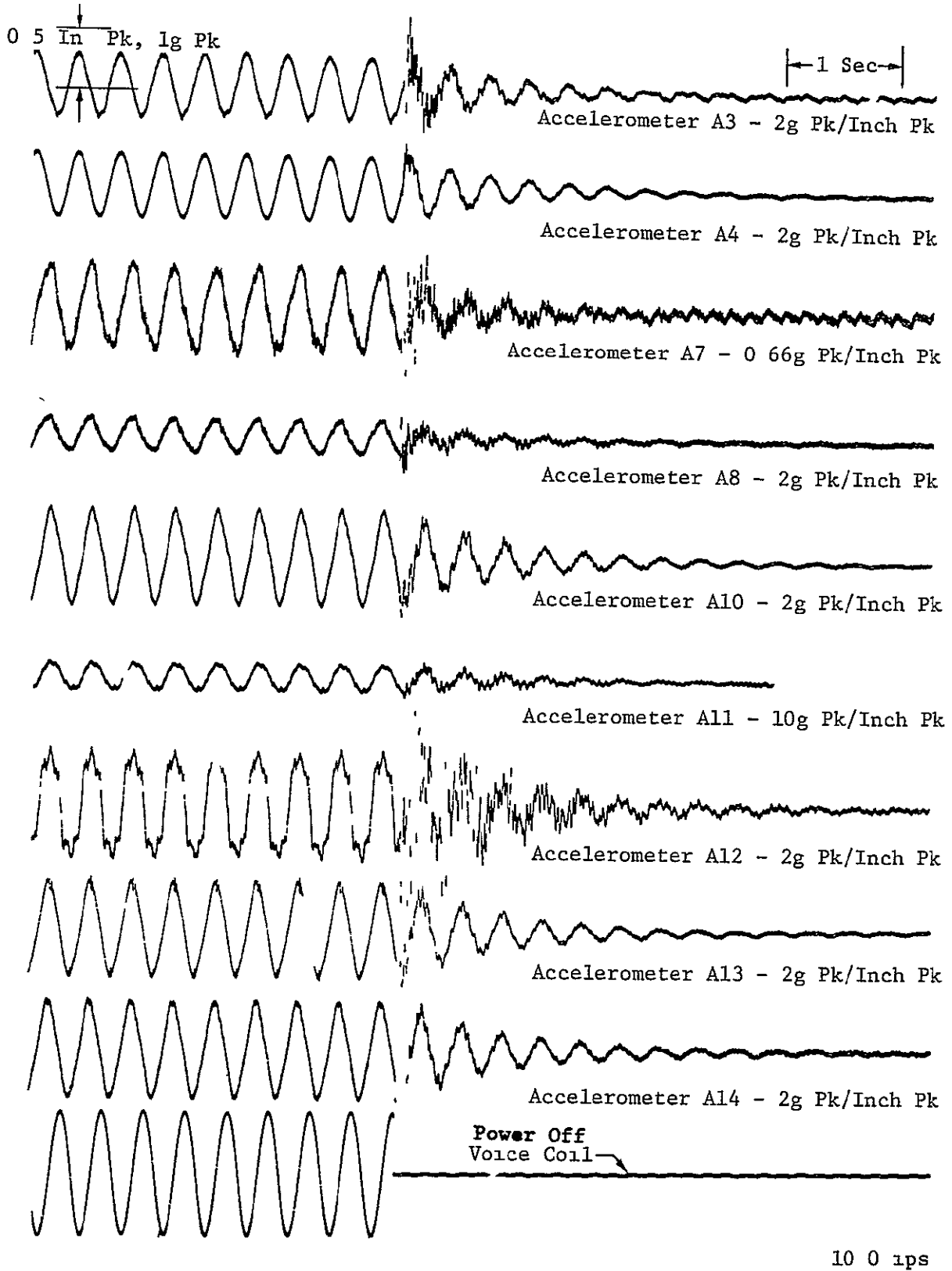


Figure 6-8 OSCILLOGRAPH RECORD, FIRST BENDING - DECAY

6.2.1 TEST ACTIVITIES

—

Satisfactory acoustic test data were obtained.

—

The test panel was supported in the test chamber between two 80 Hz cutoff exponential horns as shown by Figure 6-9. Two separate systems controlled the Altec-Lansing acoustic transducers driving the horns to ensure random excitation of the panel.

Microphones mounted adjacent to each side of the panel were used to measure the environment. Accelerations were measured by 9 accelerometers and strains by 10 strain gages. The required acoustic spectrum and the measured spectrum obtained by averaging the six microphones are shown in Figure 6-10.

The only visual indication of motion during the test was a blurring of the exposed substrate tapes visible as a white line between the solar cell modules. During the 60 second test run the wire connections to two accelerometers loosened and the signal was lost. However, the first 20 seconds of data from these runs was available and satisfactory for data reduction. The remaining instrumentation provided data for the complete run.

Visual examination after testing showed no structural damage. One solar cell, adjacent to the edge of the panel, had been cracked by finger pressure during handling. The silver mesh interconnectors at the inboard edges of the submodules showed some curling and separation from the RTV-40 bonding agent. This occurred only where the silver mesh on the substrate side of the cell groups extended beyond the cell edge (nominally, it is installed flush) so the function of the panel was not affected. However, this condition was an indication of flexing of the silver mesh which became more significant in view of the subsequently discovered failures of the mesh pigtails discussed in Section 6.9.

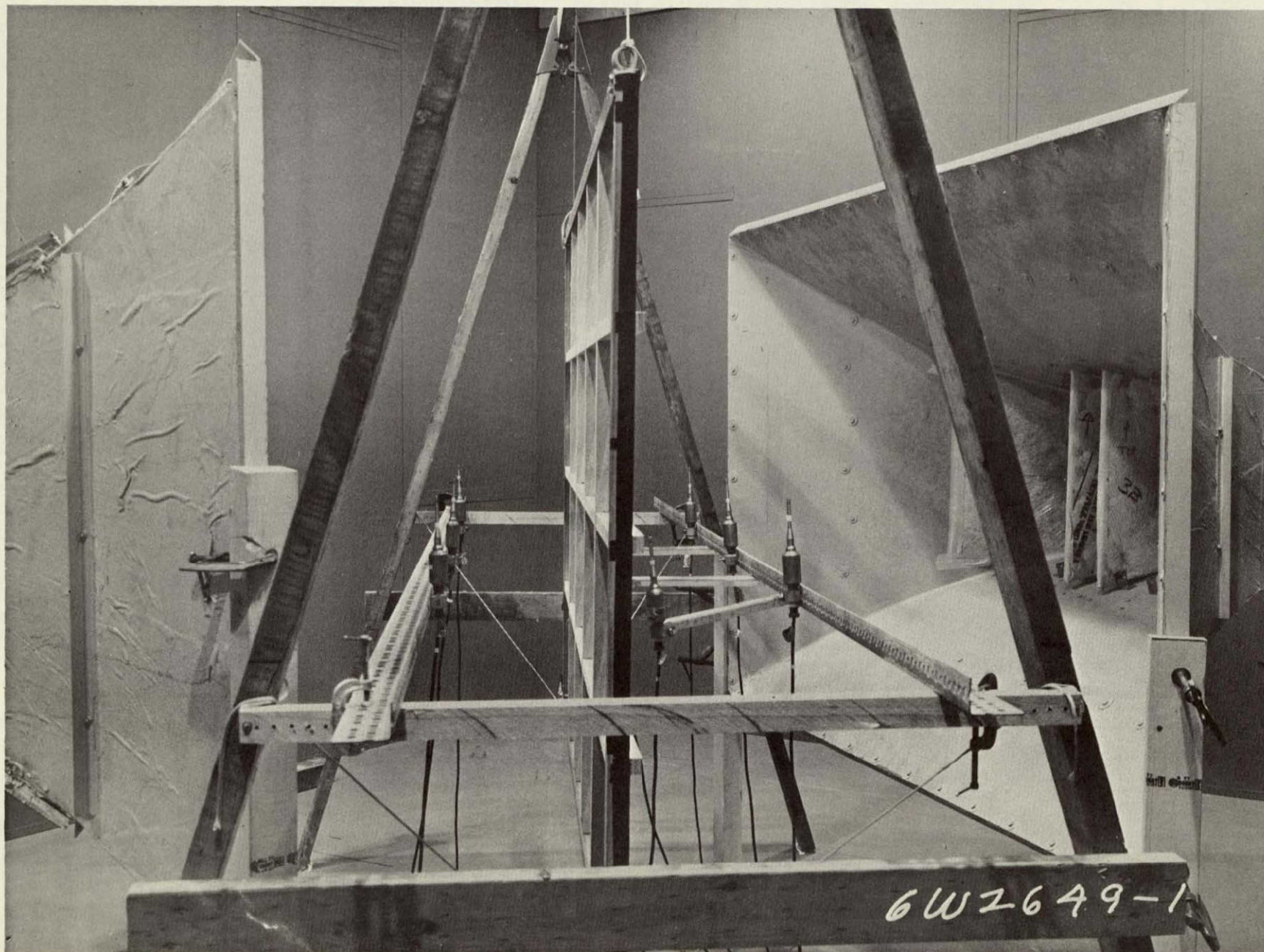
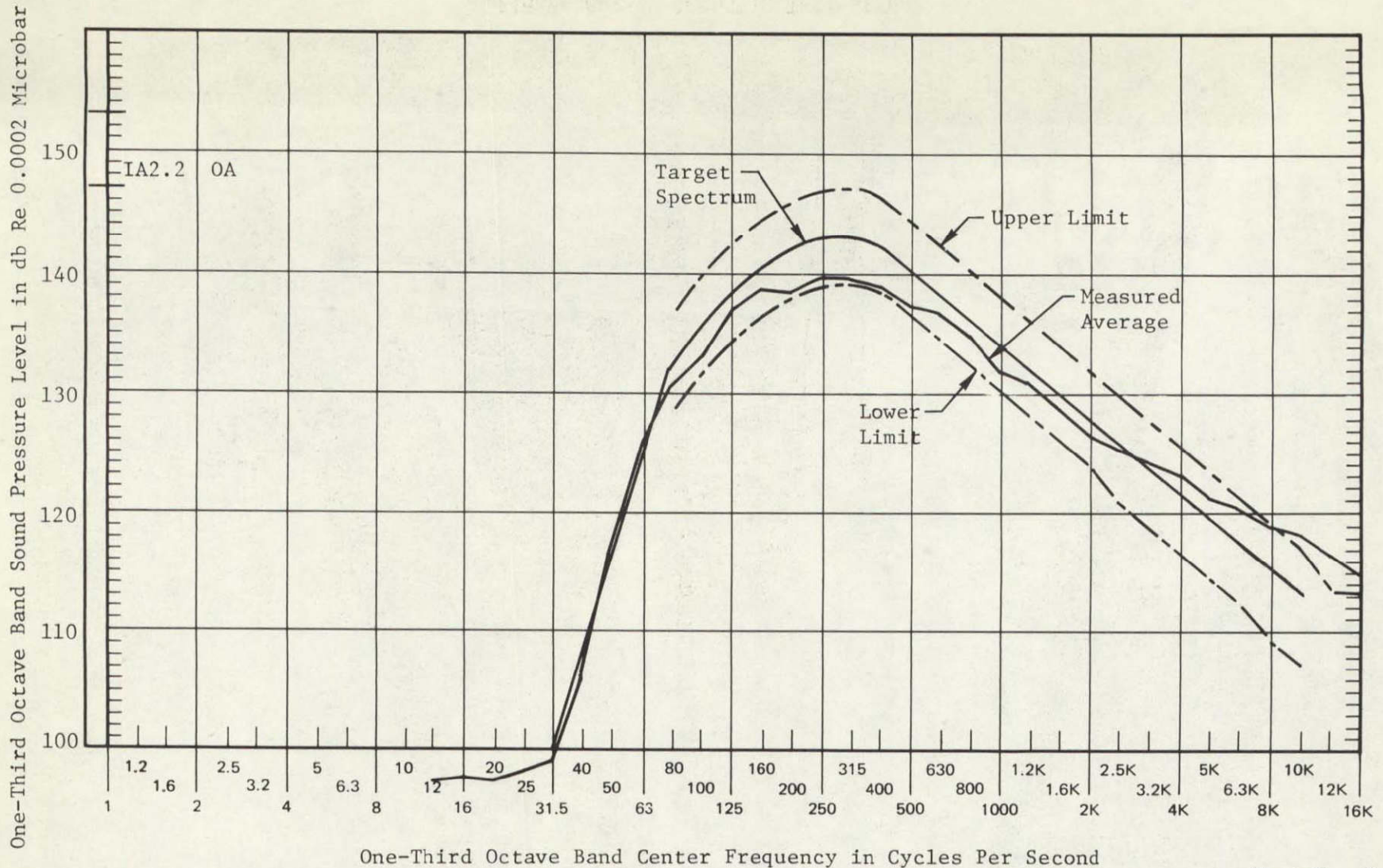


Figure 6-9: ACOUSTIC TEST SETUP



Arithmetic Average of 6 Microphones
A1, A2, A3, B1, B2, B3

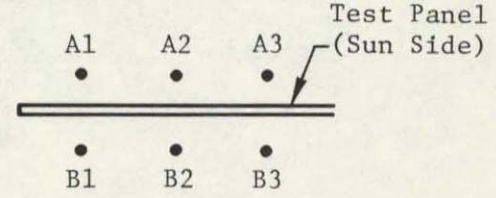


Figure 6-10: AVERAGE ACOUSTIC SPECTRUM

6.2.2 EVALUATION OF TEST RESULTS

—
The panel structure response was nominal; however, the substrate response was four times greater than estimated.

—
By simple extrapolation of the SCS-43 (4 ft. by 4 ft. panel) test results from the LASA program, the substrate response was expected to be about 75 "g" rms. The measured response in the largest substrate bay, shown in Figure 6-11, indicated a response of 305 "g" rms. This may have been, in part, due to the upward shift of the substrate resonant frequencies (from about 35 Hz to 60 or 70 Hz for the fundamental mode). In addition, the beams bounding the substrate bay had significant response during this test, whereas the beams were constrained in the acoustic test of the SCS-43 LASA panel. Despite the high accelerations, no separation of the cells from the substrate occurred and the allowable stress for the RTV-40 cell bonding agent was not exceeded.

The highest strain was measured on a main spar near the middle of the panel with an equivalent maximum 3 sigma stress of 4300 lbs/in². No structural damage was observed as a consequence of this excitation.

6.3 RANDOM VIBRATION TEST

—
This test was conducted to determine the adequacy of the test panel to withstand wide-band random excitation.

—
The excitation input during the random vibration test was along the launch vehicle roll axis which is nearly parallel to the plane of the panel in the stowed position. No formal analysis was made to predict random responses for the panel. Because of the small component of random excitation normal to the panel and the dampers attached at the tips, important dynamic response was not expected. No analysis for the longitudinal modes was made, consequently, there was no analytical basis for

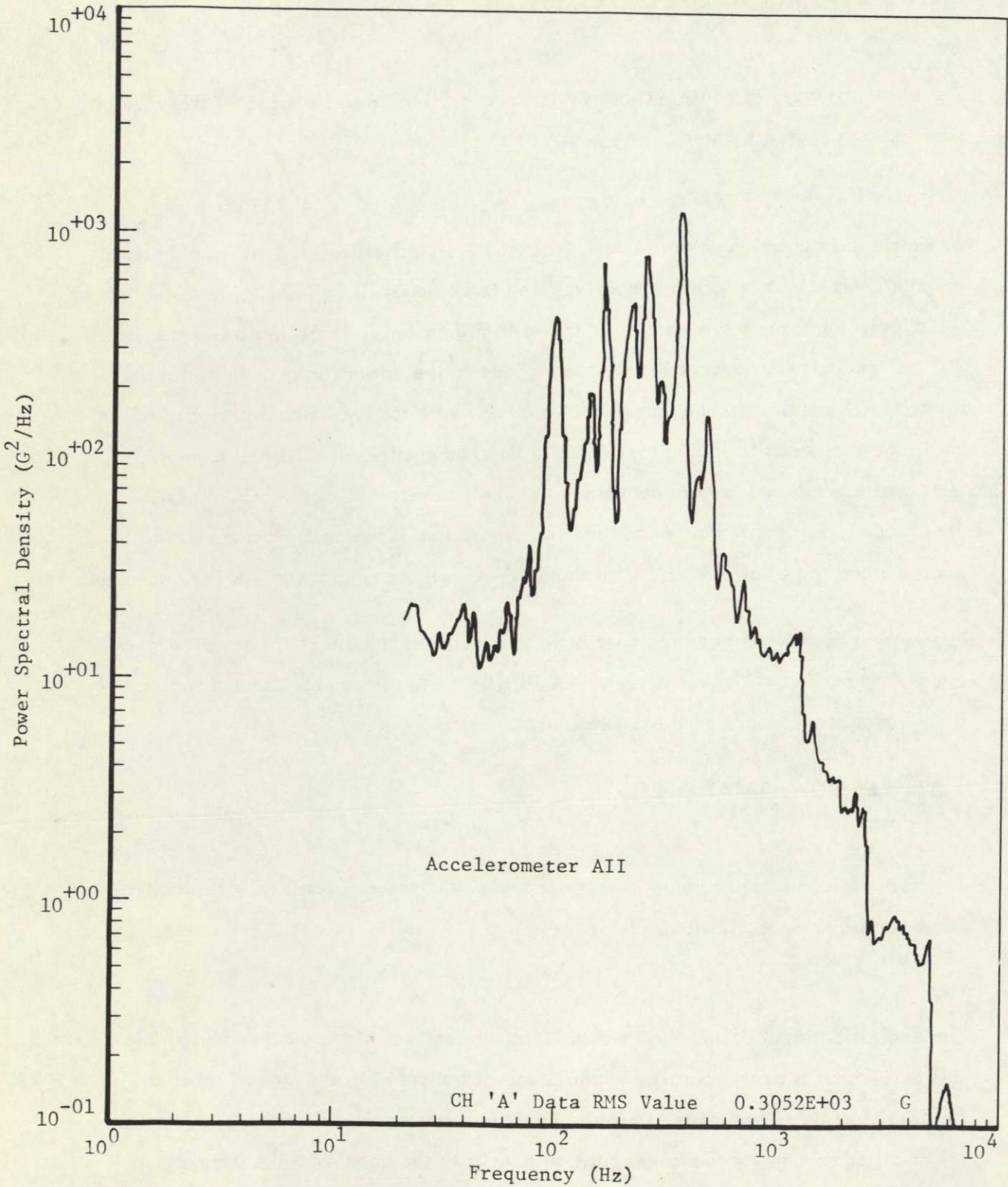


Figure 6-11: SUBSTRATE ACCELERATION RESPONSE -ACOUSTIC TEST

estimating longitudinal random response. The only area of concern was the possible effects of the concentration of mass due to the attitude control jet simulation and the sun sensor simulation. For this area, an acceleration limiter setting of 30 "g" peak was calculated for the initial test runs.

6.3.1 TEST ACTIVITIES

—

The test panel adequately withstood the random vibration environment.

—

An adapter fixture attached to a Ling 249 vibrator supported the test panel at its hinges. The panel was tilted 4° off the vertical axis of the vibrator and supported at the tip by two dampers. The test setup is shown in Figures 6-12 and 6-13. Selection and modification of the Mariner '67 type boost dampers for this and the sinusoidal test is discussed in Section 5.7.

Prior to installing the panel, evaluation of the test fixture was made to obtain the desired random vibration spectrum at both hinge points on the fixture. The required spectrum and the measured input spectrum used in this test are shown superimposed in Figure 6-14.

Test procedures were followed except that the run at full level was interrupted after 3 seconds by the 30 "g" limiter monitor accelerometer. After examination of the on-line oscillograph traces, the limit was raised to 40 "g" and the panel was excited at the required level for 48 seconds before the limiter tripped again. A third run at the specified level was then made for 12 seconds, resulting in a total exposure time of 63 seconds.

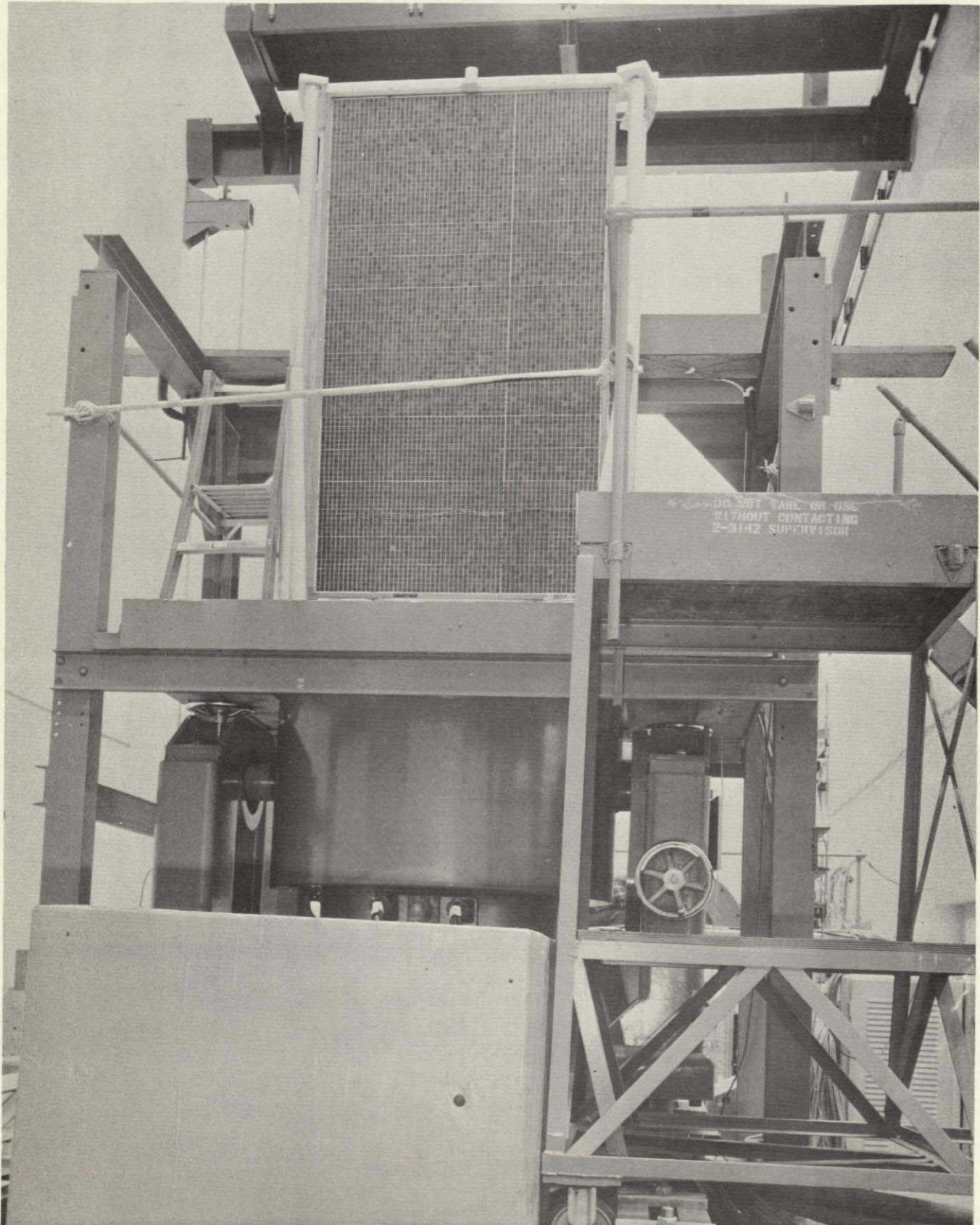


Figure 6-12: RANDOM VIBRATION TEST SETUP

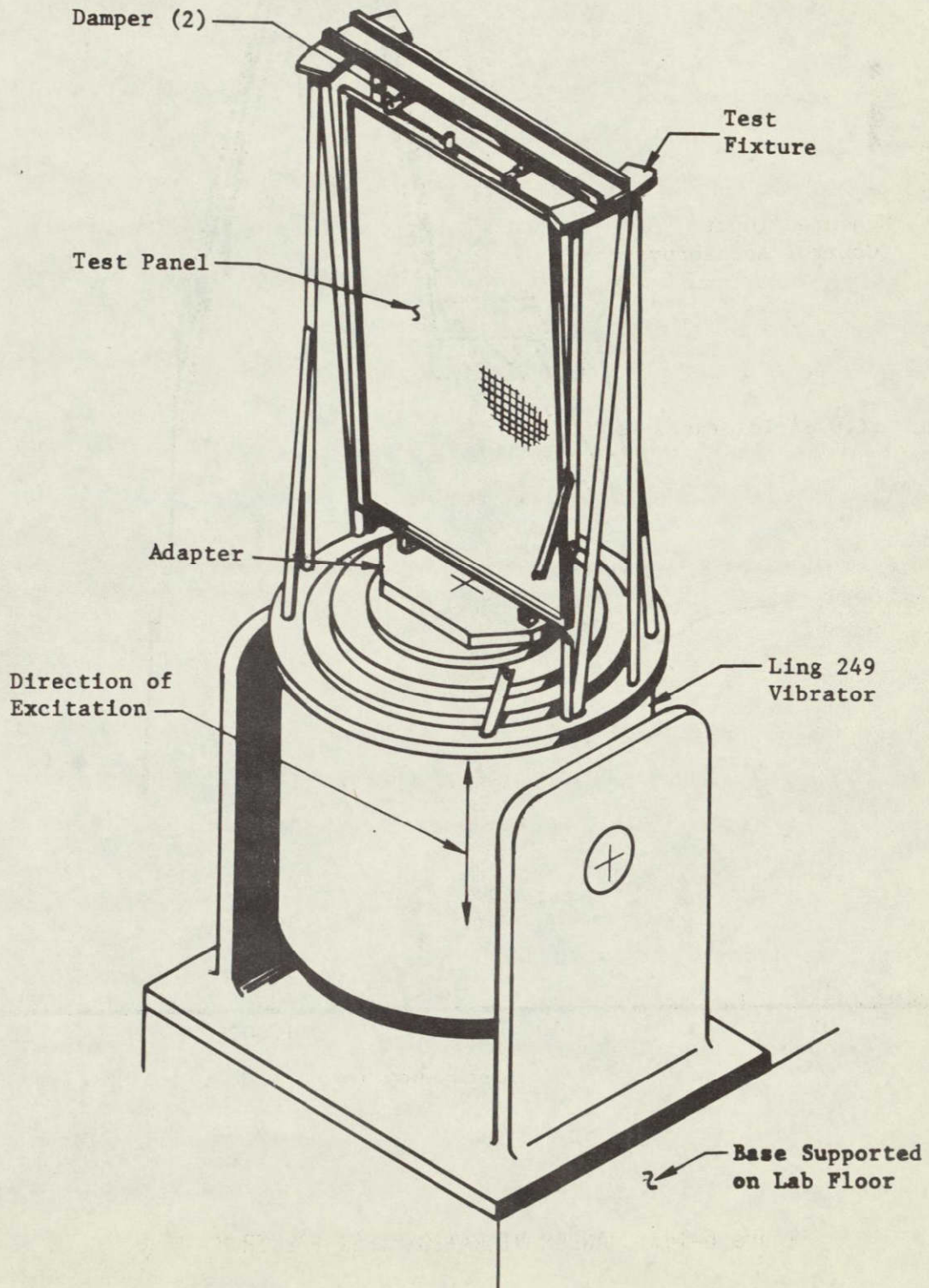


Figure 6-13: RANDOM VIBRATION TEST SETUP

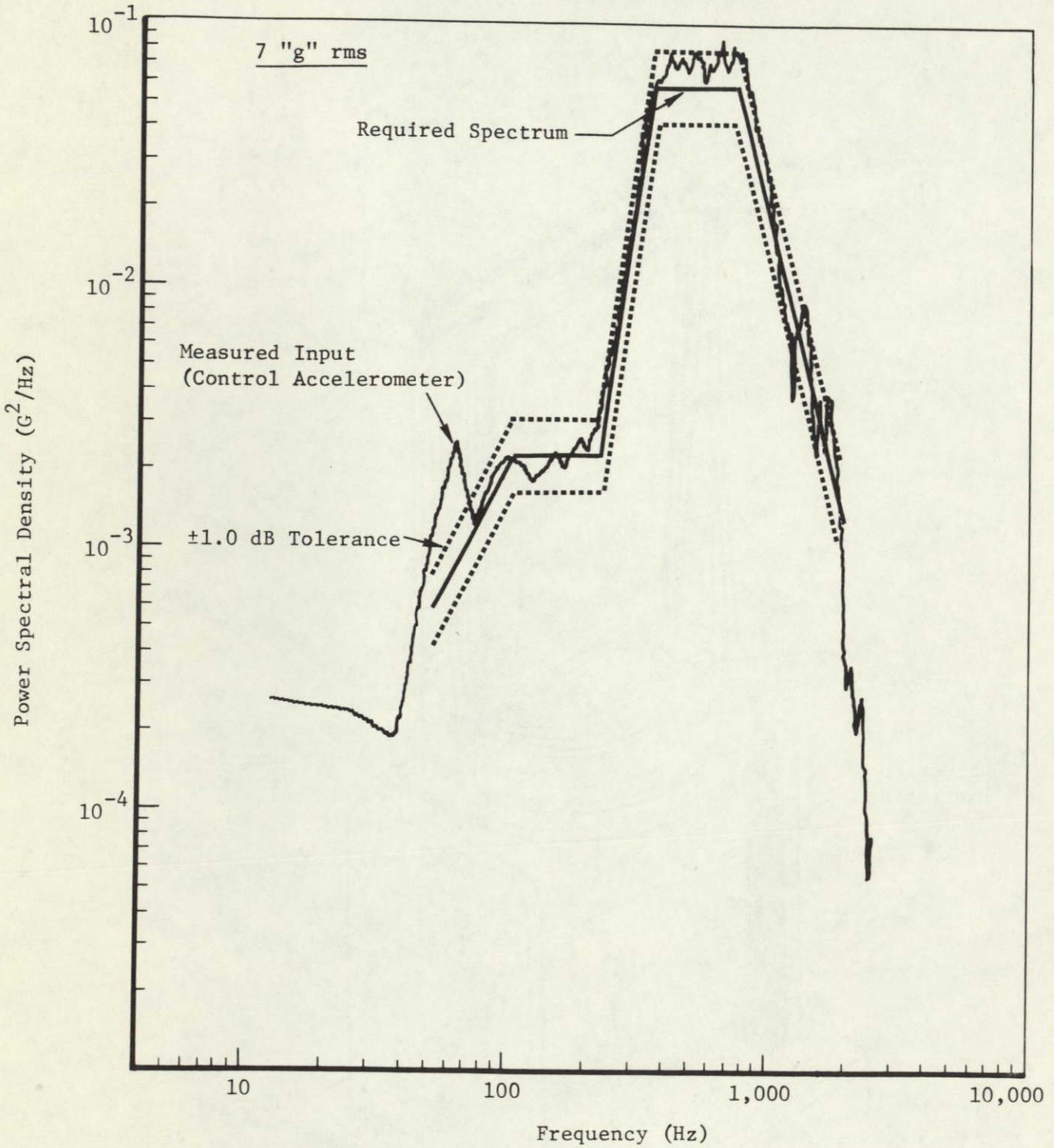


Figure 6-14: RANDOM VIBRATION TEST SPECTRUM

6.3.2 EVALUATION OF TEST RESULTS

—
Stress and acceleration levels were low in the random vibration test, as expected.

—
The area of most concern, the responses and stresses near the simulated equipment at the panel tip, did not show excessive response levels. The longitudinal response in this area, from accelerometer A16, was 6.1 "g" rms. A value of 8.05 "g" rms normal to the panel was obtained from accelerometer A10 on the longitudinal intercostal. The large substrate bay acceleration shown in Figure 6-15 was 14.6 "g" rms. The general level of 3 sigma peak stress was about 600 lb/in², with a maximum value of 1100 lb/in² in the main spar cap near the hinge.

No structural damage was observed as a result of this test. Damage to a silver mesh interconnector, possibly attributable to this test, was subsequently found, as discussed in Section 6.9.

6.4 SINUSOIDAL VIBRATION TEST

—
This test was designed to provide excitation of the panel at the hinge points that would produce response of the panel to the levels equivalent to the response when excited to the specified levels at the four spacecraft attach points.

—
To simulate the specification requirements the panel must be excited in translation normal to the panel at four points: the two hinges and the two tip latch fittings. In order to avoid using two vibrators and thus to reduce cost, the test panel was excited at the hinges only, with the panel tip supported by dampers. The analyses to determine the equivalent test levels and to select the dampers is described in Section 5.7. Details and limitations of the four-segment test approach are discussed in D2-121321-2, "Light Weight Solar Panel Development Test Report."

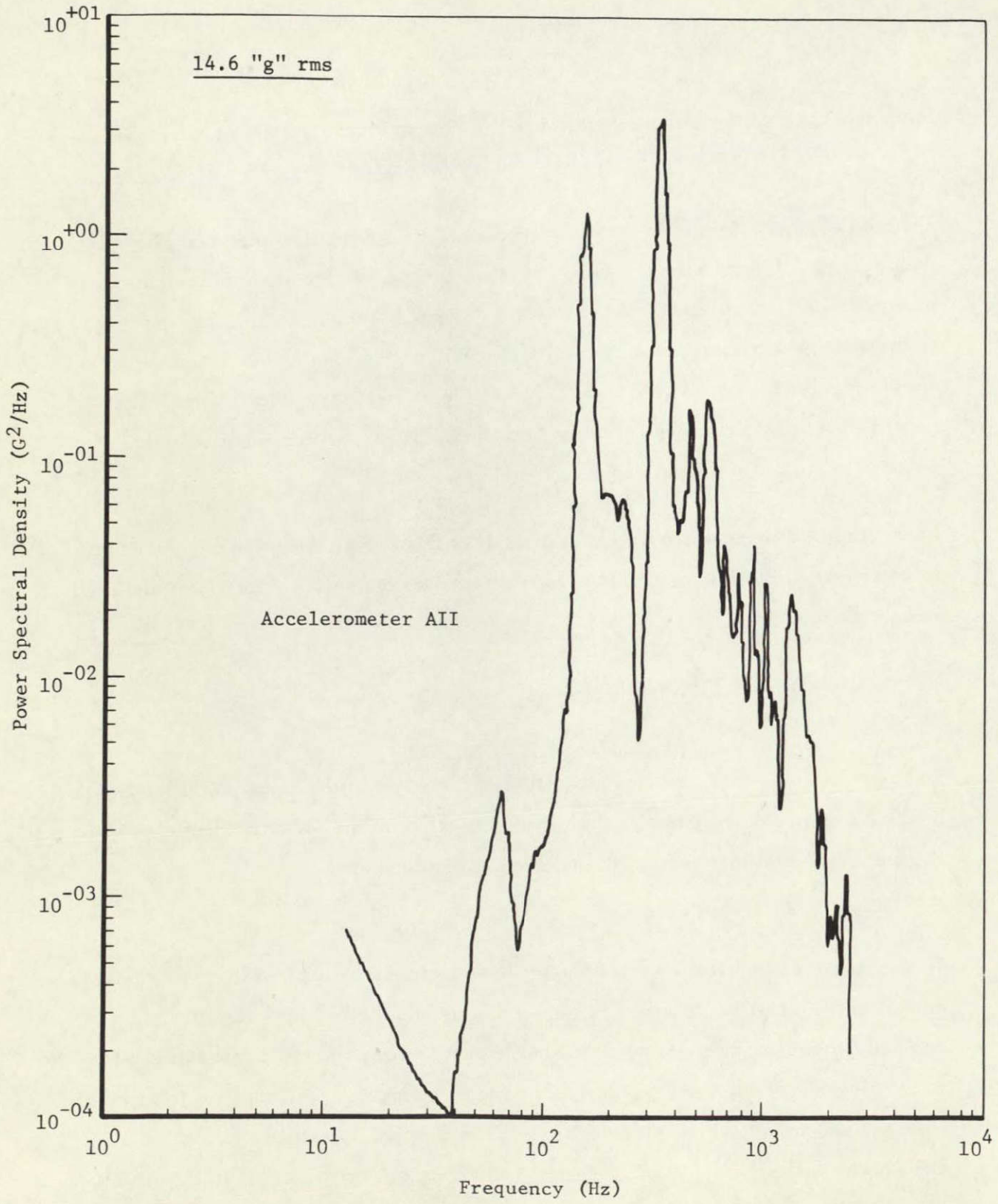


Figure 6-15: SUBSTRATE ACCELERATION RESPONSE - RANDOM VIBRATION

Objectives of this test were to subject the panel to the specification-equivalent environment and to determine important frequencies and responses. Analyses were not made to specifically predict responses; however, stresses for zero margins of safety were calculated at critical frequencies and amplitudes.

6.4.1 TEST ACTIVITIES

—
The sinusoidal vibration test was conducted in four steps to obtain responses equivalent to the specified condition.

—
The test panel was suspended by the hinges from an adapter fixture attached to the Ling 249 vibrator as shown in Figure 6-16. Tip dampers used for the random vibration supported the panel during this test. Test levels are shown in Figure 6-17. The upper chart in this figure shows the specification levels for four-point excitation. Planned and actual test levels are superimposed in the lower chart. The planned levels were achieved in four test segments, selection of which was based on the predictions of important modes and frequencies and on the limitations of the test equipment. The test was accomplished in segments to obtain "equivalent" excitation which varies with each resonant mode. A problem arises when resonances are close and the higher frequency modes require a significantly lower excitation level. Under these circumstances the excitation at the lower frequency mode can overdrive the higher frequency mode.

The following exceptions to the planned test levels were made:

- 1) As a result of measured resonant frequencies in the modal test, the levels for the first and second segments were changed to agree with the specified input increase which started at 30 Hz as shown in the upper chart of Figure 6-17. A change in frequency at which the segment test was to be stopped was also necessary.
- 2) The first segment (Segment I) was made in two sweeps, one for the constant "g" input then changing to the other at about 100 Hz for the increasing level to 2 "g" rms. During this latter sweep, difficulty in controlling the level was encountered, and two unscheduled stops were made. However, the test was re-started in each case and the required excitation was obtained.

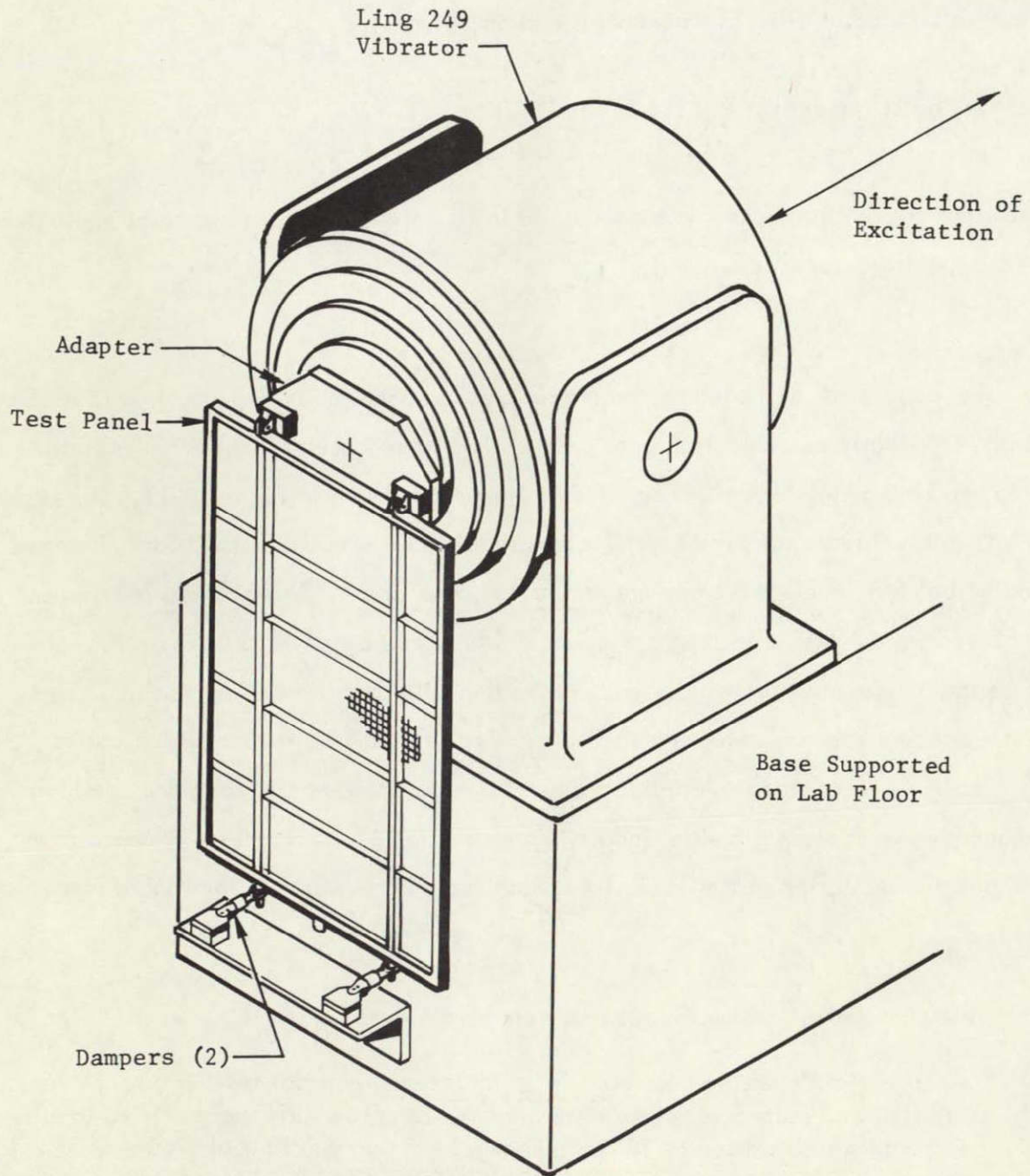
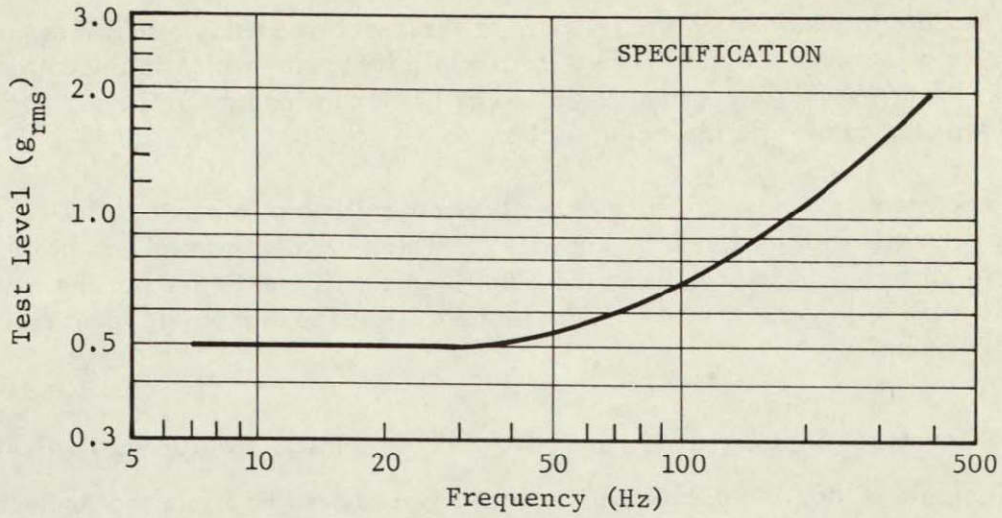


Figure 6-16: SINUSOIDAL VIBRATION TEST SETUP



Specification for Translation Excitation
(At 4 Points---Hinges and Tip Latches)

- 1 Rigid Rotation 7.9 Hz
- 2 First Torsion 19.2 Hz
- 3 First Bending 34.3 Hz

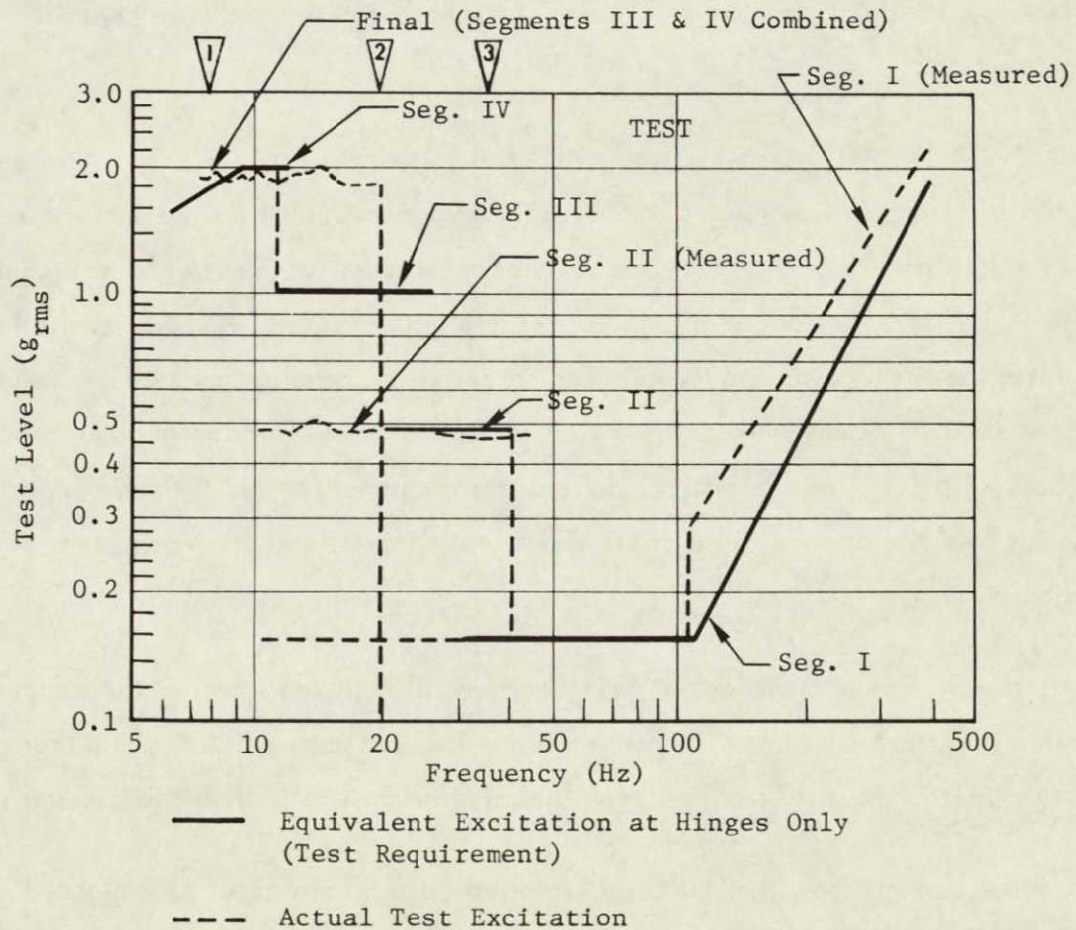


Figure 6-17: SINUSOIDAL VIBRATION TEST LEVELS

- 3) To provide information on the response of the lower frequency resonances, the sweeps of Segments II and III were started at a frequency which included the next lower segment. Segment II started at 10 Hz instead of 20 Hz and Segment III was started at 8 Hz instead of 12 Hz.
- 4) The Segment III sweep was inadvertently accomplished at a nominal 2.7 "g" peak input from the minimum frequency for which vibrator control was possible up to 20 Hz. This accomplished both the Segment III and IV tests at the same time eliminating one run by running Segment III at the higher "g" level required for Segment IV.

The actual levels for Segments I, II, and III and IV combined, are also shown in Figure 6-17. The table of limiting accelerometer levels was revised to assure that expected amplitudes would not be exceeded.

6.4.2 EVALUATION OF TEST RESULTS

—
Stresses and accelerations measured during sinusoidal vibration were well within acceptable limits.

—
The test spectrum previously calculated for the test procedures from the analytic solutions for resonant frequencies required revision to account for the resonances measured in the modal test. The analytic calculations had indicated only very low excitation forces for the first and second torsion, and for the chord bending modes. This results from the stiffness symmetry and only a small amount of mass dissymmetry about the longitudinal axis. Thus the critical motions for the panel for this test were expected to be the response at about 8 Hz of the rigid rotation mode and the response at the first bending mode.

The tip damper requirement for the 8 Hz mode was to limit the travel of the dampers to something less than 0.15 inch in order to ensure that the damper force would increase with amplitude. For the bending mode, the requirement was to limit the bending stresses.

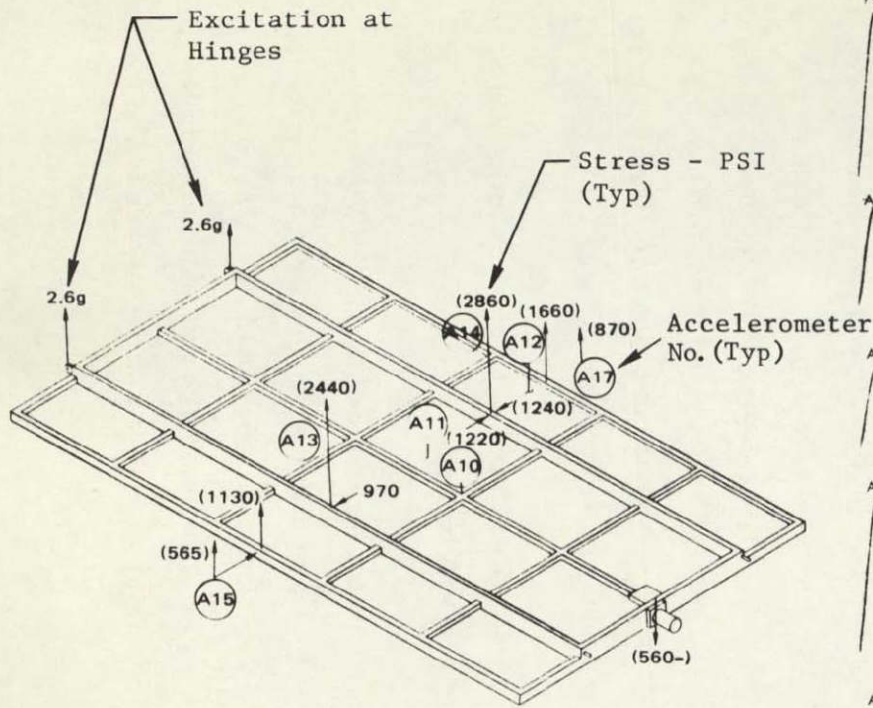
Stress measurements show that the "rigid rotation" stresses are about 15% higher than the bending mode stresses. Examination of the stress and acceleration traces show a large

component of a higher frequency which is apparently driven off-resonance by the non-linear characteristics of the damper. Accelerations and stresses for the bending mode are shown in Figure 6-18.

Although the stress values are from the Segment III and IV run that went to 20 Hz, the X-Y plots from the next lower level, Segment II, show the stress peak to be at a frequency of 18-20 Hz. Oscillograph records of the Segment III and IV run at this frequency with a 40-cycle filter provided clean traces from which phase and amplitude were obtained. The highest stress measured in the main spar caps was 3250 lbs/in² as compared to 10,900 lbs/in² for zero margin of safety. In the main beam channels the maximum stress was 1240 lbs/in² as compared to 4500 lbs/in² for zero margin of safety. Note that the ratio of about 3.5 between the maximum stress measured and the calculated stress at zero margin of safety does not mean that an increase of that magnitude in excitation is possible. A significant initial stress is in the members due to tape tension and to possible manufacturing straightness considerations. In addition, the damper non-linear characteristics could be important. The non-linear characteristics (probably due to the dampers) were seen in the oscillograph record for the starting portion of the final test sequence. The traces had the high frequency content filtered out, but an appreciable, almost harmonic, content remained. At this frequency and amplitude, the ratio of damping forces between the two dampers is about 1.5. Peak stresses from the combined components are 3250 lbs/in² as compared to 2860 lbs/in² for the bending mode condition.

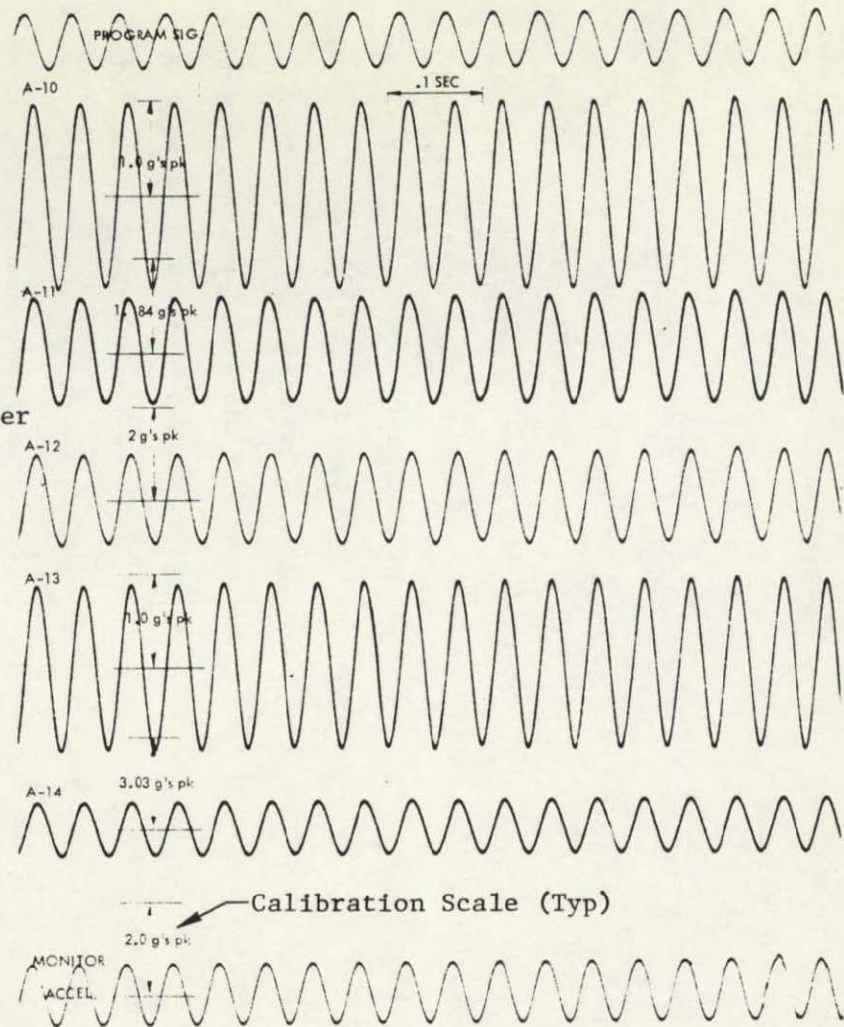
Measured stress levels were generally related to each other by ratios similar to those for the calculated zero-margin-of-safety stresses.

With one exception, the accelerations experienced during the Segment I sweep were less than 5 "g" on the structure even at high frequencies. For accelerometer A10, on the longitudinal intercostal, one sharp spike reached 15 "g". The substrate response had peak values of 8 "g" and 12.5 "g" on the large and small substrate bay, respectively. The strain gages showed their peak values at the 20 Hz bending frequency.



Frequency = 18-20 Hz

Segment IV Stress Levels



Segment II Acceleration Responses

Figure 6-18: SINUSOIDAL SWEEP TEST RESULTS - BENDING MODE

No structural damage was encountered in this test; however, another silver mesh pig-tail failure was discovered in the subsequent power output check (see Section 6.9).

6.5 STATIC LOAD TESTS

—
The static load tests demonstrated greater panel flexibility than anticipated.

—
The two specified loading conditions were: (1) 8 "g" distributed load normal to the panel and, (2) 50 pounds point loading. In the 8 "g", or bending, test the panel was supported at the hinges and the tip latch pins (two points at each end) and loaded by weights applied at the structural intersections. The weights were placed on rods which were held vertical by a guide plate as shown in Figure 6-19. In the 50-pound, or torsion, test the panel was supported at the two hinges and at one tip latch pin. The load was applied at the other tip latch pin. In both cases deflections were measured with dial gages and stresses with strain gages. Expected stresses and deflections were calculated and are compared in this section.

6.5.1 TEST ACTIVITIES

—
The test panel withstood the specified static loads without physical damage.

—
The panel was loaded to 100% of the planned test load in both the bending and torsion condition. As the load was applied in increments, deflections higher than initially predicted were noted. Increased flexibility was expected because of the lower stiffness indicated by the modal survey. However, as the test weight was increased from zero to 100%, the deflections remained linear and the strain gage readings indicated that stresses were not excessive. The torsional condition, shown at 100% load in Figure 6-20, was of the greatest concern. In this condition, a loading in excess of 40 pounds was sustained for 40 minutes without damage or permanent set to the panel. At one point, a dial gage probe slipped off the structure and damaged a solar cell.

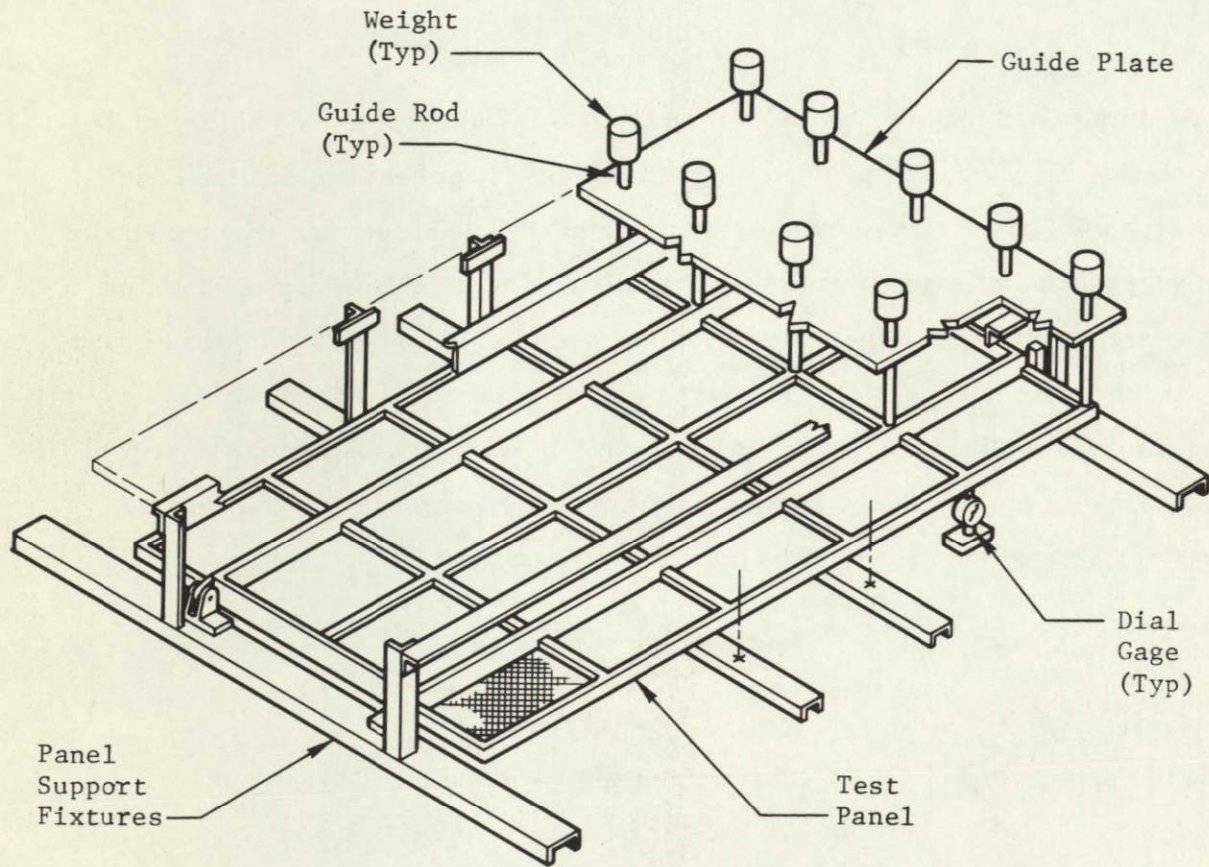


Figure 6-19: STATIC LOAD TEST SETUP

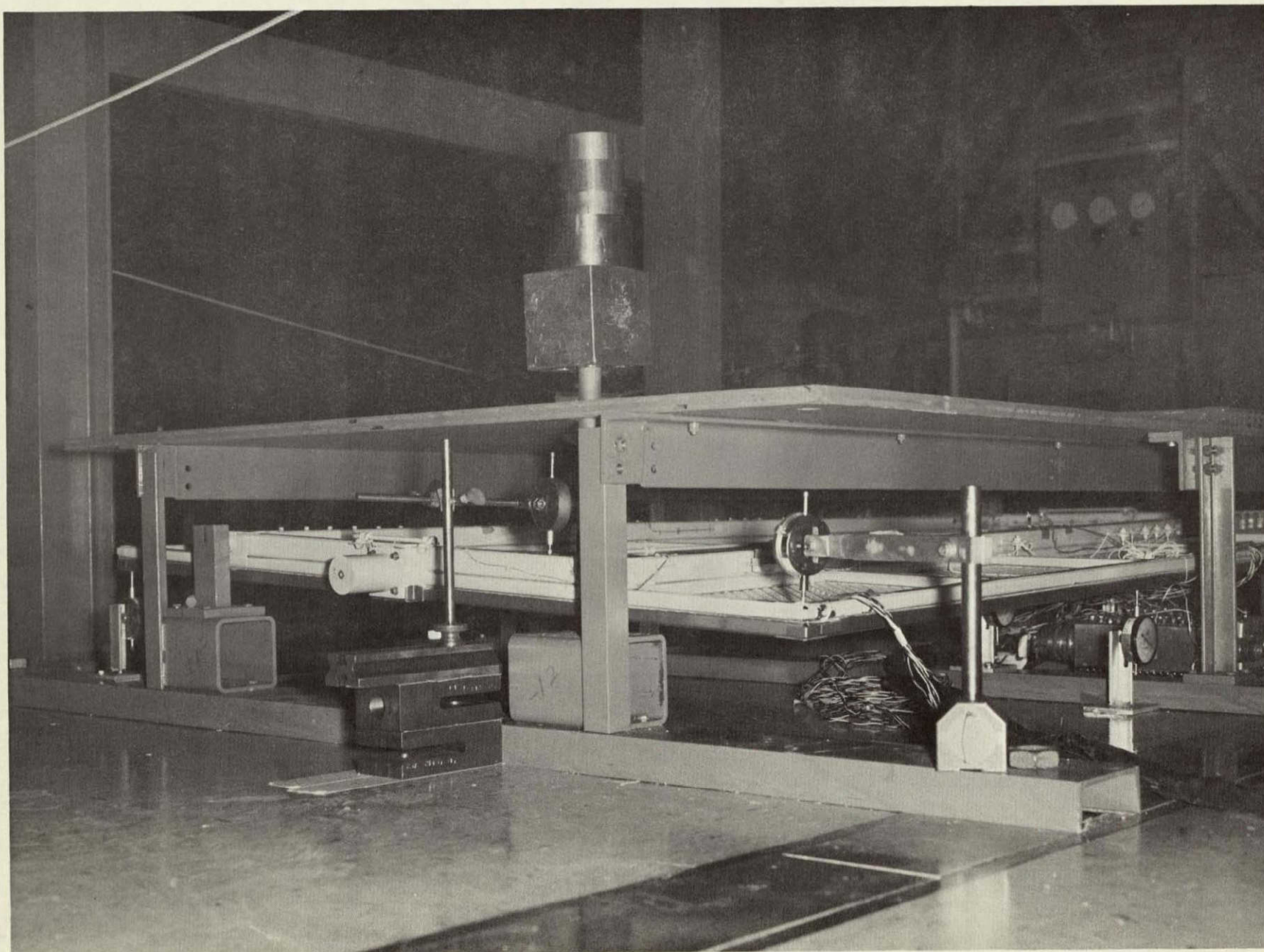


Figure 6-20: TORSIONAL LOAD APPLIED

6.5.2 EVALUATION OF TEST RESULTS

—

Deflections, under static load, were greater than predicted but stresses did not exceed allowable limits and no damage occurred.

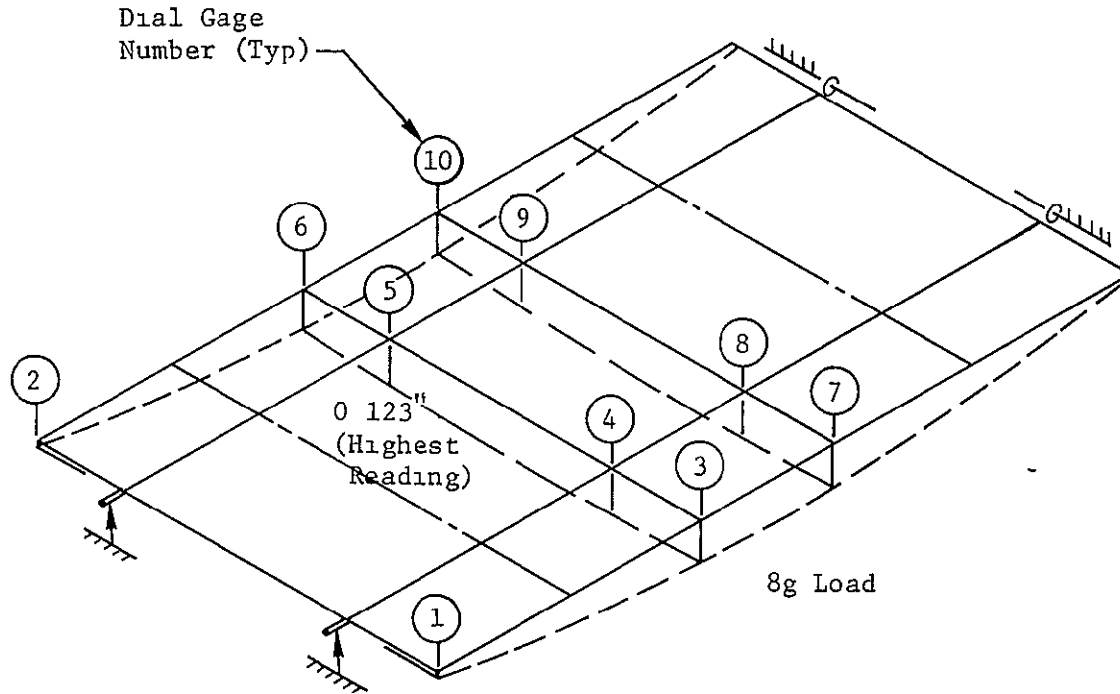
—

The deflections, plotted at the measurement stations, for the bending and torsion tests are shown by Figures 6-21 and 6-22, respectively. Measured and calculated stresses are shown in Figure 6-23. Measured stresses did not exceed allowable limits.

Bending deflections at the middle of the panel exceeded the calculated values by an average of 20%. The torsional deflections were about 50% greater than the calculated values. This reduction in stiffness is validated by the results of the modal test. When adjustment of the calculated frequencies is made for the added instrumentation weight and the measured weight of the panel, the calculated stiffness approximated the stiffness required to produce the measured deflections.

The cause of the greater-than-expected deflections cannot be determined definitely without additional testing and analysis; however, some facts pertinent to the problem are:

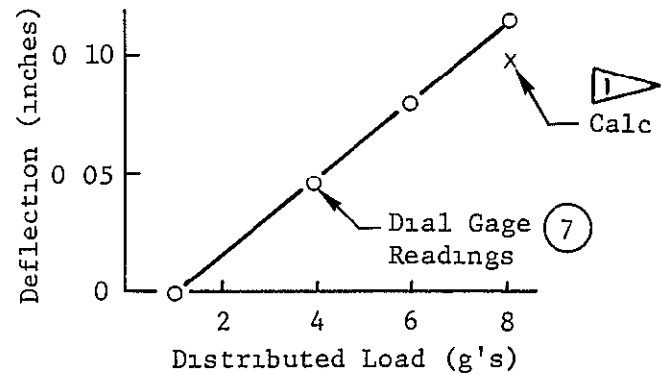
- 1) The stiffness of the Large Area Solar Array (LASA) panel, as indicated by a modal survey, was predicted accurately using the same assumptions that were used in the analysis of this panel. Therefore, the explanation of the stiffness anomaly probably lies in the structural differences between the two panels.
- 2) The primary difference is that, in the LASA panel, the neutral axes in bending and the centers of section rotation in torsion for each member were on the same plane, whereas, in this panel, the axes of the main spars and the lateral spars are offset from the axes of the other members.
- 3) The analysis of this panel used the assumption that all torsional loads were carried by the deeper of the two rectangular members comprising the "picture frame" shape described by the main spars and lateral spars. These members were assumed to be of continuous cross section, but, in fact, the interior shear web was intermittent to allow joining the cross members. Also, these members were assumed to retain the rectangular cross section shape with the panel loaded in torsion, but, because of the absence of bulkheads or stiffeners, some deforming of the cross section could occur.



Note Plots of all Dial Gage Readings are Linear

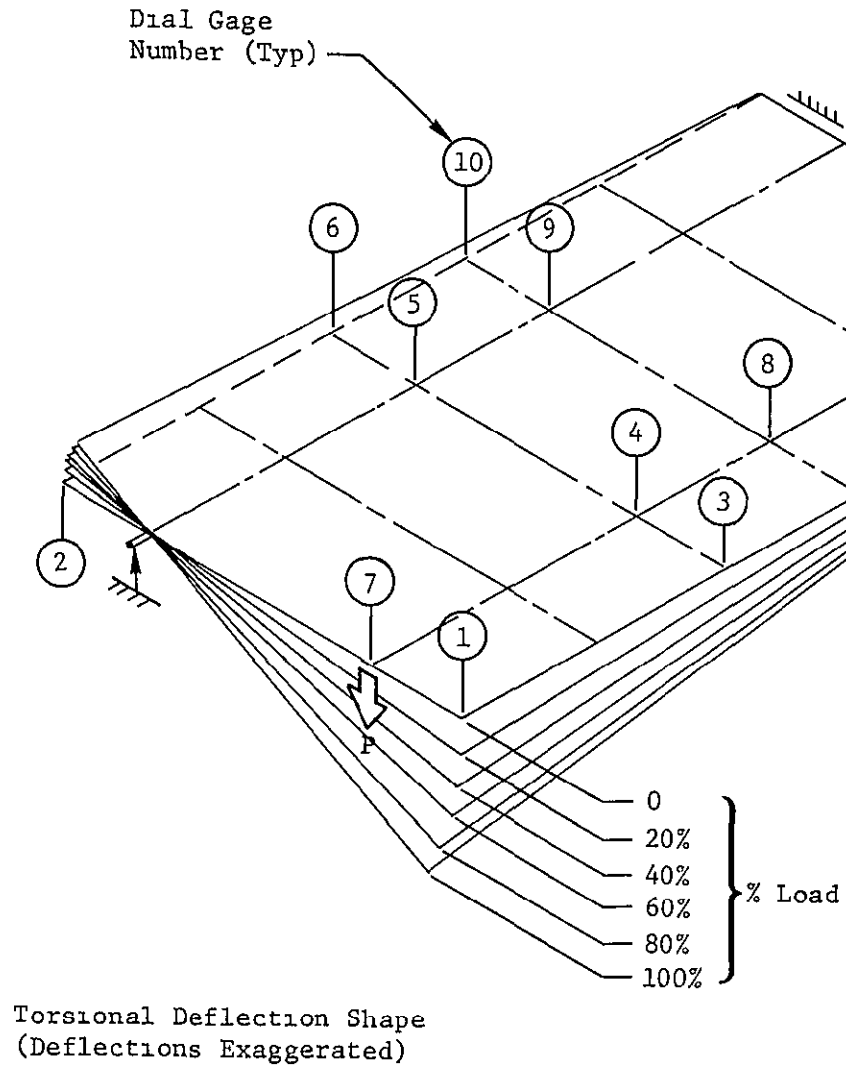
Bending Deflection Shape (Deflections Exaggerated)

1 Measured Deflections were consistently about 1.2 times the Calculated Deflections

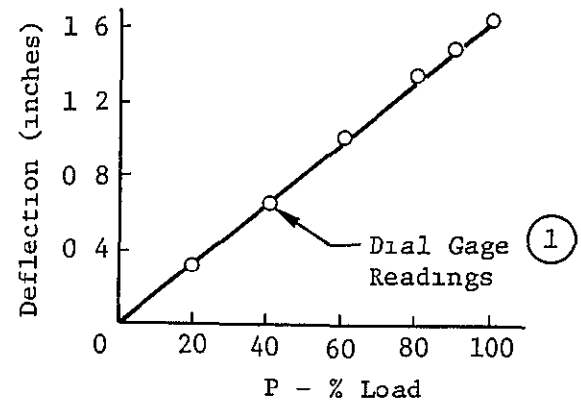


Typical Load-Deflection Plot

Figure 6-21 DEFLECTIONS - 8g LOAD



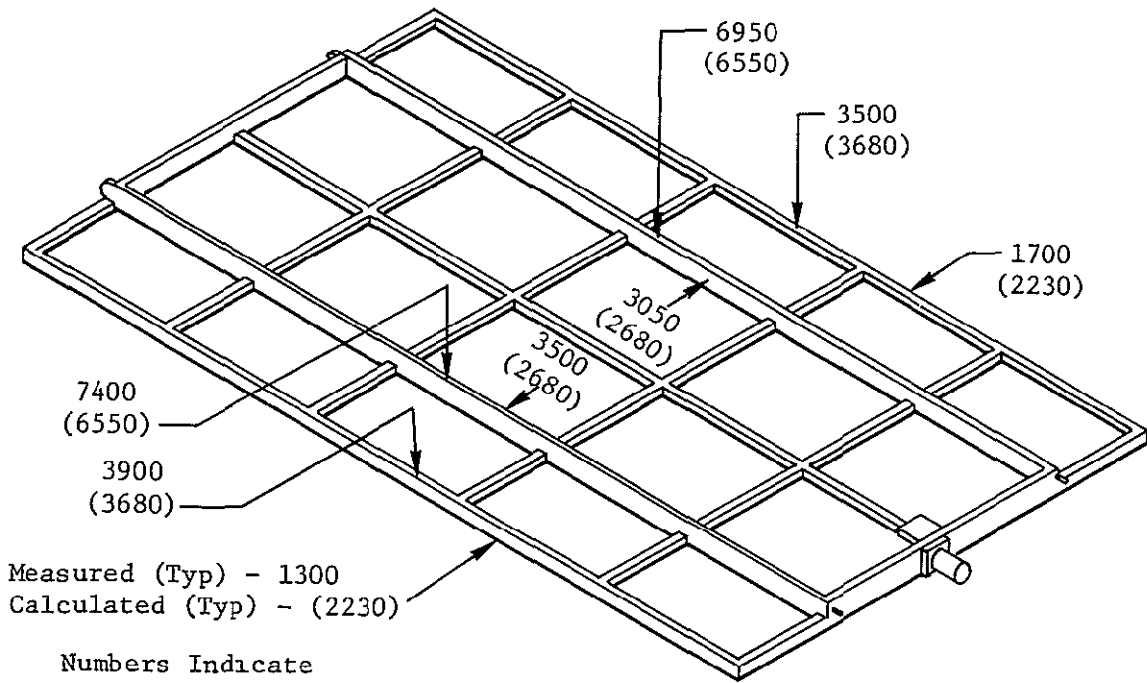
Note Plots of all Dial Gage Readings are Linear



Typical Load - Deflection Plot

Figure 6-22 DEFLECTIONS - 50 LB LOAD

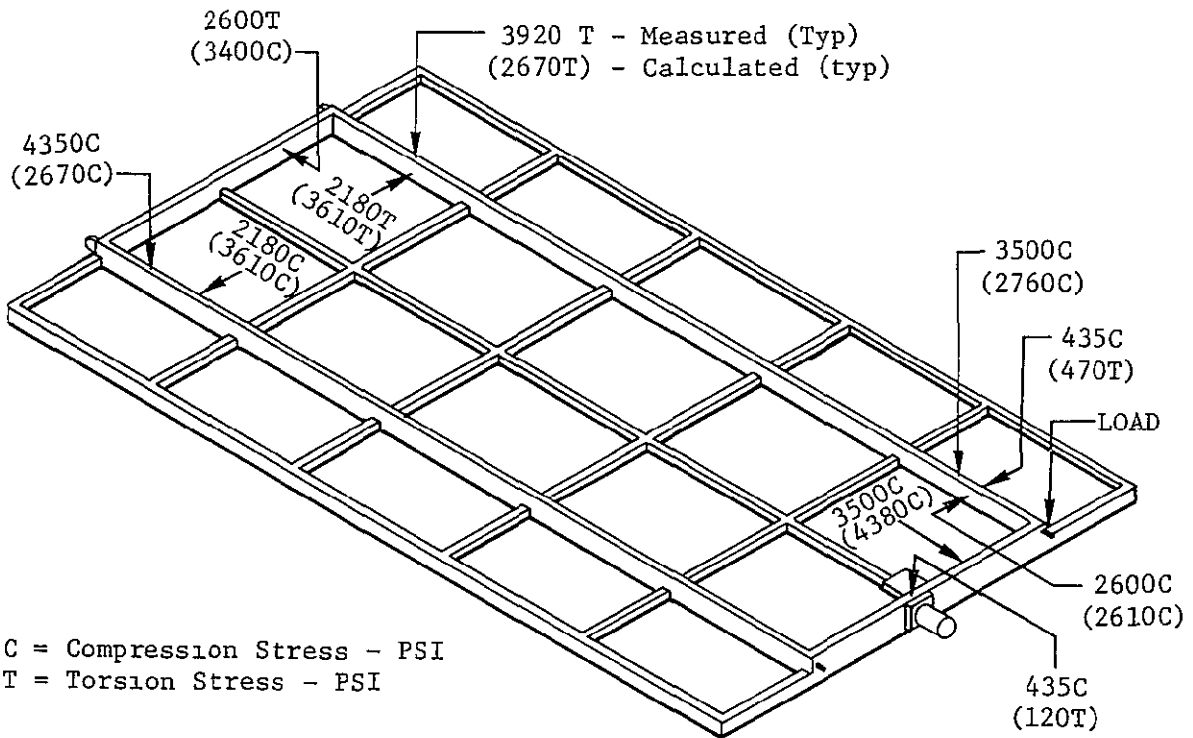
D2-121773-2



Measured (Typ) - 1300
Calculated (Typ) - (2230)

Numbers Indicate
Compression Stress
in PSI

BENDING (8g)



C = Compression Stress - PSI
T = Torsion Stress - PSI

TORSION (50 Lb)

Figure 6-23 STRESS COMPARISONS - STATIC LOAD TESTS

- 4) The computer simulation of the corner joints of the "picture frame" members assumed complete rigidity, whereas the practical case generally has less than complete rigidity. Also, an "L" joint occurs on this panel but a "T" joint was used on the LASA panel.

To adequately model all of these factors would, at least, double the analytical effort with a consequent increase in computer time, but would, in all probability, provide an accurate assessment of structural stiffness

6 6 THERMAL-VACUUM-SHOCK TESTS

—

These tests were conducted to expose the test panel to "type approval" levels of temperature and vacuum, to obtain voltage-current data at Earth and Mars intensities, and to determine operating parameters of the zener diodes.

—

The test panel was exposed to a range of temperatures and solar simulator intensities while in a vacuum of 10^{-5} torr. A history of the actual test sequence and conditions is given in Figure 6-24. The test activities are described herein in chronological order in accordance with the test history. The zener diode tests are not identified in the test history, but were performed throughout the testing.

No specific predictions of results were made for these tests. The primary test objectives were to expose the panel to the environment and to obtain performance data.

6.6.1 TEST ACTIVITIES

—

The test panel adequately withstood the thermal-vacuum-shock environment.

—

The test setups and activities are summarized chronologically as follows:

- 1) Initial Setup---The test panel was suspended in the 50,000 cubic foot space simulator as shown in Figure 6-25. Solar intensities were produced by seven hexagonal-section beams of light directed from the solar simulator onto the

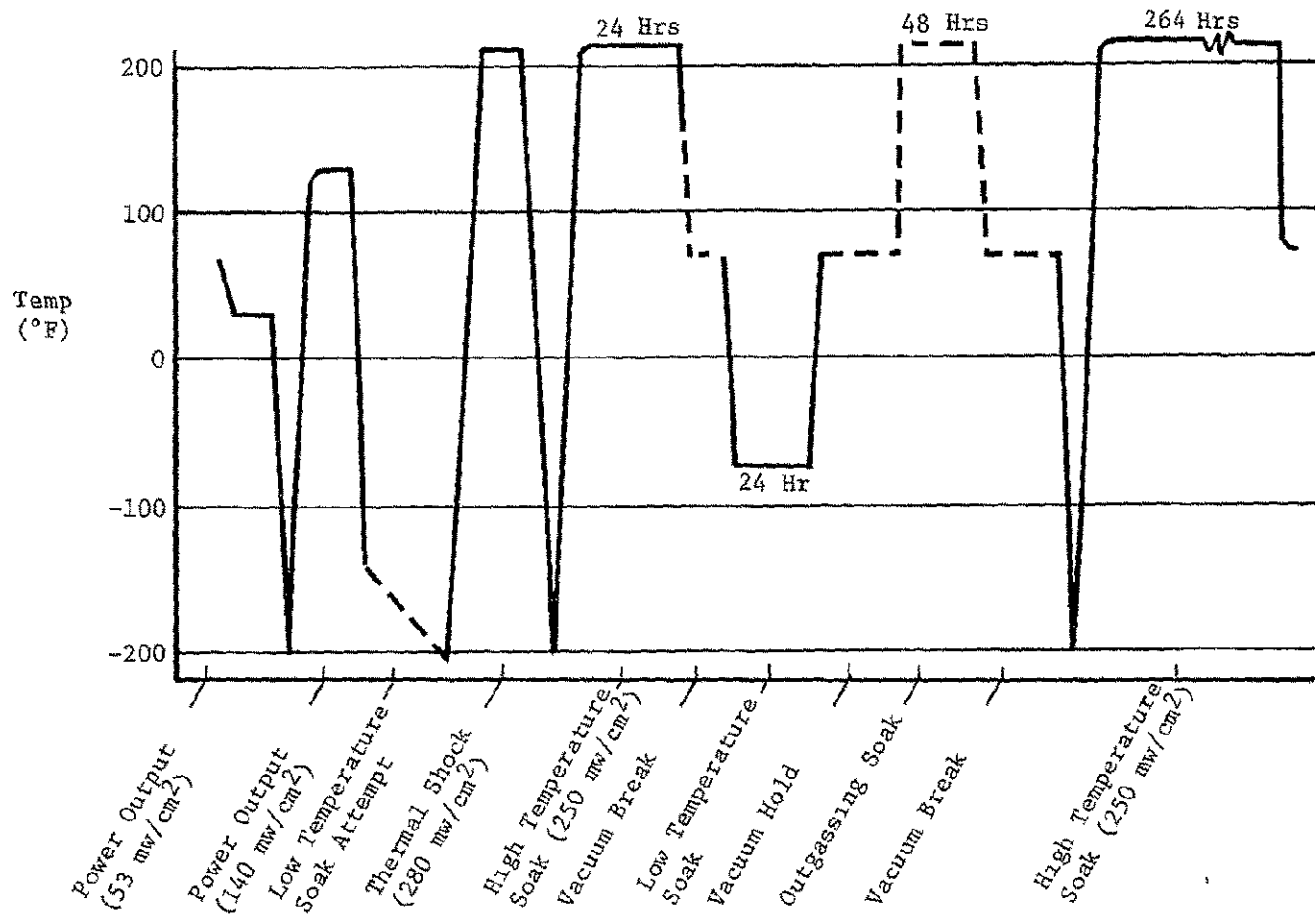


Figure 6-24 THERMAL-VACUUM-SHOCK TEST HISTORY

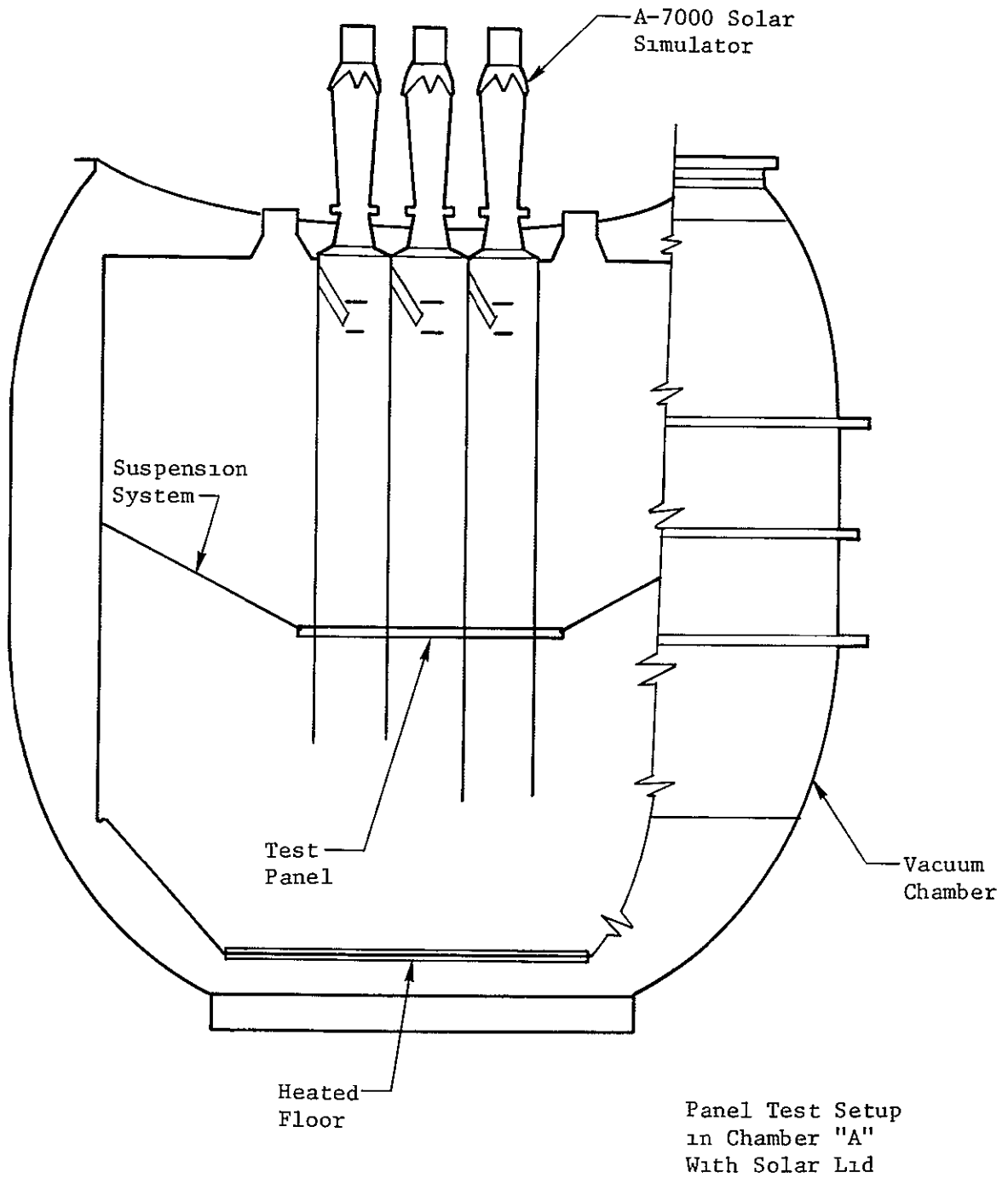


Figure 6-25 THERMAL-VACUUM-SHOCK TEST SETUP

panel surface as shown in Figure 6-26. Instrumentation consisted of 30 chromel constantan thermocouples located on the structure, the dark side of the solar cell modules, and the zener diodes. A control thermocouple was located on the dark side of a solar cell near the center of the panel. A block diagram of the test equipment hookup is shown in Figure 6-27. In addition, the zener diodes for three of the active solar cell modules (modules 3, 7, and 11) were connected to an external power supply and were isolated from the panel electrical system. The zener diodes for the other three active modules were connected in parallel with the modules as in the flight configuration. Quantities of 3, 4, and 5 zener diodes per module were tested for both of the sets of three active modules as shown in Figure 6-26.

- 2) Power Output Tests in Vacuum---The vacuum chamber was evacuated and voltage-current data was taken at intensities of 53 mW/cm^2 (50 W/ft^2 , near Mars), and at 140 mW/cm^2 (130 W/ft^2 , near Earth). Current to the three sets of isolated zener diodes was adjusted to maintain a diode temperature of 230°F . This was done to evaluate the heat sink properties of the panel structure and the zener diode mounting clips.
- 3) Low Temperature Soak Attempt---Data from the initial illumination at 53 mW/cm^2 indicated that the required -67°F could be obtained on the test panel with the solar simulator. With the solar simulator at minimum intensity, panel temperatures could not be maintained below 0°F , so the test was deferred (see item 6).
- 4) Thermal Shock Test---Starting at -202°F , the solar simulator was turned on at an intensity of 280 mW/cm^2 during the up-shock and reduced to 250 mW/cm^2 after four hours to maintain the required 212°F upper temperature. The solar simulator was then turned off to achieve the thermal down-shock to -202°F which occurred in one hour. Maximum measured rates of change were 225°F per minute during up-shock and 140°F per minute for down-shock. Temperature, voltages, and zener diode currents were recorded.
- 5) High Temperature Soak - First 24 Hours---The intent of this test was to expose the test panel to a temperature of 212°F in vacuum for 288 hours. The heat source, the solar simulator lamps, required increasing power to maintain the necessary intensity, and after 24 hours, had degraded so that the 212°F temperature could not be maintained. Investigation showed that energy reflected from the solar cells was damaging the lenses of the solar simulator. During repair of the lenses, the low temperature soak and the panel outgassing were performed.
- 6) Low Temperature Soak---The solar panel was reoriented in the test chamber to a position one foot above the floor with the panel sun side down. An aluminum box was suspended over the panel with the open end of the box in the plane of the panel and the closed end three feet above the plane of the panel as shown in Figure 6-28. The interior of the box was bare aluminum and the outside was

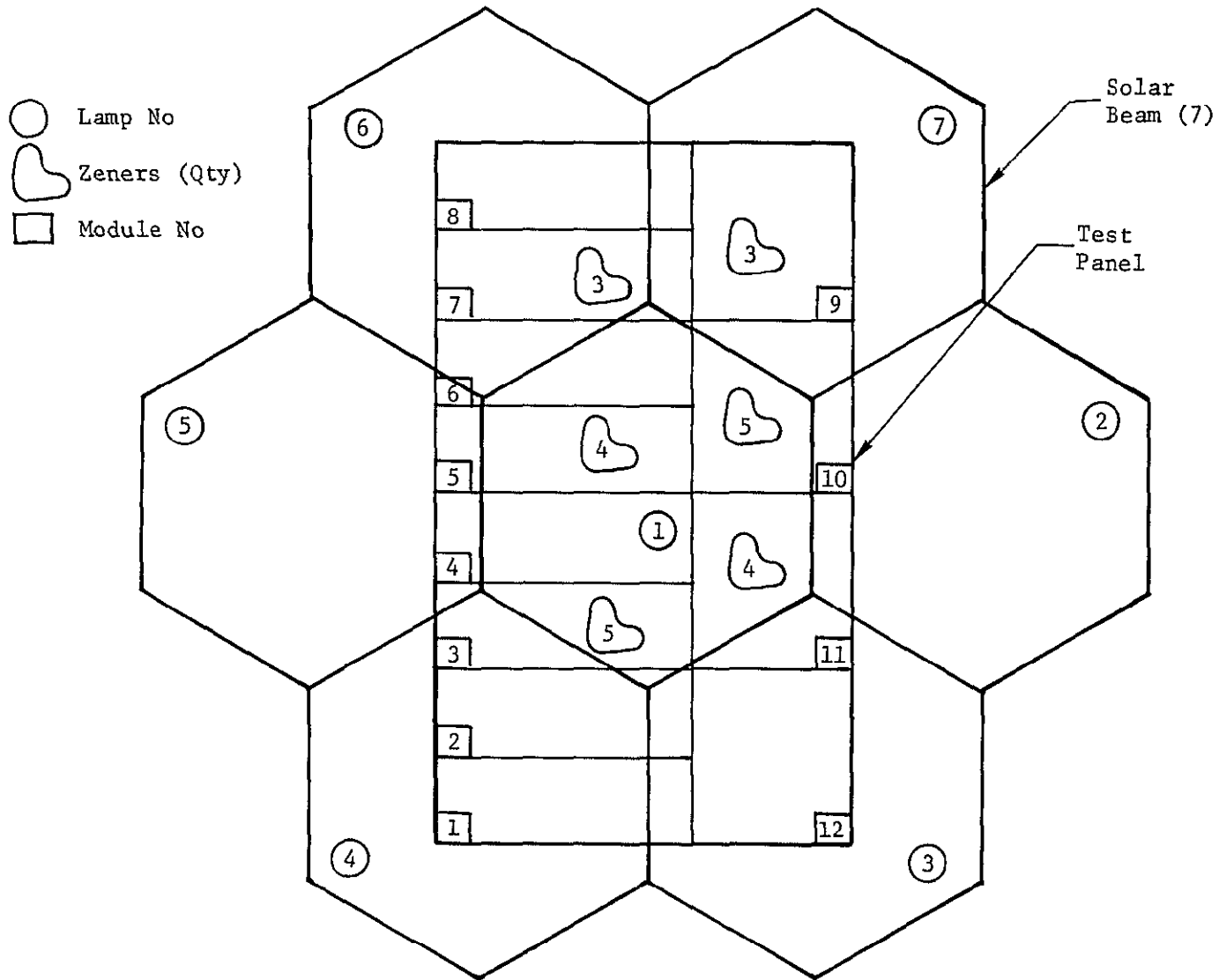
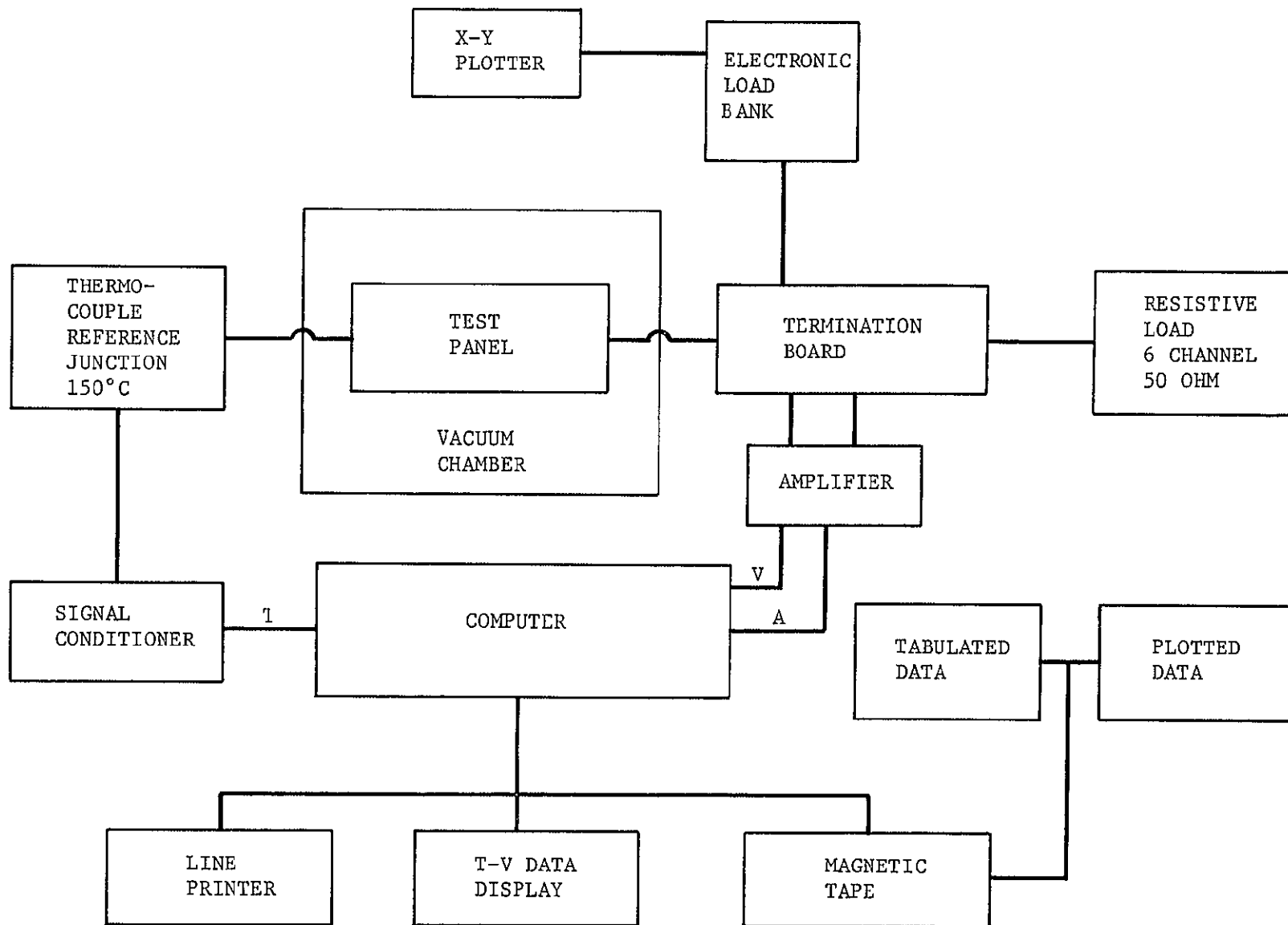


Figure 6-26 SOLAR SIMULATION---THERMAL-VACUUM-SHOCK TEST



BLOCK DIAGRAM

Figure 6-27 THERMAL-VACUUM-SHOCK TEST EQUIPMENT

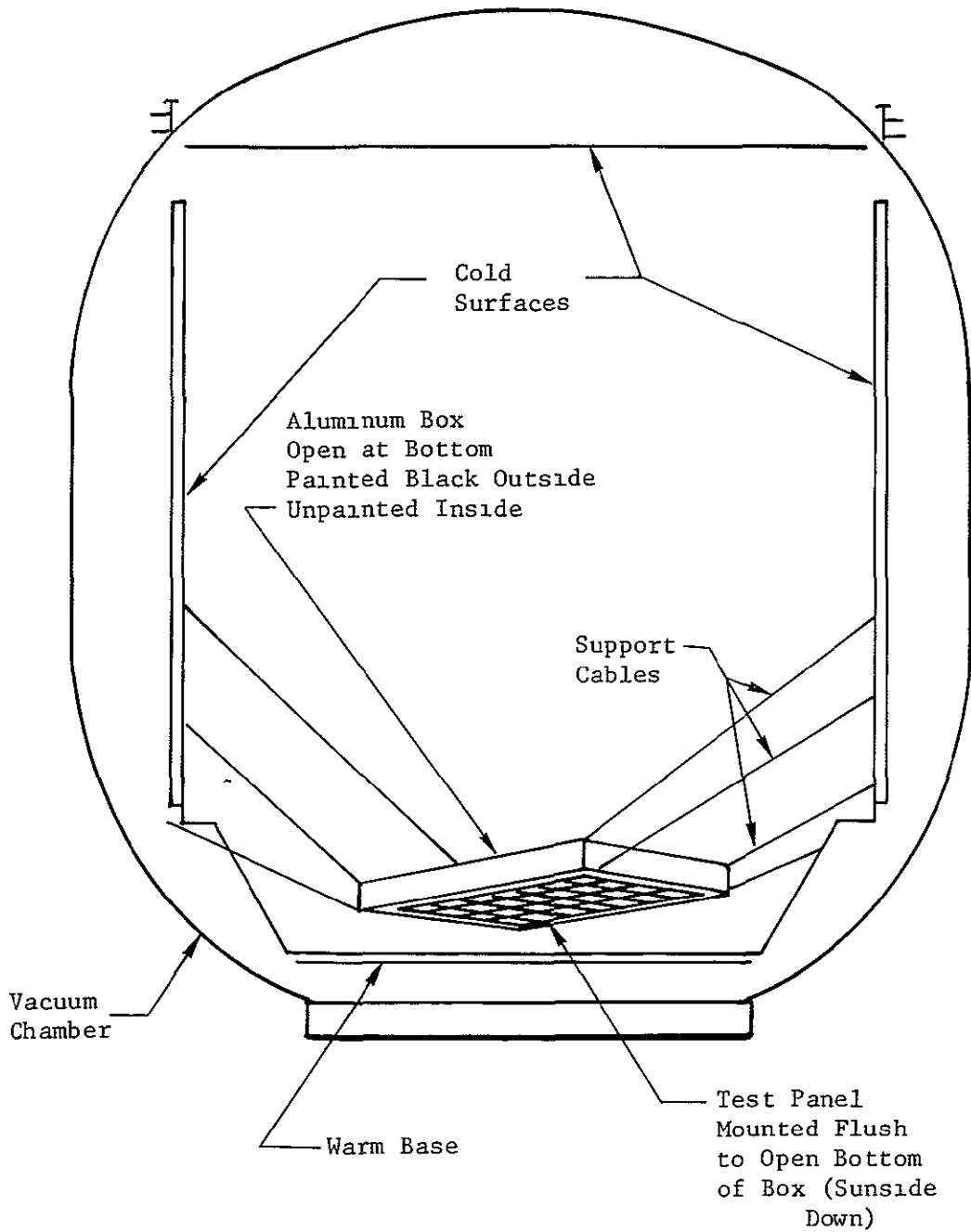


Figure 6-28 LOW TEMPERATURE SOAK SETUP

painted black. The vacuum chamber was evacuated to 10^{-5} torr and the floor was heated to control the panel temperature at -67°F for 24 hours. The panel temperature was then raised to 70°F and held until the start of the outgassing soak.

- 7) Outgassing Soak---Using the low temperature soak setup, the panel temperature was raised to 212°F by increasing the floor temperature. This condition was held for 48 hours to outgas the panel.
- 8) High Temperature Soak - Final 264 Hours---After repair of the solar simulator lenses, the test panel was reinstalled in the initial setup condition except that the plane of the solar cells was positioned 4° off the normal to the light beams to avoid reflecting into the optics of the solar simulator. The test was then completed successfully. Current to the three sets of isolated zener diodes was adjusted to maintain a diode temperature of 230°F . One unscheduled thermal shock of the panel occurred when the power to the central solar lamp was interrupted for 15 minutes. Temperature differences exceeded 250°F between the hottest and coldest measured thermocouples, but no damage to the panel occurred.

6.6.2 EVALUATION OF TEST RESULTS

The test panel did not degrade when subjected to the thermal-vacuum-shock environment, and performance with only three zener diodes per solar cell module was adequate.

No significant structural or electrical degradation of the test panel occurred as a result of the thermal-vacuum-shock tests. Voltage-current and temperature data were obtained which substantiated the analytical predictions of the thermal and electrical performance of a flight configuration panel of the Light Weight Solar Panel design (see Figure 2-2, Section 2.0). Important characteristics of this design that were demonstrated by the thermal-vacuum-shock tests are:

- 1) The lower solar cell operating temperature---Compared to the contract-specified nominal of 55°C at one A.U. and 140 mW/cm^2 , the predicted solar cell operating temperature for the test panel was 45.5°C and the temperature measured in these tests was 48.5°C . The measured value is high because of variations on the high side in the solar simulator intensity.
- 2) The short solar cell warmup time provided by the open substrate design---This is important because of the short time (about 2 minutes) that the zener diodes

operate during thermal up-shock conditions as shown in Figure 6-29. The shorter operating time indicates that a less severe derating factor can be applied to the zener diodes, thus allowing the use of three zener diodes per cell module.

- 3) The favorable heat sink properties of the beryllium structure---This is indicated by the low (15°F) zener diode operating temperature shown in Figure 6-29.
- 4) The ability of the open substrate design to withstand high thermal gradients---The test panel was inadvertently subjected to a temperature differential of 250°F during the final high temperature soak and no damage occurred.

The thermal up-shock test data shown in Figure 6-29 was obtained from a solar cell module with a series of only three zener diodes connected in parallel with the module. The zener diode current was about 1.5 amps at 50 volts for tests with 3, 4, and 5 zeners (75 watts of total rated diode capability). A safe maximum diode temperature is 230°F, which is far above the indicated 15°F obtained during the thermal up-shock test. Zener temperatures dropped immediately following zener diode current cut-off, indicating that the structure was dissipating the zener diode thermal energy at a rapid rate.

6.7 SUBSTRATE FREQUENCY CHECK

—

The substrate frequency checks were conducted to determine if any significant relaxation of substrate tension occurred as a result of the environmental tests.

—

The substrate frequency checks were conducted once at the start and once at the completion of the series of environmental tests. A comparison of the results of the two checks was used to determine if any significant relaxation in the tension of the fiberglass substrate tapes had occurred. The frequencies of one small and one large substrate bay near the center of the panel were measured. A substrate bay is a rectangular area of the substrate, about 12 inches by 17 inches, bounded by the dark side frame structural members.

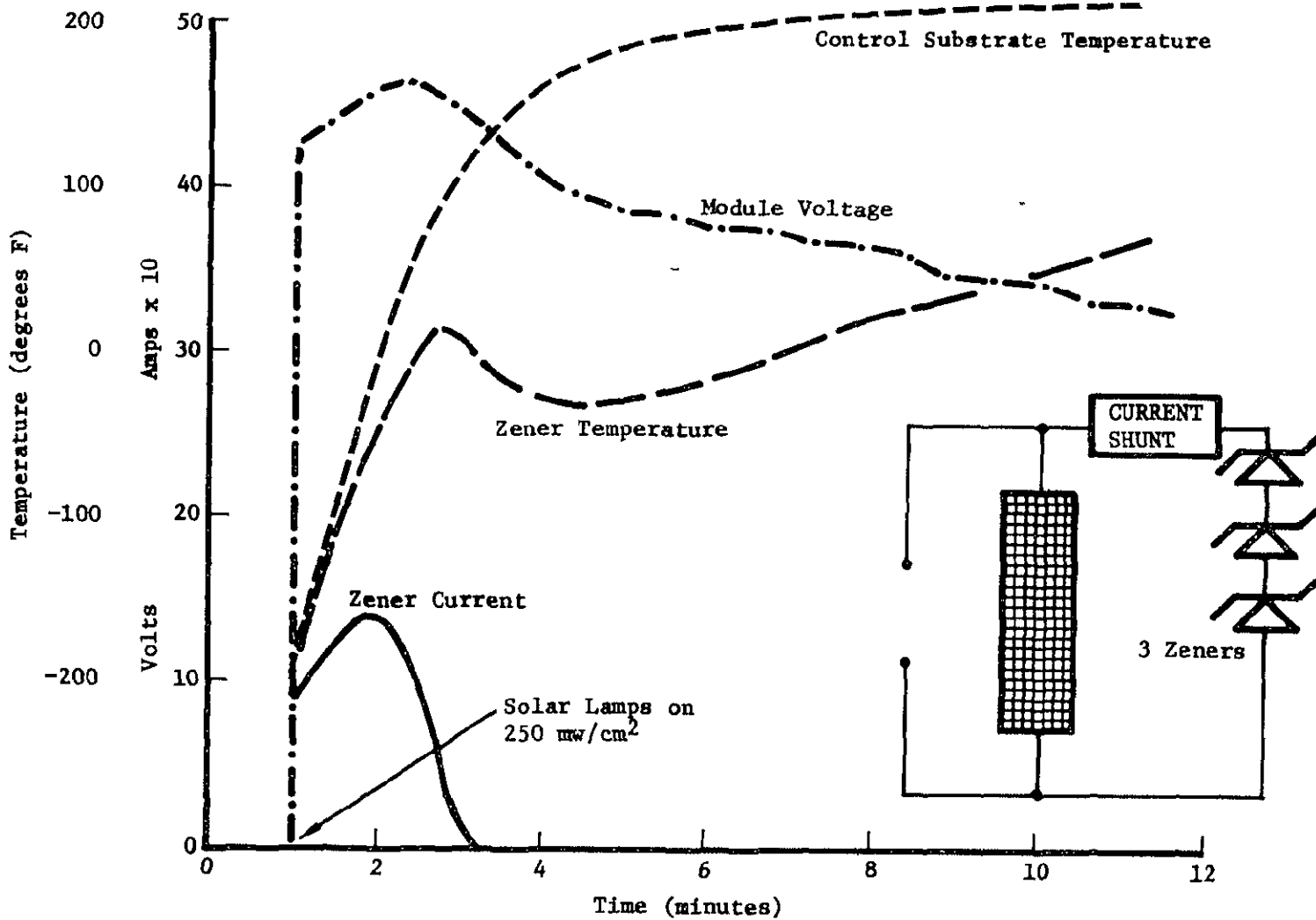


Figure 6-29 ZENER DIODE TEST DATA

6.7.1 TEST ACTIVITIES

—

The frequencies of the two substrate bays were adequately measured.

—

The test panel was installed in the same fixture used for the modal survey as shown in Figure 6-30. On both of the substrate bays, accelerometers were mounted on small blocks undercut to receive a string harness. A string was attached, in turn, to each block, routed over a pulley, and weighted as shown in Figure 6-30. The string was cut to excite the substrate and the responses from the accelerometers were recorded for each of the two bays in turn.

6.7.2 EVALUATION OF TEST RESULTS

—

The 6% reduction in substrate frequency does not significantly affect the performance of the panel.

—

The measured substrate frequencies, before and after the environmental tests, are tabulated below:

	Fundamental Frequency-Hz	
	Pre-Test	Post-Test
Large Substrate Bay	74	69
Small Substrate Bay	78	74

The fundamental frequency dropped 4 to 5 Hz during the test series. The test most likely to cause a relaxation of substrate tension was thermal-vacuum-shock, this test included a thermal soak of 212°F for 12 days under vacuum. The 6% drop in frequency represents a small amount of relaxation of substrate tension and does not significantly affect panel performance.

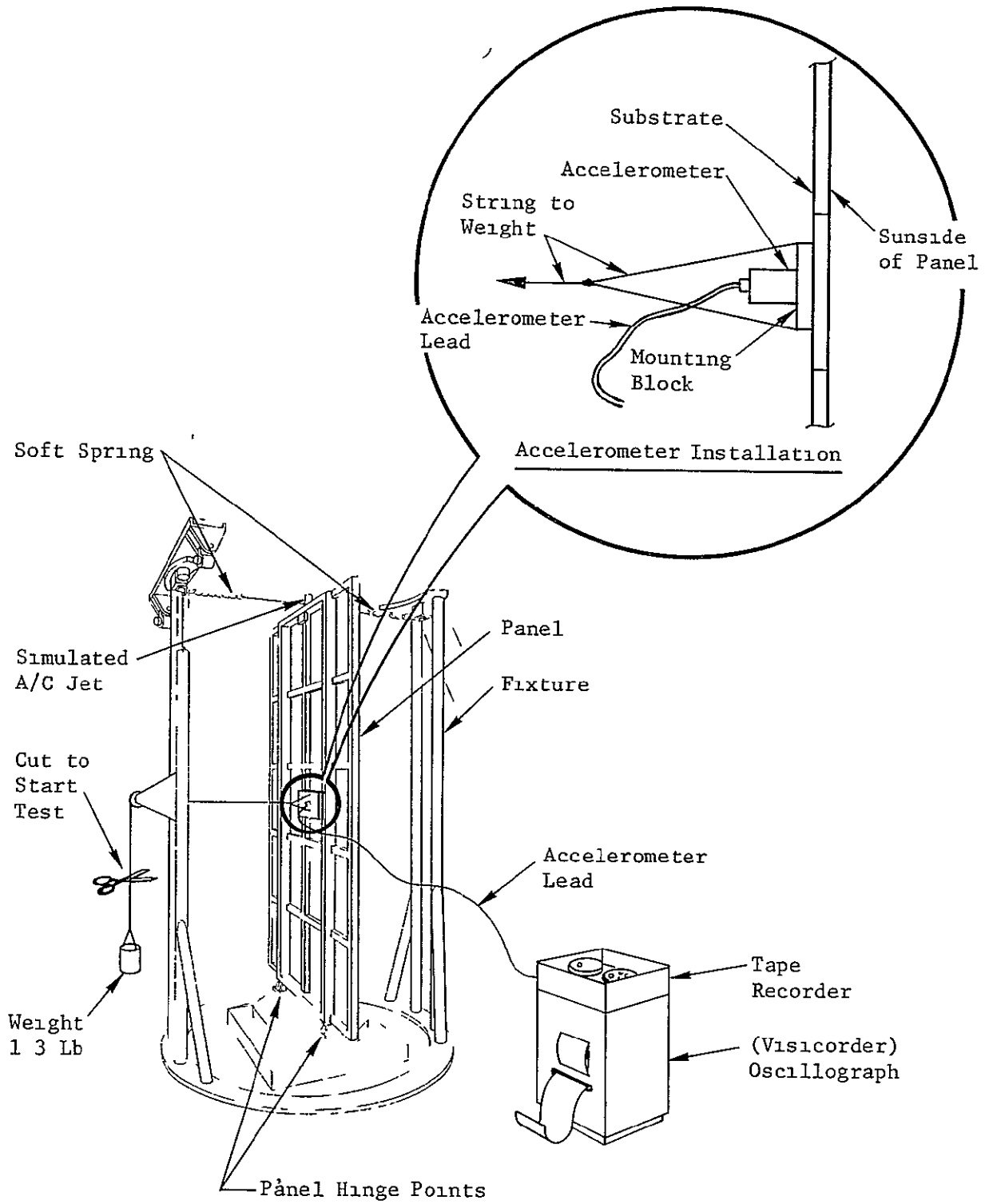


Figure 6-30 SETUP FOR SUBSTRATE FREQUENCY CHECK

6.8 POWER OUTPUT CHECKS

—

The power output checks were conducted to determine if any electrical degradation of the test panel had occurred during the test program.

—

A power output check of each of the six active solar cell modules was performed before and after each environmental test as shown in Figure 6-31. No specific power output values were predicted. The power outputs measured were used for comparison to determine if any environmental test had caused electrical degradation.

6.8.1 TEST ACTIVITIES

—

Power output data was satisfactorily obtained, except for the first two checks.

—

The test panel was set up in a tripod-mounted holding frame under the solar simulator as shown in Figure 6-31. The solar simulator beam is a 40-inch diameter, spectrally filtered, collimated beam with a uniformity of $\pm 3\%$, as shown in Figure 5-17, Section 5.0. A 500-watt electronic load bank was used to vary the load to the live cell modules. Voltage versus current curves were plotted on an X-Y plotter. A JPL-furnished, balloon flown, standard cell, BFS 301, was used to verify the beam intensity. A six-point thermocouple probe was used with a time-versus-temperature recorder to determine temperature stabilization.

A total of seven power output checks were required, however, data from the first two checks was later found to be invalid. This anomaly is discussed in Section 5.8. The remaining power output checks, numbers 3 through 7, were successfully completed.

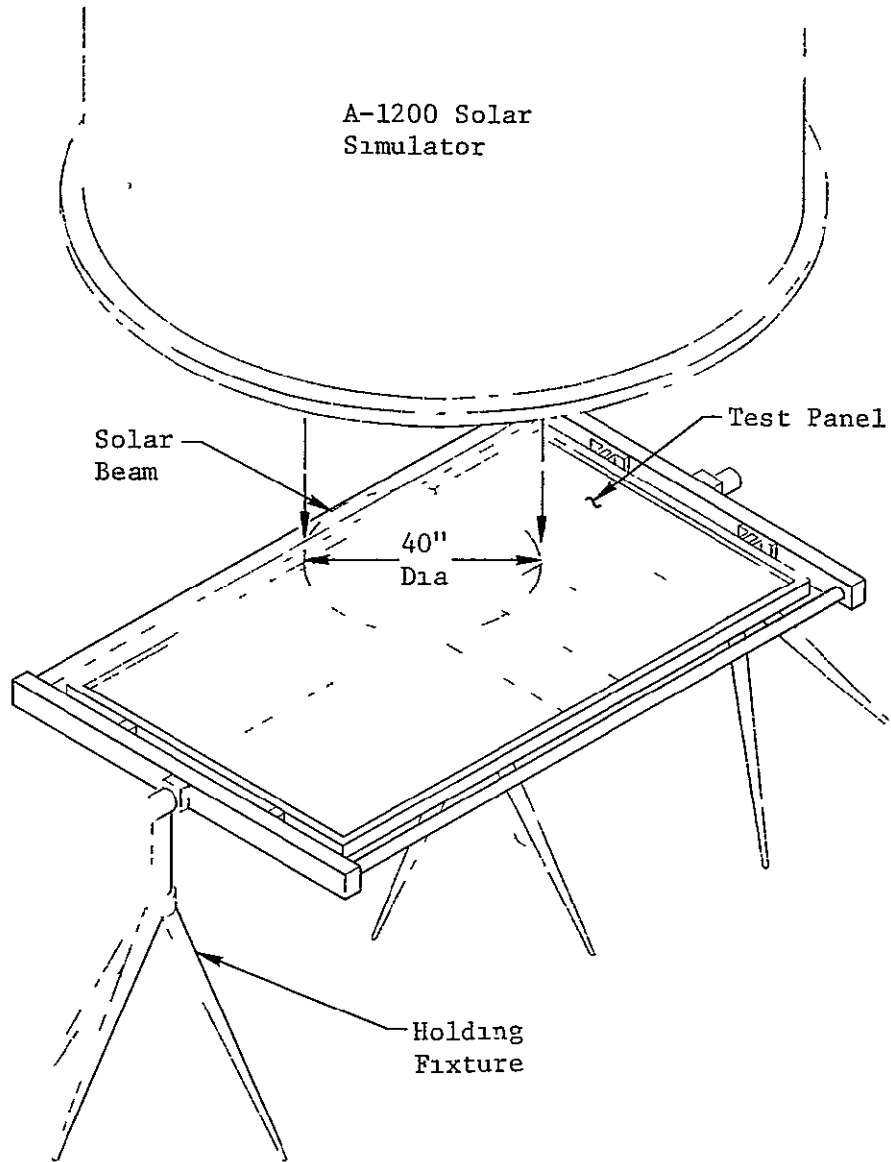


Figure 6-31 SETUP FOR POWER OUTPUT CHECK

6.8.2 EVALUATION OF TEST RESULTS

—

The results of the power output checks indicated no measurable degradation.

—

The results of power output checks 3 through 7 are given in Figure 6-32. A significant feature of the pattern of variation is that it is random rather than a steady decline in output. Considering this factor, it is concluded that no electrical degradation occurred that could be determined within the $\pm 4\%$ accuracy of the test measurements. The number of solar cells that were broken or cracked during the test or in handling the panel were insignificant and not large enough to move the maximum power point of any module outside of the 4% experimental accuracy.

6.9 DAMAGE EVALUATION

—

Solar cells and silver mesh pigtails were found damaged following testing.

—

Throughout the test program the panel was periodically inspected for damage. No structural damage was found and none was indicated by the test results. However, several instances of breakage of the silver mesh interconnector pigtails from the solar cell modules to the buses and between submodules were encountered and two types of cracking of the solar cell assemblies were found. These failures, and some cosmetic effects which did not constitute functional damage, are discussed in this section.

6.9.1 DAMAGE OF SILVER MESH PIGTAILS

—

The test program has proven the silver mesh pigtail design to be unsatisfactory.

—

The silver mesh pigtail design has been found to be vulnerable to damage throughout subassembly, installation, and testing. These pigtails, shown on the solar cell

Power Output Test	Test Accuracy %	Date (1970)	Module 3		Module 5		Module 7		Module 9		Module 10		Module 11		P _m (Avg)
			P _m (W)	%											
3	+4	4-10	23 5	104.0	25 3	104 0	25 2	104 0	24 5	104 0	24 1	104 0	24 4	104 0	
	-4			100 0		96 0		100 0		96 0		100 0		96 0	
4	+4	4-20	24 7	109 9	24 7	101 6	25 0	103 2	24 6	104.4	23 9	103 1	24 6	104.8	
	-4			105 7		97 6		99 2		100 4		99 1		100.8	
5	+4	4-24	24 7	109 9	25 1	103 6	24 9	102 8	24 4	103 6	24 1	104 4	24 2	103 6	
	-4			105 7		99 6		98 8		99 6		100 4		96 4	
6	+4	5-4	25 1	111 3	24.0	98 9	24.2	99 7	23 8	101 0	24 0	103 6	24 1	102 6	
	-4			107.0		95 1		95 9		97 1		99 6		98.7	
7	+4	7-2	23 3	107 6	23 9	98 5	24 2	99 7	23.8	100 9	24.0	103 6	24 0	102 7	
	-4			103 5		94 7		95 9		97 1		99 6		98 7	
Averages			24 3		24 6		24 7		24 2		24 0		24 3		24 4*

*Predicted power output of the 560-cell module at the normalized condition is 23 00 watts

Date Corrected for Solar Intensity = 140 mw/cm² P_m = Maximum module power as corrected
 Panel Temp = 55°C
 Normalized to Test No 3 Performance

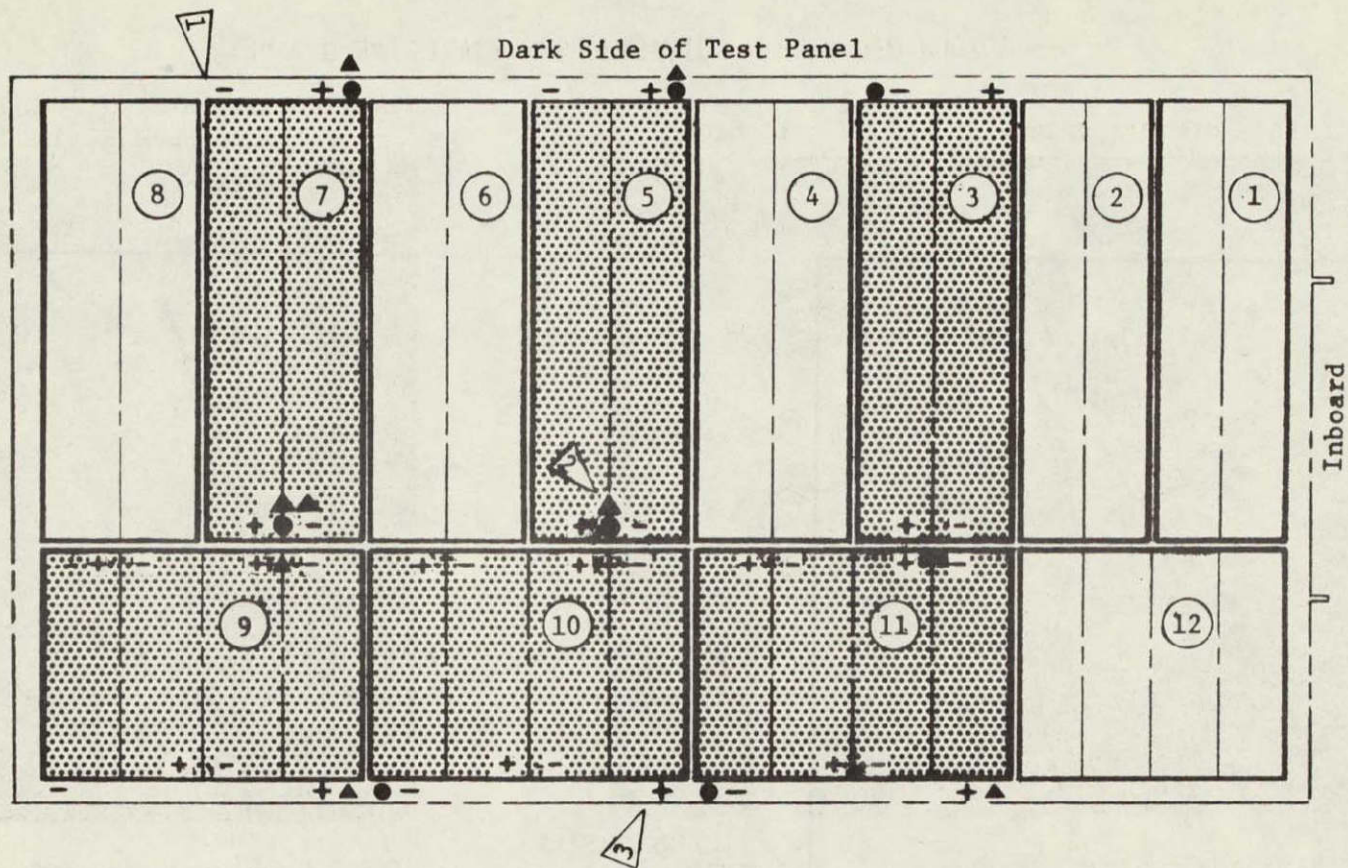
Figure 6-32 POWER OUTPUT TEST DATA

submodule assemblies in Figure 4-5, Section 4, are about one inch long by 1/8 inch wide when folded double from the original 1/4-inch width, and protrude from the extreme corners of each submodule assembly. They are subject to bending over the solar cell edges, either during handling of the submodule or during bonding, where vacuum bag pressure is applied. During vibration testing, a flexing of the pigtails occurred due to the motion of the cells and substrate relative to the structure and buses. The failures that occurred during the test program were not evident in a visual examination but were detected by electrical continuity checks. In all eight cases, the breaks in the silver mesh were hidden by the RTV-40 thermal control coating which also held the broken mesh together. When a suspected pigtail was probed, continuity would be broken and sometimes the pigtail would separate physically.

A record of failures of the silver mesh pigtails is given in Figure 6-33. An examination of a broken section of silver mesh, shown in Figure 6-34, indicated that fatigue was the probable cause of failure. This figure also shows typical installations. The seven failures during manufacturing were repaired by soldering splice pieces of silver mesh across the breaks. These failures involved all three pigtail configurations: the positive-to-bus, negative-to-bus, and submodule-to-submodule connections. Four of the eight failures found during testing were repaired with conventional wire, similar to the recommended design described in Section 10. These repairs were made after the sinusoidal vibration test so the recommended design has not been subjected to any vibration environment. However, the type of wiring used is similar to that used on the zener diode installation which withstood all testing.

The number and frequency of failures encountered on this program indicates a basic flaw in the pigtail concept, because of the following factors:

- 1) The pigtails are subject to breakage because of flexing during fabrication and testing.
- 2) The breakage is not easily detectable after the cell modules are bonded to the substrate.
- 3) No redundancy is provided.



- Silver Mesh Pigtail Replaced During Fabrication
- ▲ Silver Mesh Pigtail Broken During Test
- ▒ Active Module
- ▢ See Photo No. 1, Figure 6-34
- ▣ See Photo No. 2, Figure 6-34
- ▤ See Photo No. 3, Figure 6-34

Figure 6-33: SILVER MESH PIGTAIL DAMAGE

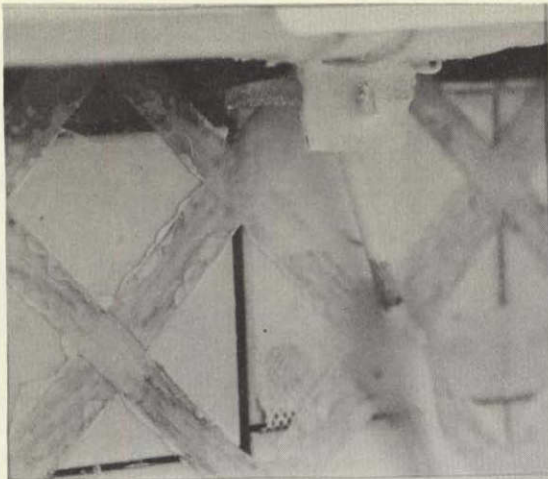


Photo 1: TYPICAL NEGATIVE TERMINAL

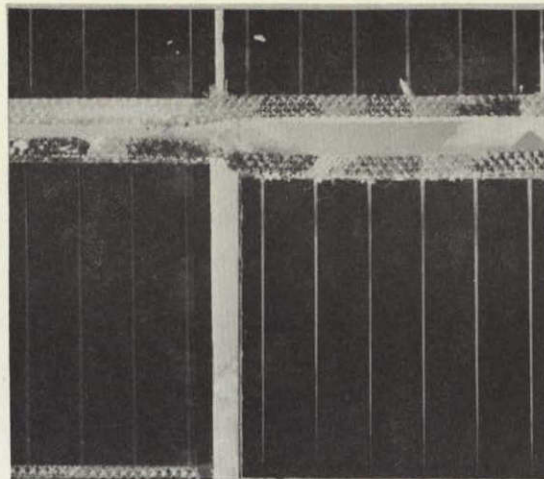


Photo 2: TYPICAL SUBMODULE INTERCONNECT

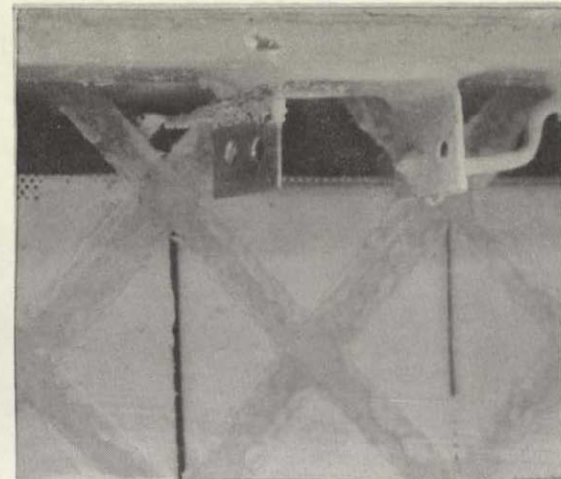


Photo 3: TYPICAL POSITIVE TERMINAL

154

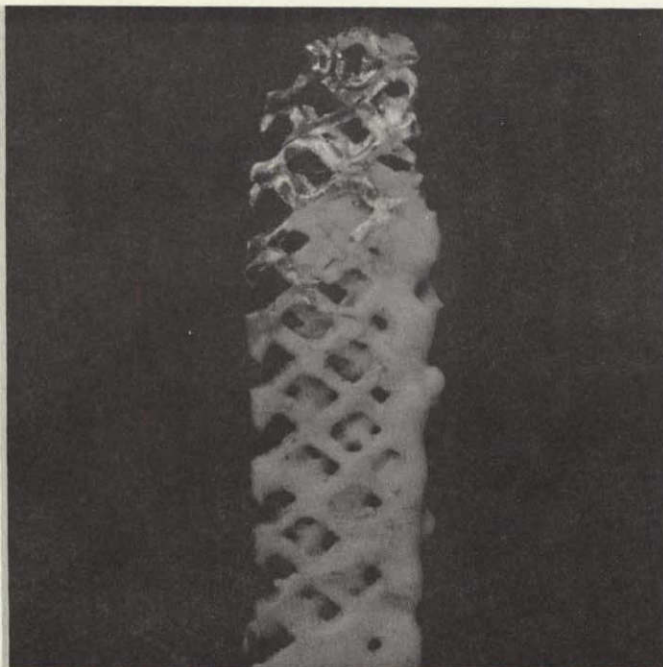


Photo 4: BROKEN SILVER MESH PIGTAIL --- RTV 40 COATING PARTIALLY REMOVED

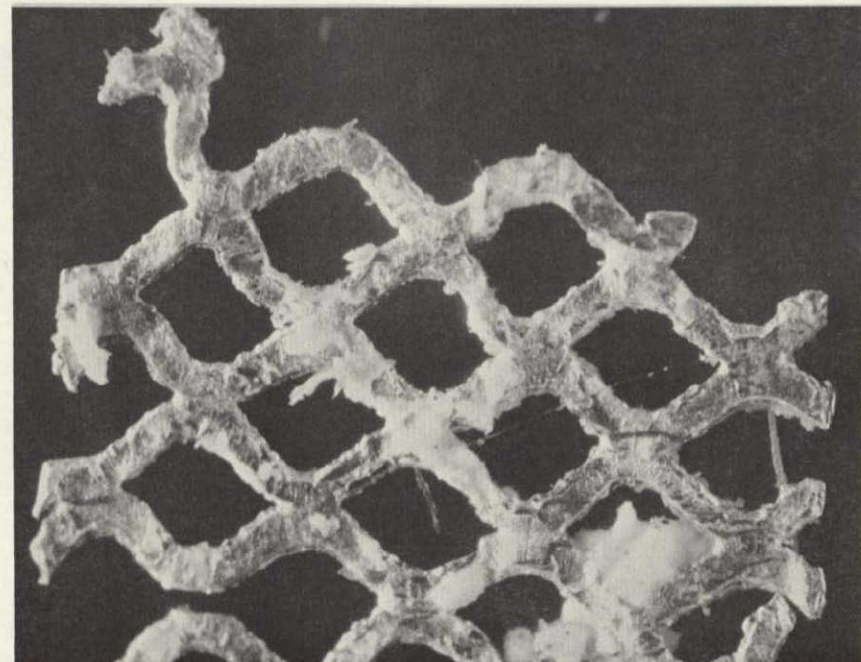


Photo 5: BLOWUP OF BROKEN PIGTAIL---UNFOLDED

D2-121773-2

Figure 6-34: SILVER MESH PIGTAILS---ENLARGED PHOTOS

The breakage during testing could not be attributed to any one test because of the difficulty of detection. However, the first failure was noted at the time of the power output check following the acoustic test. Subsequent failures were noted while trying to determine the measurement anomaly on the first two power output tests, after the random vibration test, and during the thermal-vacuum test. The failures occurred only at the positive-to-bus and submodule-to-submodule connections.

6.9.2 DAMAGE OF CELLS AND COVERGLASSES

—
Mechanical breakage of cells and edge cracks were found on about 1.4% of the cell assemblies.

—
Mechanical breakage, which severely cracked seven cell assemblies, occurred four times during testing. The first instance was discovered at the time of the setup for the acoustic test. Two cell assemblies adjacent to the inboard, or hinge, edge of the panel were broken. The appearance of the fracture and the proximity of finger marks on the structure indicated that these cells were cracked by finger pressure during handling. The second instance occurred during the static load test and was a result of the greater than expected torsional deflection of the panel. As the loading was increased, the dial gage probe at the unsupported outboard corner of the panel slipped off the slanting structural surface and contacted the extreme corner cell, causing the breakage. The last two instances occurred during handling after the thermal-vacuum-shock test.

Edge cracks were found in both cells and coverglasses and were generally barely discernable, hairline cracks extending about 1/8 inch from the edge of the cell or, in some cases, running diagonally across a cell corner. Triangular chips at the edges were also noted on some cells. Approximately half of the reported discrepant cells were cracked or chipped sufficiently to be rejected on a flight panel. Of the 36 cells and 55 coverglasses that were cracked, 13 cells and 18 coverglasses were found to be cracked at the start of the test program. Additional cracking of 23 cells and

37 coverglasses, affecting 0.93% of the cell assemblies on the panel, was noted following the test program. The location of the cracked cells and coverglasses was generally distributed over the panel and throughout the test program as tabulated in Table 6-2. The total quantity of cells on the panel was 6480.

TABLE 6-2
REPORTED CRACKED SOLAR CELLS (C) AND COVERGLASSES (CG)

Module No.	Power Output Test Number						
	1 (initial)	2 (after Modal Survey)	3 (after Acoustic)	4 (after Random)	5 (after Sinusoidal)	6 (after Static)	7 (final after Environ. Test)
1	1 c, 1 cg				2 cg		
2							
3	1 c, 3 cg	1 c			1 c, 1 cg		
4		2 c, 2 cg			2 cg		2 c
5	4 cg				1 cg	1 cg	
6	1 c					3 cg	
7	9 c, 5 cg			1 c, 4 cg		2 c, 4 cg	1 c, 3 cg
8		2 cg	1 c, 1 cg		1 c	1 c, 1 cg	1 cg
9	2 cg	1 cg		1 c			1 cg
10		2 c		2 cg			1 cg
11	1 c, 3 cg	3 c		1 c, 1 cg			1 cg
12				2 c, 2 cg		1 c, 1 cg	
Total	13c, 18cg	8c, 5cg	1c, 1cg	5c, 9cg	2c, 5cg	4c, 10cg	3c, 7cg

GRAND TOTAL: 36 cells, 55 coverglasses

6.9.3 COSMETIC EFFECTS

—

The test instrumentation and economic tooling were responsible for some cosmetic blemishes on the panel which will be eliminated for flight equipment.

—

These cosmetic blemishes consisted of a stained area on the dark side of the substrate, several small patches where the RTV-40 coating was peeled off when temporary instrumentation tape was removed, and a vapor deposit on the sun side structure. The function of the test panel was not affected in any case.

The stained area on the substrate was caused by the filler material used at the joints in the bonding platen "bleeding" on the substrate. The substrate will be separated from the platen by a plastic sheet when the panel substrate is bonded in the future.

The instrumentation wiring for the various tests was attached to the RTV-40 coated structure with tape. Removal of these temporary tapes caused some peeling of the coating which was later touched up locally.

The brownish-grey vapor deposited film on the sun side structural members was observed after the high temperature soak. It is believed to be an outgassing product from the primer on the members. A minimum quantity of this film was noted on the solar cells and the power output was not affected.

SECTION 7.0: MANUFACTURING AND MATERIEL

The manufacturing sequence, fabrication and assembly techniques, special tooling, and materiel activities are described in this section. The completed test panel is shown in Figures 7-1 and 7-2.

7.1 MANUFACTURING PLAN

The manufacturing plan, in following the sequence used in assembling the Large Area Solar Array (LASA) panel, avoided any significant problems.

The manufacturing plan, as in the LASA program, consisted of the following basic sequences:

- 1) Detail Fabrication---Including the long-lead beryllium and titanium details.
- 2) Subassembly---Including the beryllium cap-channel assemblies commonly called "sticks" and the solar cell stacks and seven-cell groups.
- 3) Major Subassembly---Including the sun side and dark side structural frames, the substrate, and the solar cell submodules.
- 4) Structural Assembly---Which involves the bonding of the substrate between the sun side and dark side frames.
- 5) Final Assembly---Which involves the installation of the solar cell submodules and other components on the structure assembly.

The above sequence was followed throughout manufacturing with no significant problems. Other important features of the manufacturing plan included the early definition of beryllium details and the provisions in the panel design to allow the use of existing LASA tooling. The formed beryllium channel shapes and gages were identified as early as possible to allow material to be collected and the LASA form die to be reworked commensurate with schedule requirements.

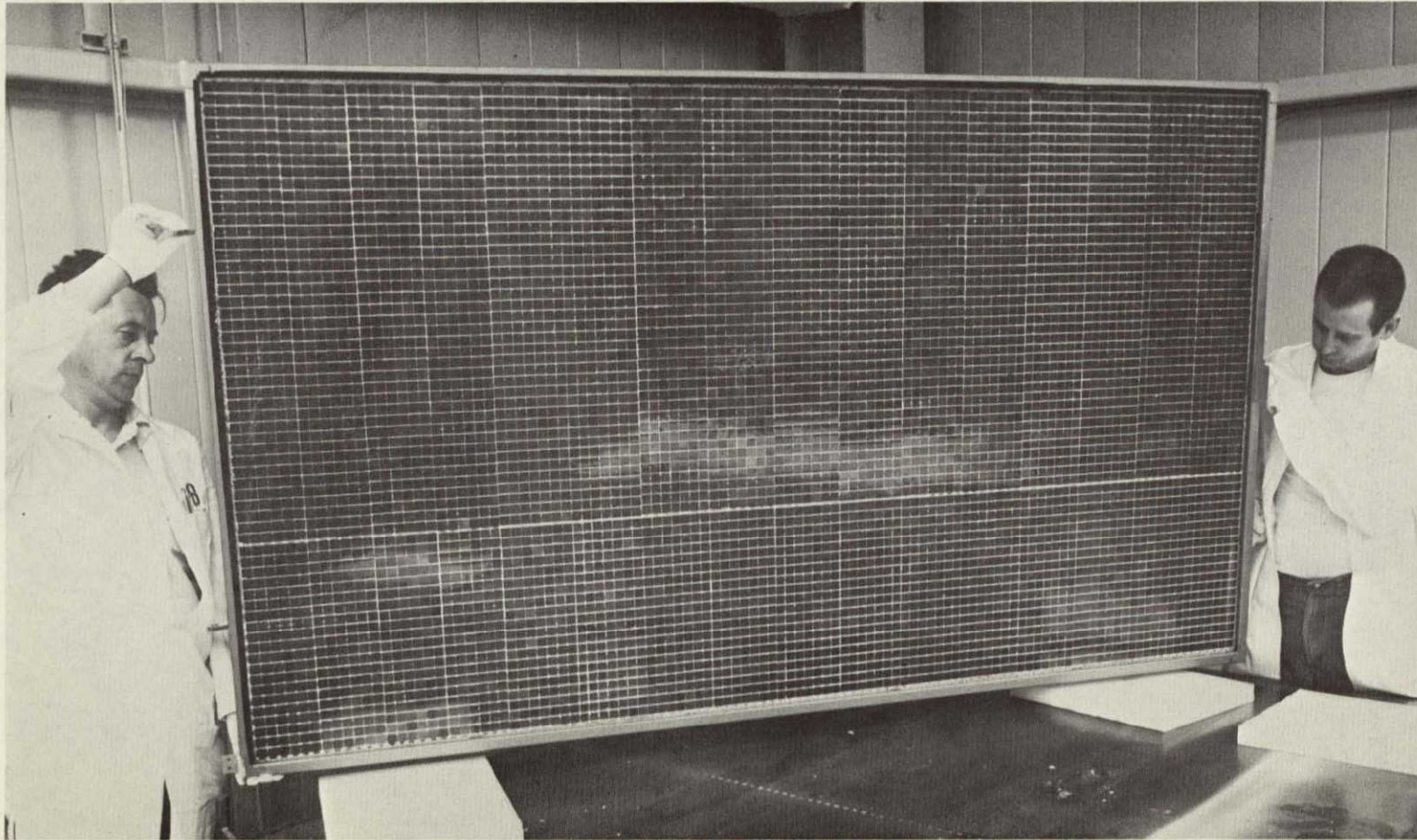


Figure 7-1: TEST PANEL - SUNSIDE

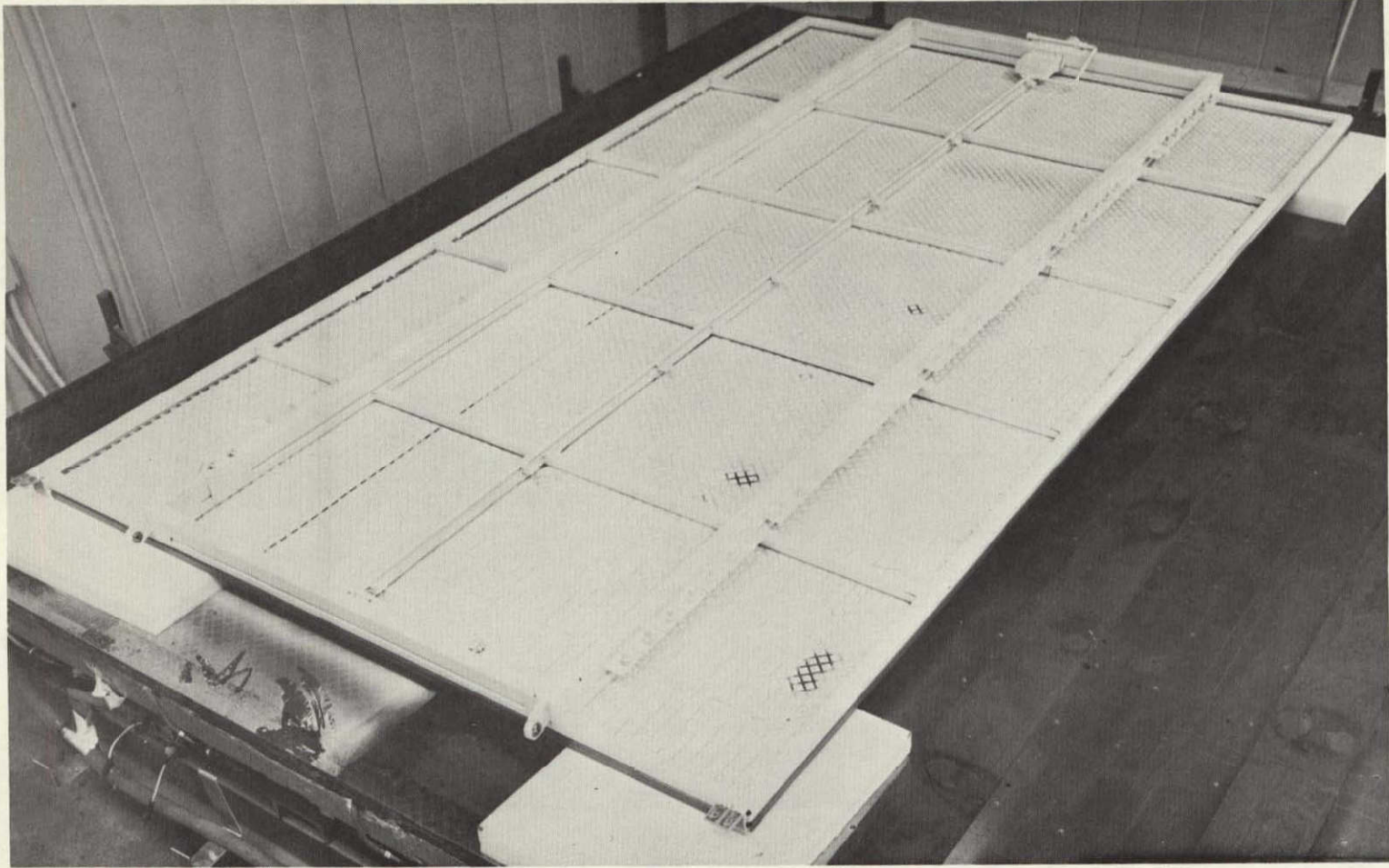


Figure 7-2: TEST PANEL - DARKSIDE

7.2 DETAIL FABRICATION

—

Beryllium channels were successfully formed to the required straightness tolerances.

—

Beryllium Details---Beryllium sheet material was obtained in strips in the widths required for forming channels or in net widths for flat parts from purchases and from surplus LASA Program stock.

The beryllium channel forming was done in a stainless steel die from the LASA program. The channel form die, shown in Figure 7-3, was modified to accept punches for all three different size channels and to provide support for and position the three punches. New material guides were also made.

The die was heated and the forming done in the hot platen press, shown in Figure 7-4, with ceramic platens on the top and bottom. The part was loaded in the die outside the press, moved into the press, and both die and part heated to 1,375°F. The part was "creep formed" by lowering the upper platen at 0.1 to 0.2 inch per minute until the punch bottomed the part.

The channel straightness required by the design is 0.002 inch in 10 inches, and the channel flange perpendicularity requirement is 0.005 inch. These straightness requirements are to prevent inducing stresses into the sticks when the stick components are forced straight during bonding. To produce channels to the required straightness, fluid pressure was applied vertically by means of a stainless steel bladder to force the die and hence the channel to conform to the flat bottom press platen. Fluid pressure was applied horizontally by means of an expanding stainless steel tube to force the channel flanges to conform to the perpendicular sides of the punch and the straight fixed side bar of the die.

A pressure of 6 to 8 psi was applied to the upper bladder for two minutes, then reduced to zero. A pressure of 200 psi was applied to the steel side tube and the 6 to 8 psi reapplied to the upper bladder for 10 to 20 minutes. The upper platen was then

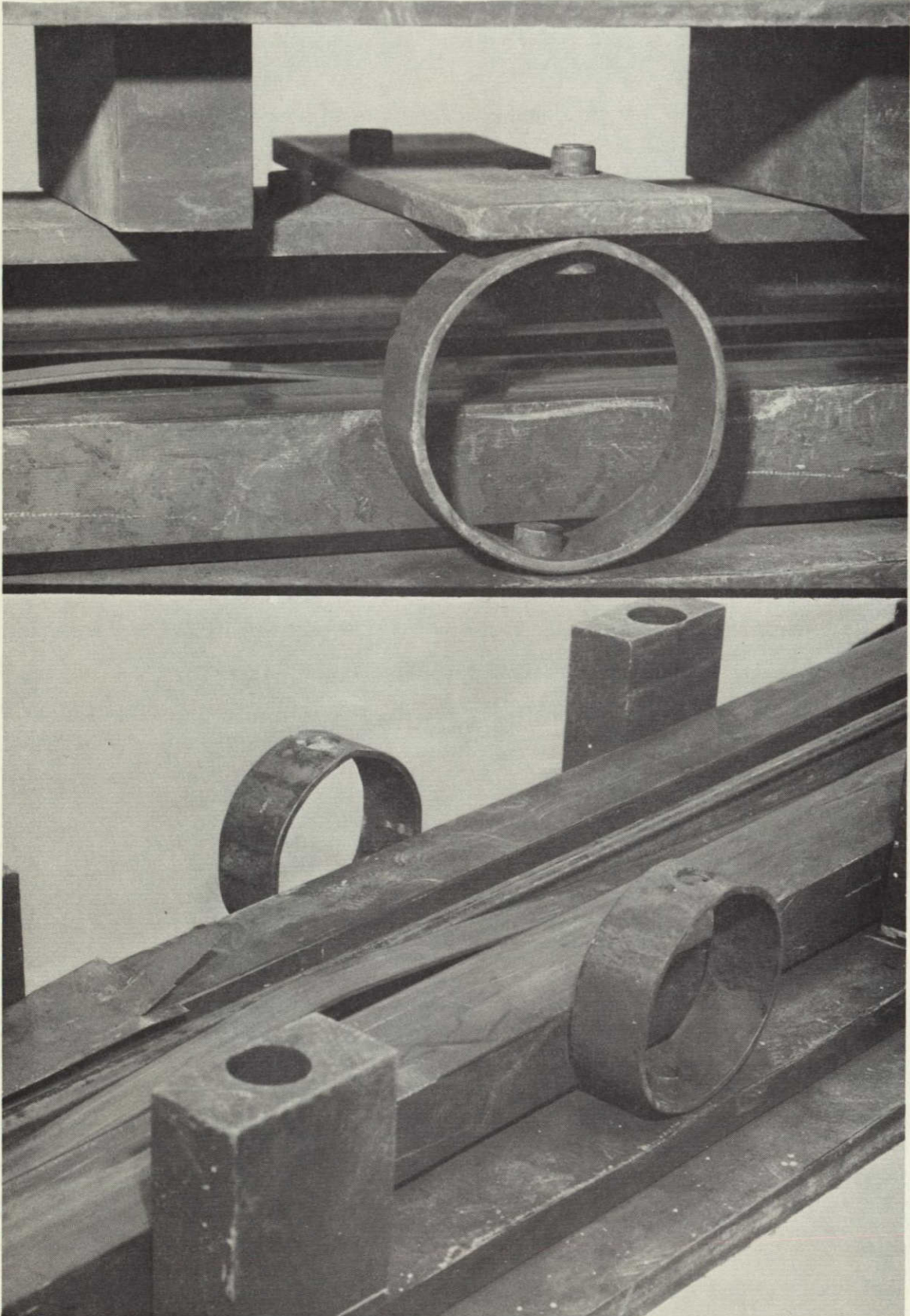


Figure 7-3: CHANNEL FORM DIE

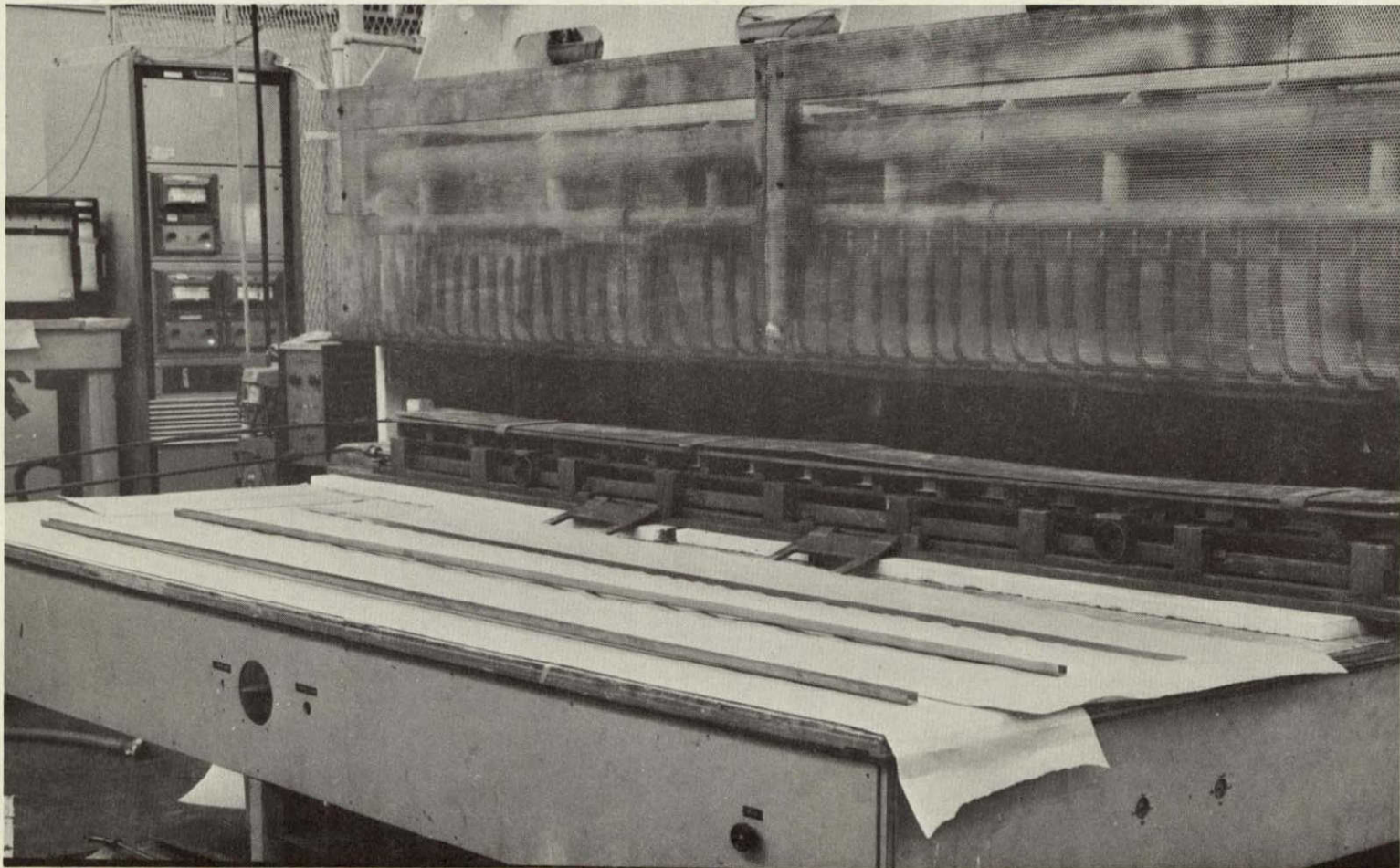


Figure 7-4: HOT PLATEN PRESS

raised slightly to take the platen weight, but not the upper bladder pressure, off the part; then the part and die were cooled to 800°F (from 1375°F) and removed from the press. At 500°F, the part was removed from the die, inspected, then sent to trimming where excess flange height was removed by cutting with an abrasive wheel.

Channels were then sent to penetrant inspection, followed by chem-mill and priming with a baked-on epoxy primer. Unformed beryllium parts were cleaned or chem-milled and primed. Beryllium test specimens were regularly bonded and lap shear tested to prove the continuous effectivity of the cleaning and priming processing. Chem-milling and cleaning were done using an etch tank containing an ammonium bifluoride/phosphoric acid solution and a de-smut tank containing a sulfuric/chromic/phosphoric acid solution.

The beryllium parts for the LASA Phase II were chem-milled, cleaned, and primed by a subcontractor. The shorter parts required for this program allowed the use of equipment from LASA Phase I, and a cost savings was achieved as the result.

The zener diode brackets were designed to utilize LASA surplus beryllium channel material. Two long channels were bonded back-to-back with AF-126 adhesive, the flanges were cut off from one side to make a T-shaped part, then the part was cut to length and drilled. These parts, which were hand-held for cutting to length with an abrasive saw and drilled with conventional aluminum backup plates, demonstrate that, in many cases, special methods are not required for beryllium fabrication.

Titanium and Steel Parts---Titanium sheet stock of the various gages was cleaned and primed; then gussets, clips, and fillers were cut from the sheets. Titanium hinge fittings, tip latch fittings, and the cruise damper fitting were machined from solid plate. The hinge and tip latch fittings, originally designed to be welded, were rough-machined, then finished by electrical discharge machining using a graphite electrode. This resulted in a cost savings of 30 percent per fitting. The sun sensor and attitude control simulators were machined from mild steel bar stock.

7.3 STRUCTURAL SUBASSEMBLY BONDING

—
Significant cost reduction was achieved through the use of new bonding techniques.
—

A major difference from the LASA program in the bonding of the test panel structure was the use of a baked-on, corrosion-inhibiting, adhesive primer (Boeing Specification BMS 5-59) with the AF-126 adhesive. This primer, applied immediately after each etch cleaning, provided the critical metal/epoxy interface required for reliable bonds. Significant cost savings were achieved through the use of this primer. Its use enabled parts to be handled, fitted up, and even cut to size without degrading the bond. This allowed the fabrication of beryllium parts as stock which were cut on assembly or even after assembly to the proper length. Parts were solvent-wiped just before applying adhesive to the primed surfaces. Assembly and bonding procedures were controlled by use of the LASA Process Specification Document, D2-113354-1.

Structural Member Subassemblies---The subassemblies, or "sticks" were bonded in the stick assembly bonding tool shown in Figure 7-5. This tool was constructed for the LASA program and was modified for use on this program by reworking the Teflon mandrels to suit the three different size channels used on the test panel.

The channels and flat strips comprising the sticks were "fitted up" to check the parts for accuracy, then adhesive was placed on primed channels, and caps and shear webs were assembled over the Teflon material. A thin, heat-resistant, mylar adhesive tape was used to hold the parts in the proper relationship to each other. Parts were then placed into the fixture, and after inspection an "okay to bond" was obtained from Quality Control. Heat for the bonding temperature was supplied by an electric blanket under the baseplate of the tool, and pressure was applied from line pressure through a regulator to an air bladder on the tool. The sticks were bonded by heating to a temperature range of 225°F to 250°F with a pressure of 17-100 psi. The assembly was maintained at that temperature and pressure for a minimum of one hour. After bonding, the sticks were cut to length and miter cut where required, then inspected.

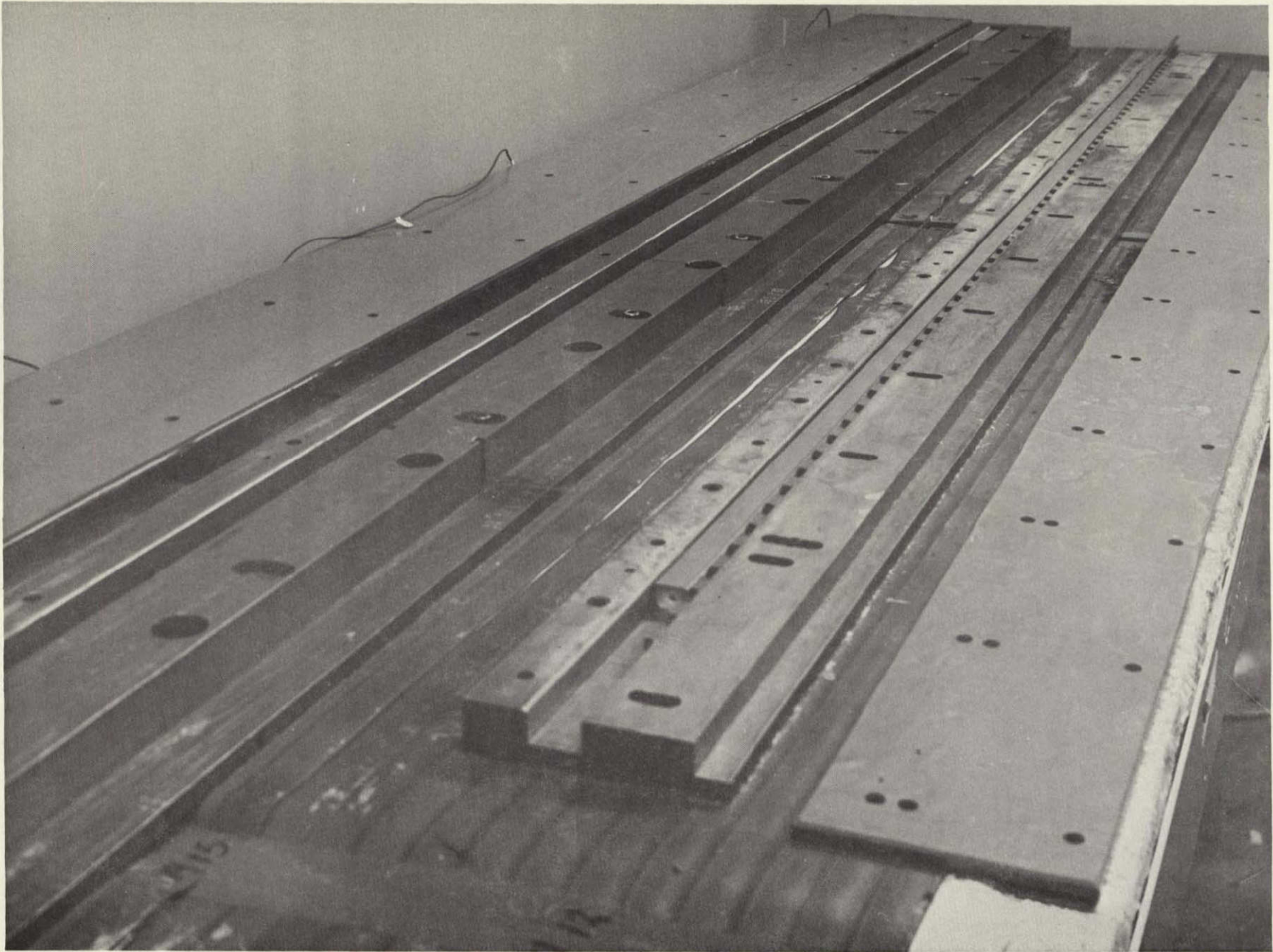


Figure 7-5: STICK ASSEMBLY TOOL

To utilize available surplus beryllium material, two of the outboard spar channels were spliced. This was accomplished by bonding beryllium splice angles inside the channels using the LASA splice tool.

Sun Side and Dark Side Frames---These major assemblies were bonded in the LASA panel bonding jig which was modified to incorporate a "spring and plate" pressure application system. This system was used to avoid vacuum-induced side pressures during bonding. The modified bonding jigs for sun side and dark side frame bonding are shown in Figures 7-6 and 7-7. The six-inch-square aluminum plates, threaded studs, and springs, comprising the spring and plate devices, are detailed in Figure 7-7.

The sun side frame bonding was accomplished in one cycle. Details to be bonded were wiped clean with Methyl Ethel Keytone (MEK). AF-126 adhesive was placed on one face of each mating surface; and tubular members, gussets, and clips were jig-located on the bonding platen. Shimming of gussets, if required, was done at this time. Rubber pads were placed on top of gussets and spring pressure plate setups were placed over each gusset and adjusted to give the required vertical bond pressure. Rubber-faced, calibrated, spring-loaded clamps were placed to apply horizontal pressure to clips previously taped in place at the inside and outside of each corner joint (Figure 7-6). After the "okay to bond" was obtained, an aluminum coarse mesh screen, shaped to form a cover, was placed over the assembly. A nylon cover was placed over the aluminum frame; aluminum foil for insulation was placed over the nylon; and two hair dryer-type fans were placed in opposite corners of the aluminum frame for warm air circulation. This heating arrangement avoided temperature variations and the temperature was held to within plus or minus 5°F of the desired temperature. Heat was derived from heating blankets under the jig base, and bonding was accomplished with a temperature of 225°F to 250°F for one hour.

The dark side frame was bonded using the techniques described above. Two bond cycles were used on the dark side, one for vertical pressure (gussets) and one for horizontal pressure (clips, doublers, and vertical gussets). The gussets at the inter-costals are on top of the tubular members which means that the substrate surface of

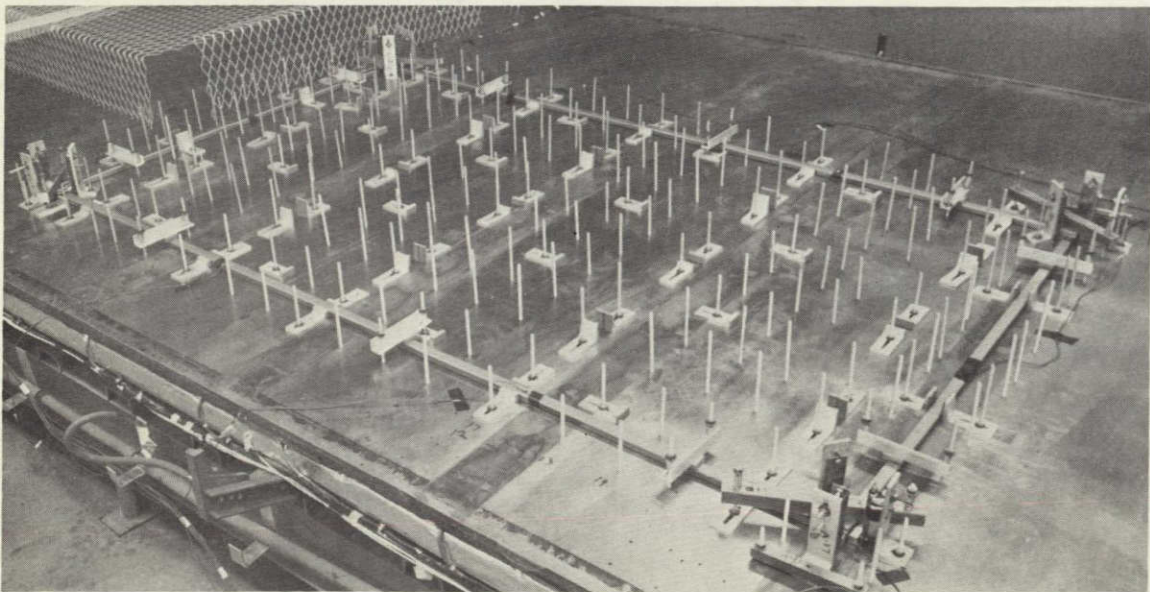
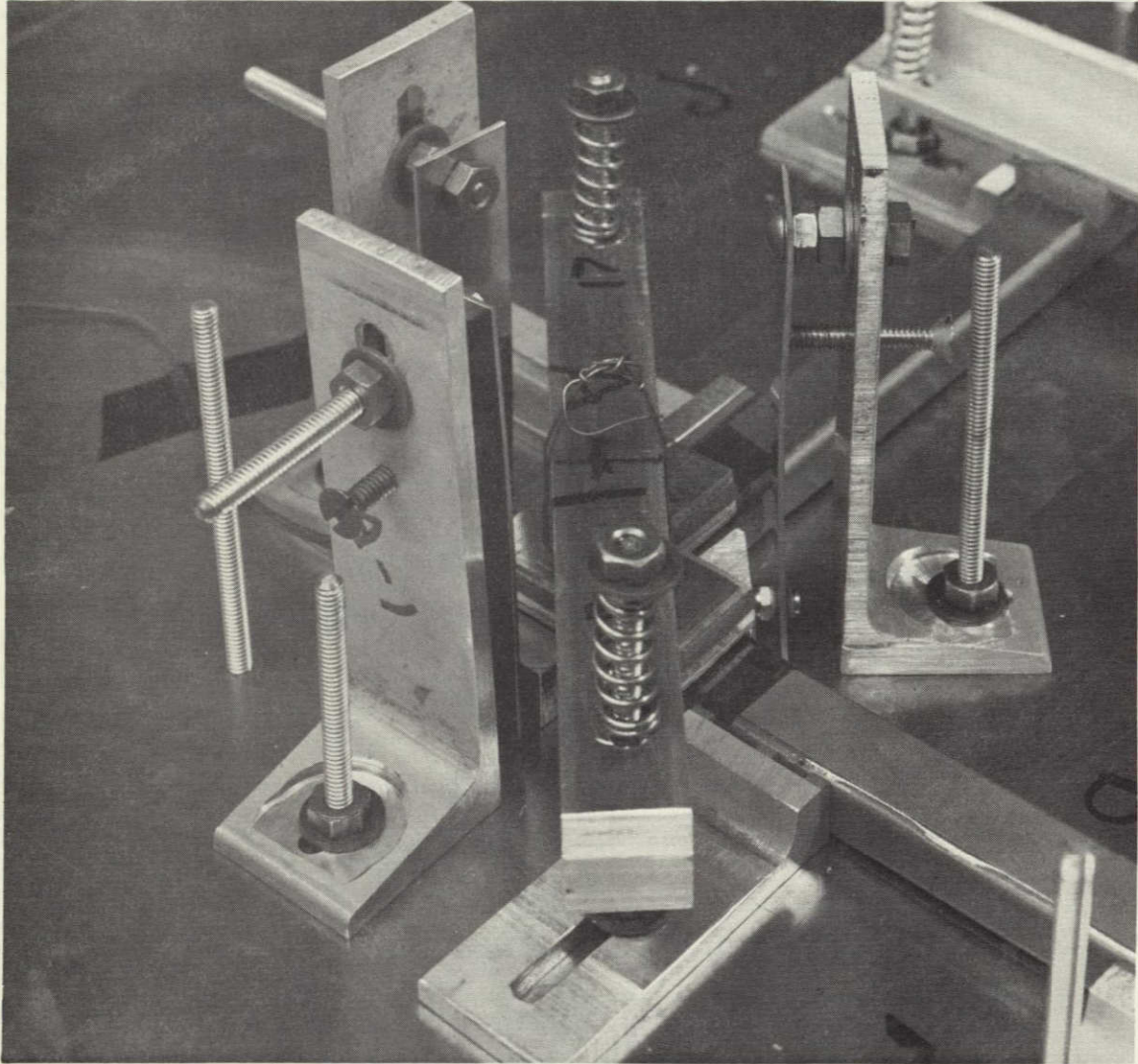
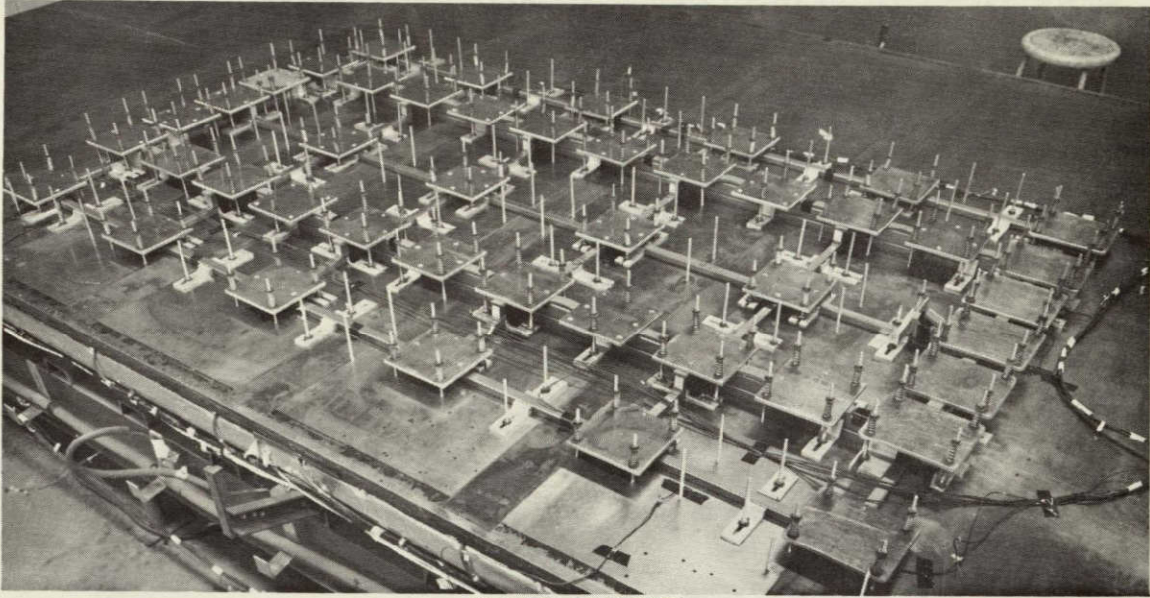


Figure 7-6: FRAME BONDING - SUNSIDE FRAME



GUSSET BONDING

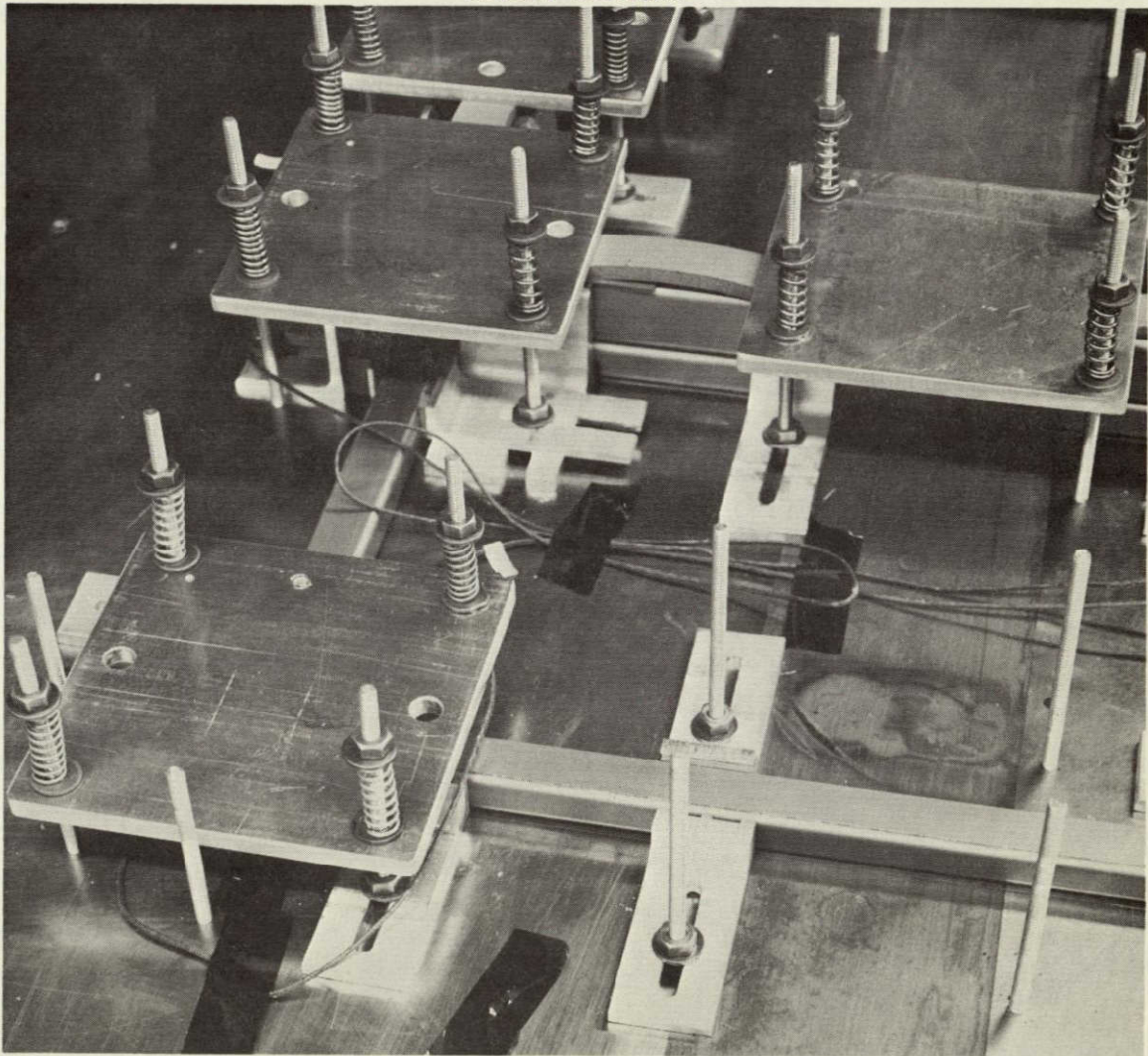


Figure 7-7: FRAME BONDING - DARK SIDE FRAME

the dark side frame is not flat. To prevent the substrate from having sharp planar irregularities which would have resulted in possible bending of the solar cells, ramps were installed. These ramps consisted of layers of adhesive in different length strips, built up to the thickness of the gussets. Figure 7-7 shows the plates and springs in position to bond the gussets, as well as the deep member of the main spar to the standard depth member of the main spar.

7.4 SUBSTRATE BONDING

—
Pretensioning the fiberglass substrate tapes was unnecessary because of the difference between the thermal expansion of the steel platen and the fiberglass.

—
The substrate was bonded on the structure bonding jig platen with a tension bar frame to hold the tape ends. To obtain more accurate spacing and alignment of the tapes, an additional row of removable alignment pins was added to the platen.

The substrate was made of fiberglass tapes pre-impregnated with epoxy resin in the uncured or "B" stage. The tapes were laid and spaced using locating pins along the outside edges of the tool and the added row of temporary pins along the center of the bonding platen. The tapes were tensioned by hand and held in place with double-backed tape. The tapes were covered with a Teflon parting film and a nylon vacuum bag was sealed to the outer edges of the jig baseplate. A 10-inch minimum vacuum was drawn and the jig baseplate was heated to 300°F. The assembly was cured for 30 minutes at 300°F and for 4 hours at 350°F. Expansion of the steel bonding platen provided the slight tension required to straighten the tapes. After curing, cooling to 150°F, and removing the vacuum bag and Teflon parting films, the substrate assembly was visually inspected and the node bonds checked. The substrate was stored in its tension bar frame.

7.5 STRUCTURE FINAL ASSEMBLY

—
The threaded stud and pressure plate bonding tool, although economical, is not recommended for use on future production.

—
The sun side frame and the dark side frame were joined to the substrate using the same bolt, plate, and spring setup as was used on the dark side frame. Additional bolt, plate, and spring assemblies were used to apply bonding pressure along the length of the members between plates used at member-to-member joints. This system of bonding eliminated the vacuum bag and the more costly spacers, bars, and plates required on LASA to protect the beryllium structural members from the vacuum bag side pressures. AF-126 adhesive was placed on the sun side frame which was then set on the bonding platen, dark side and adhesive up, and positioned to scribe lines on the platen. Spacing bars were placed to support the dark side intercostals and to apply bonding pressure to the substrate. Threaded studs were placed in position to accept aluminum pressure plates. Short pieces of plastic tubing were placed on the threaded studs to prevent the threads from damaging the substrate strands. The substrate, still in its tension frame, was abraded with Scotchbrite and cleaned with MEK, then was slowly and carefully lowered over the studs onto the sun side frame. The substrate was tensioned to 12 pounds per linear inch of edge by adjusting the air cylinders and heating the tension bars, shown in the substrate/frame bonding operation in Figure 7-8. The final positioning of the substrate nodes relative to the sun side frame was accomplished by shifting the position of the substrate frame on the bonding tool. After this was done, the dark side frame, with adhesive applied, was placed on top of the substrate and positioned to the sun side frame. Silicone rubber was placed on the upper surface of all dark side frame areas where pressure would be applied. Bolts, springs, and plates were installed; and springs were adjusted to apply the required pressure on the adhesive. The substrate/frame bond setup is shown in Figure 7-9.

The aluminum cover, nylon cloth, and aluminum insulation were placed over the assembly. The small fans were placed in the corners, heat from the blankets under

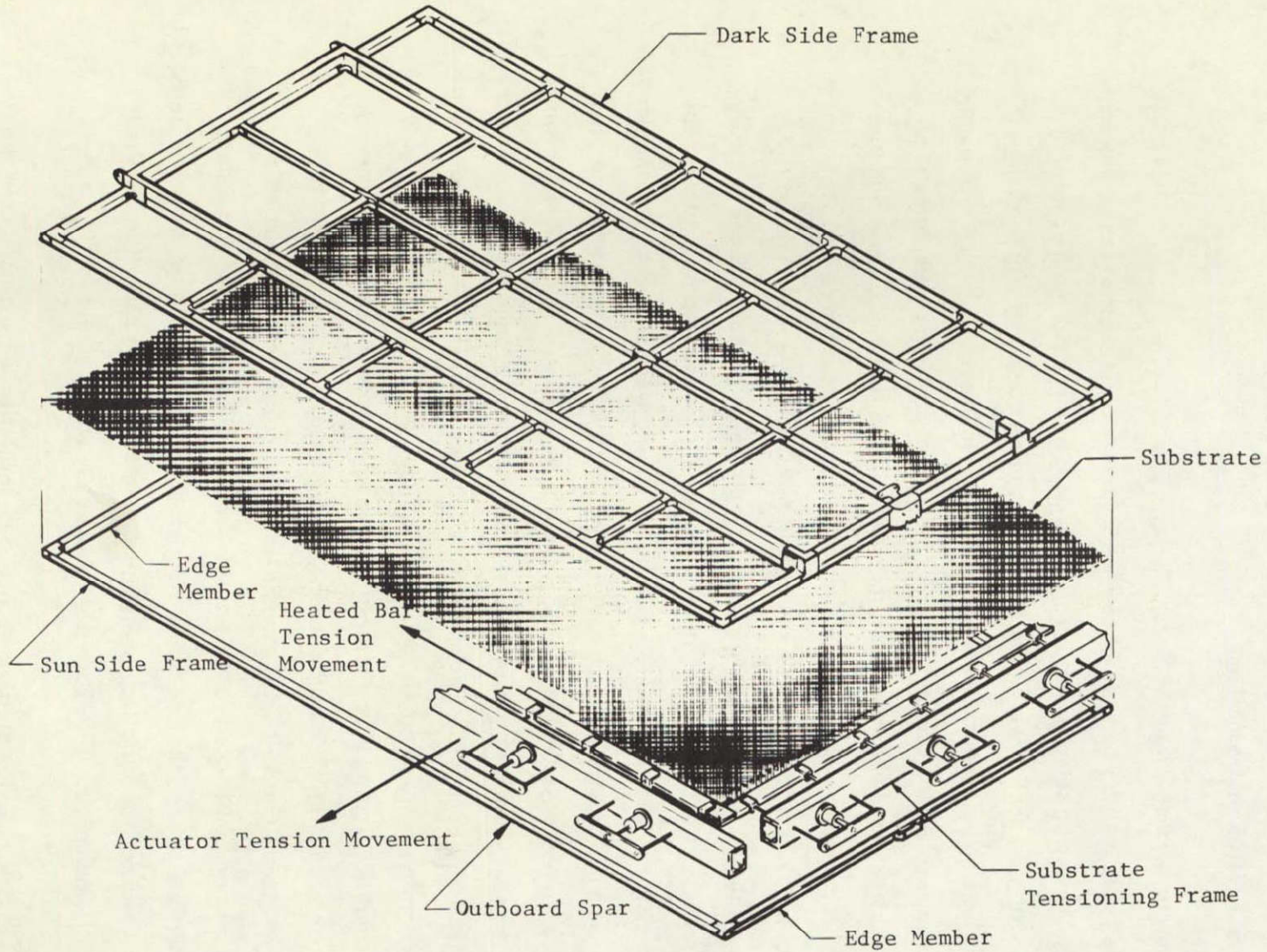


Figure 7-8: SUBSTRATE/FRAME BONDING

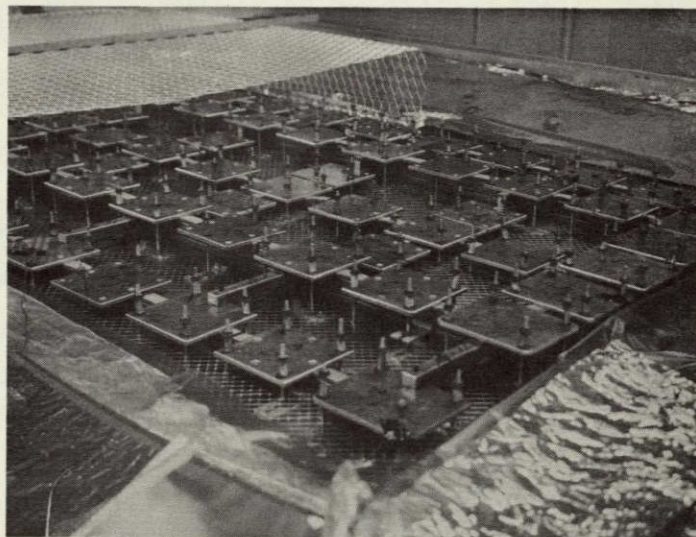
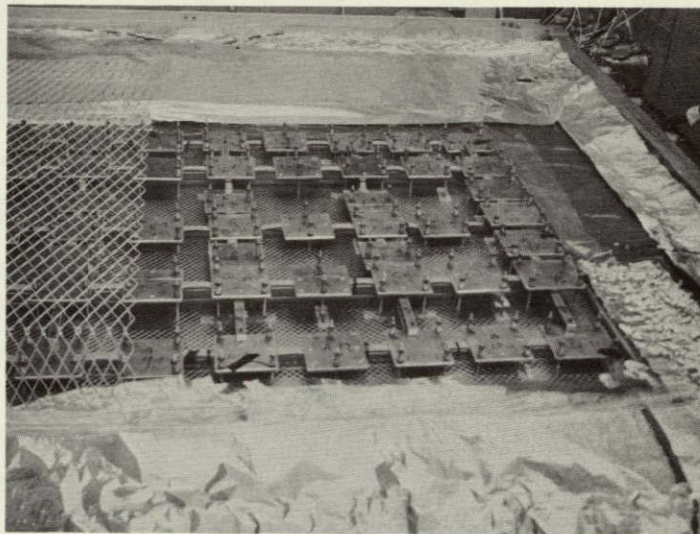


Figure 7-9: SUBSTRATE/FRAME BOND SETUP

the platen was turned on, and the panel was bonded by heating to 225°F - 250°F for one hour. After cool-down, the cover was removed and the threaded studs were carefully removed from the platen. Figure 7-10 shows the completed structural frame assembly, and Figure 7-11 shows the titanium hinge cruise damper and tip fitting installations.

In some places, the removal of the threaded studs from between the substrate tapes caused separation of the tape-to-tape bond. These were repaired with Boeing Specification BMS 5-59 room-temperature cure adhesive. Some separation of this adhesive was later noted during the test program. For this reason, and because of the excessive time required to install the studs, and the care required to guide the substrate onto them, the spring and plate devices are not recommended for use other than on one-time developmental tooling. Tools similar to those used on LASA are recommended for the fabrication of flight-quality units.

7.6 SOLAR CELL, CELL GROUP, AND SUBMODULE ASSEMBLY

—
Modified LASA solar cell module assembly tools were used for solar cell interconnections.

—
The build-up of the "live" (electrically connected) solar cell submodules involved three levels of subassembly:

- 1) The assembly of individual cells and coverglasses.
- 2) The assembly into seven-cell groups.
- 3) The assembly of 20 or 40 cell groups into submodules.

Solar Cell Assemblies---The test panel contains 6,480 solar cell assemblies (coverglasses installed), 3,360 of them connected electrically by expanded silver mesh interconnectors. The remaining 3,120 cell assemblies were not electrically connected but were installed on the panel to simulate weight. Solar cell assemblies were made

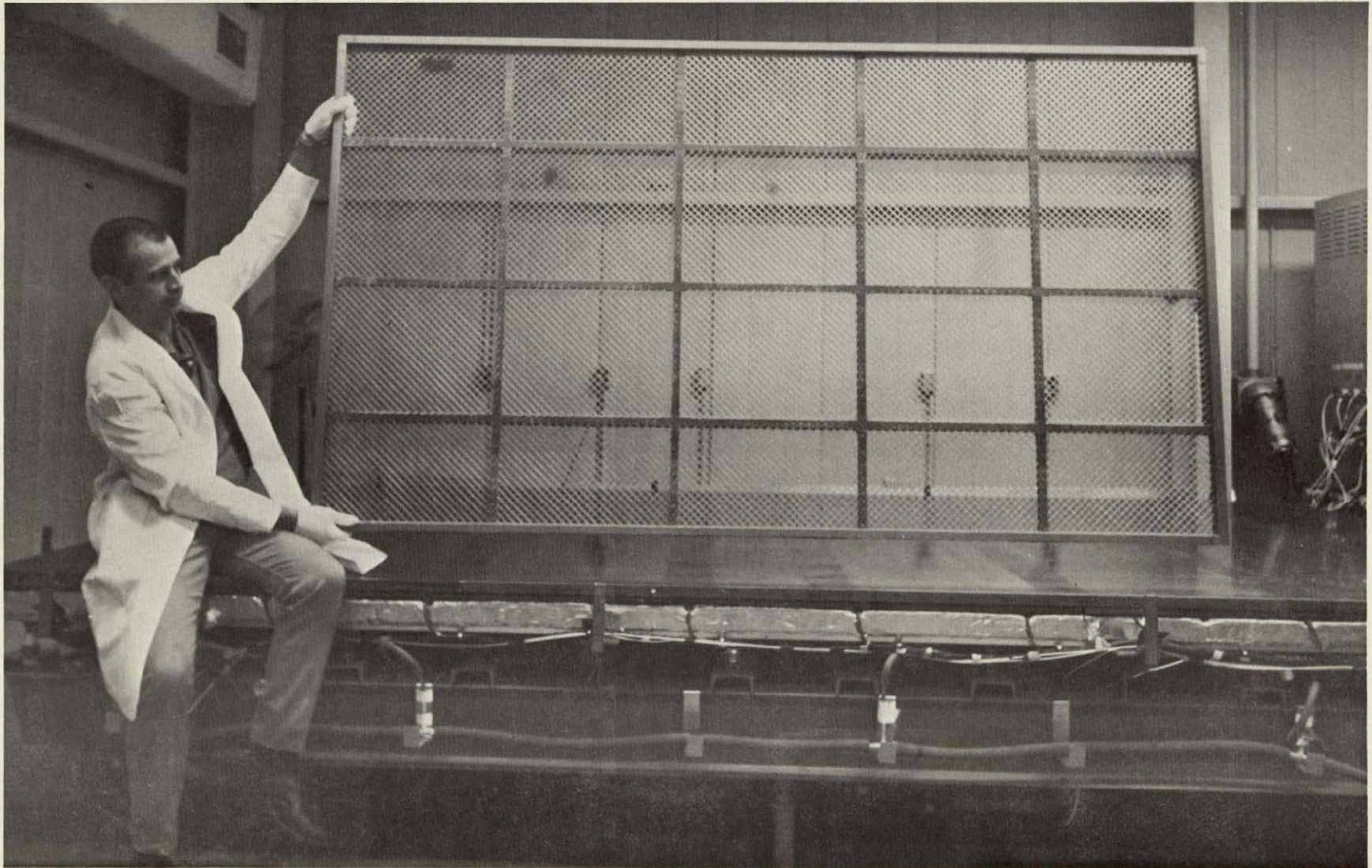


Figure 7-10: COMPLETED STRUCTURAL FRAME ASSEMBLY

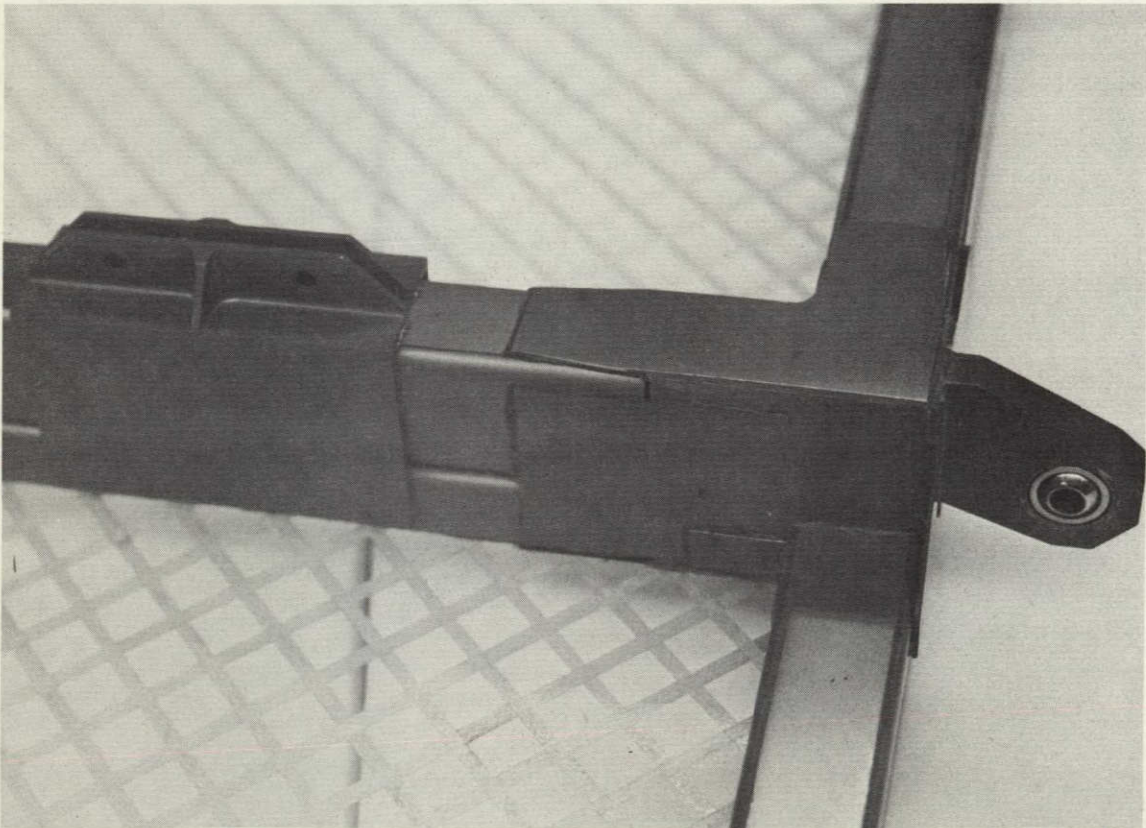
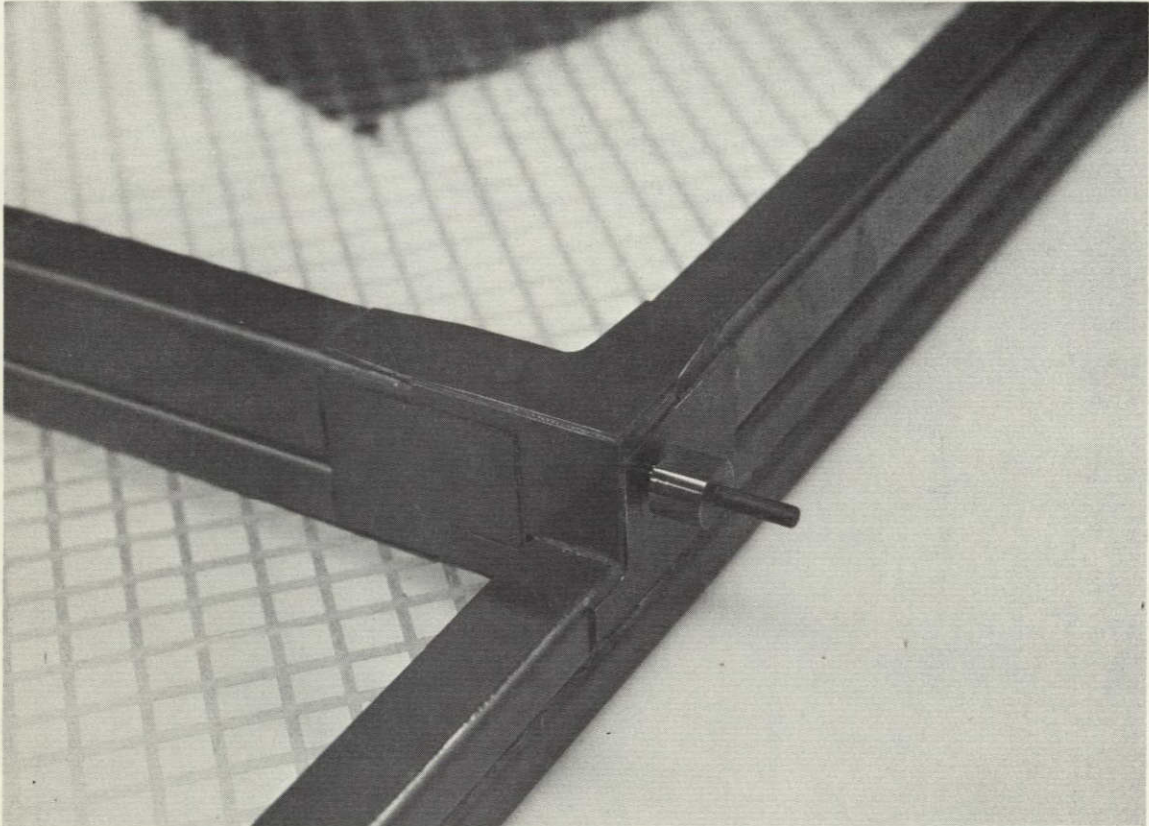


Figure 7-11: TITANIUM HINGE, CRUISE DAMPER, AND TIP FITTING INSTALLATIONS

by installing a 0.003-inch-thick LASA surplus coverglass on the sun side of each solar cell. Solar cells were separated by power output grades; then cells and coverglasses were swab-cleaned with MEK, rinsed with ethyl alcohol, air dried, and placed in clean containers. Solar cells were then placed sun side up in a holding fixture, adhesive was added, then the coverglasses were placed on top of the adhesive. After ten minutes, pressure (weight) was added to the coverglass to assure an adhesive bonding thickness of 0.001 inch or less. Assemblies were cured for 12 hours at room temperature before handling and 36 hours before cleaning.

Cell Groups---Solar cell groups were made by joining seven solar cell assemblies with a silver mesh interconnector in the LASA seven-cell soldering fixture shown in Figure 7-12. Four-hundred-eighty solar cell groups, each containing seven cell assemblies were connected electrically in the module soldering fixture shown in Figure 7-13. After cleaning, the cell assemblies were placed in the seven-cell soldering jig, dark side up. The cells were interconnected in parallel. Interconnectors made of expanded silver mesh were cleaned with nitric acid, cut to size, and formed to shape using the interconnector template tool. Solder cream was applied by a stencil to three places on each solar cell in the group of seven cells. The interconnector was then positioned over the solder cream locations. Using LASA-developed soldering schedules, the interconnector was pulse-soldered to the solar cell. Groups were then stored by power output grade in labeled storage containers. The solar cell soldering template is shown in Figure 7-14.

Submodules---Solar cell submodules were assembled by placing seven-cell groups in the module soldering fixture (Figure 7-13), with each newly added group being soldered to the previous group by the same process as used for cell group soldering. Six submodules had 40 live cell groups, and 12 submodules had 20 live cell groups. Submodules were then inspected and packaged in a clean, labeled plastic case.

The unconnected groups of solar cells were made up of three modules, each containing 80 six-cell groupings, and three modules, each containing 80 seven-cell groupings. These modules were made by placing individual solar cell assemblies in the assembly tool until the required number of cells had been placed. Cells were then

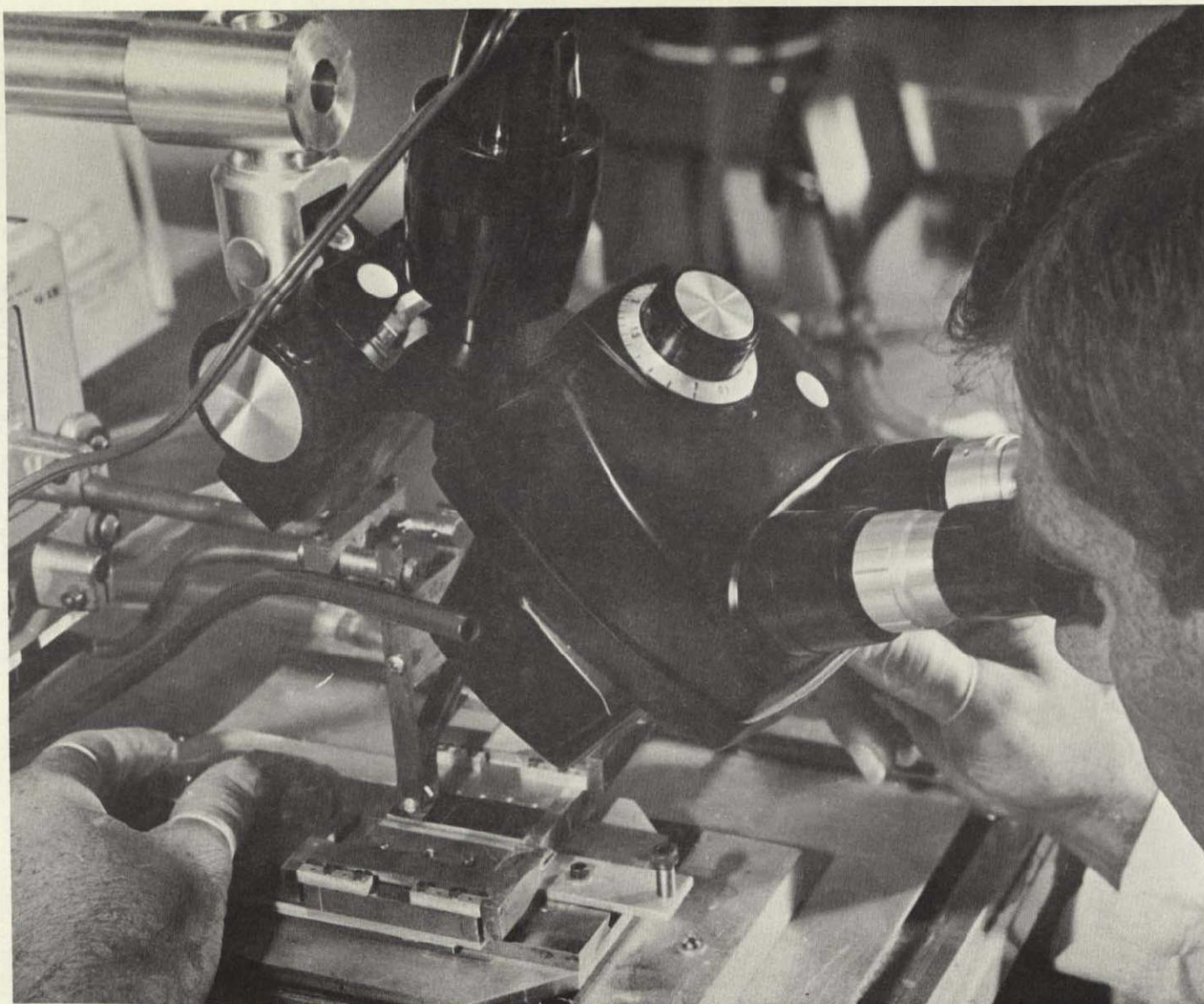


Figure 7-12: SEVEN-CELL SOLDERING FIXTURE

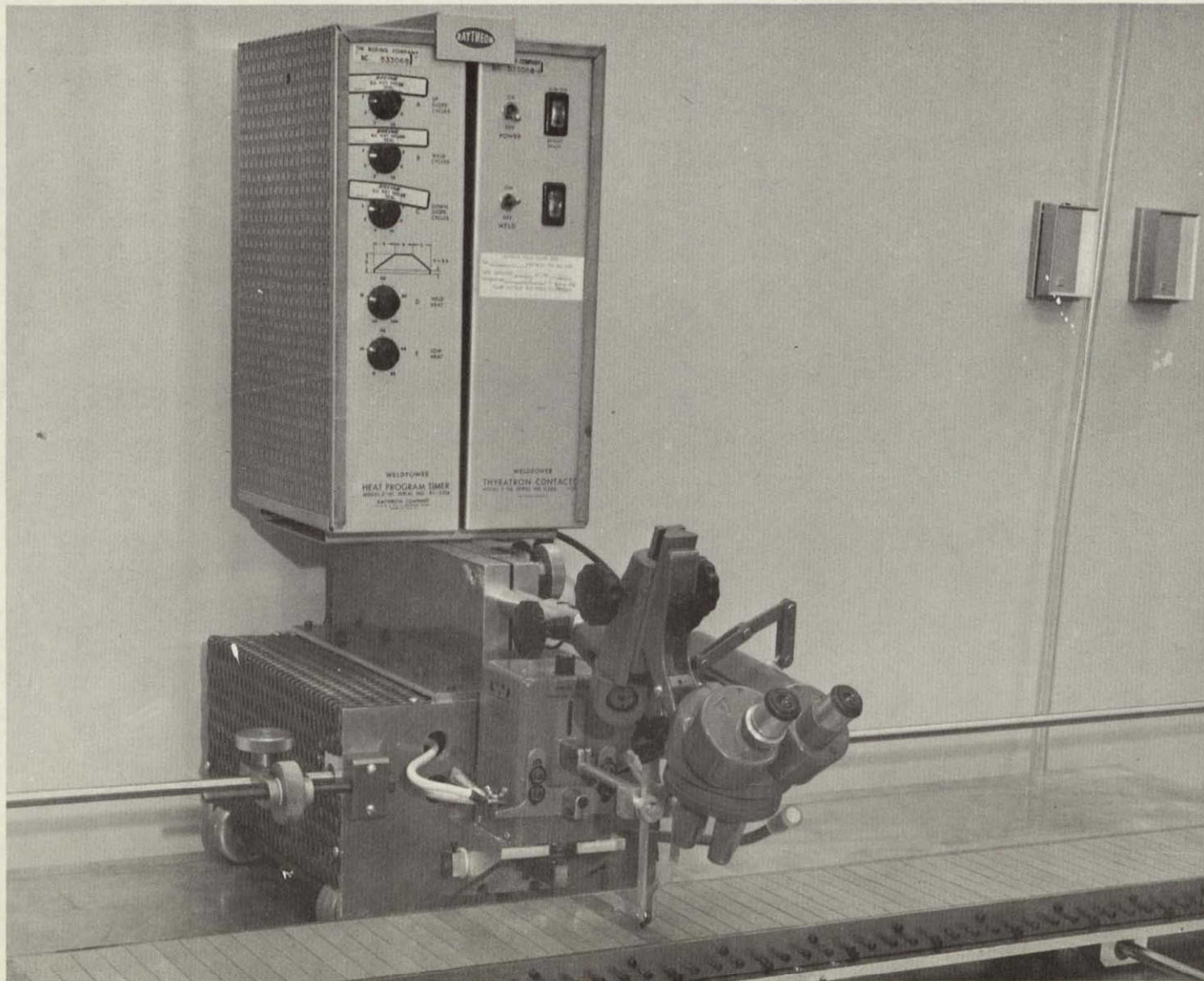


Figure 7-13: MODULE SOLDERING FIXTURE

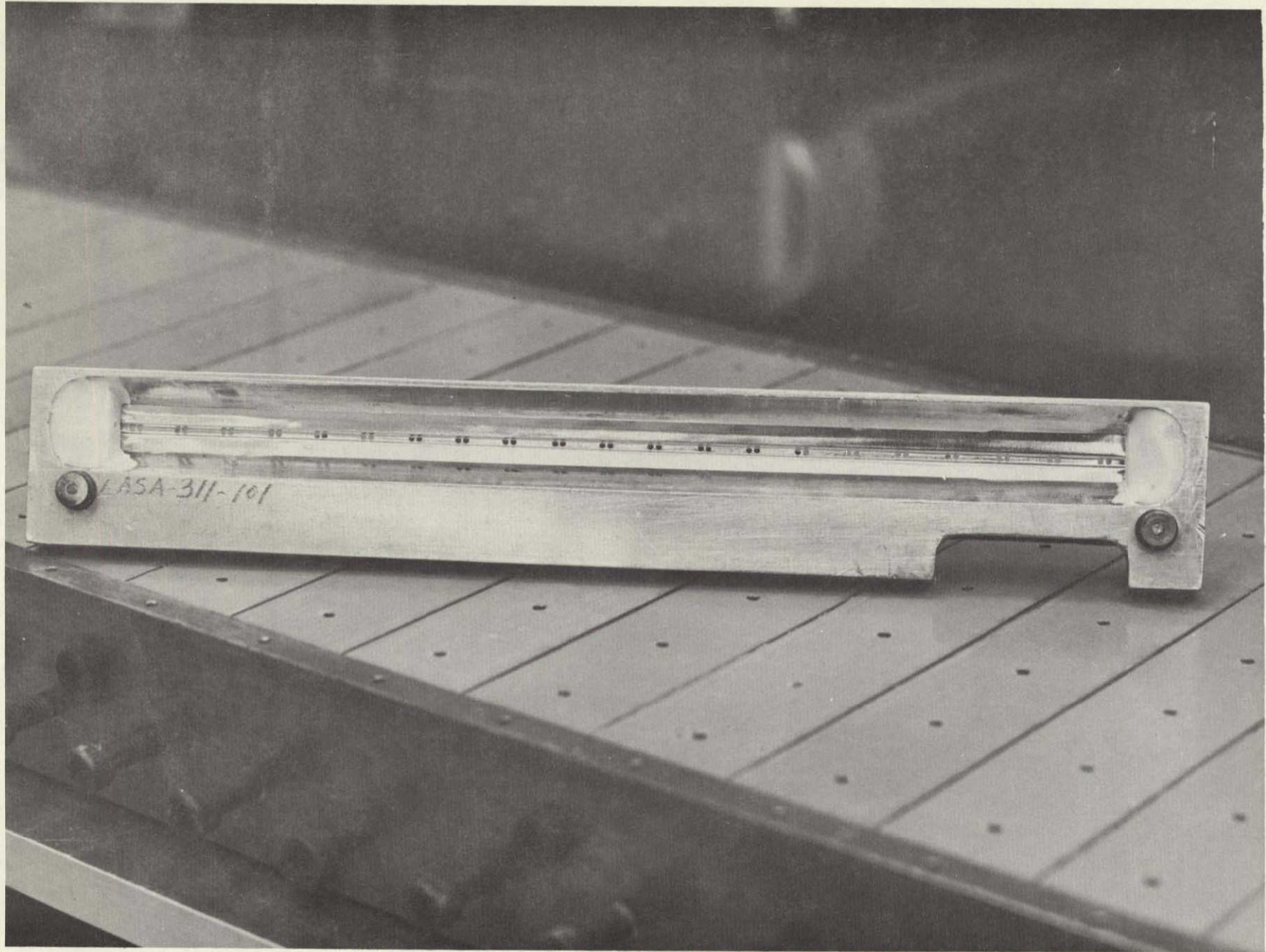


Figure 7-14: SOLAR CELL SOLDER TEMPLATE

temporarily joined into a module by placing low-tack adhesive tape over the cells in the tool. These modules were stored in identified plastic cases.

7.7 TEST PANEL FINAL ASSEMBLY

—

The economical solar module installation technique developed on LASA was successfully used on the test panel assembly.

—

The solar cell modules were bonded to the substrate with RTV-40, a room-temperature vulcanizing silicone rubber compound. A primer was placed on the sun side of the substrate and the dark side of the solar cells. Adhesive was sprayed onto the solar cell modules and allowed to partially cure. Just prior to bonding the modules to the substrate, adhesive was applied to the substrate with a urethane foam paint roller. The structural assembly was set on the bonding platen, sun side up, and the solar cell modules were placed on the frame. Polyurethane foam cushions covered with a Teflon film were set under the substrate between the dark side members. A one-piece masonite sheet was placed over the solar cells and a vacuum bag sealed around the entire assembly. The masonite provided a stiff backing to assure no bending of solar cells. It also flexed sufficiently to conform to irregularities in the substrate plane caused by the dark side frame gussets and adhesive ramps. Bonding was performed at approximately one lb/in² for six hours at room temperature.

After bonding, the silver mesh pigtails protruding from the ends of the submodules were soldered to the appropriate connections. Some damage to these pigtails was encountered as a result of bending during handling and bonding. These damaged pigtails were replaced by silver mesh splice pieces soldered in place. Subsequent failures of these pigtails are discussed in Section 6.9. A recommended design which would eliminate the pigtails is described in Section 10.

Other electrical items installed on the test panel included the zener diodes and brackets, blocking diodes, bus bars, and wiring. The copper bus bars were made by placing

net-trimmed copper foil, rough-trimmed Kapton insulating material, and unsupported thermoplastic adhesive in a vacuum bag, then in a beryllium stick bonding tool for heat application and vacuum pressure containment. Resulting bus bar assemblies were removed from the tool and trimmed to size. The zener diode brackets were attached to the main spars using a silicone rubber adhesive, RTV-630. The bus bars were bonded to the frame using the same room-temperature vulcanizing silicone adhesive.

Mechanical parts and mass-simulated equipment items were mechanically fastened to the test panel. These items included the tip latch pins, the cruise damper latch, and the simulated sun sensor, attitude control jets, tubing, and clamps.

The RTV-40 thermal control coating was the same silicone rubber compound used to attach the solar cell modules to the substrate. The substrate dark side was masked, as were certain instrumentation points and electrical connections, before application of the sprayed coating. The coating was then sprayed on the exposed dark side surfaces, and was dried for four hours at 125°F. The panel was then cleaned, inspected, and placed in its shipping container, ready for testing.

7.8 MATERIEL

—

The beryllium sheet was the major materiel cost item for the test panel.

—

Only fifty-five percent of the beryllium strip material for the test panel had to be purchased. The remainder was transferred from the LASA program surplus stock. Minor amounts of other items such as special adhesives, Kapton tape, zener and blocking diodes, and solder paste had to be purchased.

Test fixture material purchased consisted of small quantities of commercially available materials and standard parts. Some of the items purchased were: magnetic recording tape, adjustable camera tripod for supporting the panel, standard steel shapes, strain gages, aluminum plate, and steel tubing and plate.

D2-121773-2

One set of Xenon lamps for the solar simulator was purchased to perform the high temperature long term test (288 hours).

Problems encountered in "on schedule" delivery of beryllium material were solved without impact on the program by receiving the material in partial lot shipments.

Another problem encountered in the purchase of materials occurred during the test program when two Xenon lamps had to be returned to the manufacturer because of defects. The delay in getting the space chamber ready for the thermal-vacuum-shock test caused by the return of the lamps had no impact on the program at the time, but did use up some ahead-of-schedule time.

SECTION 8.0: QUALITY ASSURANCE

Unplanned events occurred on approximately 8% of the parts fabricated and less than 3% were scrapped.

Program surveillance was accomplished as stipulated in the "Quality Assurance Plan" set forth in Section 4 of D2-121318-1, "Mars Mission Solar Array Program Plan."

No major problems were encountered by Quality Assurance on this program. Configuration control of the panel during fabrication was maintained through use of the Boeing Integrated Record System (IRS). The panel was inspected after each test and the inspection results were recorded and are reported in Section 6.0. One-hundred shop fabrication orders were initiated by Manufacturing and approved by Quality Assurance.

Quality Assurance encountered problems of a minor nature, such as broken or cracked coverglass or solar cells, soldering discrepancies, priming, bonding, dimension errors and broken, cracked or gouged channel stock. A total of 65 UER's (Unplanned Event Records) and 35 pickups (minor shop errors) were written during fabrication. This quantity of UER's is considered to be minimal in view of the quantity of parts fabricated and the development status of the program. This opinion is also based on the fact that 45% of the beryllium parts were fabricated from surplus stock from a previous program.

Quality Assurance statistics for the fabrication program are shown below:

<u>Nature of Discrepancy Encountered During Fabrication</u>	<u>Quantity</u>
Broken or cracked coverglass or solar cells and soldering discrepancies - - - - -	15
Priming - - - - -	3
Bonding - - - - -	5
Dimensional Errors - - - - -	19

D2-121773-2

Broken, cracked, or gouged channel stock - - - - -	9
Miscellaneous - - - - -	<u>14</u>
Total - - - - -	65

Parts and Assemblies Fabricated (excluding solar cells):

557 Parts 100%

Nonconforming Parts - UER* Actions:

Rework Required	7	1.25%
Use As Is	22	3.95
Use to Make Smaller Part	3	.55
Scrapped	<u>13</u>	<u>2.34</u>
Total	45	8.09%

Solar Cell Assembly 6480 Parts 100%

Nonconforming Parts - UER* Actions:

Rework Required	10	.0015%
Use As Is	11	.0017
Scrapped	<u>3</u>	<u>.0005</u>
Total	24	.0037%

Note: Some edge-cracked solar cells were not cracked severely enough to be rejectable (see Section 6.9.2).

*Unplanned Event Record, Boeing Standard Form No. U3 4282 6040.

SECTION 9.0: CONCLUSIONS

The conclusions reached during the design, fabrication and testing of the light weight solar panel are presented below.

9.1 DESIGN CONCLUSIONS

Conclusions concerning the Light Weight Solar Panel design are:

- 1) The design goal of 20 watts per pound specific power output has been met. Under the contract-specified condition of 10 watts per square foot output, the specific power output of the test panel design is 20.6 watts per pound. This figure is based on a basic panel weight of 14.07 pounds which includes only the structure, cell stack, and wiring. The power output of a possible flight-configuration panel, using higher efficiency solar cells, is 23.0 watts per pound (see Figure 2-2). This configuration, with the weights of three zener diodes per solar cell module added to the basic panel weight, produces 20.3 watts per pound.
- 2) The panel design can accommodate a 40% increase in the weight of supported equipment, from 8.00 pounds to 11.22 pounds, with only a 3.3 percent decrease in specific power output.
- 3) The panel design requires redesigned submodule power-out pigtails for the power transfer to the buses since the handling and test environment causes damage to silver mesh pigtails.

9.2 MANUFACTURING CONCLUSIONS

Experience in the manufacturing of the light weight solar panel test panel has led to the following conclusions:

- 1) The use of plates, springs and threaded studs to provide bonding pressure is economical but the probability of damage to the assembly makes this bonding technique undesirable for flight-article tooling.
- 2) The use of the Boeing Specification BMS 5-89 primer was very successful in reducing the cost of panel assembly.
- 3) The expanded silver mesh solar cell module and submodule power-out pigtails are not sturdy enough to withstand handling during the fabrication of the panel. There is no problem with the silver mesh as a solar cell interconnector.

9.3 TEST CONCLUSIONS

From the test results it is concluded that:

- 1) Fiberglass substrate tension reduces a very small amount when exposed to 100°C for twelve days or extreme temperature changes at rates as high as 300°F/minute for short time intervals.
- 2) The panel structure is adequate to withstand an 8 "g" static load normal to the panel and a 50-pound load applied at one tip latch pin with supports at the other three attach points.
- 3) The solar panel assembly and solar cell module functions are not damaged or degraded by temperatures of -100°C for 24 hours, +100°C for 288 hours, and when exposed to thermal down-shock rates of 225°F/minute for one minute.
- 4) The solar cell module and submodule power-out silver mesh pigtails are inadequate for the handling and test environments to which they were exposed. Silver mesh is suitable as a solar cell interconnector.
- 5) The first resonant frequencies of the panel assembly in the pin-free condition, in bending, shear, and torsion are 28.4, 22, and 12.2 Hz, respectively.
- 6) The first resonant frequencies of the large and small fiberglass substrate bays are 68 and 78 Hz, respectively.
- 7) The solar panel assembly will withstand an acoustic field of 148.2 db for one minute with no structural damage.
- 8) The solar panel will withstand a specified wide-band random vibration spectrum at an input acceleration of 6.9 g rms for one minute.
- 9) The primer used on bonded structural members will discolor when exposed to twelve days of solar simulation of 1.8 suns.
- 10) Three 50-watt zener diodes per solar cell module are adequate because of the favorable heat sink properties of the beryllium structure and diode mounting clips.

SECTION 10.0: RECOMMENDATIONS

It is recommended that:

- 1) The basic light weight panel design be considered suitable for flight hardware on interplanetary missions by virtue of having met the requirements of this contract.
- 2) The design of the solar cell module and submodule power-out pigtails be re-designed to increase the reliability of the connection and provide dual path operation as illustrated in Figure 10-1. The recommended design uses dual, stranded-wire connectors.
- 3) A series of component tests be run on the redesigned module and submodule power-out connectors to verify the design.
- 4) Bonding pressure for final assembly of the panel be applied from a rigid beam structure supported by the heated platen.
- 5) Composite materials having near equivalent structural properties similar to beryllium be investigated to replace the beryllium parts to reduce panel costs.
- 6) A primer with similar properties to the Boeing Specification BMS 5-89, but without the characteristic of discoloration under solar simulation, be substituted for the BMS 5-89 primer.
- 7) Three 50-watt zener diodes per solar cell module be used.

- ① Wire (No. 26) Route as Shown to Provide Stress Loops
- ② Zener Diode Lead (Ref)
- ③ Bond Wire to Structure and Substrate Using RTV 882
- ④ Solder Wire to Silver Mesh Interconnects

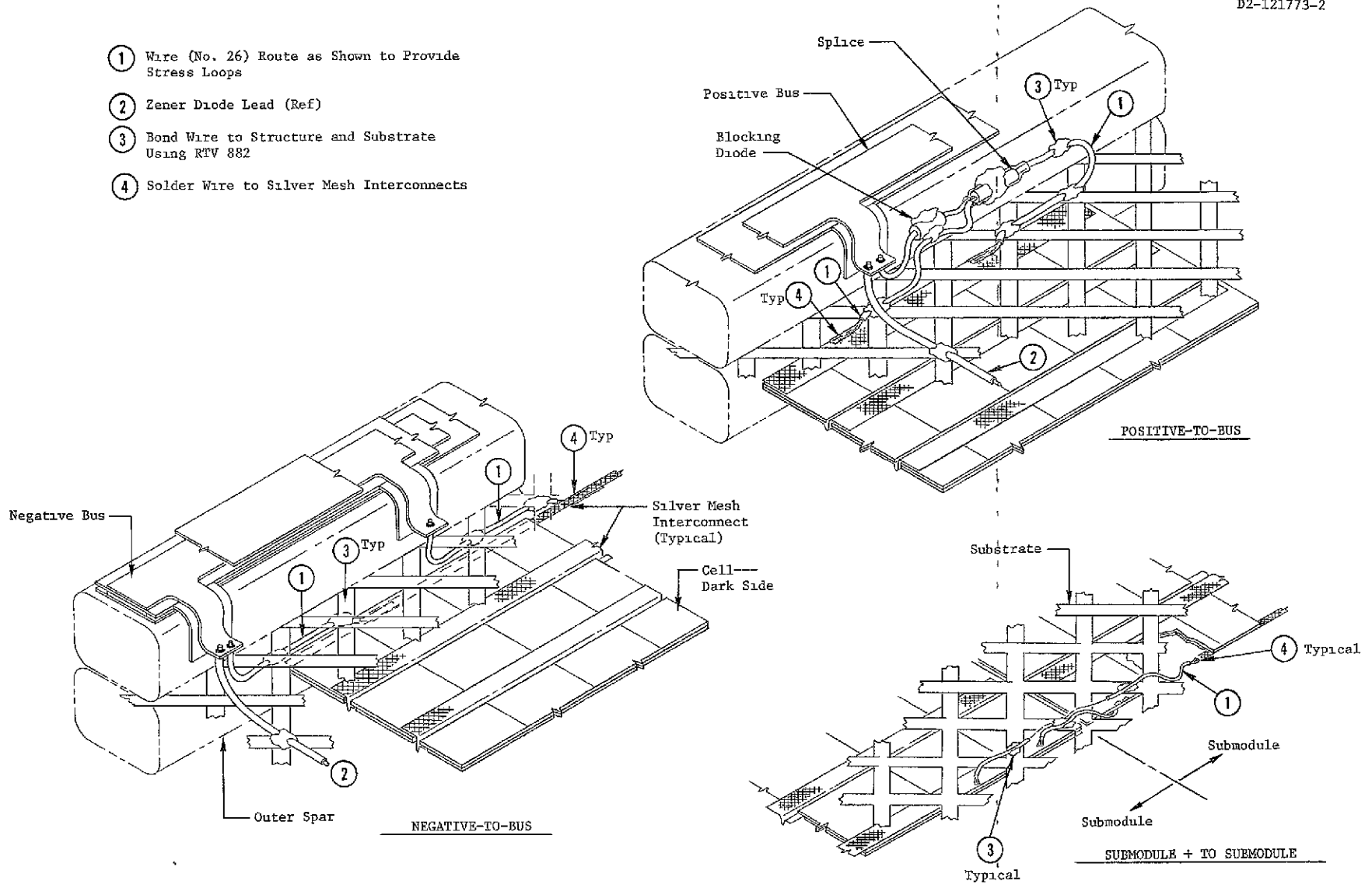


Figure 10-1 RECOMMENDED ELECTRICAL INSTALLATION

FOLDOUT FRAME

FOLDOUT FRAME 2

SECTION 11.0: NEW TECHNOLOGY

The purpose of this contract was to apply new technology developed under the Large Area Solar Array (LASA) development program to new and different requirements. Therefore, no new technology was developed. Only the application of existing and recently developed technology was made in producing and testing the light weight solar panel. Two procedures for improving the bonding costs of the panel were used that are different from the procedures used on LASA.

- 1) Bonding heat is normally applied to panels the size of the Light Weight Solar Panel in an autoclave, which is large and expensive, or by covering the panel with insulation and using heat blankets as was done with LASA. The latter method resulted in temperature differentials across the panel. The use on the Light Weight Solar Panel of an insulated cover setup above the platen, with hair dryer-type fans to circulate the air, resulted in temperature differentials of only $\pm 5^{\circ}\text{F}$.
- 2) The use of the baked-on epoxy primer, Boeing Specification BMS 5-89, allowed a minimum number of large pieces to be cleaned and primed while still in large sizes. The large pieces were cut to size on assembly, MEK-wiped, then bonded. This resulted in easier handling, fewer individual parts to process, and, as a result, reduced costs. However, discoloration under simulated sun light was an undesirable characteristic.

SECTION 12.0 REFERENCES

1. D2-121318-1, Mars Mission Solar Array Program Plan
2. D2-121321-1, Mars Mission Solar Array Test Plan (Volume I)
3. D2-121718-1, Mars Mission Solar Array Analysis Documentation
4. D2-121319-1, Mars Mission Solar Array Semi-Annual Progress Report
5. D2-121321-2, Light Weight Solar Panel Development Test Report (Volume II)
6. D2-121321-3, Light Weight Solar Panel Development Test Report (Volume III)
7. D2-121773-1, Test Procedures - Light Weight Solar Panel Development
8. E. L. Ralph, "Performance of Very Thin Silicon Solar Cells," paper presented at the 6th Photovoltaic Specialists Conference, Cocoa Beach, Florida, March 28-31, 1967.